KERNFORSCHUNGSANLAGE JÜLICH GmbH
Institut für Kernphysik

WORKSHOP ON ELECTRON COOLING

Bad Honnef, May 1982

edited by

G.P.A. Berg
W. Hürlimann
J.G.M. Römer

The Workshop was organized by

J. Debrus
F. Hinterberger
S.A. Martin

Jül - Spez - 159
Juli 1982
ISSN 0343-7639

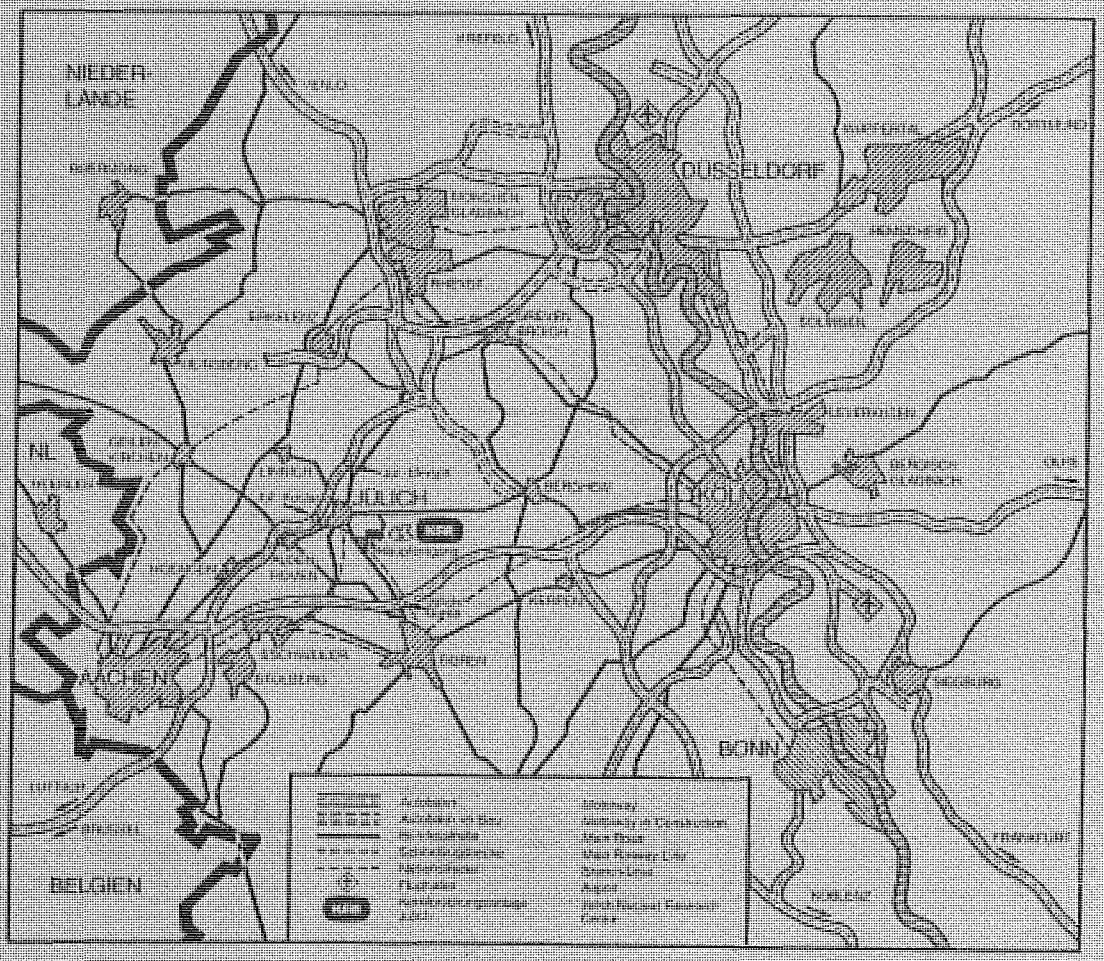

Als Manuskript gedruckt

Spezielle Berichte der Kernforschungsanlage Jülich – Nr. 159

Institut für Kernphysik Jül – Spez – 159

Zu beziehen durch: ZENTRALBIBLIOTHEK der Kernforschungsanlage Jülich GmbH
Postfach 1913 · D-5170 Jülich (Bundesrepublik Deutschland)
Telefon: 02461/610 · Telex: 833556 kfa d

WORKSHOP ON ELECTRON COOLING

Bad Honnef, May 1982

edited by

G.P.A. Berg
W. Hürlimann
J.G.M. Römer

The Workshop was organized by

J. Debrus, Physikzentrum Bad Honnef
F. Hinterberger, ISKP Universität Bonn
S.A. Martin, KFA Jülich

The "Workshop on Electron Cooling" was organized by the KFA Jülich and the University of Bonn. It is a contribution to the discussion about ideas and plans for future activities of the Nuclear Physics community in Nordrhein-Westfalen.

The aim of the workshop was to discuss the status of high resolution accelerator technology for protons and light ions (Li) in the energy region between 100 MeV and 1.0 GeV. It seems that the recent developments (electron cooling on recirculators) open new possibilities for the high precision nuclear physics in the energy regime up to about 1 GeV.

The present "Workshop notes" are copies of the transparencies presented during the talks and discussions or a manuscript when the speaker could provide one. These notes do not intend to cover the complete talks given at the workshop. But it should be a help for those who want to continue to work in this interesting field. It should not be made reference to these informal notes but rather contact the speaker for correct references or use those given in manuscripts. Therefore the list of participants contains the addresses. We hope the workshop notes will be useful for refreshing the many different pieces of information given during the workshop and they may help to guide the further discussion on new experiments in nuclear physics.

The organizers gratefully acknowledge the expertise of all guests, who contributed to the workshop and transfered their past experiences and future ideas to other participants.

We are also grateful to the KFA Jülich, the Institut für Strahlen- und Kernphysik, Universität Bonn, for their financial support as well as the Deutsche Physikalische Gesellschaft for the kind hospitality.

Workshop on Electron Cooling

Physikzentrum Bad Honnef, May 27 - 28, 1982

Final Program

Thursday, May 27

Chairman: H. Daniel

10.00 F. Hinterberger (Univ. Bonn)
"Welcome and introductory remarks"

10.15 S. Martin (KFA Jülich, IKP)
"First ideas about a Cooler-Synchrotron (COSY) at Jülich"

11.00 Coffee break

11.30 F. Mills (FERMILAB)
"Review of the principles of electron cooling"

12.45 Break for lunch

Chairman: K.H. Maier (HMI Berlin)

14.00 H.V. von Geramb (Univ. Hamburg)
"The need for small cross section measurements at medium energies"

14.30 R.E. Pollock (IUCF)
"Indiana storage ring with electron cooling
- Research at IUCF
- General comments on Recirculators and beam cooling
- Design and construction of the Indiana cooler ring"

16.00 Coffee break

Chairman: R. Santo

16.30 H. Poth (KFZ Karlsruhe, LEAR-CERN)
"Electron-cooling in combination with internal targets"

17.30 C.A. Wiedner (MPI Heidelberg)
"Is a recirculator for the BIG KARL spectrograph feasible?"

19.00 Grill

Friday, May 28

Chairman: H. von Buttlar (Univ. Bochum)

9.00	F. Osterfeld (KFA Jülich) "The challenge of physics with a high-energy light-ion facility"
10.00	D. Husmann (Univ. Bonn) "Acceleration and storage of polarized particle beams"
11.00	Coffee break
11.30	F. Mills (FERMILAB) "Antiproton accumulators at FERMILAB and recent results of electron-cooling"
12.45	Break for lunch

Chairman: F. Hinterberger

14.00	B. Franzke (GSI Darmstadt) "SIS 12 - a look to the possibilities of electron-cooling of heavy ions"
14.45	Coffee break

Chairman: K.H. Maier

15.15	Panel discussion and summary by R.E. Pollock (IUCF)
17.00	End of the Workshop

LIST OF PARTICIPANTS

G.P.A. Berg
IKP
KFA Jülich GmbH
Postfach 1913
5170 Jülich

W. Bräutigam
IKP
KFA Jülich GmbH
Postfach 1913
5170 Jülich

P. v. Brentano
Institut für Kernphysik
Universität Köln
Universitätsstr. 14
5000 Köln 41

K.L. Brown
SLAC
P.O. Box 4349
Stanford, Ca. 94305
USA

H. von Buttlar
Institut für Experimentalphysik III
Ruhr Universität
Universitätsstr. 150
Gebäude NB
4630 Bochum

H. Daniel
Physik Department
Technische Universität München
James-Franck-Str. E18
8046 Garching

P. David
ISKP
Universität Bonn
Nußallee 14 - 16
5300 Bonn 1

J. Debrus
ISKP
Universität Bonn
Nußallee 14 - 16
5300 Bonn 1

K. Erdman
TRIUMF
4004 Wesbrook Hall, UBC Campus
Vancouver, B.C.
V6T 2A3
Canada

J. Ernst
ISKP
Universität Bonn
Nußallee 14 - 16
5300 Bonn 1

K. Euler
ISKP
Universität Bonn
Nußallee 14 - 16
5300 Bonn 1

B. Franzke
GSI
Postfach 11 05 41
6100 Darmstadt 11

G. Gaul
Institut für Kernphysik
Universität Münster
Von-Esmarck-Str. 10a
4400 Münster

H.V. von Geramb
Institut für Theoretische Physik
Universität Hamburg
Jungiusstr. 9
2000 Hamburg 36

Chr. Günther
ISKP
Universität Bonn
Nußallee 14 - 16
5300 Bonn 1

F. Hinterberger
ISKP
Universität Bonn
Nußallee 14 - 16
5300 Bonn 1

H. Huebel
ISKP
Universität Bonn
Nußallee 14 - 16
5300 Bonn 1

W. Hürlimann
IKP
KFA Jülich GmbH
Postfach 1913
5170 Jülich

D. Husmann
Physikalisches Institut
Universität Bonn
Nußallee 12
5300 Bonn 1

K.H. Maier
HMI für Kernforschung
Postfach 39 01 28
1000 Berlin 39

N. Marquardt
Institut für Experimentalphysik III
Ruhr Universität
Universitätsstr. 150
Gebäude NB
4630 Bochum

S. Martin
IKP
KFA Jülich GmbH
Postfach 1913
5170 Jülich

T. Mayer-Kuckuk
ISKP
Universität Bonn
Nußallee 14 - 16
5300 Bonn 1

F. Mills
Fermilab
P.O.Box 500
Batavia, Il. 60510
USA

P. Morsch
IKP
KFA Jülich GmbH
Postfach 1913
5170 Jülich

F. Osterfeld
IKP
KFA Jülich GmbH
Postfach 1913
5170 Jülich

R.E. Pollock
Physics Department
Indiana University
Bloomington, Ind. 47401
USA

H. Poth
LEAR-Gruppe
CERN
CH-1211 Geneve 23
Switzerland

P. von Rossen
ISKP
Universität Bonn
Nußallee 14 - 16
5300 Bonn 1

J. Reich
IKP
KFA Jülich GmbH
Postfach 1913
5170 Jülich

J.G.M. Römer
IKP
KFA Jülich GmbH
Postfach 1913
5170 Jülich

M. Rogge
IKP
KFA Jülich GmbH
Postfach 1913
5170 Jülich

R. Santo
Institut für Kernphysik
Universität Münster
Von-Esmarck-Str. 10a
4400 Münster

W. Schott
Physik Department
Technische Universität München
James-Franck-Str. E18
8046 Garching

O.W.B. Schult
IKP
KFA Jülich GmbH
Postfach 1913
5170 Jülich

A. Scott
Department of Physics
University of Georgia
Athens, Georgia 30602
USA

H. Wahl
ISKP
Universität Bonn
Nußallee 14 - 16
5300 Bonn 1

C.A. Wiedner
MPI für Kernphysik
Postfach 10 39 80
6900 Heidelberg

P. Wucherer
IKP
KFA Jülich GmbH
Postfach 1913
5170 Jülich

L. Zemlo
INR
Hoia 63
Warszawa
Poland

Table of Contents

1. F. Hinterberger (Bonn)
   Welcome and introductory remarks
2. S. Martin (KFA, TRIUMF)
   First ideas about a Cooler-Synchrotron (COSY) at Jülich
3. F. Mills (Fermilab)
   Review of the principles of electron-cooling
4. H. von Geramb (Hamburg)
   The need for small cross section measurements at medium energies
5. R. Pollock (IUCF)
   Indiana storage ring with electron-cooling
6. H. Poth (KfK, LEAR)
   Electron-cooling in combination with internal targets
7. C. Wiedner (MPI Heidelberg)
   Is a recirculator for the BIG KARL spectrograph feasible?
8. F. Osterfeld (KFA)
   The challenge of physics with a high-energy light-ion facility
9. D. Husmann (Bonn)
   Acceleration and Storage of polarized particle beams
10. F. Mills (FERMILAB)
    Antiproton accumulators at FERMILAB and recent results of electron-cooling
11. B. Franzke (GSI)
    SIS 12 - a look to the possibilities of electron-cooling of heavy ions
12. Panel discussion
    Chairman: K.H. Maier (HMI Berlin)
13. R. Pollock (IUCF)
    Summary

Welcome and introductory remarks

F. Hinterberger
Institut für Kernphysik
Universität Bonn

Gentlemen,

it is a pleasure for me to welcome you at this workshop on electron cooling. Originally Prof. Mayer-Kuckuk wanted to present a welcome adress but right at the moment he is hindered to be here. He will join us at 11.30.

Before starting the workshop with a review of the discussions on a cooler synchrotron by Sig Martin and with an outline of the work that should be done I would like to make a few remarks on the aim of this meeting.

During the last one and a half years there have been a lot of discussions among nuclear physicists from Nordrhein-Westfalen on the following questions.

What kind of upgrading of the JULIC cyclotron facility should be envisaged?

What kind of particles should be used and what is the most interesting energy range?

What kind of machines could be used to match the different experimental requirements and the existing JULIC facility?

The wanted energy range and particle range can easily be summarized

Light ions: p, d, t, ^{3}He, α, ^{6}Li, ^{7}Li,.....
Energy range: 5 MeV/N - 500 MeV/N

The requirements regarding beam properties depend on the experiments. But in any energy range the quest for a very high energy resolution and a complete channel resolution in nuclear reaction experiments was apparent.

Well, those discussions are not yet finished. But during that time Sig Martin studied the potentialities of synchrotrons and cooler rings. He also made rough estimates of the feasibility as well as of the costs for the energy range 50 MeV/N up to 1 000 MeV/N.

In summarizing I would say some of us were fascinated by the possibility to produce high-current beams (up to 100 μA) with an extremely good beam quality, that is energy resolution of better than 10^{-4} and emittances of the order of 0.1 mm·mrad, with a widely variable time structure (DC → Δt < 100 psec).

But there was also a large scepticism of how to use such circulating beams in experiments. I will only mention two problems:

- the problem of measuring nuclear reactions in the vicinity of zero degree with a high-resolution magnetic spectrometer.
- the problem of making external beams which can be used in external target stations.

Coming back to the actual purpose of this workshop.

There are essentially two aims (i) to bring together experimentalists to explore the potentialities of using cooled storage rings in nuclear reaction experiments.
(ii) to learn the methods of electron cooling. It is apparent that the methods in beam cooling are rapidly developing. Pioneering work was done at Novosibirsk, the Fermilab and the CERN laboratories.
The electron cooling method was especially developed in view of the planned low energy antiproton ring experiments.

So, I am happy that we have experts from the Fermilab and the LEAR group with us.

Now some technical remarks regarding the workshop.

As announced in the circular it is planned to lay down the results of the workshop in a Jülich Internal Report. This report should contain the manuscripts of the contributions - if available - or at least the most important viewgraphs and the main topics in a condensed form. In addition the essential results of discussions should also be written down.

To this end we have asked Georg Berg from the Big Karl group in Jülich to be our workshop secretary. He and his colleagues from the Big Karl group will try to do this job.

Before closing I would would like to acknowledge the financial support by the KFA Jülich as well as the supports given by the government of Nordrhein-Westfalen und the University of Bonn.

I hope that this workshop will be very helpful for the future planning and that it will stimulate the phantasy of the experimentators of how to use cooled storage ring beams.

I hope also that all of you will have a nice time here in the Physikzentrum which is known as a very pleasant host for workshops and our sincere thanks go to Frau Ingeborg Kluth and Dr. J. Debrus.

Problems:

Electron cooling
Storage rings
Cooler-Synchrotron: one ring or two rings?
preaccelerators
internal targets (heating vs. cooling)
cooling of $Z>1$ beams
vacuum requirements
beam extraction (continuous or pulsed)
polarized beams
high-resolution spectroscopy (near $\Theta = 0°$?)
smooth energy variation for resonances?

First ideas about a Cooler-synchrotron (COSY) at Jülich

S.A. Martin
Institut für Kernphysik
Kernforschungsanlage Jülich

SPECTROSCOPY WITH P, D, ..., α AT BIG KARL - JULIC

DEV. + IMPROVEMENTS OF EXPERIMENTS :

- SMALL ε
- EFF. USE OF THE BEAM
- NO BEAM STOP
- TUNABLE DUTY CYCLE
- E - VARIATION: "FINE" <1 MeV
  LARGE RANGE
- THIN TARGETS
  RECOIL SPECTROSCOPY
- POLAR. ATOMIC TARGETS

WHY IMPROVEMENTS ?

→ DISC. WITH BIG KARL USERS

SPECTROMETER

45 MeV / u p d ^3He α

→ $\Delta E/E \approx 10^{-4}$ → $5 \cdot 10^{-5}$

$\Delta\Omega \approx 4$ msr

→ TARGET LIMITS

→ SMALL ANGLES

→ BEAM $d p/p \approx 3 \cdot 10^{-3}$

$\varepsilon \approx 10\ \pi$ mm mr

$I \approx 1\ \mu A$

FEED

DIFF. IN BEAM - ACC

MATCHING

BEAM ANALYSIS

I_0	10 μA	100 nA	100 μA
E	5 - 50 variabel	< 50	≤ 500 (1000) variabel
E/ΔE Acc	$3 \cdot 10^4$	100	
E/ΔE Exp.	10^5		10^3 10^4 10^5
Zeit	dc	10 nsec 100 sec, 0.5 nsec	10 nsec 10 μsec, 1 nsec (dc)
Teilchen	p, d, ^{3}He, α pol.	≤ 60	≤ Li
EXPER. EQUIPM.	Spectr.	γ-Spectr.	Spectr. CARP (recoil) SINDRUM
	SSM		HHM

→ RECIRCULATOR

→ COSY

SYNCHROTRON WITH e-COOLING

Bad Honnef Juni 1980

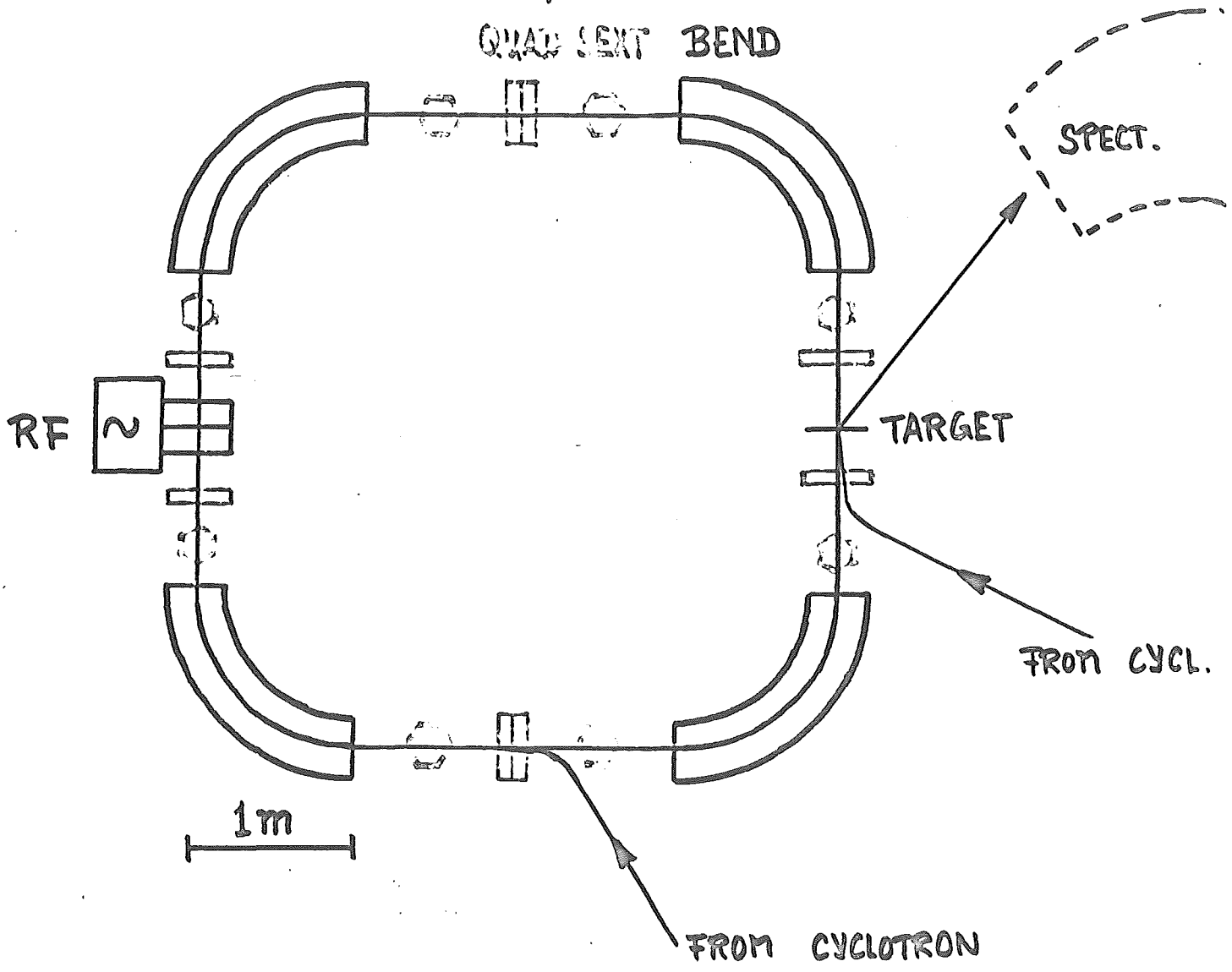

SCHRITTE zum REZIRKULIERER

1. SEPTUM MAGNET
   - STRAHLSTOPP WEG v. TARGET
   - MONITOR ZÄHLER
   - KOINZIDENZEXPERIMENTE
2. HALBER RING zum STRAHLSTOPP
   - ACHROMAT
   - 0°- EXPERIMENTE
3. GANZER RING f. STRIPPING INJEKTION
   - N-fache Intensität für PROTONEN
4. HF
   - HÖHERE INTENSITÄT d. KORREKTUR d. ENERGIEVERL.
   - INJEKTION ohne STRIPPING
5. REZIRKULIERER als BY-PASS IM COSY

SYNCHROTRONS

Vorteile	Nachteile
E-variabel	ΔE schlecht
billig	duty cycle
	Vacuum (10^{-9})
	injection + extraction

internes Target + e-Kühlung

E-Variabilität 100 – 1000 MeV
20 – 100 "

nicht sehr kostspielig ~ 20 MDM

$\Delta E/E \leq 10^{-5}$

duty cycle variable 1% ... 100%

Injektion
- sehr einfach mit stripping
- möglich mit Kickers

Extraktion
- möglich für 100% duty cycle (slow)
- wird untersucht für e-Kühl-Ring!

SEC BEAM CHARACTERISTICS

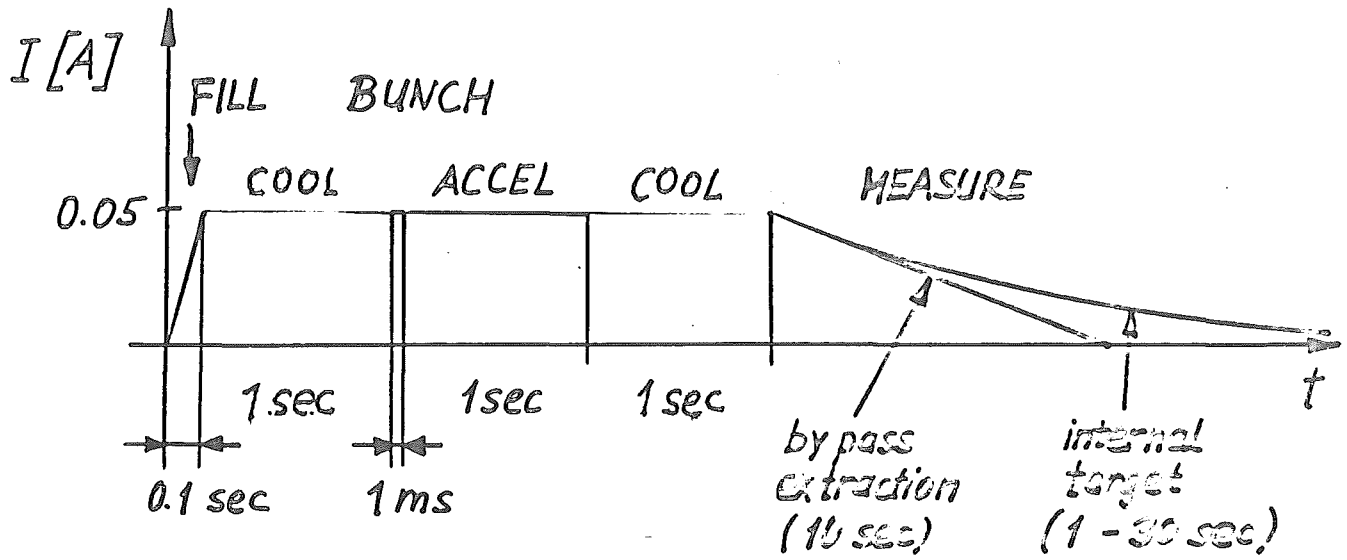

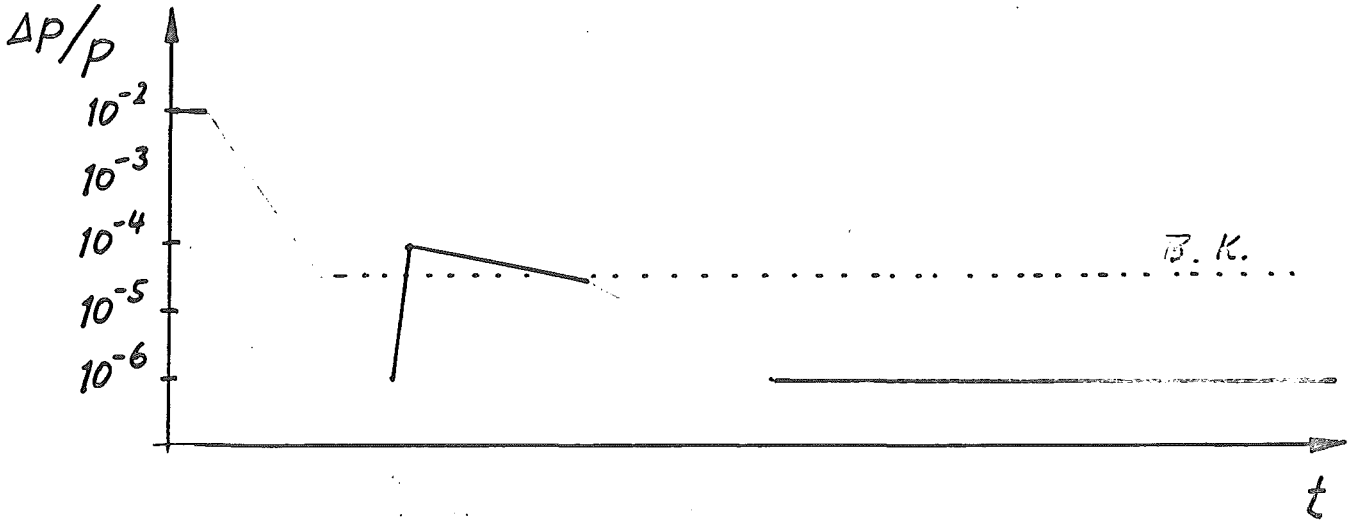

	JULIC	SEC	
	achr. mode	internal Target	by pass extr.
beam current I	1 μA	30 mA	5 nA
target thickness T	50 μg/cm²	0.05 μg/cm²	50 μg/cm² *
resolution power $\frac{P}{\Delta P}$	600	10^6	
$I \cdot T$ [Ag/cm²]	$5 \cdot 10^{-11}$	$1.5 \cdot 10^{-9}$	$2.5 \cdot 10^{-13}$
$I \cdot T \cdot \frac{P}{\Delta P}$	$3 \cdot 10^{-8}$	$1.5 \cdot 10^{-3}$	$2.5 \cdot 10^{-7}$

* affected by target thickness!

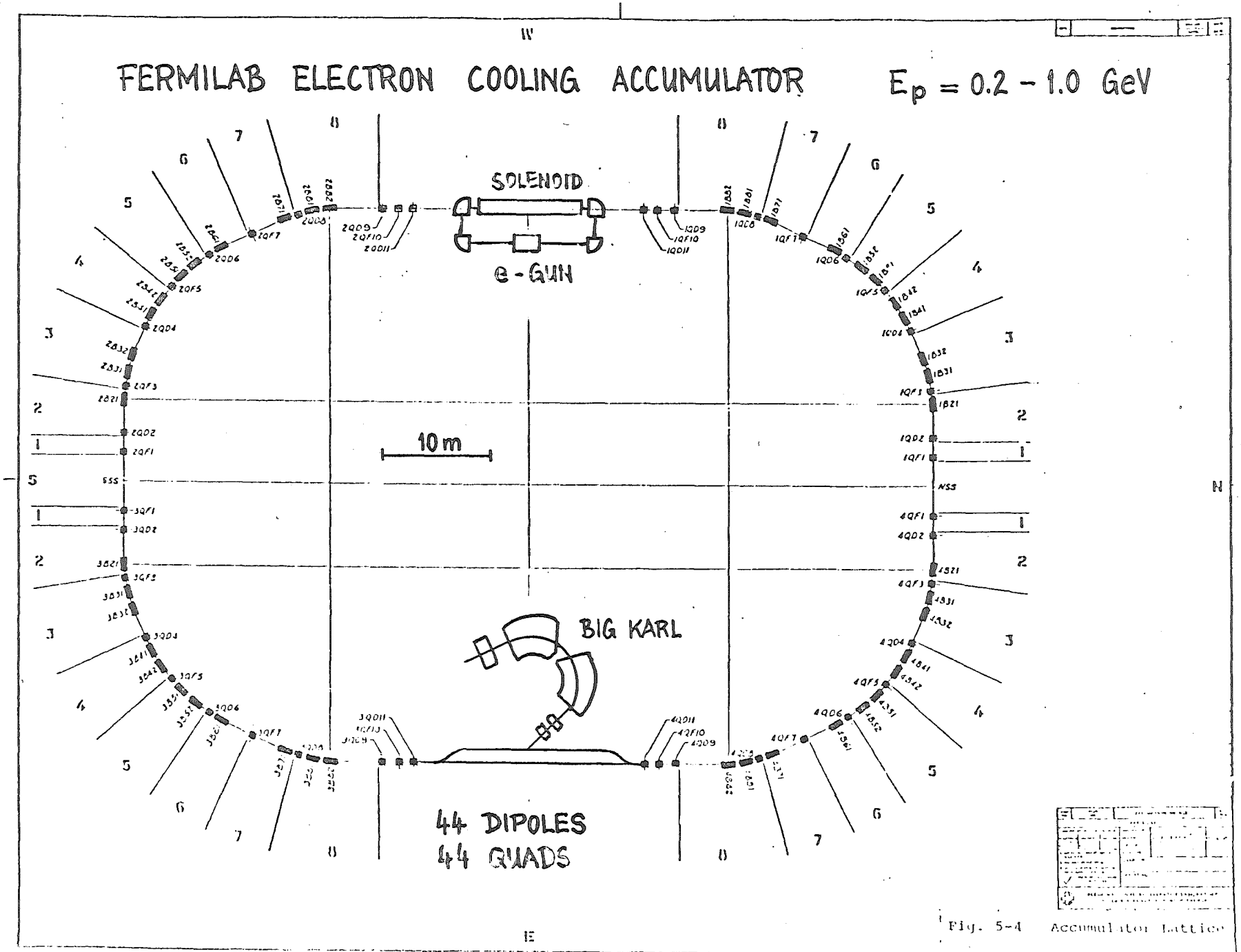

Fig. 5-4 Accumulator Lattice

FERMI E-COOLING RING ACCUMULATOR

ENERGY	0.2 – 1.2 GeV	
ℓ	9.17 m	
R	32.35 m	U = 203.2 m
REVOL. TIME	1200 – 750 usec	
SUPER PERIODICITY	2 (1 COOLING)	
FOCUSING	FODO SEPAR. FUNCTION	
WORKING POINT	γ_H	4.102
	γ_V	5.367
	γ_T	4.084

MAGNETE:	DIPOLES	QUADRUPOLES
NUMBER	44	44
LENGTH [m]	1.22	0.61
Eff. LENGTH "	1.31	0.68
FIELD [KG]	6.2	(1 × 3.5)(1×3.0), < 2.3

VACUUM CHAMBER $a_H = \pm 8.9$ cm

$a_V = \pm 2.5$ cm

ACCEPTANCE OF DIPOLES $A_V = 47\pi$ mm · mrad

$A_H = 40\pi$ "

$\Delta p/p = \pm .25\%$

$= 2.37\%$ (injection)

ANGLES IN E-COOLING SECTION:

$\Theta_H = 1.8$ mrad

$\Theta_V = 2.2$ mrad

$\Theta_{perp} \sim \gamma \frac{\Delta p}{p} \approx 5 - 10$ mrad

Kosten:

1.	MAGNETE	~ 4000 TDM
2.	Netzgeräte	740
3.	e-Kühler	2000
4.	HF	260
5.	Diagnostik	230
6.	Ver- und Entsorgung	270
7.	Instrumentierung	580
8.	Vakuum	
	RING	2370
	TARGET	2070
	KRYOANLAGE	2930
	Sa. Gerät	15460
	Bau	~ 5000

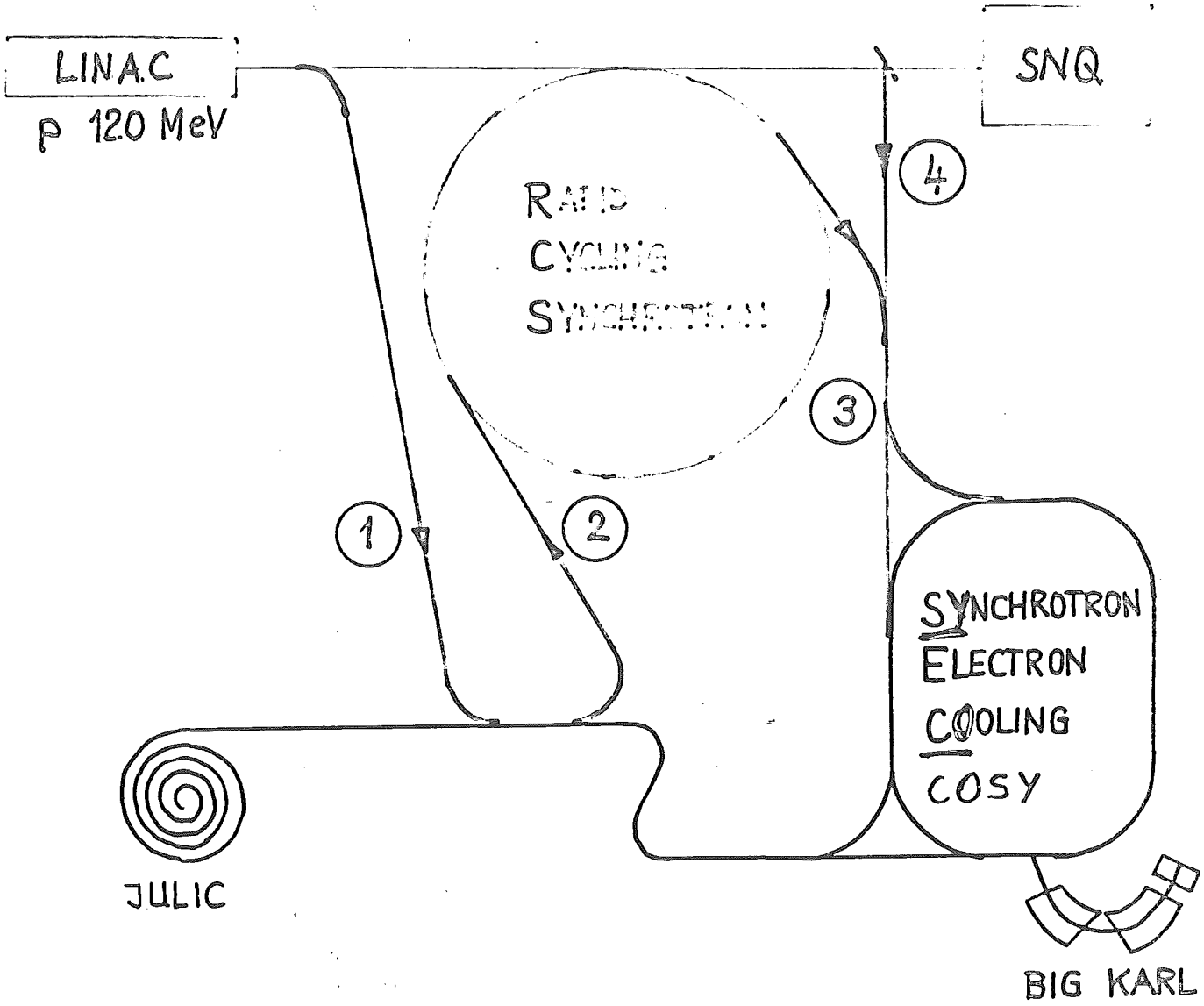

(1) Einschuss in JULIC - Strahlführung vom LINAC

(2) Bedienung des RCS der SNQ mit JULIC

(3) Füllen des SEC mit Protonen zwischen 100 und 1100 MeV vom RCS

(4) Benutzung des SEC als Exoten - Akkumulator

WORK :

1 Injection : Cycl. → SYNCHR.
LINAC → SYNCHR.
Stripper
KICKER
STACKING

2. e - COOLING : SOLENOID
e-GUN
OPTIC
Bell calculations (THEORY)

3. CONDITIONS IN COOLED BEAM
BEAM QUALITY
ACCELERATION
EXTRACTION

4. LATTICE - PARTICLE DYNAMICS — W. SCHOTT
SPACE CHARGE EFFECTS — S. MARTIN

5. INTERNAL TARGETS — Ch. WIEDNER

6. COMPUTER

7. TECHNOLOGY HF
MAGNETE
DIAGNOSTIC

8. GEN. SUPPORT

Review of the principles of electron-cooling

F. Mills
Fermi National Accelerator Laboratory
Batavia, Illinois

F. Mills
26 May 82

Electron Cooling is the slowing down and equilibration of ions by coalomb scattering in an electron gas. There is a close analogy to stopping power phenomena.

Single Collision

The proton receives, on the average, a longitudinal momentum transfer (⟶ Friction force + Diffusion) and on the average, no transverse momentum ⟶ Diffusion

$$\vec{F}(v_p) = \sum_{\substack{\text{impact parameters} \\ \text{electron velocities}}} \left(n \; \sigma \; v \; \Delta P_{\text{long.}} \right)$$

$$= -\frac{4\pi n e^4}{m} \ln \frac{b_{max}}{b_{min}} \int \frac{(\vec{v}_p - \vec{v}_e)}{|\vec{v}_p - \vec{v}_e|^3} f(\vec{v}_e) d\vec{v}_e$$

$$= K \nabla_{v_p} \int \frac{f(v_e)}{|\vec{v}_p - \vec{v}_e|} d\vec{v}_e$$

Note the analogy to Electrostatics $\vec{E} = -\nabla \int \frac{\rho \, d\vec{r}_1}{|r - r_1|}$

Then there is a story to be told about electron velocities, proton velocities and impact parameters and transformations between laboratory and moving systems.

First some orders of magnitude.

Take 200 Mev Protons, 110 kv electrons, $I = 5$ A, 5 cm diameter and $T_e \sim 1$ eV; $B = 1$ kg.

$n_e \sim 10^8$, $\omega_{pe} \sim 6 \times 10^8$ Hz, $\omega_{ce} \sim 1.8 \times 10^{10}$ Hz

$$\beta_e = \sqrt{\frac{2T_e}{mc^2}} \sim 2 \times 10^{-3}$$

Impact Parameters

$$b_{min} \sim \frac{e^2}{T_e} \quad \text{(Distance of minimum approach)}$$

$$\sim \frac{2r_e}{\beta_e^2} \sim 1.4 \times 10^{-7} \text{ cm}$$

$\ln = 10$

$$\rho_e = \frac{m v_e c}{eB} = \frac{\beta_e c}{\omega_{ce}} = 3.4 \times 10^{-3} \text{ cm}$$

$\ln = 3$

$$\lambda_D = \sqrt{\frac{T_e}{4\pi n e^2}} \sim .07 \text{ cm}$$

For $b > \rho_e$, the collision is adiabatic for the transverse (gyro) motion of the electron. Momentum can be transferred only along the field lines, and only if there is an angle between $\vec{V_p}$ and $\vec{B}$.

The above Friction force must be modified, essentially by removing $T_{e\perp}$ from the above formula. "Magnetic Cooling"

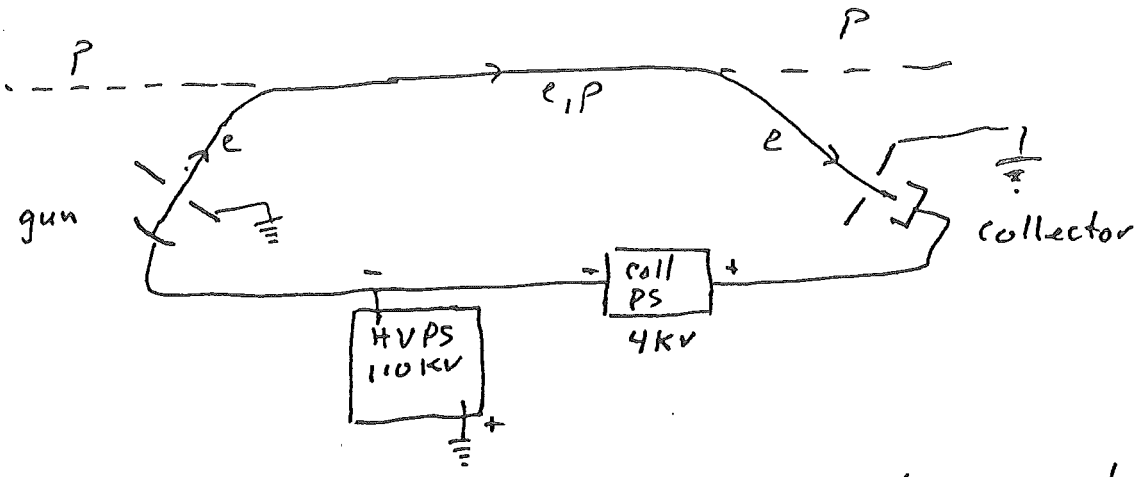

To contain the beam against space charge, at low energies, the beam must be in a magnetic field. To obtain low temperature, the cathode must also be immersed. To obtain good collection the collector must be immersed.

Consequences

1. Magnetic cooling for ~25% of coulomb log

2. $\Delta E_{\parallel} = mv\,\Delta v_{\parallel}$, $\frac{\Delta v_{\parallel}}{c} = \frac{\Delta E}{pc} = \frac{T_e}{\beta\gamma mc^2}$

$\beta_{\parallel} \sim 3\times10^{-6}$, while $\beta_{\perp} \sim 3\times10^{-3}$

Since $\beta_{\perp}$ is unimportant for magnetic cooling, and $\beta_{\parallel}$ is so small, the magnetic part of cooling is important.

3 space charge

a) Potential of ebeam $V \sim \frac{30I}{\beta}\left[1 + 2\ln b/a\right]$

~ 1kV for 5 A - moves operating point.

b) Radial Field $E_r = \frac{4\pi n e \cdot \pi r^2}{2\pi r} = 2\pi n e r$

Rotation of ebeam $= \frac{m}{2e}\omega_p^2 r$.

$\omega \equiv \frac{v_{drift}}{r} = \frac{E_r c}{B r} = \frac{mc}{2eB}\frac{\omega_p^2 r}{r} = \frac{\omega_{pe}^2}{2\omega_{ce}}$

for the above parameters

$$\omega \sim 8.9\times10^{6}\ Hz \quad , \text{ or } \frac{\omega}{\beta c} = .05\ \frac{\text{radian}}{\text{meter}}$$

This adds another velocity component to e beam, which is equivalent to a temperature increase.

Proton Velocities

If the proton velocity exceeds the electron velocity in the moving system, then cooling will be dominated by the proton velocity, and will be slower. Equality is when $v_{p\perp} \sim v_{e\perp}$. Now

$$\frac{v_{p\perp}}{c} = \frac{p_\perp}{mc} = \frac{p\theta_p}{mc} = \beta\gamma\theta_p$$

For $\beta\gamma \sim .7$ and $\beta_{e\perp} \sim 2\times10^{-3}$, $\theta_{p\perp} \sim \frac{2\times10^{-3}}{.7} = 3\times10^{-3}$.

If the lattice β function $\beta_L \sim 20m$, then the proton emittance is $\frac{\varepsilon}{\pi} = \beta_L \theta_p^2 \simeq 100\ \pi$ mm mrad - this is not too restrictive.

Further for emittances much smaller than this, the magnetized cooling can become dominant.

Transformations between Laboratory and Moving Systems

The important transformations to remember are that

$$n_{moving} = \frac{1}{\gamma}\, n_{Lab}$$

$$\Delta t_{Lab} = \frac{1}{\gamma}\, \Delta t_{moving}$$

$$p_\perp = \text{invariant} \Rightarrow \frac{v_\perp}{c} = \beta\gamma\theta$$

$$\frac{v_{\parallel}}{c} = \beta\frac{\delta p}{p}$$

Friction Forces

Electrostatic Analogy for non-Adiabatic Collisions

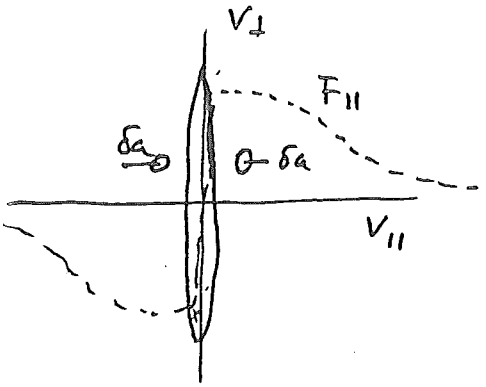

1.) If $|V_p| >> |V_e|$ $\qquad \kappa = \frac{4\pi n e^4}{m} L\eta$

$$\vec{F} = -\frac{k \vec{V_p}}{|V_p|^3}$$

2) F_{11} near origin: By Gauss's Law

$$2 F_{11} \cdot \delta a = \frac{\kappa}{\pi V_{\perp e}^2} 4\pi \delta a$$

$$\text{or } F_{11} = \frac{2\kappa}{V_{e\perp}^2}$$

Expressed in rate of change of $\frac{\delta p}{p}$ in lab system ($V_{11} = \beta c \frac{\delta p}{p}$

$$\left(\frac{\dot{\delta p}}{p}\right)_{lab} = \frac{8\pi n_L c}{1836 \beta \gamma^2} \left(\frac{mc^2}{T_e}\right) r_e^2 L\eta$$

$$\simeq 10^{-3}/\text{sec} \quad \text{for } L = \ln \frac{\rho_s}{b_{min}} = 10 \quad \eta = .04 = \frac{L_{cool}}{C}$$

and previous parameters. (200 Mev etc)

For $\frac{\delta p}{p} = 10^{-3}$ $\quad \Delta E_e \cong 160 eV$

Such Friction Forces are easy to measure by stepping e beam voltage and measuring time for p beam to follow.

Transverse Cooling

$$m \frac{dV_\perp^*}{dt^*} = F_\perp^* \qquad \tau^* = \frac{m_p V_\perp^*}{F_\perp^*}$$

$$\simeq \frac{\gamma^3}{2\pi n r_p r_e c L\eta} \left(\frac{T_{e\perp}}{mc^2}\right)^{3/2} \simeq 12 \text{ sec for above parameters}$$

If $\beta_{p\perp} < \beta_{e\perp}$, the magnetic cooling can be dominant

Magnetized Cooling

For $V_p > \beta_{e\parallel}$ $\left(L_A = \ln \frac{r_D}{\rho_e} \sim 3\right)$

$$\vec{F}^{*A}_{\perp} = -\frac{8\pi n e^4}{m_e} L_A \frac{V_{p\perp}^2 - 2V_{p\parallel}^2}{V_p^7} \frac{\vec{V}_{p\perp}}{V_p^3}$$

$$F^{*A}_{\parallel} = -\frac{6\pi n e^4 L_A L^A}{m} \frac{V_{p\perp}^2}{V_p^2} \frac{V_{p\parallel}}{V_p^3} \quad *$$

Main Points

1. There is no cooling if $V_{\perp p} = 0$
2. for finite $V_{\perp p}, V_{\parallel p}$, the velocity vector rotates toward the $\perp$ direction, then reduces in magnitude
3. for $V_{p\parallel} \sim 0$, the cooling is much faster than that by non adiabatic term when $V_{\perp e} > V_{\perp e}$ (Most Novosibirsk results are in this regime). For Fermilab cooling, the [redacted] contribution is substantial.

* There is a factor of 2 mistake in this formula (From CERN 77-08) which was corrected by Rosenbluth (unpublished)

Technique of Electron Beam

1. Gun - Novosibirsk, CERN

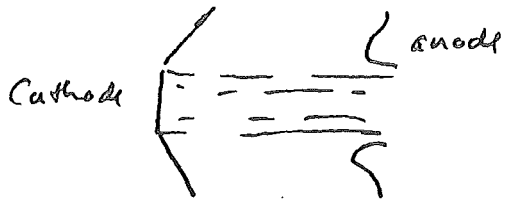

Flat Cathode

or Fermilab

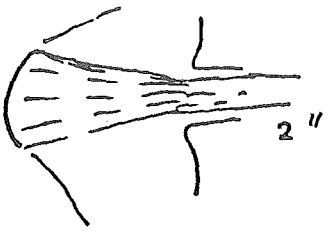

Converging beam.

Both are Pierce guns immersed in Magnetic field. In the accelerating region, there is no radial electric field. In the anode hole, a radial field is turned on in a length < gyrolength This induces a gyro oscillation of e beam which must be removed by later lenses (usually electrostatic) This is called "resonance optics". In the Fermilab gun, this corresponds to ~ 1000 eV.

A recent Fermilab gun design (Oleksiak) turns the field on adiabatically and the induced gyromotion is ~ 1eV

The converging gun, because of the constancy of magnetic moment, increases the electron temperature in proportion to the (beam area)$^{-1}$.

2. Toroid

a. Centripetal Drift.

The field lines force the e beam to turn the corner, but there is an equivalent Electric field causing a centripetal acceleration $\frac{V^2}{R_{Toroid}}$. This causes an $\frac{E \times B}{B^2}$ drift which must be compensated by a transverse magnetic field, which is exactly the field required to bend the ebeam around the toroid.

b. Temperature:

It is convenient to adjust the Toroid field to get an integer number of gyro orbits, to cancel out

inhomogeneities in the Toroid Field (More resonant optics)

3. Solenoid

Field uniformity and Field line Straightness is crucial to obtain low $T_{e\perp}$. At Fermilab the field lines were mapped with a low velocity ebeam + screen + transit, to align Solenoid coils and make corrections. Fields were mapped with a Hall probe. The coils were designed to ensure that errors were adiabatic to the gyromotion. Typically errors imply field additions to electron temperature < 0.25 eV, except for 1 0.5 m coil which has several percent field error. For large amplitudes, the effective cooling length is reduced by about 5%. Dipole corrections can steer the Field lines and ebeam to proton direction.

4. Collector

Secondary Emission and backscattered electrons are the major source of electron loss. These must be controlled, or the beam fills with electrons bouncing between cathode and collector. These electrons tend to bunch and make the beam noise. They resonate with the ion plasma frequency (see below)

Ideally one would like a suppressor grid as in a pentode. We (P. McIntyre) have achieved this in the following way.

The collector is ~4kV above the cathode voltage. The collector anode is several hundred volts above the cathode so that the ebeam slows down to several hundred volts then is accelerated to the collector.

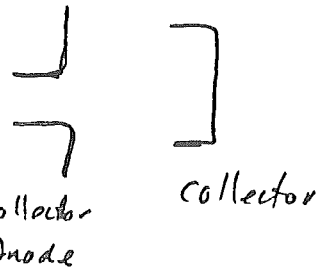

One might expect the e beam to blow up under these conditions, but what is found is that if the collector anode potential region is extended, ions are trapped in this region in a stable manner. The e beam is gas focussed and then accelerated to the collector. e beam losses are $\sim 2 \times 10^{-4}$, and the beam is quiet..

5. Neutralization

In principal, some improvement is possible against space charge effects by neutralizing the e beam. This hope was frustrated by the presence of a two stream drift instability (Rosenbluth) which is accentuated if the potential surfaces surrounding the beam is split (which might allow controlled neutralization). This was abandoned, and the beam is stripped of electrons and ions by an EXB system in the collector Toroid region. This seems to work well, as evidenced by the measurements of e-beam tune shifts of the p beam, and by measured potential shifts of the e beam when e beam current is changed (the cooled proton velocity changes)

Orbit effects of e beam on p beam

1. Toroid has strong dipole filed $\sim 0.7\ B\ R_{Toroid}$

$$\theta = \frac{0.7 \times 0.1T \times .46\,m}{2.14\ Tm} = .015\ rad.$$

Must be corrected by two dipoles at each end to get correct position and angle

2. Coupling – Solenoid + Toroid give tune shift

$$\Delta\nu = \pm \frac{1}{4\pi} \frac{BL}{B\ell} \simeq .02$$

3. e beam space charge tune shift

$$\Delta\nu = \frac{n_e r_p}{2\gamma^3\beta^2} L\beta_L \simeq .01 \text{ for } 5A$$

Quad strengths must be readjusted to maintain stable lattices. If the e beam has non uniform distribution, non linear resonances can be driven (but weakly)

Proton Diagnostics

Position electrodes in Quads and in Cooling region
Wire Scanners to determine injection conditions
Current Monitors to observe beam bunching (and cooling into rf bucket)
Longitudinal High Frequency (~ 500 MHz) current monitor to observe unbunched beam Schottky Signal
Residual Gas Profile Monitors for Horizontal + Vertical

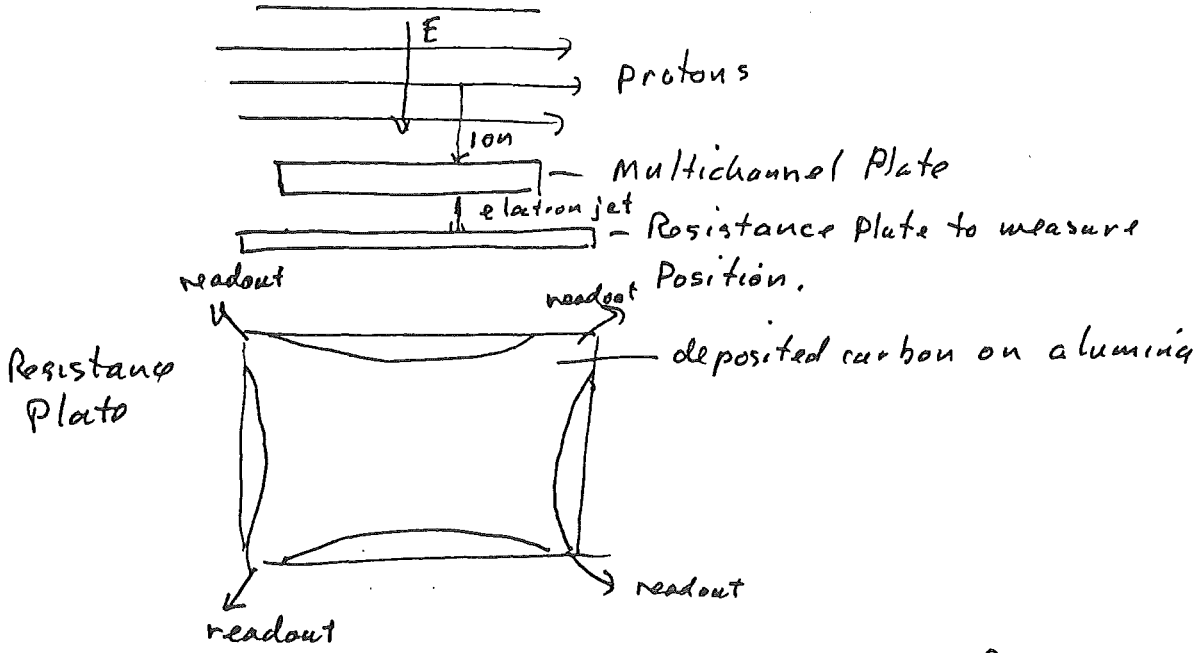

4 current pulses are sampled and digitized for each ion event. 512 such events are taken to form a profile. H_2 gas is puffed to raise pressure to ~ 5×10^{-9} Torr to get rapid profile result. A sequence of 4 profiles can be recorded at specified times

The need for small cross section measurements at medium energies

H.V. von Geramb
Institut für Theoretische Physik
Universität Hamburg

THE NEED FOR SMALL CROSS SECTION MEASUREMENTS AT MEDIUM ENERGIES

H.V. von Geramb *
Theoretische Kernphysik
Universität Hamburg

The experimental and theoretical studies of high momentum components in the nuclear wave functions have opened many new structures in this century. Guided by the famous Rutherford experiment, high energy electron and hadron scattering were instrumental in the discovery that hadrons are built out of quarks and gluons. In recent years classical nuclear physics extended its projectile energies and improved the resolution for complex nuclear studies. Medium energy nuclear physics aims towards new phenomena associated with mesonic degrees of freedom, properties of metastable superhigh dense nuclear matter and many body physics with relativistic energies. It shall ultimately join nuclear and particle physics results in a unified description.

The nuclear physics community has proposed and operates accelerators for electrons, π- and μ-mesons, hadron accelerators for protons and antiprotons. The research topics covered with these facilities are the elastic and inelastic scattering to determine ground state and transition form factors for charge and matter, measurements of nuclear deformations and electromagnetic transition rates, mesonic degrees of freedom and baryon resonances, search of dibaryons.

* Contribution to Electron Cooling workshop in Bad Honnef 27./28.5.1982

Medium energy scattering is thereby guided from the picture that high energy particles ($k>>k_F$) see nucleons in a nucleus as *quasi free* and the total nucleon nucleus interaction is a coherent sum where the elemantary process is driven by the NN scattering amplitude. This idea implies a transition region from the low energy domain where long range correlations dominate and the high energy situation where the impulse approximation (IA) is valid. To get a feel, in Fig. 1 is shown the theoretical total cross section based on IA, here the Kerman, McManus, Thaler (KMT) approach and data for p-^{12}C, ^{16}O. From this figure we may conclude that the IA deteriorates below 5oo MeV and yields an overestimate of 25-3o% around 2oo MeV projectile energy. The depression of the cross section around 2oo MeV reflects the minimum in the NN cross section. As a reminder I show it in Fig. 2 (pp total cross sections).

The deviation of KMT from data is presently understood as many body blocking, Fermi averaging effect in the nuclear medium. It is this effect and the experimental access which makes medium energy scattering an almost ideal laboratory. It may be considered somewhat a misfortune, that the threshold adds new degrees of freedom just in the same energy region but beauty is seldom alone.

Many body theory with its developments as variational or perturbative approaches offer a genuine mean for investigating nuclear interaction. The fictitious infinite translationally invariant system of nucleons is known as nuclear matter. A microscopic calculation of nuclear matter is generally accepted to yield a major achievement as prelude to the systematic (microscopic) evaluations of properties of finite nuclei. Reactions are part of these evaluations.

To speak of scattering or reactions, we speak of mapping of geometric (coordinate space) quantities in nuclei into momentum space. They are manifest in the measurement of angular or momentum transfer distributions.

With very weakly interacting probes (electrons) the first Born approximation with plane waves is sometimes sufficient and in this instand the plane wave Fourier-transformation is the mathematical tool to transform momentum space and coordinate space quantities into each other. This transformation makes it obvious how global features (radius,diffuseness etc.) are related to small momentum transfer. In order to see finer details, we need higher and higher momentum transfers, i.e. high incident momenta. Present electron and hadron experiments with incident momenta of 5oc to 2ooo MeV/c permit to see structures as fine as o.o1 fm (1o millifermi). This is much smaller than the nucleon form factor . In terms of the driving NN potential (which is still assumed to be a valid tool to describe NN and therefrom derived N-nucleus interactions) the OPE (one pion exchange) contribution gives a good description only at very large distances (r>2fm). At shorter distances heavier meson (or multiple mesons) exchange is important. In the last two decades many purely phenomenological studies of nuclear forces become known. Today, a hybride view is taken. The Paris-group developes a meson theory of nuclear forces that combines the best features of the field theoretical and OBE calculations. The result is a purely theoretical NN potential for r>o.8 fm and a phenomenological finite potential for even shorter ranges (Phys.Rev. C21 (198o) 861). This potential reproduces well the NN data up to 35o MeV (lab) contains central, tensor, spin-orbit and a squared spin-orbit terms in agreement with general invariant-principles. The weak but important energy dependence is incorporated with momentum dependent terms in the central potential.

$$V(r,p^2) = V_o(r,p^2)\Omega_o + V_1(r,p^2)\Omega_1$$

$$+ V_{LS}(r)\Omega_{LS} + V_T(r)\Omega_T + V_{So2}(r)\Omega_{So2}$$

$$\Omega_o = \frac{1-\vec{\sigma}_1\cdot\vec{\sigma}_2}{4}$$

$$\Omega_1 = \frac{3+\vec{\sigma}_1\cdot\vec{\sigma}_2}{4}$$

$$\Omega_{LS} = \vec{L}\cdot\vec{S}$$

$$\Omega_T = 3\frac{(r\cdot\sigma_1)(r\cdot\sigma_2)}{r^2} - \sigma_1\cdot\sigma_2$$

$$\Omega_{SO2} = \frac{1}{2}\left[(\vec{\sigma}_1\cdot\vec{L})(\vec{\sigma}_2\cdot\vec{L}) + (\vec{\sigma}_2\cdot\vec{L})(\vec{\sigma}_1\cdot\vec{L})\right]$$

$$V_x(r,p^2) = V^a(r) + \left(\frac{p^2}{m}\right) V^b(r) + V^b(r)\left(\frac{p^2}{m}\right)$$

$$p^2 = -\hbar^2\left[\frac{1}{r}\frac{d^2}{dr^2}\,r - \frac{\vec{L}^2}{r^2}\right]$$

This potential cannot be used directly in structure and reactions due to its strong short range behaviour but a reaction typ G-matrix does. Low density expansion of nuclear matter suggest it as effective interaction between incident projectile and target nucleons. The reaction matrix contains several important features:

- it is energy dependent
- complex
- density dependent
- it may be computed with techniques of infinite nuclear matter
- allows a full microscopic and selfconsistent treatment of structure and reactions

- permits to compare results from other sources ($\pi, \mu, e^{\pm}$ scattering)
- may be extended to antiproton scattering.

In Fig. 3 to 6 I give an example of the density dependence (density and fermi momentum is related by $\rho = \frac{2}{3\pi^2} k_F^3$) k_F = o.1/o.5/o.9/1.3 fm^{-1} at 16o and 4oo MeV. Figs. 3 and 5 show the radial dependence of the singlet even reaction matrix. Figs. 4 and 6 show its Fourier transformed $0 < k < 5$ fm^{-1}. The other components are shown in Figs. 7 to 1o. Medium energy physics with projectile energies up to 1 GeV are ideal means to investigate the momentum transfer region of 2-6 fm^{-1} (4oo - 12oo MeV/c). For the two nucleon potentials it means to investigate the radial region o.8 - 1.5 fm. Herewith we achieve access to baryon resonances on and off the energy shell.
Experimentally and theoretically we approach this field from various directions. A great deal is known from meson-nucleon and meson- nuclear scattering about the on-shell formation and decay of baryons. At least a semiquantitative understanding of the underlying dynamics can be set forward. Lower energy phenomena deal with the same isobars but as virtual constituents. I recall the activities centered around possible pion-condensation studies just above nuclear saturation.
Enhancement and quenching in magnet transitions are expected due to the strong $(\vec{\sigma}\cdot\vec{\sigma})(\vec{\tau}\cdot\vec{\tau})$ force in the NN→NΔ. Compare the coupling constants NN -> NN: $f^2/4\pi$ = o.o8

$$NN \rightarrow N\Delta: \frac{(ff^*)}{4\pi} \sim o.16$$

It is the central point of this contribution to make clear that all this effects in whatever way we may look at are associated with differential cross sections of typically μbarn/sr down to a few nbarn/sr. We should not exclude pbarn/sr.

Finally, let me give you a typical example, which has been done in collaboration with M. Coz, H.O. Meyer, J.R. Hall, W.W. Jacobs and P. Schwandt:

Cross section and analyzing power angular distributions for proton elastic scattering from ^{12}C have been measured recently at the Indiana University Cyclotron Facility. The data with 122, 160 and 200 MeV polarized proton beams cover an angular region from about 5^{o} to 160^{o} in the lab and constitue an experimental study of momentum transfers up to 6 fm^{-1}. It was natural to look for an optical model potential (OMP) which reproduced these data.

With projectile energies above the pion threshold, it is known that the nucleus should not be considered only as an assembly of nucleons interacting through a two-body force. It is certain that baryon resonances as well as mesons exist in nuclei in addition to the nucleons. In particular one cannot understand the large momentum properties of any nuclear state without introducing mesonic degrees of freedom. This point is equivalent to proclaim the failure of the phenomenological or microscopic optical potential which *knows only of nucleons*.

We approach the analysis by a synthesis of two parallel fields. The first is concerned with a full microscopic treatment of the optical model potential within the nuclear matter approach. It is based on a free NN potential (Hamada-Johnston, Paris) which reproduces practically all NN data below 150 MeV in the two nucleon centre of mass system. This is the subpion threshold region. The second is the explicit incorporation of N^{*} + nucleus doorway states, an approach initiated by Kisslinger. He uses a doorway isobar channel where a *created pion* and a nucleon form a N^{*} baryon, that in particular may be a $\Delta(1236)$. For the purpose of elastic proton scattering we treat the nucleus as an assembly of nucleons which has a sizeable coupling to N^{*} intermediate states. Such a synthesis has been followed by Green and others in generating isobar configurations in nucleon-nucleon scattering analysis. The most reliable way to take this into account is with coupled equations. Alternatively, a corrected effective nucleon-nucleon operator may be constructed which would account for these additional mesonic currents

We follow the coupled channel approach. The first channel labelled with the subscript zero consists of the projectile and the target nucleons in its ground state. The associated channel Hamiltonian contains the average interaction as we know it from the microscopic or the phenomenological optical potentials. The second channel distinguishes a quasi-bound particle composed of a nucleon and a pion in a $J^{\pi} = 3/2^{+}$ state, a mass equal to 1.15 the nucleon rest mass, and the target nucleus in a low excited state. The choice of this second channel reflects the dominance of the J = 3/2 pion-nucleon correlation.

As a consequence the target is excited into a non normal parity state $o^{-}(1^{+},2^{-},3^{+}..)$. The second channel has a Hamiltonian containing the average interaction between the two constituents.

The coupled equations for the two channel situation read

$$
\begin{aligned}
E u_o - (T_o + V_{oo}) u_o &= V_{o1} u_1 \\
(E+Q) u_1 - (T_1 + V_{11}) u_1 &= V_{1o} u_o \, .
\end{aligned}
\qquad (1)
$$

The value for Q is taken to be -14o MeV. This is in the spirit of the weakly bound particle model which has its origin in the Born Oppenheimer approximation in the original Butler-Peierls stripping model and equal the pion production threshold.

We treated the coupling potentials V_{o1}, V_{1o} and the diagonal potential V_{11} phenomenologically. They were described by Woods-Saxon form factors with a geometry typical for ^{12}C.

However, the phenomenological treatment may be replaced by a microscopic one. In its simplest form, a folding model procedure may be based on the transition potential N + N -> N + Δ of Sugawara and v. Hippel.

Within this model we have performed a numerical analysis of 122, 160 and 200 MeV elastic proton scattering data from ^{12}C. The results for the differential cross sections are shown in Fig. 11 and polarization results are displayed in Fig.12. In these figures the dashed lines are obtained by dropping the effects of the mesonic coupling; they represent standard optical model analyses. The solid lines were obtained with the fully coupled equations, and beyond any doubt, they significantly improve the description of the experiment, particularly at large momentum transfer, without offsetting the previously obtained good agreement at the small scattering angles.

Concerning the experimental future we wish to make two remarks. The above analysis for the available data is limited to a threshold region where the mesonic effects are only marginal. However, we expect a severe enhancement of the intermediate bound state formation, due to the unique pion-nucleon correlations manifest in the Δ(1236) resonance, when the proton energy increasesabove 250 MeV. The experimental verification of this supposition must receive high priority. Since these particular mesonic effects are essentially localized beyond 90°, complete measurements should be made which go as close as possible to 180°. The other remark concerns the possible effects within the present approach for reactions other than elastic scattering. Since low energy pion-

production and absorption is dominated by the intermediate Δ formation, an extended coupled equation system should explain (p,π), (π,p) data. With minor modifications our approach is also applicable for inelastic transitions, where charge exchange and transitions to non-normal parity states are privileged because of the spin-isospin character of the transition potential.

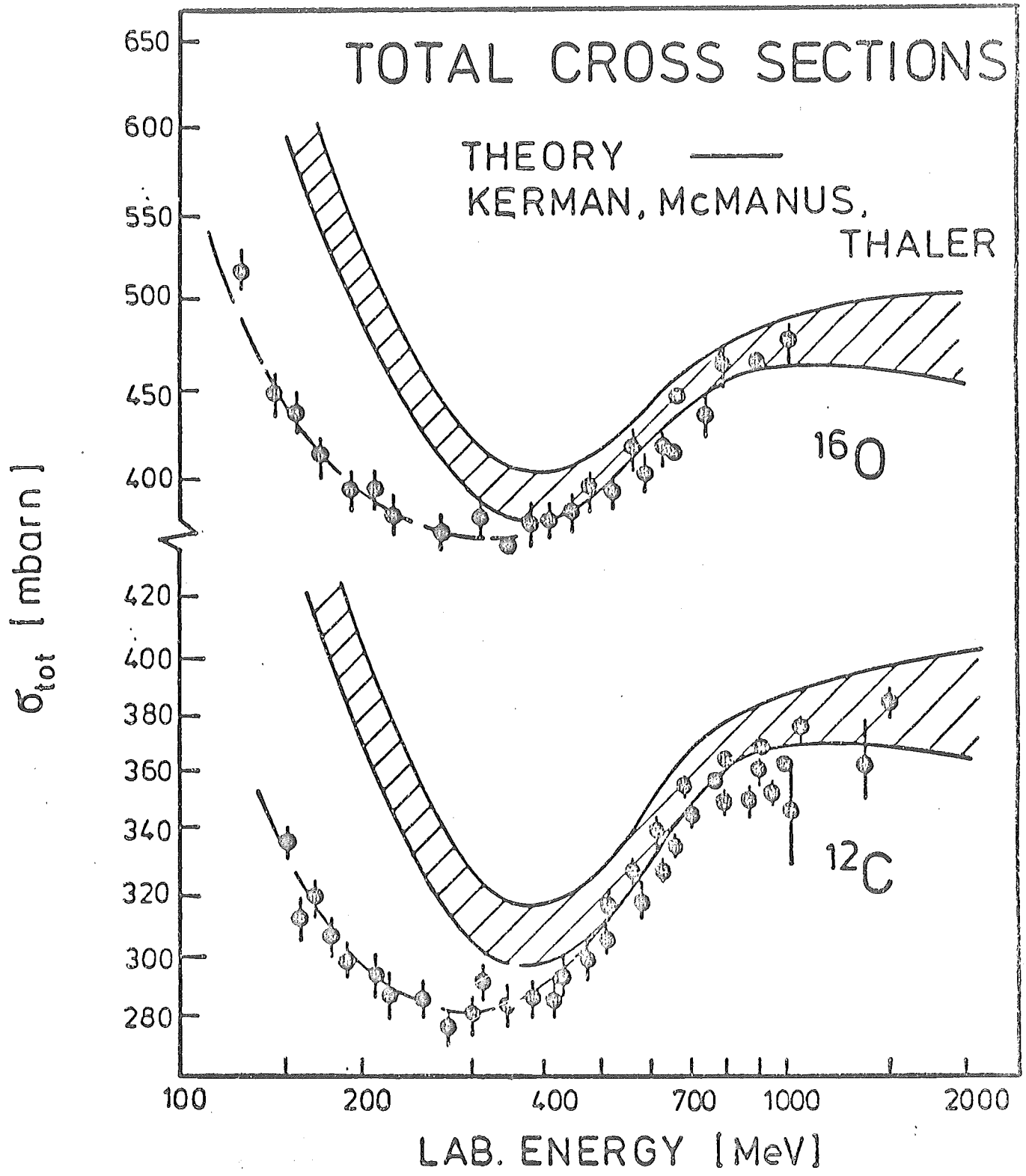
TOTAL CROSS SECTIONS
THEORY
KERMAN, McMANUS,
THALER
^{16}O
^{12}C
σ_{tot} [mbarn]
650
600
550
500
450
400
420
400
380
360
340
320
300
280
100
200
400
700
1000
2000
LAB. ENERGY [MeV]

Fig. 1

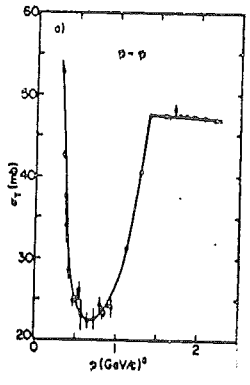

Fig. 2

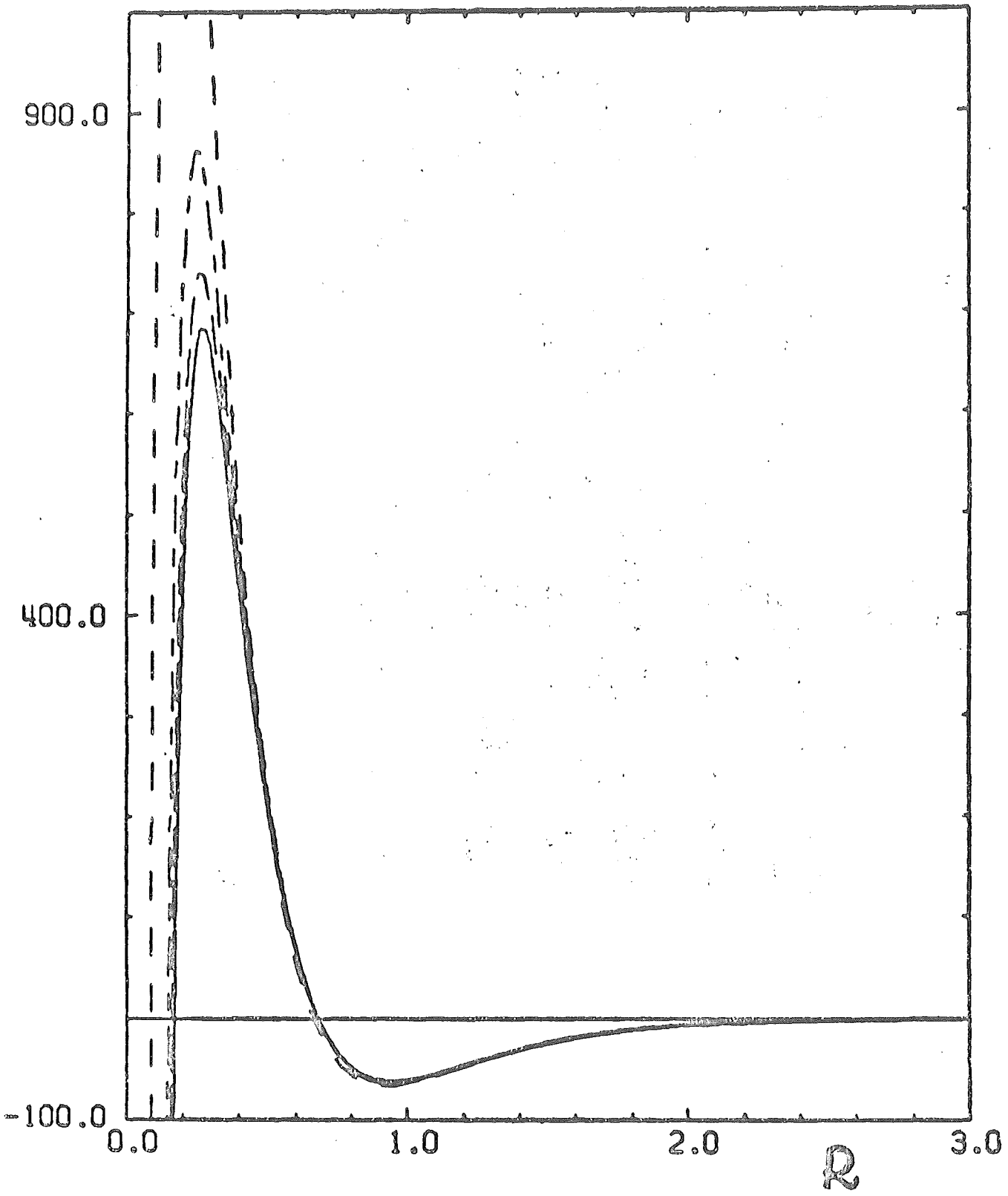

CENTRAL SINGLET INTERACTION. T = 1. REAL. ELAB = 160 MEV. P.

Fig. 3

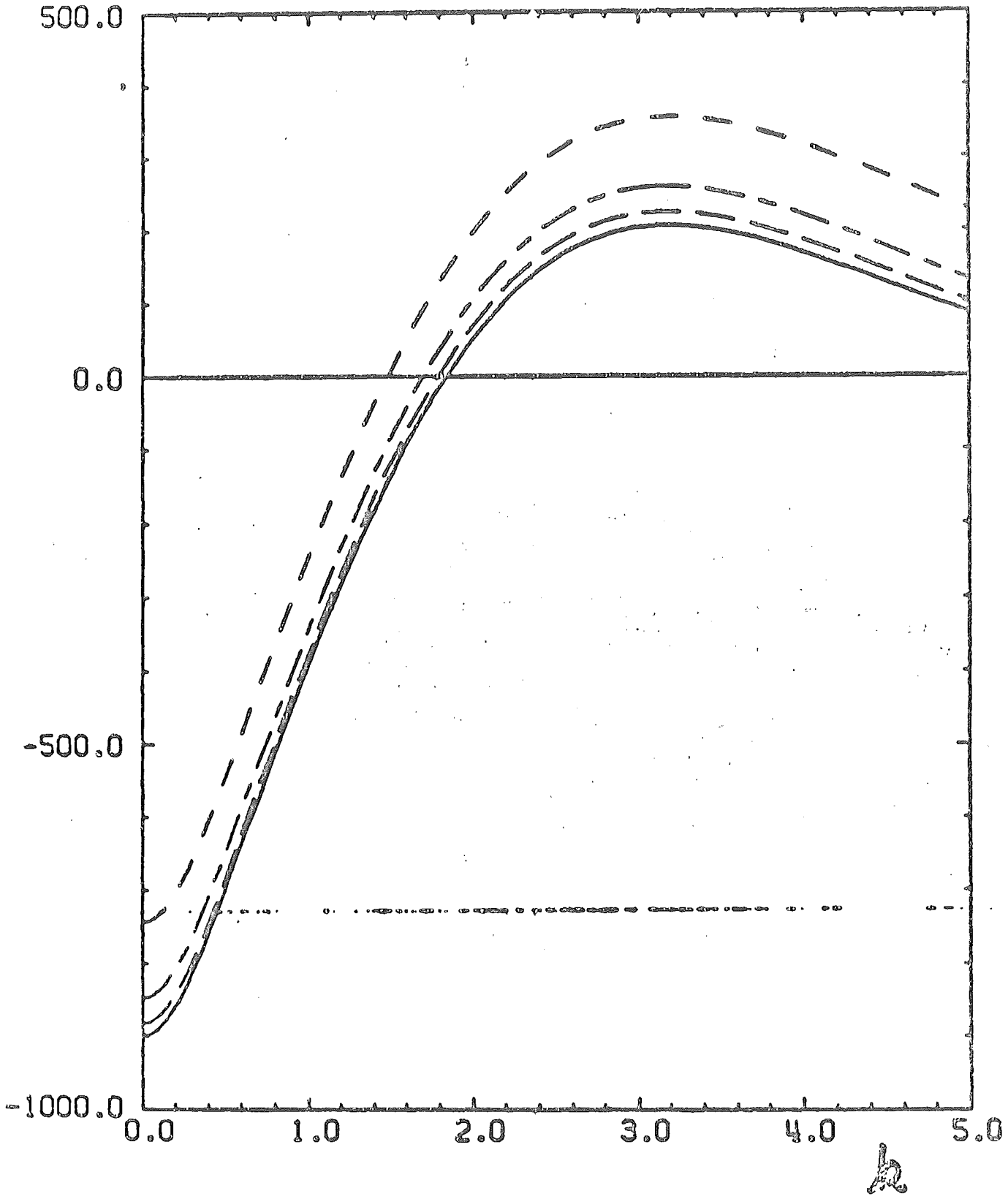

CENTRAL SINGLET INTERACTION. T = 1. REAL. ELAB = 160 MEV. P.

Fig. 4

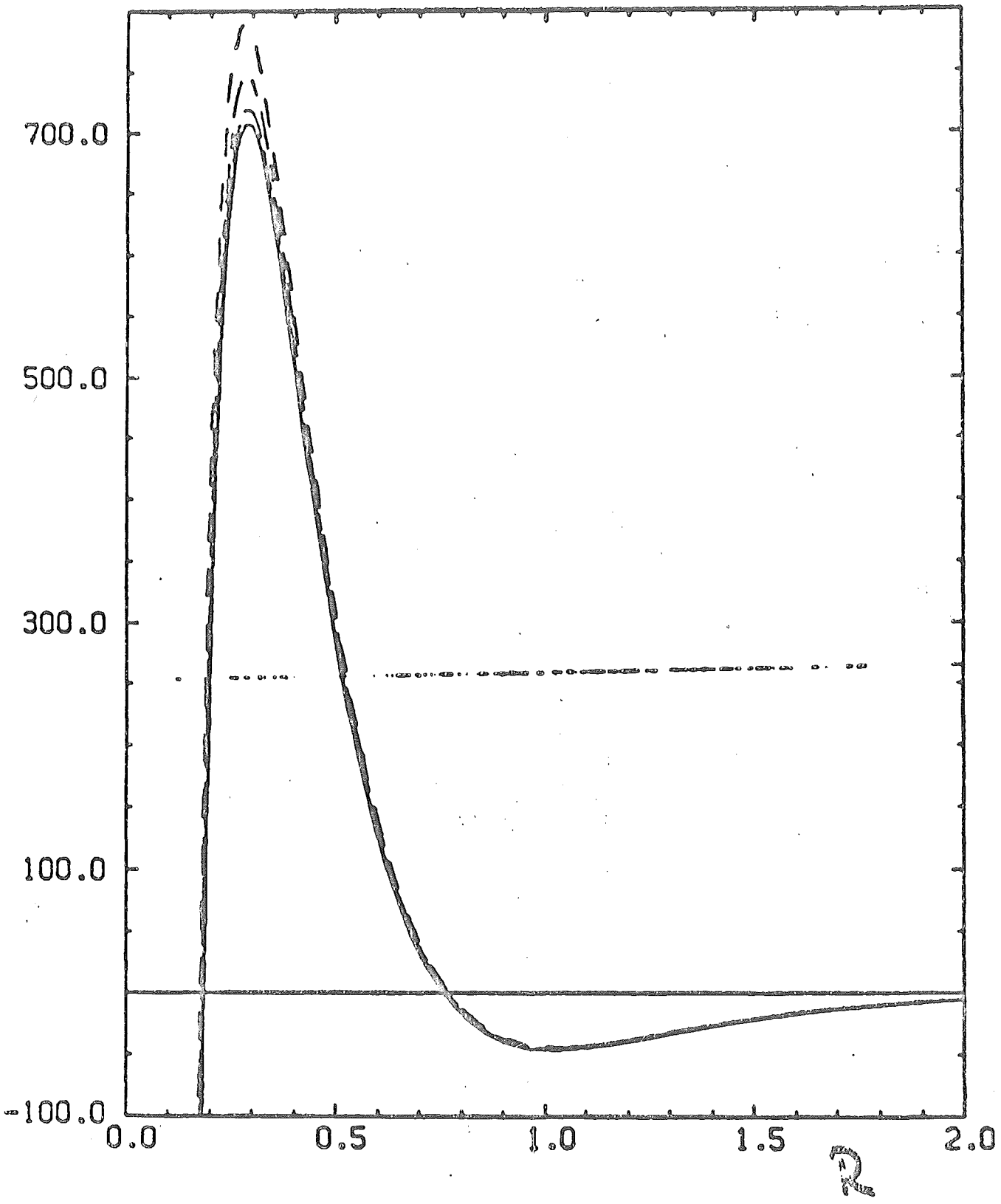

CENTRAL SINGLET INTERACTION. T = 1. REAL. ELAB = 400 MEV. P.

Fig. 5

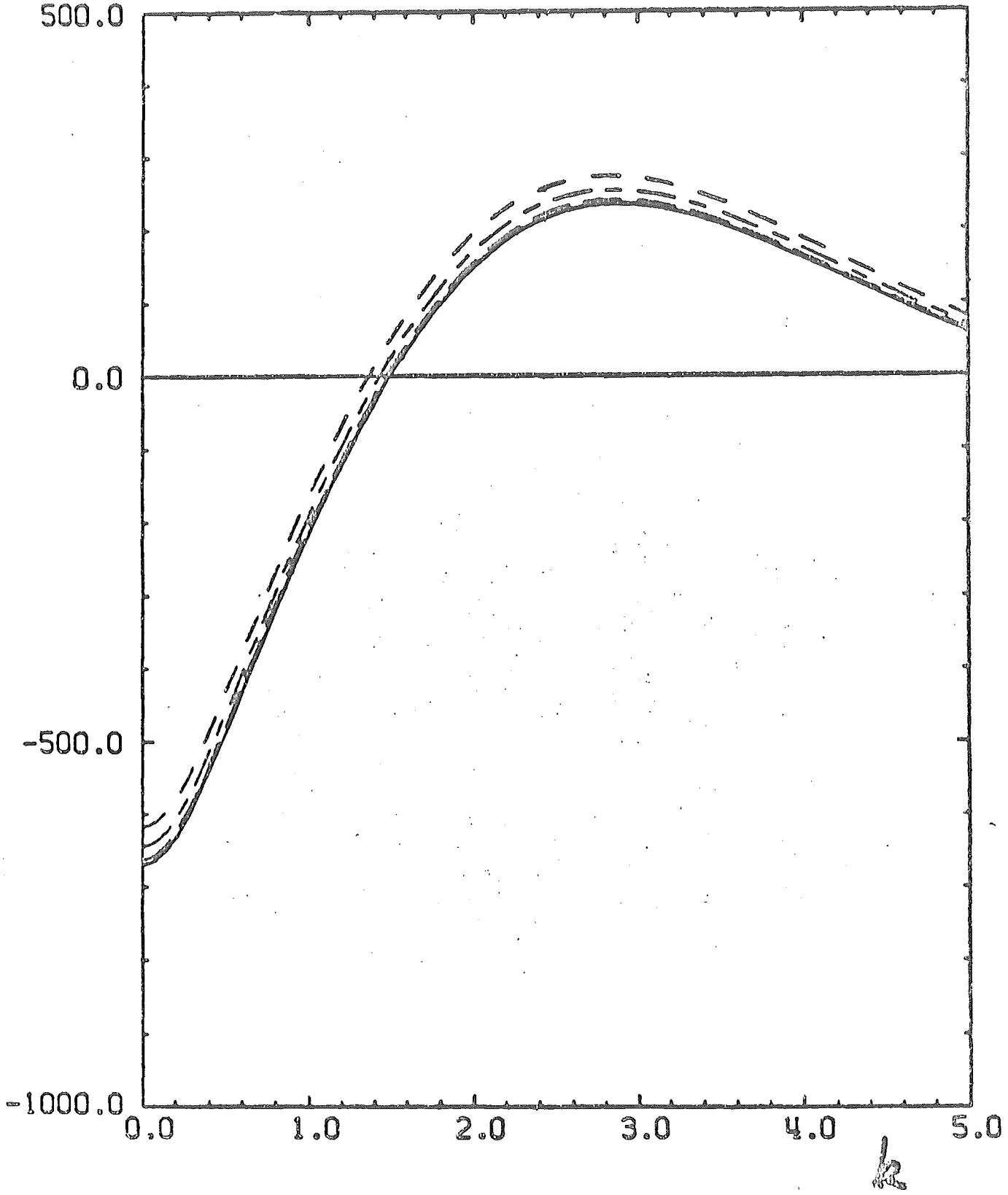

CENTRAL SINGLET INTERACTION. T = 1. REAL. ELAB = 400 MEV. P.

Fig. 6

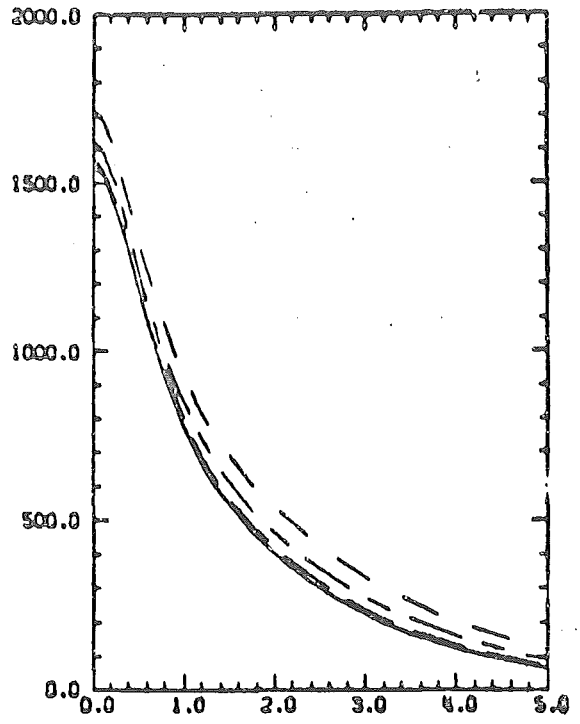

CENTRAL S = 0. T = 0. REAL. 400 KEV. P4

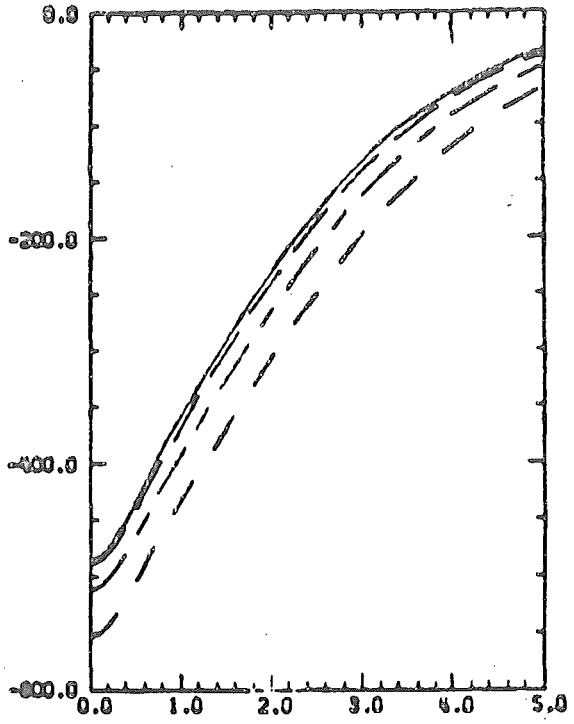

CENTRAL S = 0. T = 0. IMAG. 400 KEV. P4

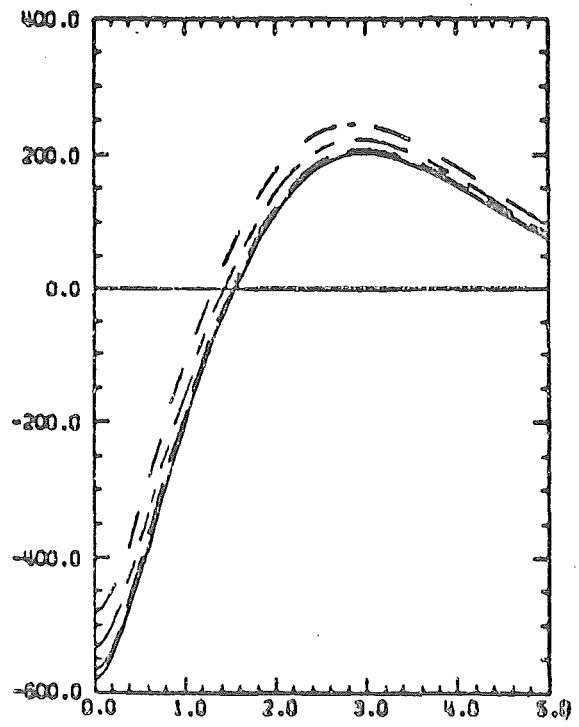

CENTRAL S = 1. T = 0. REAL. 400 KEV. P4

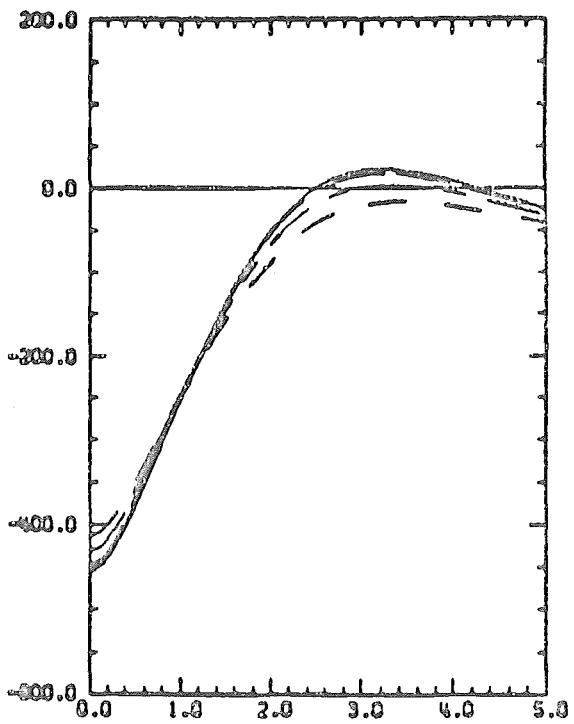

CENTRAL S = 1. T = 0. IMAG. 400 KEV. P4

Fig. 7

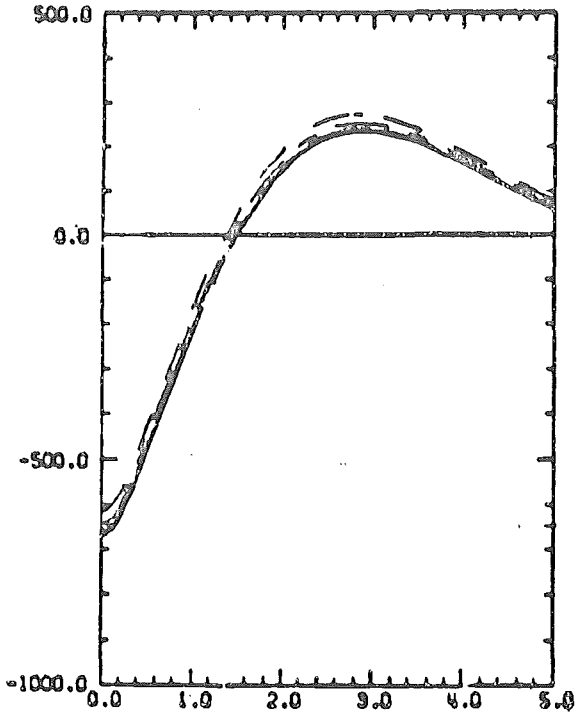

CENTRAL S = 0. T = 1. REAL. 400 KEV. PU

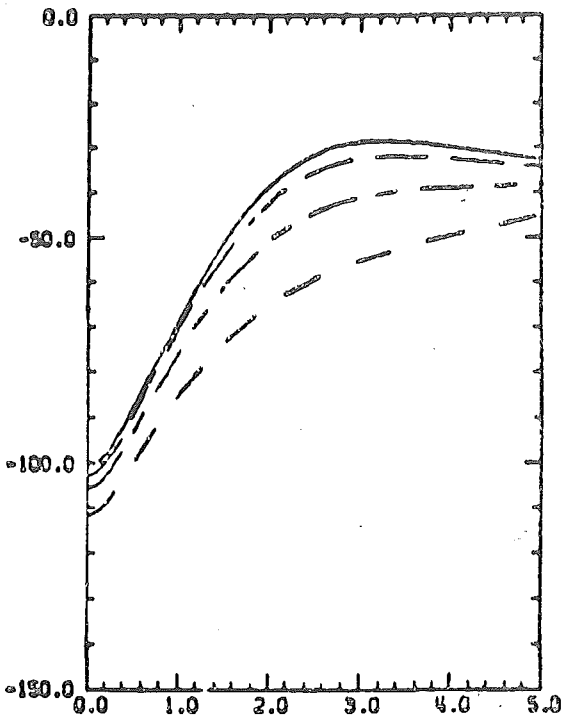

CENTRAL S = 0. T = 1. IMAG. 400 KEV. PU

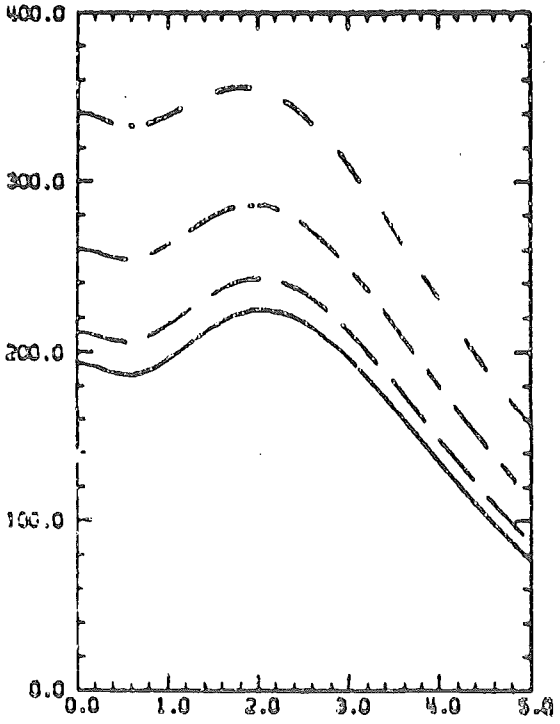

CENTRAL S = 1. T = 1. REAL. 400 KEV. PU

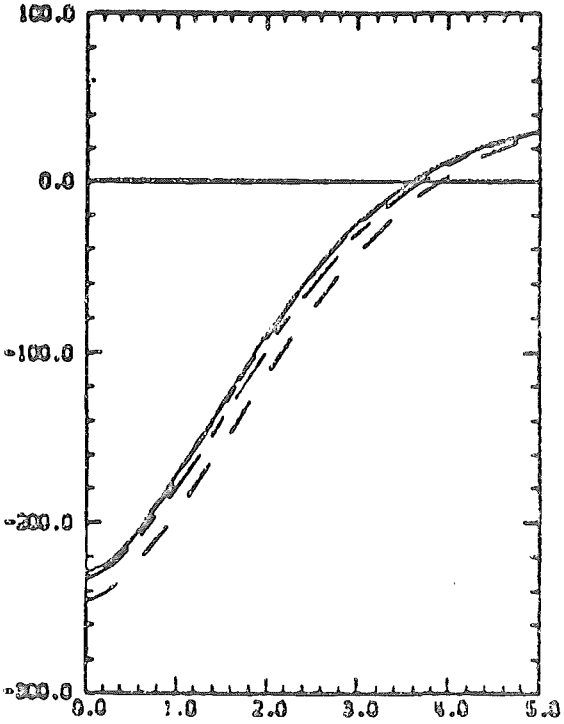

CENTRAL S = 1. T = 1. IMAG. 400 KEV. PU

Fig. 8

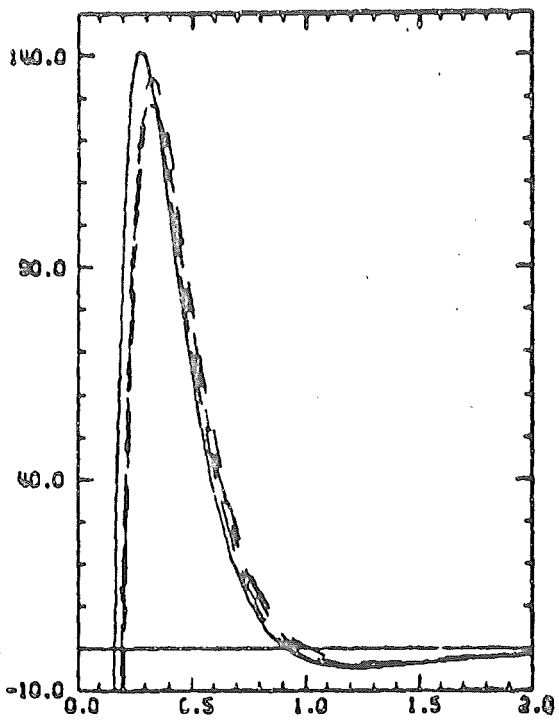

L-S. Y = 0. REAL. 400 KEV. PW

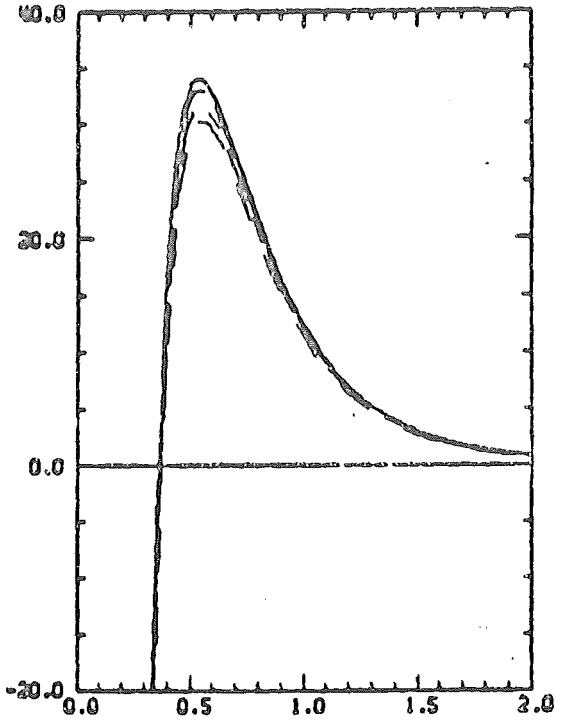

L-S. Y = 0. IMAG. 400 KEV. PW

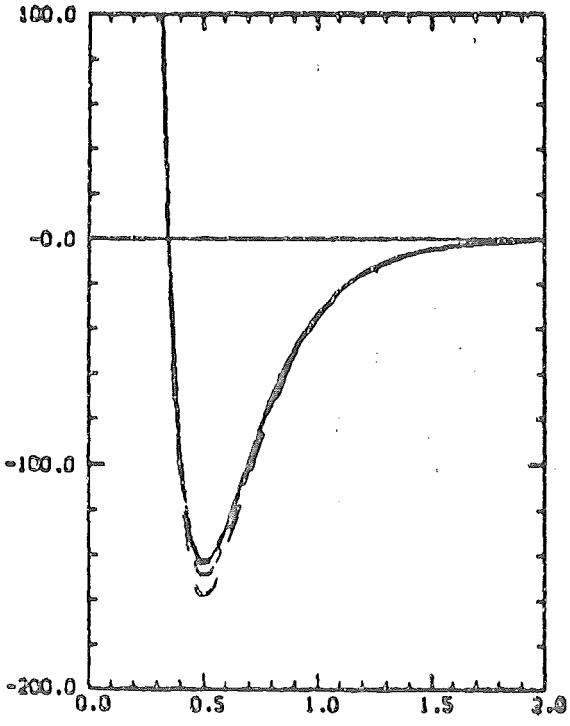

L-S. Y = 1. REAL. 400 KEV. PW

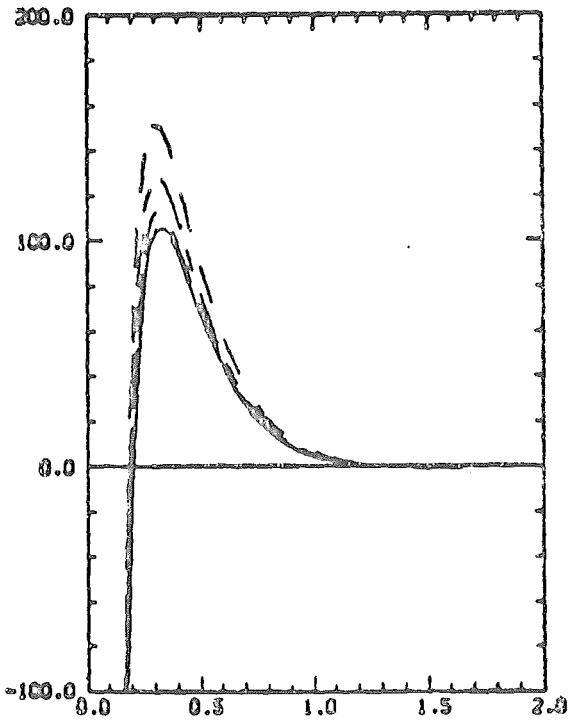

L-S. Y = 1. IMAG. 400 KEV. PW

Fig. 9

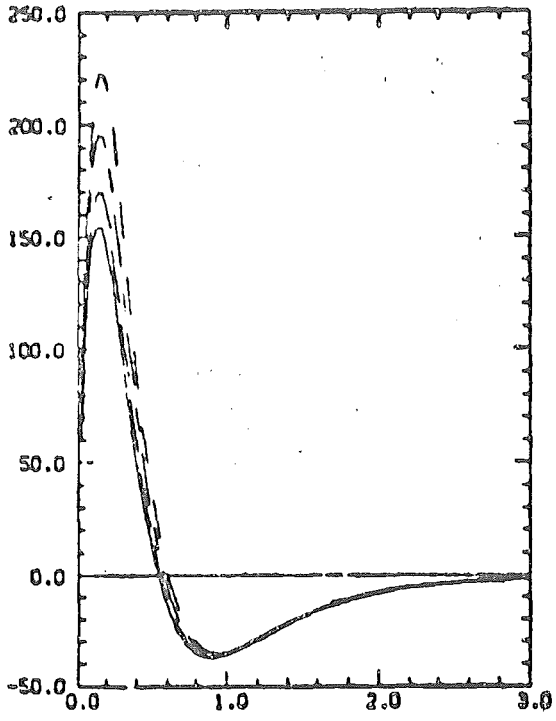

TENSOR. T = 0. REAL. 400 MEV. PN

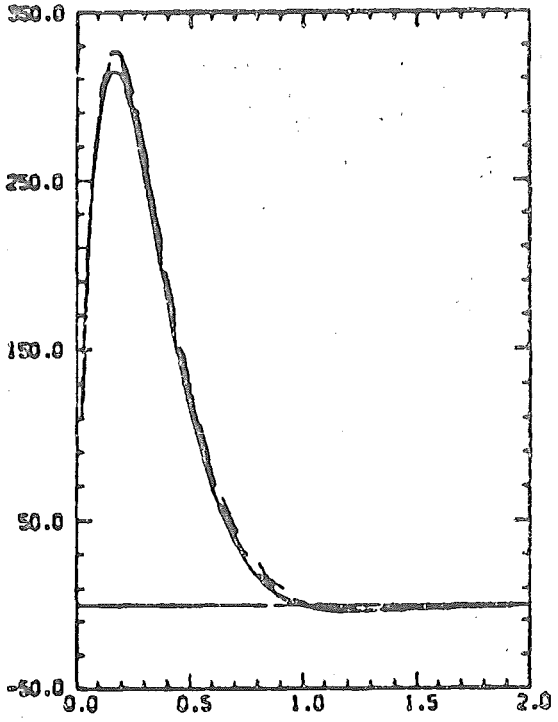

TENSOR. T = 0. IMAG. 400 MEV. PN

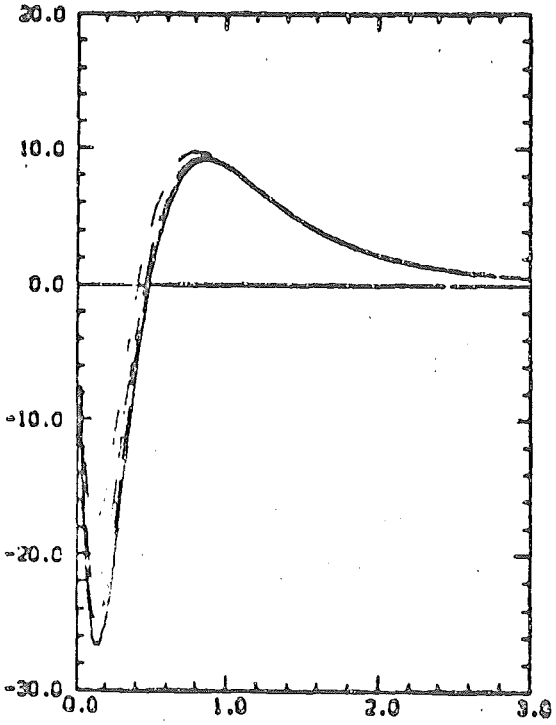

TENSOR. T = 1. REAL. 400 MEV. PN

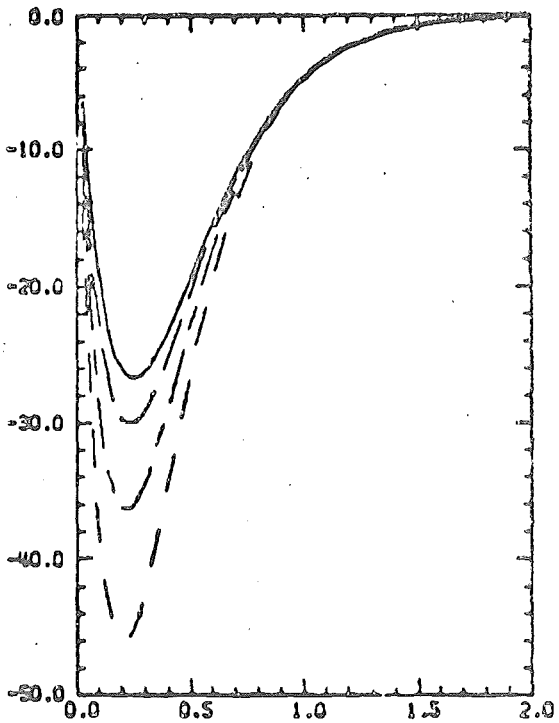

TENSOR. T = 1. IMAG. 400 MEV. PN

Fig. 10

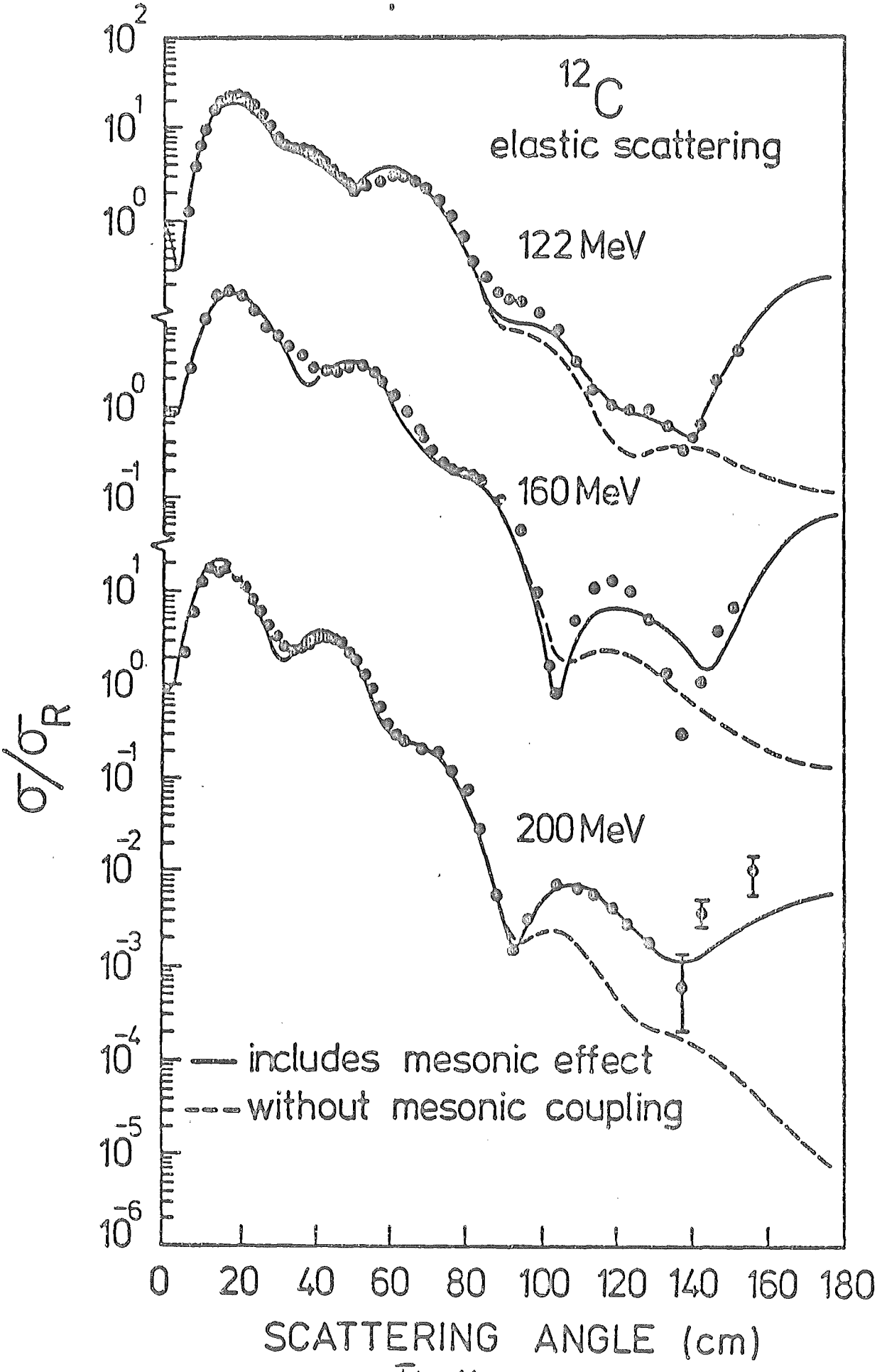
^{12}C
elastic scattering
122 MeV
160 MeV
200 MeV
— includes mesonic effect
--- without mesonic coupling
σ/σ_R
10^{2}
10^{1}
10^{0}
10^{0}
10^{-1}
10^{1}
10^{0}
10^{-1}
10^{-2}
10^{-3}
10^{-4}
10^{-5}
10^{-6}
0 20 40 60 80 100 120 140 160 180
SCATTERING ANGLE (cm)

Fig. 11

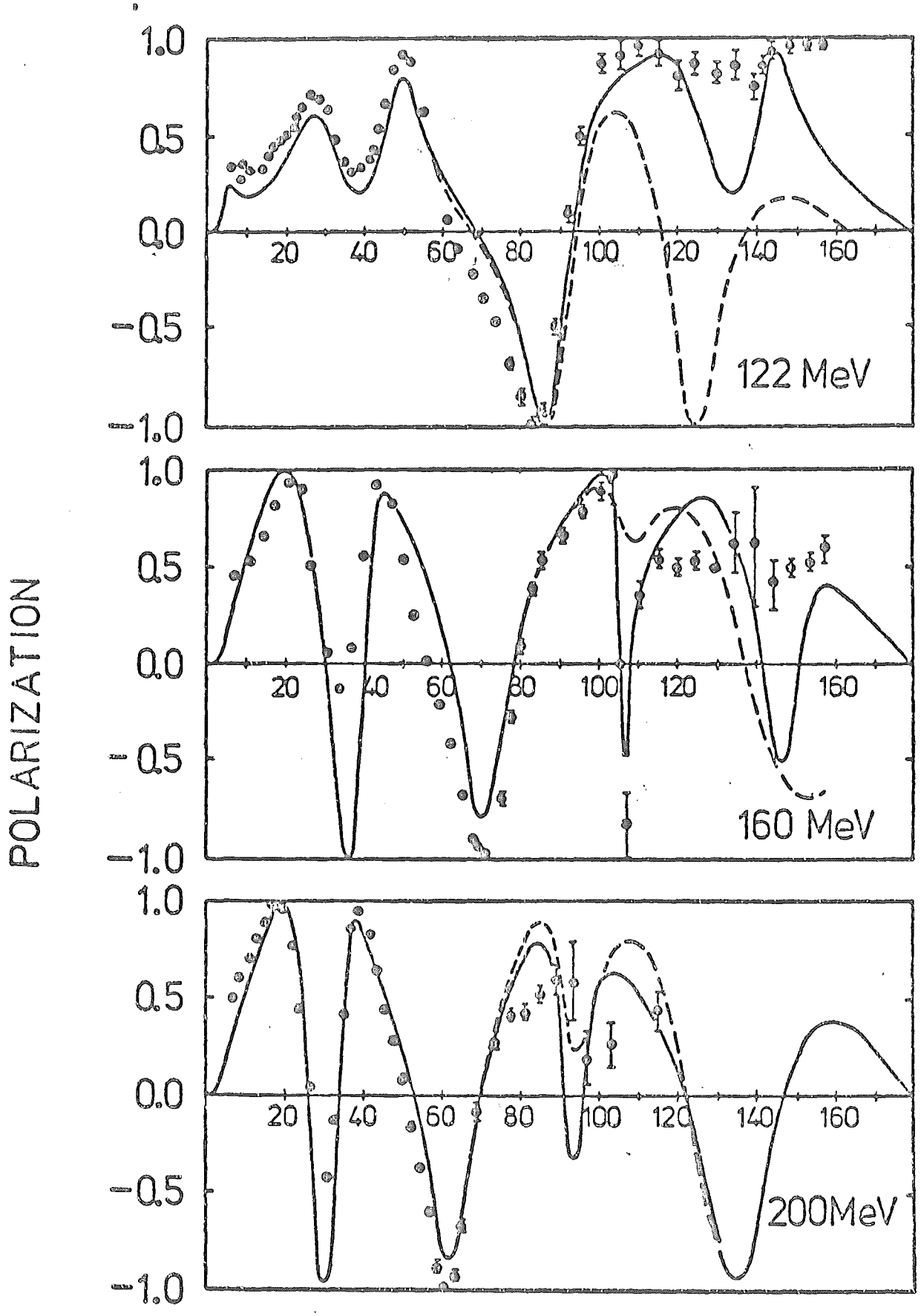
POLARIZATION
1.0
0.5
0.0
-0.5
-1.0
20
40
60
80
100
120
140
160
122 MeV
160 MeV
200MeV

Fig 12

Indiana storage ring with electron-cooling

R.E. Pollock
Indiana University Cyclotron Facility
Bloomington, Indiana

First talk

Research at IUCF

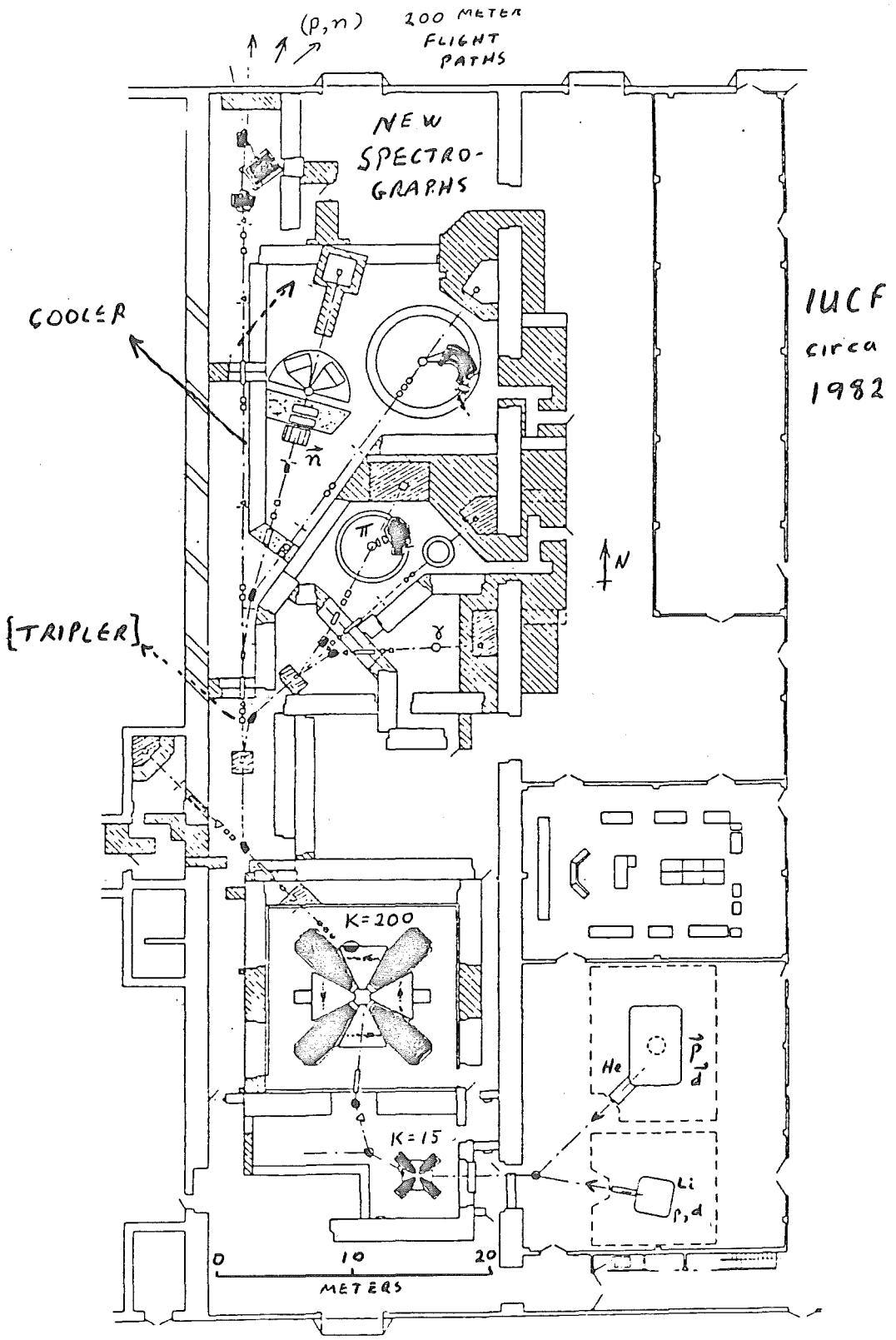

Fig.III-1: IUCF 1981 floor plan.

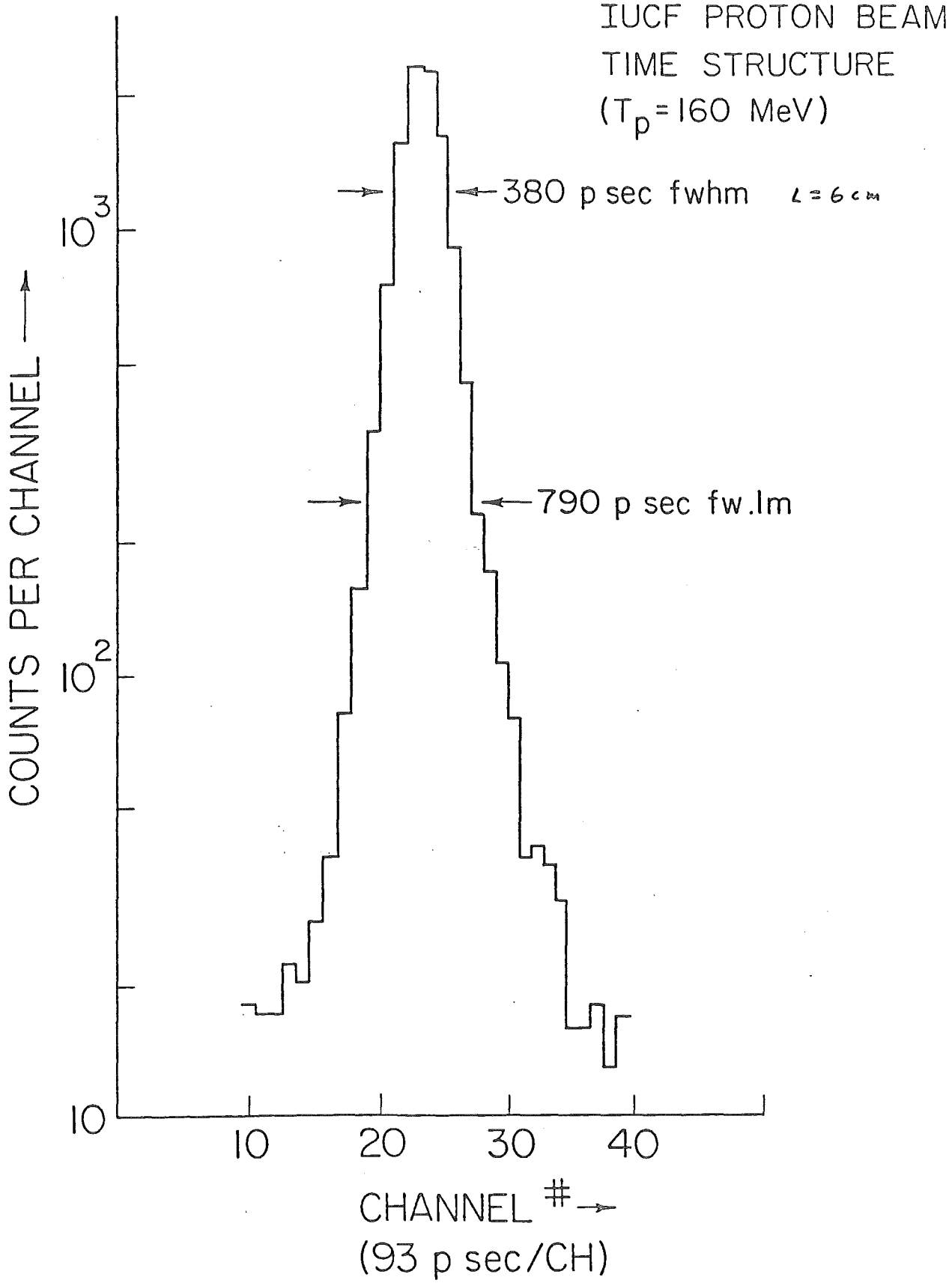
IUCF PROTON BEAM
TIME STRUCTURE
(T_p = 160 MeV)
380 p sec fwhm
L = 6 cm
790 p sec fw.lm
COUNTS PER CHANNEL
10^3
10^2
10
10
20
30
40
CHANNEL #
(93 p sec/CH)

IUCF 459

SUMMATION 4691 4941 = 115A2R

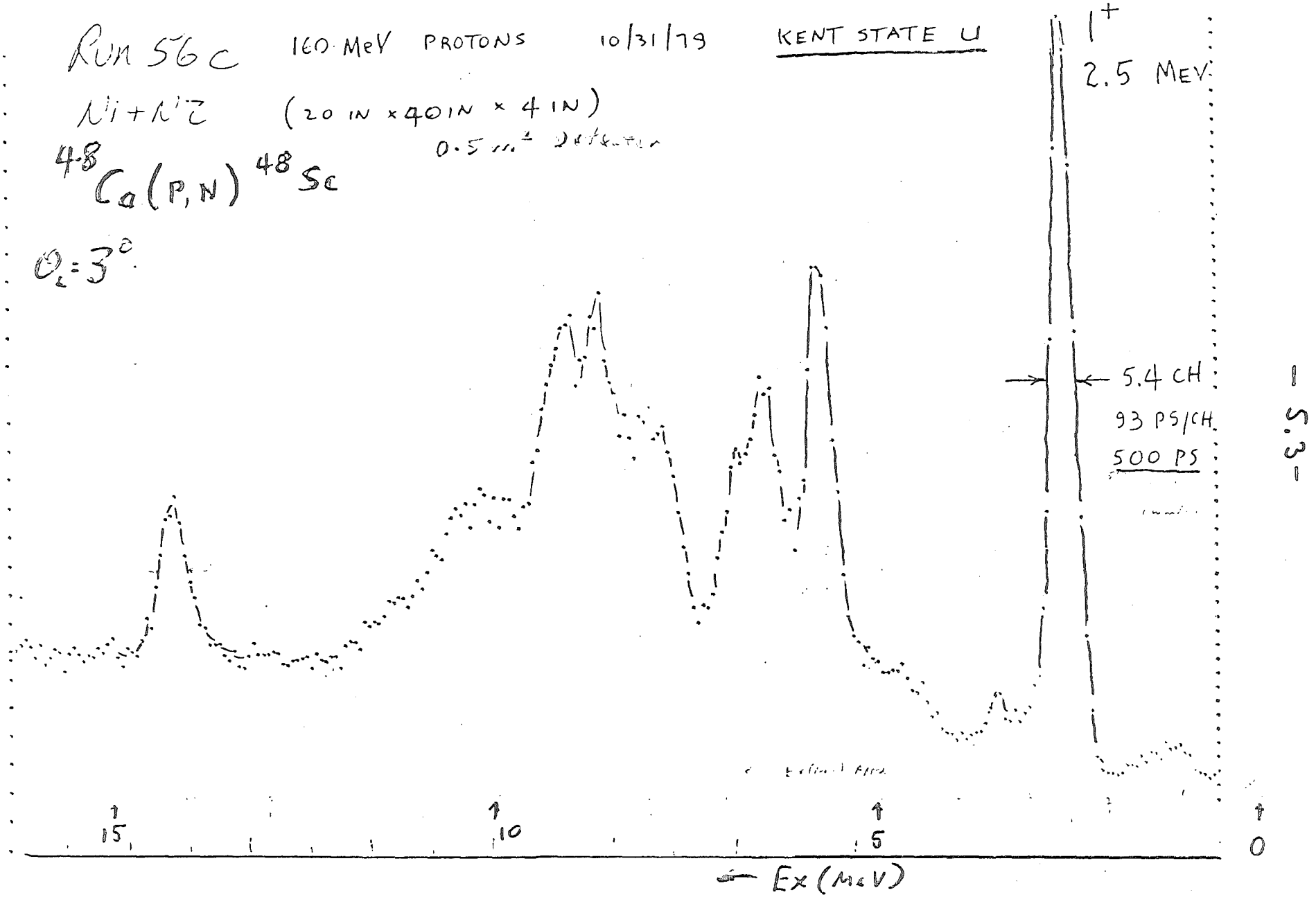

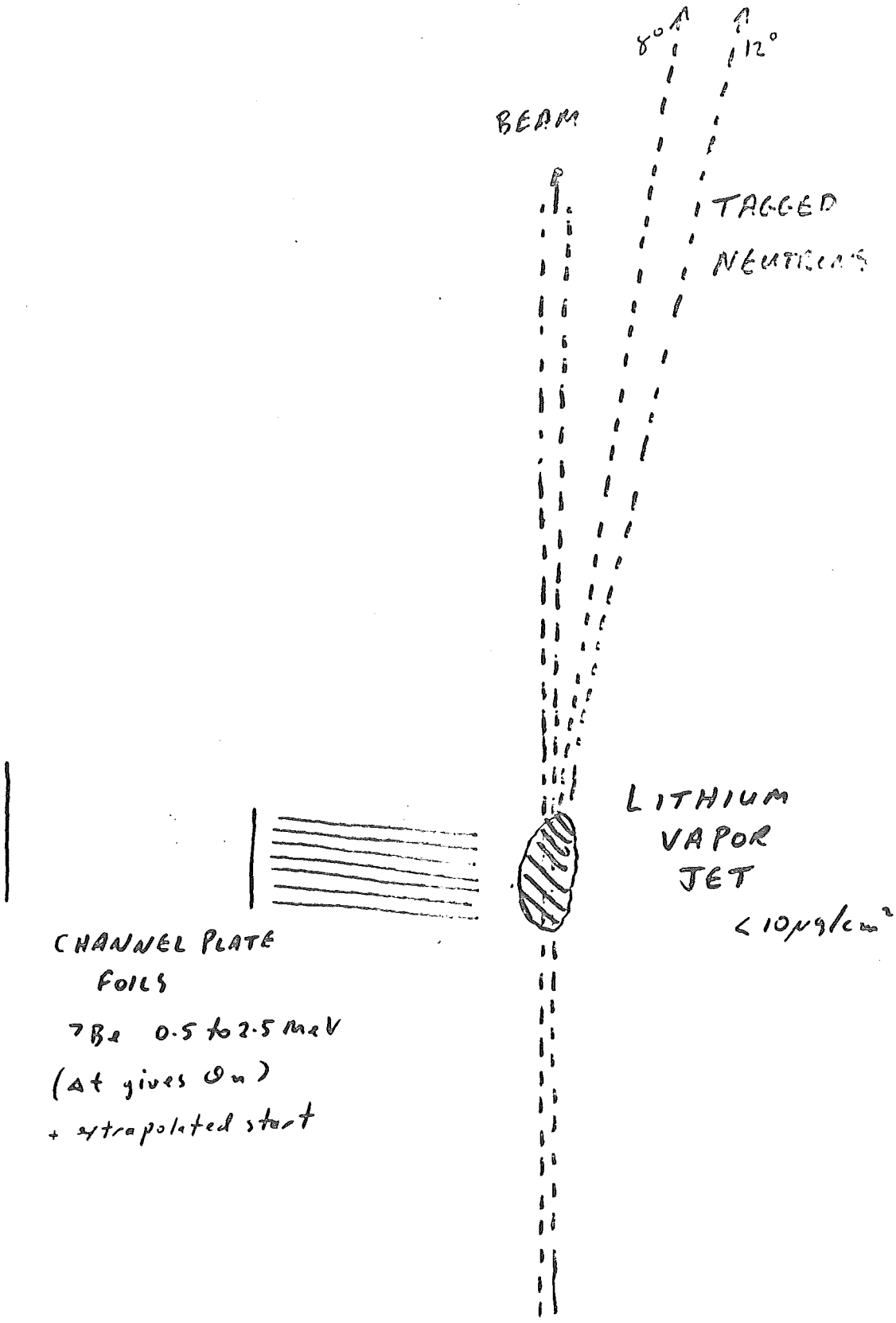
8°
12°
BEAM
TAGGED
NEUTRONS
LITHIUM
VAPOR
JET
< 10 μg/cm²
CHANNEL PLATE
FOILS
⁷Be 0.5 to 2.5 MeV
(Δt gives Θn)
+ extrapolated start

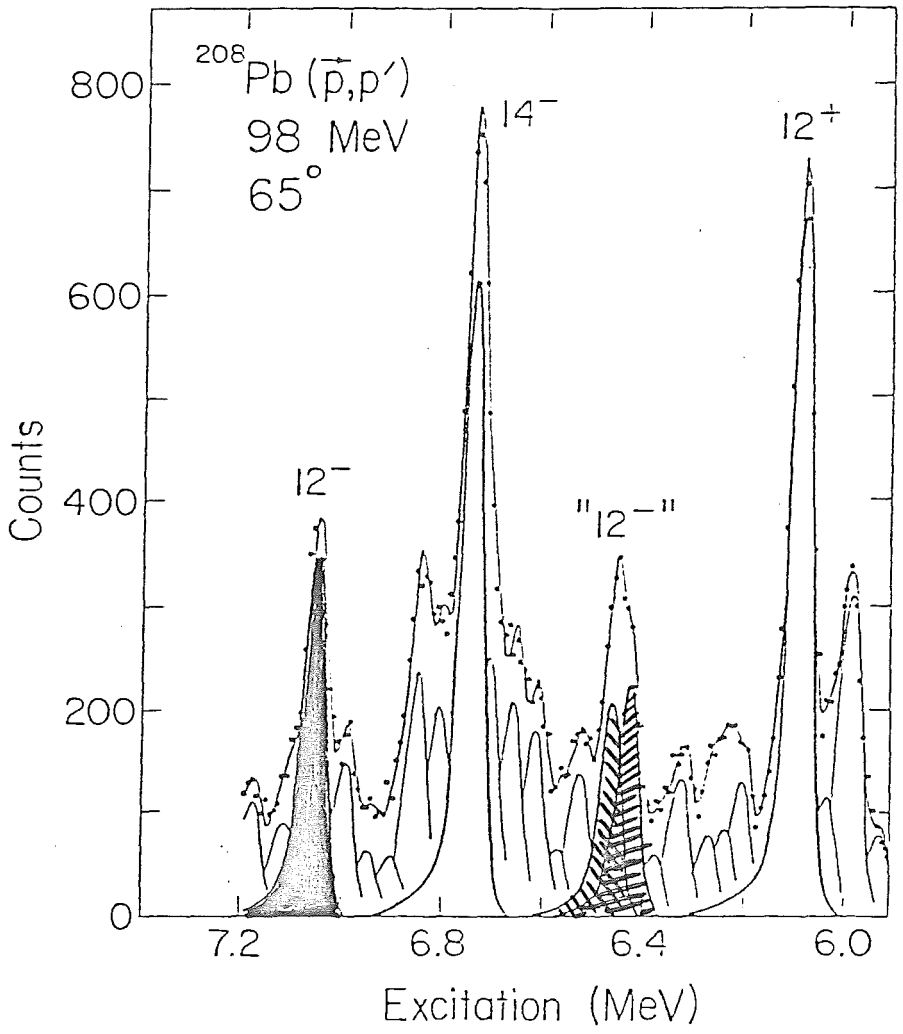

Fig. IIB-6. ^{208}Pb(p,p') at higher resolution, showing that the lower 12^- excitation was not resolved from a neighboring line in the 135-MeV measurements.

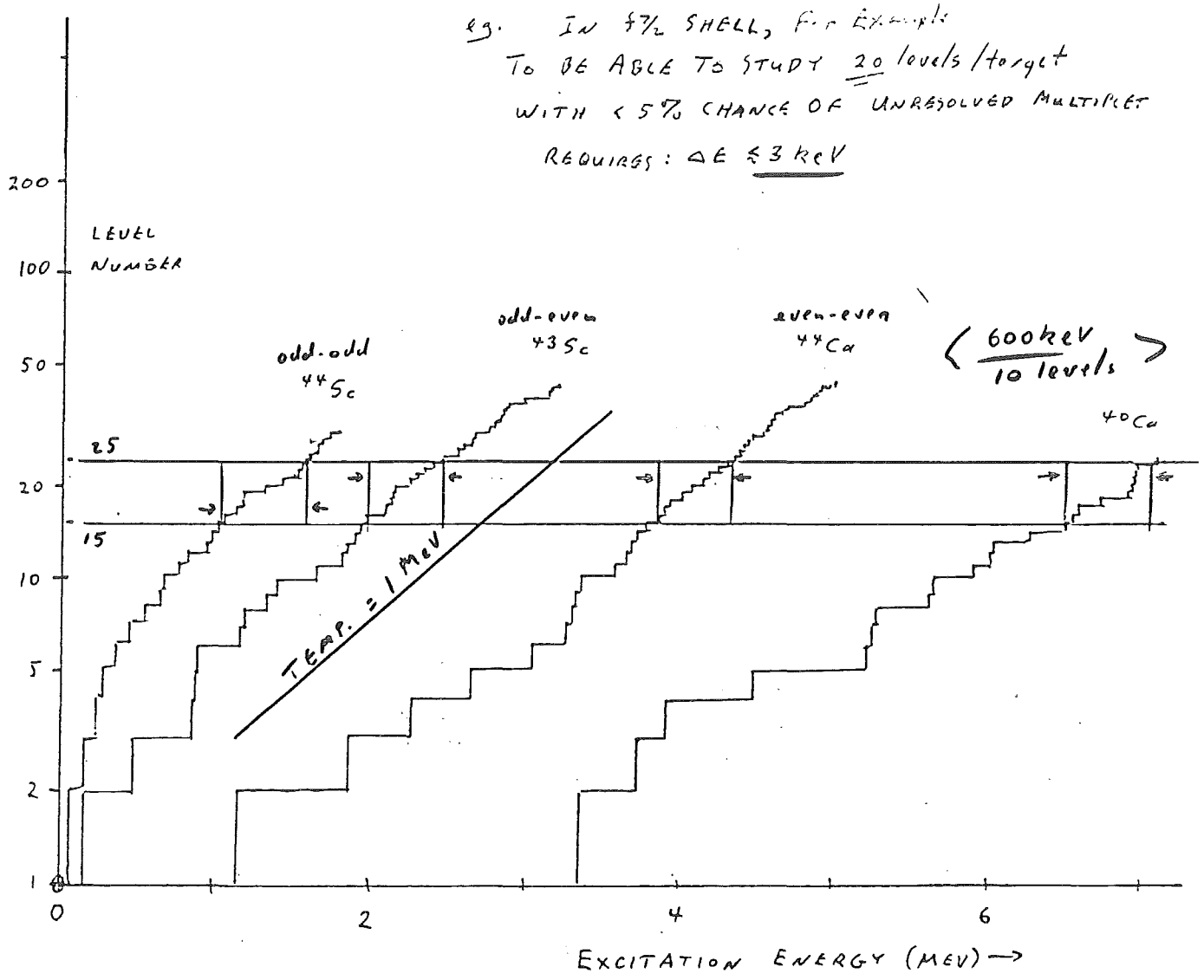
eg. IN f7/2 SHELL, for Example
TO BE ABLE TO STUDY 20 levels/target
WITH < 5% CHANCE OF UNRESOLVED MULTIPLET
REQUIRES: ΔE ≤ 3 keV
LEVEL NUMBER
200
100
50
25
20
15
10
5
2
1
odd-odd 44Sc
odd-even 43Sc
even-even 44Ca
40Ca
< 600 keV / 10 levels >
TEMP. = 1 MeV
0
2
4
6
EXCITATION ENERGY (MEV) →

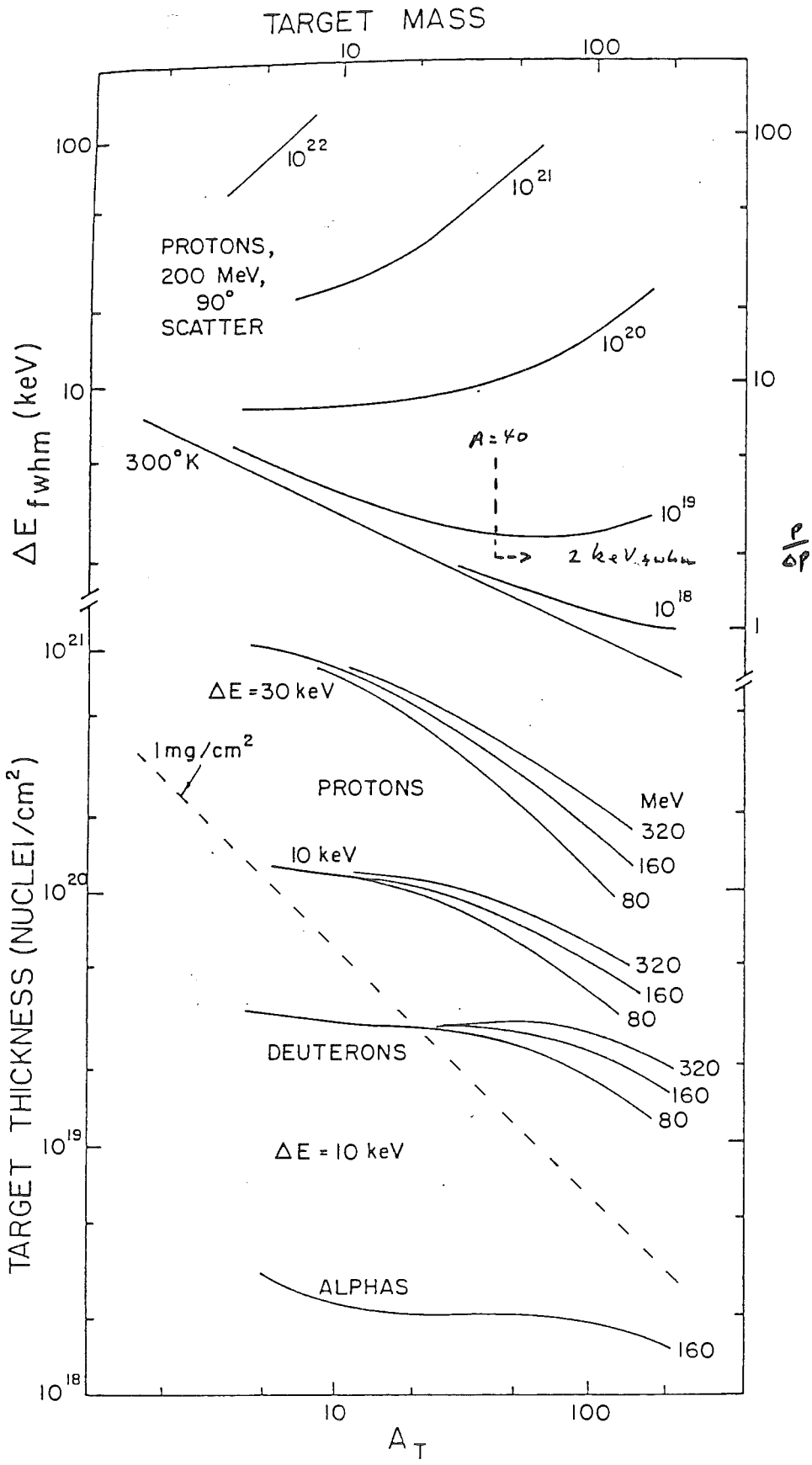
TARGET MASS
10
100
100
10
1
ΔE_{fwhm} (keV)
10^{22}
10^{21}
10^{20}
10^{19}
10^{18}
PROTONS,
200 MeV,
90°
SCATTER
300°K
A=40
--> 2 keV fwhm
$\frac{P}{\Delta P}$ = 150,000
10^{21}
10^{20}
10^{19}
10^{18}
TARGET THICKNESS (NUCLEI/cm^2)
ΔE = 30 keV
1 mg/cm^2
PROTONS
MeV
320
160
80
10 keV
320
160
80
DEUTERONS
320
160
80
ΔE = 10 keV
ALPHAS
160
10
100
A_T

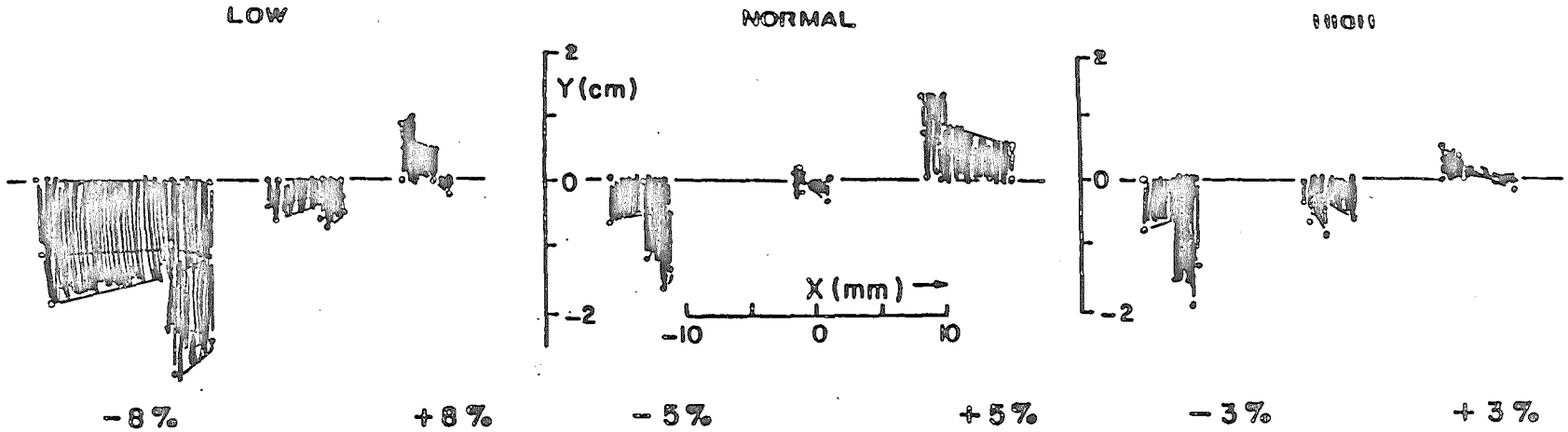

3.6 Tesla-meter Spectrometer

ABOVE - as proposed (July 80)

BELOW - revised Feb 82

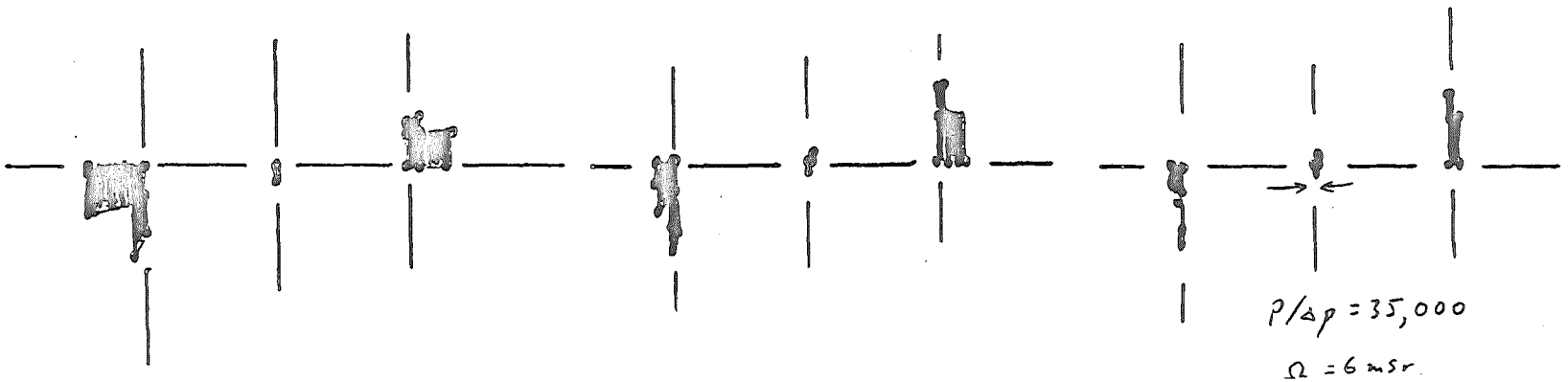

$p/\Delta p = 35{,}000$

$\Omega = 6$ msr

no event reconstruction

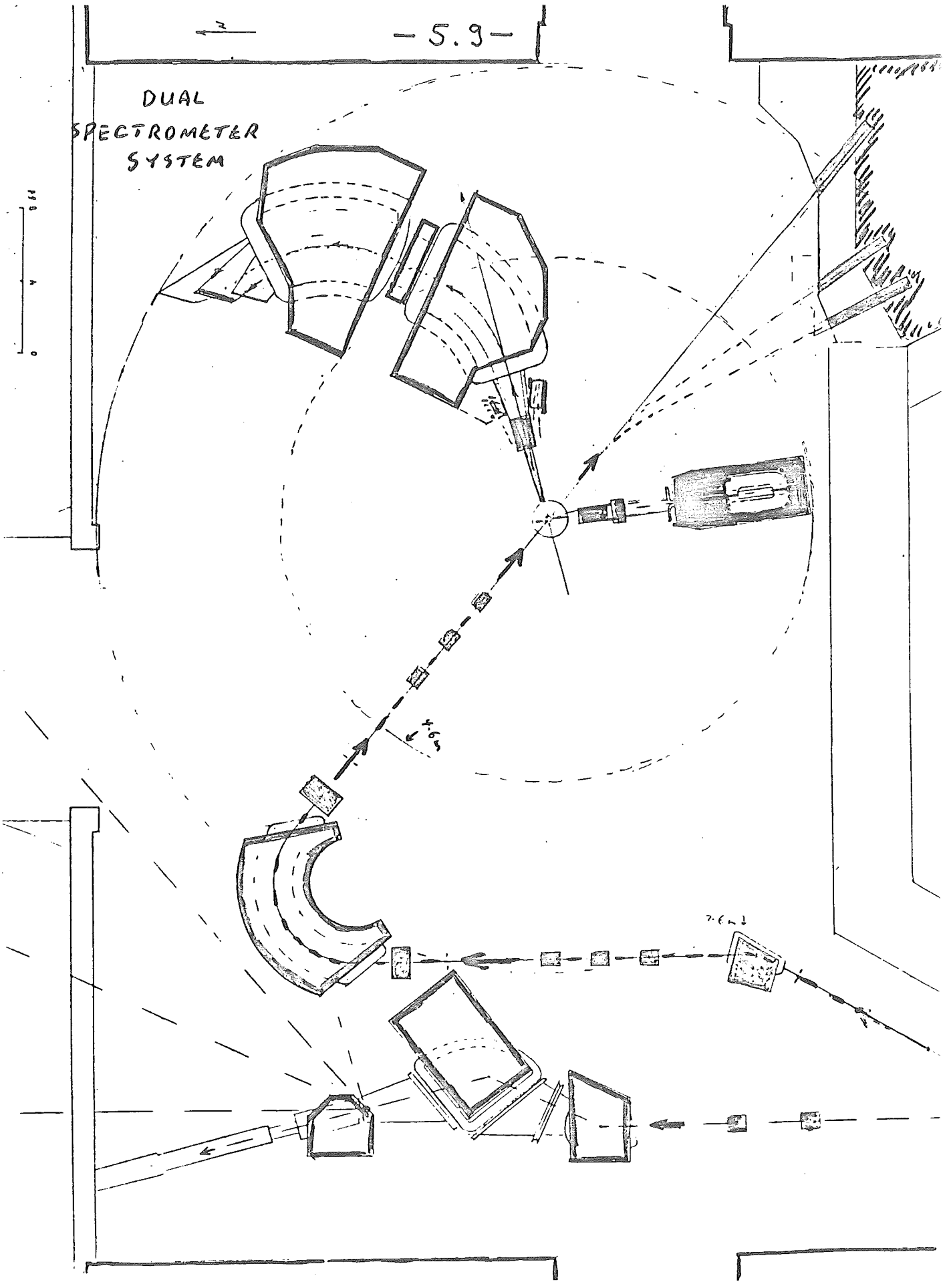
DUAL
SPECTROMETER
SYSTEM

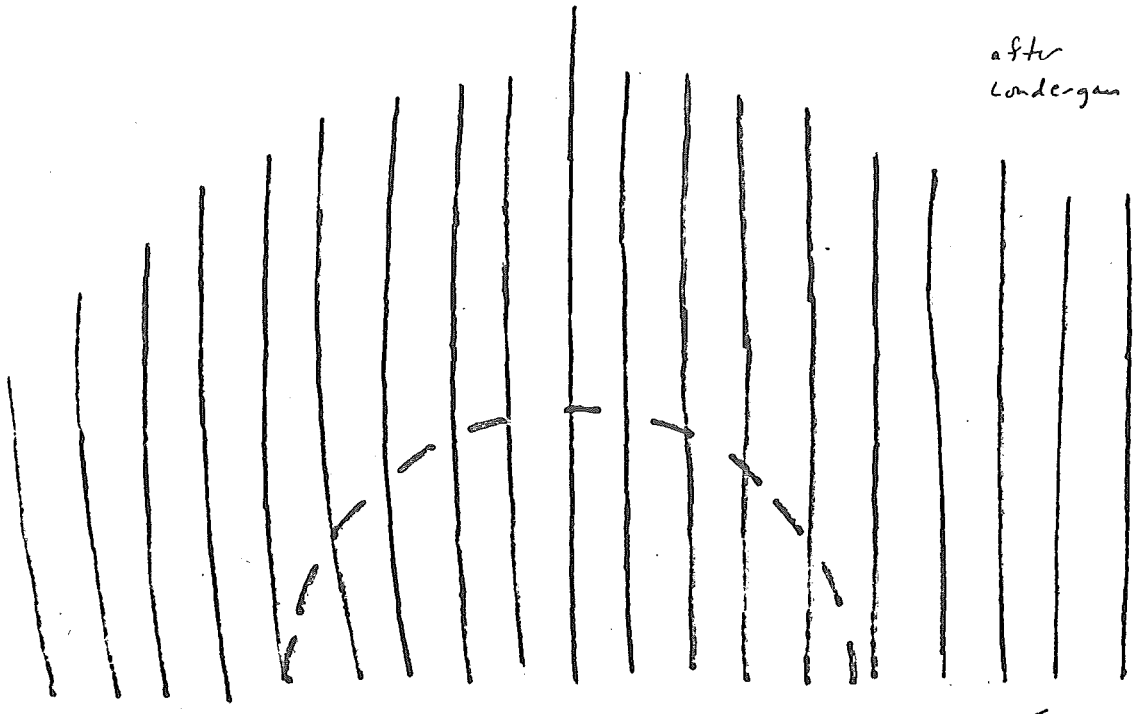
after
Londergan
12C
156 MeV p.
156 MeV
protons

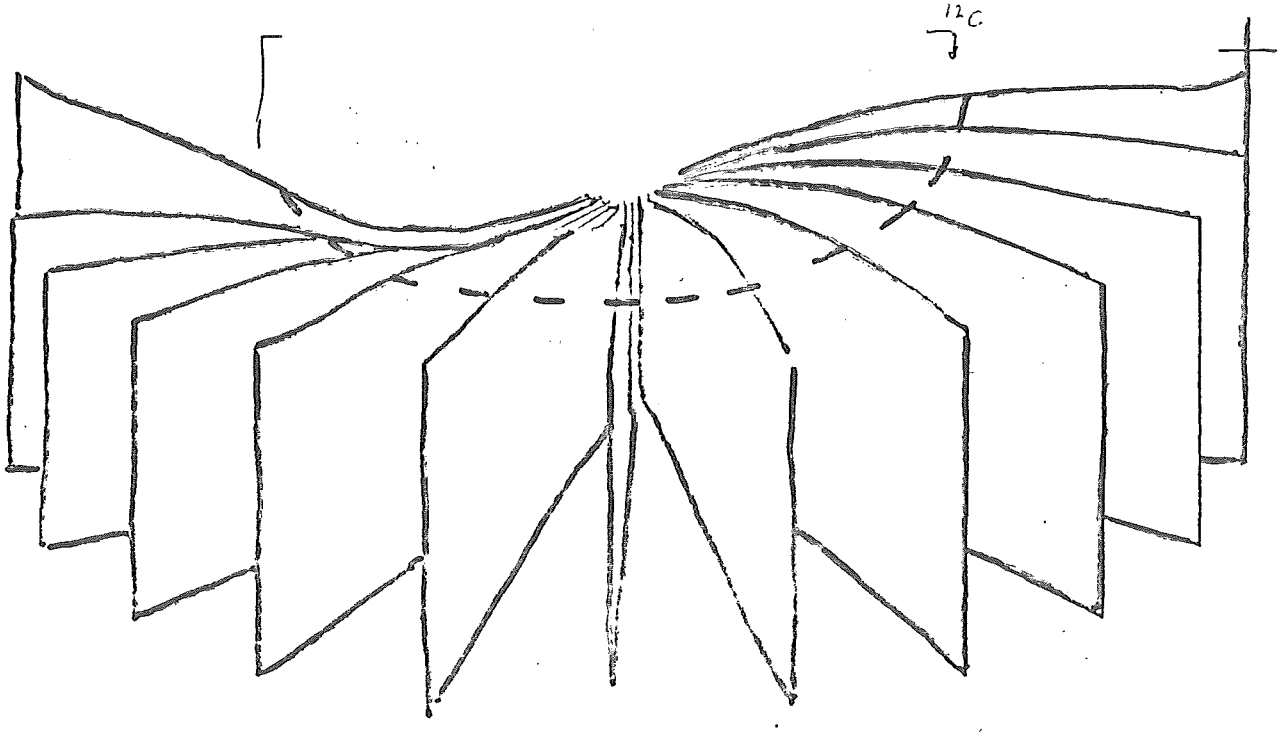
12C.

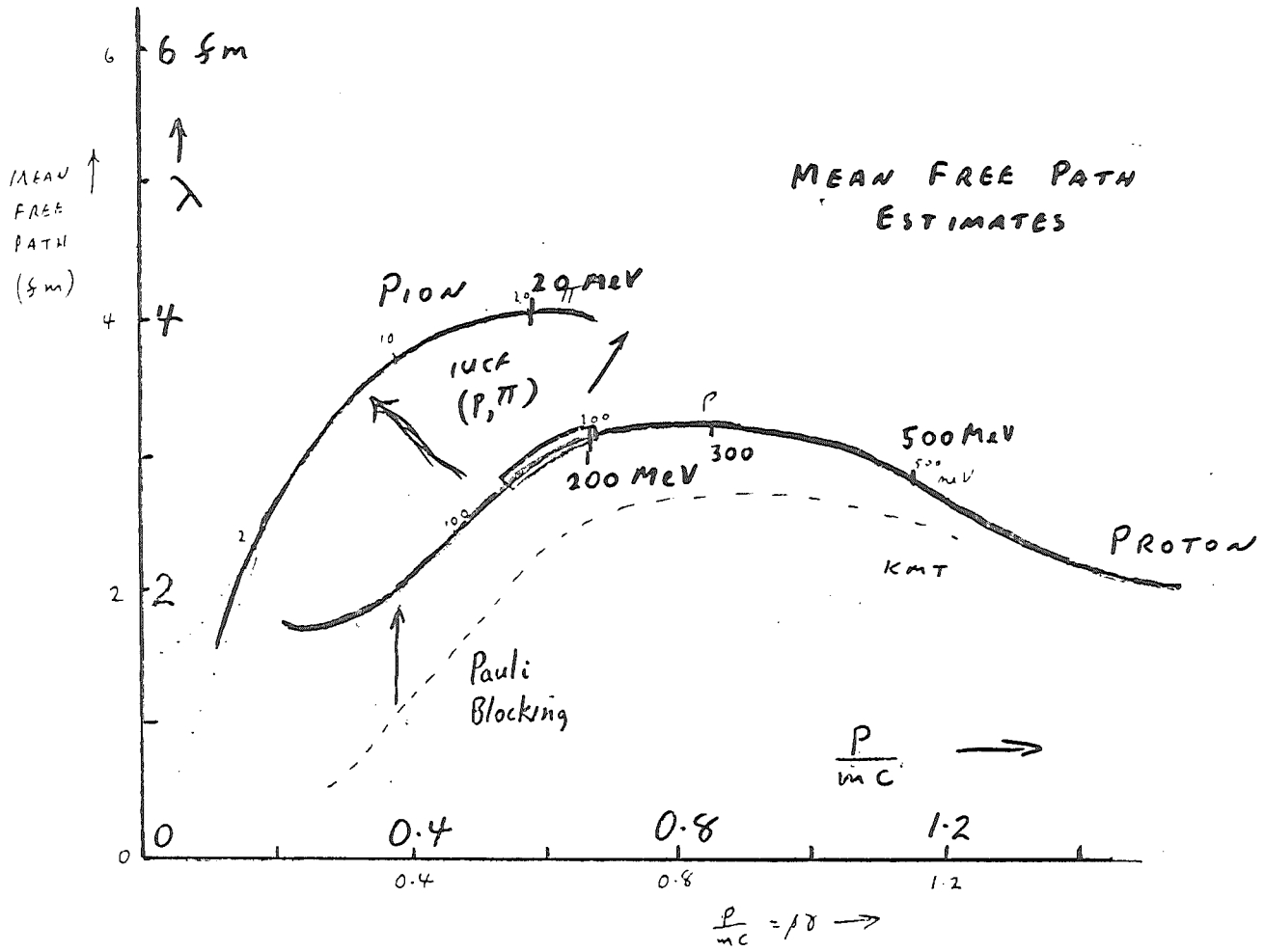
MEAN FREE PATH ESTIMATES
MEAN FREE PATH (fm)
6 fm
λ
PION
20 MeV
IUCF (P,π)
200 MeV
300
500 MeV
PROTON
KMT
Pauli Blocking
p/mc
p/mc = βγ
0
0.4
0.8
1.2
2
4
6

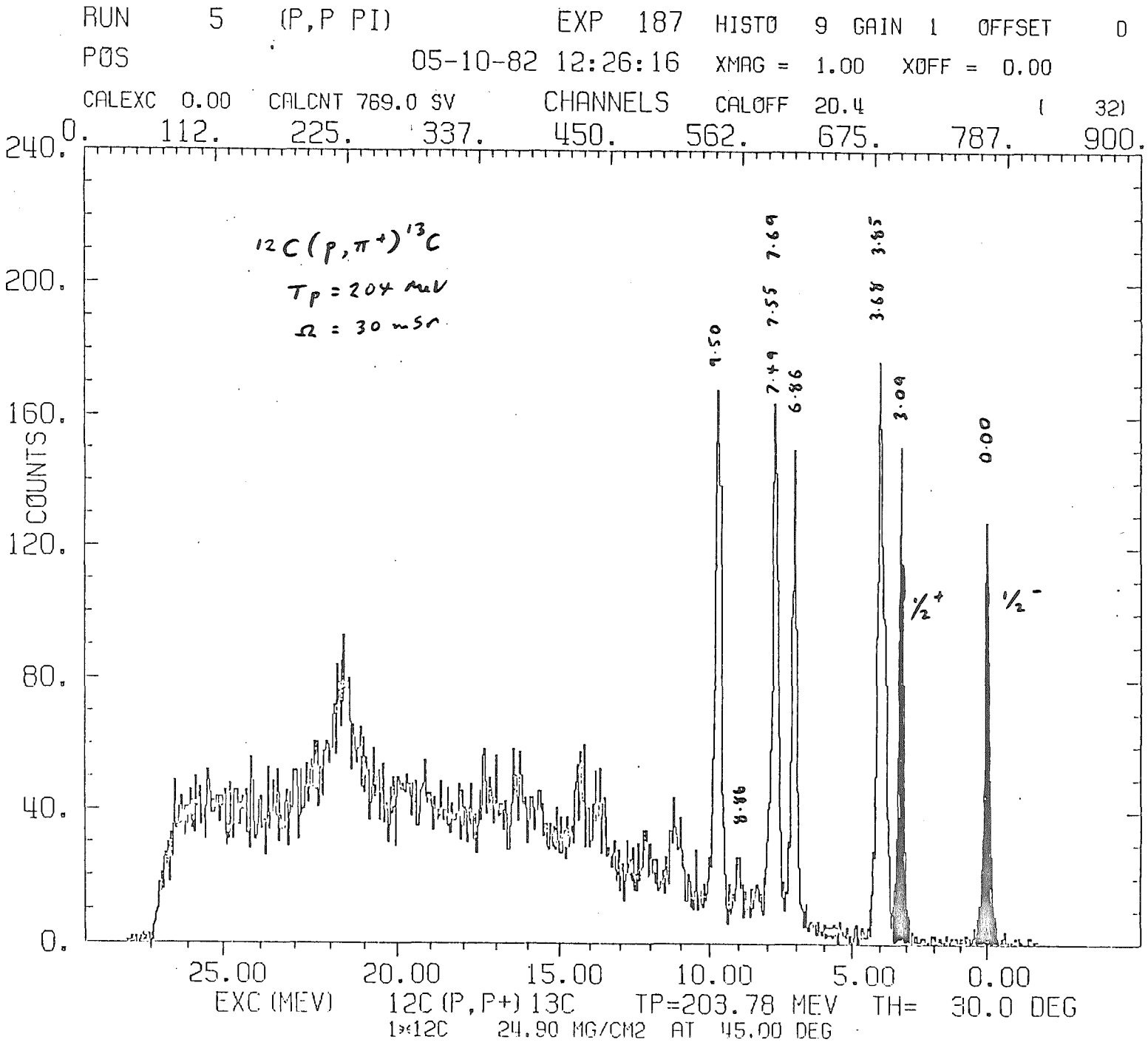
RUN 5 (P,P PI) EXP 187 HISTO 9 GAIN 1 OFFSET 0
POS 05-10-82 12:26:16 XMAG = 1.00 XOFF = 0.00
CALEXC 0.00 CALCNT 769.0 SV CHANNELS CALOFF 20.4 (32)
0. 112. 225. 337. 450. 562. 675. 787. 900.
240.
200.
160.
120.
80.
40.
0.
COUNTS
$^{12}C(p,\pi^+)^{13}C$
T_p = 204 MeV
Ω = 30 mSr
9.50
8.86
7.69
7.55
7.49
6.86
3.85
3.68
3.09
0.00
½+
½-
25.00 20.00 15.00 10.00 5.00 0.00
EXC (MEV) 12C (P,P+) 13C TP=203.78 MEV TH= 30.0 DEG
1×12C 24.90 MG/CM2 AT 45.00 DEG

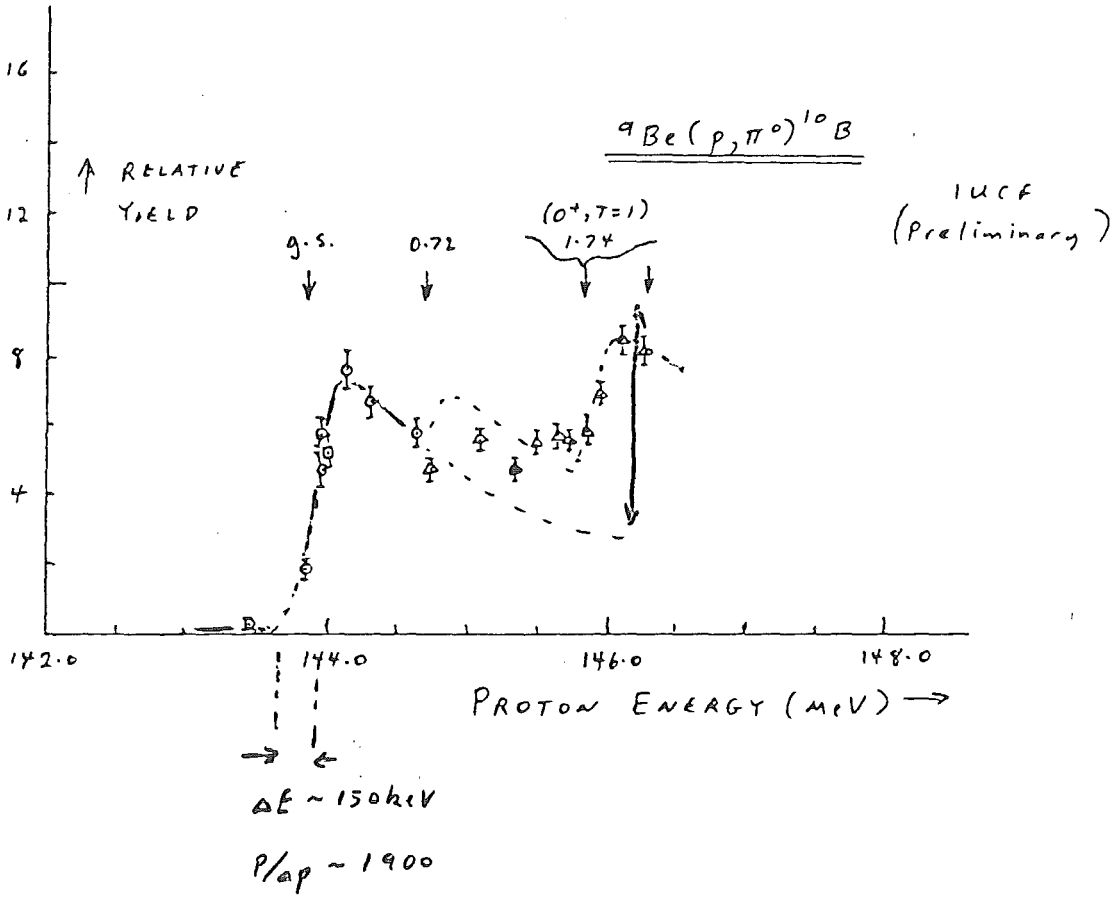
$^9Be(p,\pi^0)^{10}B$
IUCF
(Preliminary)
RELATIVE YIELD
16
12
8
4
g.s.
0.72
$(0^+,T=1)$
1.74
142.0
144.0
146.0
148.0
PROTON ENERGY (MeV) →
ΔE ~ 150keV
P/ap ~ 1900

Second talk

General comments on recirculators and beem cooling

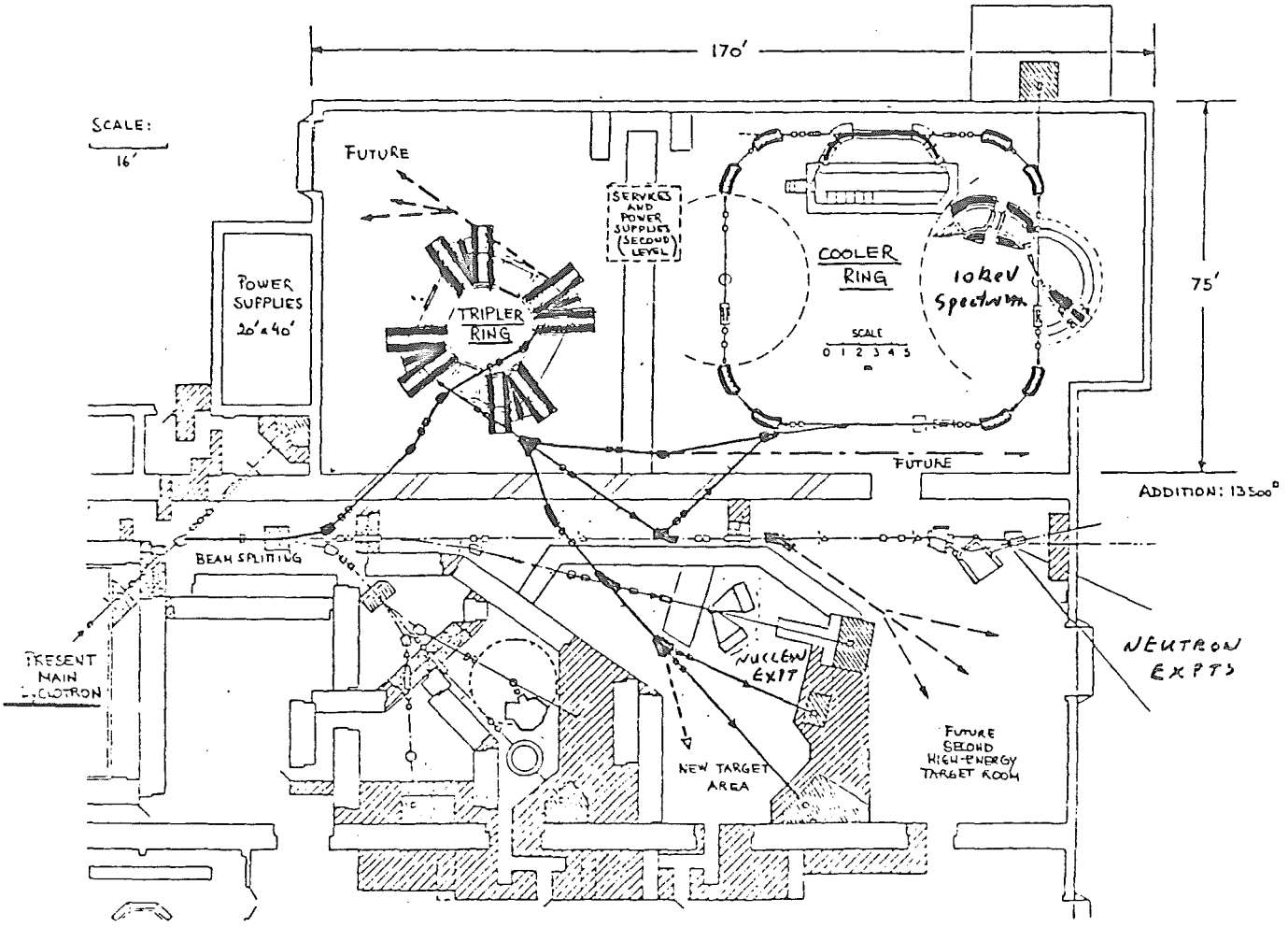

Fig.III-13: Proposed IUCF floor plan 1988.

RECIRCULATION MODES

I SINGLE PASS (GEIGER + MARSDEN - 1913)

THICK TARGET ~ 10 mg/cm^2

LOW BEAM CURRENT ~ 100 nA

VERY LOW EFFICIENCY ~ 10^{-5} nuclear reactions per beam particle

II UNCOOLED (10^2 TO 10^4 TURNS)

THIN TARGET ~ 100 µg/cm^2

HIGH BEAM CURRENT ~ 100 µA

MODERATE EFFICIENCY ~ 10^{-4} to 10^{-3}

III COOLED (10^6 TO 10^7 TURNS)

ULTRA-THIN TARGET ~ 100 µg/cm^2

VERY HIGH BEAM CURRENT ~ 100 mA

HIGH EFFICIENCY ~ 10^{-1}

EFFICIENCY OF BEAM USE:

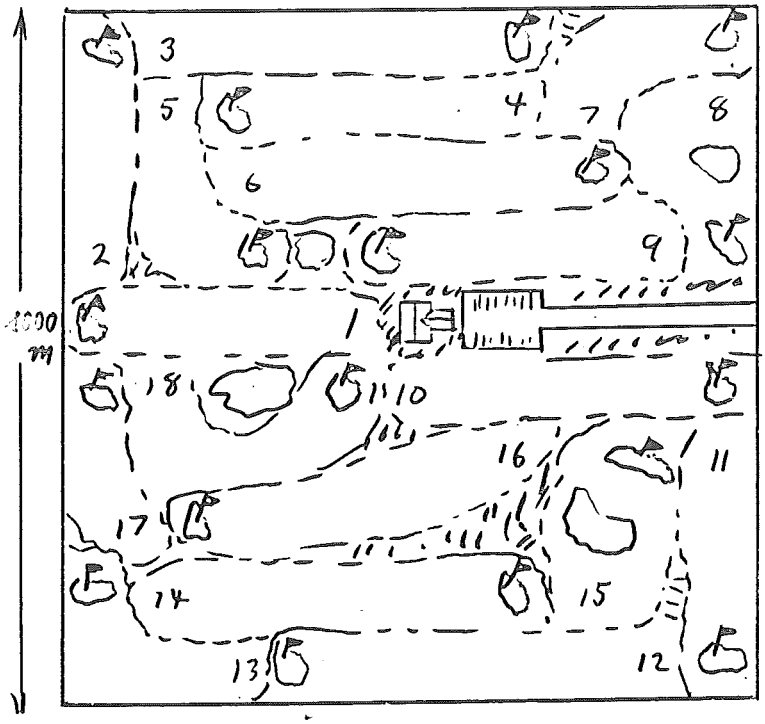

A BLINDFOLDED GOLFER SET DOWN AT RANDOM ON AN 18 HOLE COURSE HAS A PROBABILITY IN ONE SHOT FOR A HOLE-IN-ONE

$$P = \frac{18\,(\text{HOLE AREA})}{\text{COURSE AREA}} \sim 10^{-2}$$

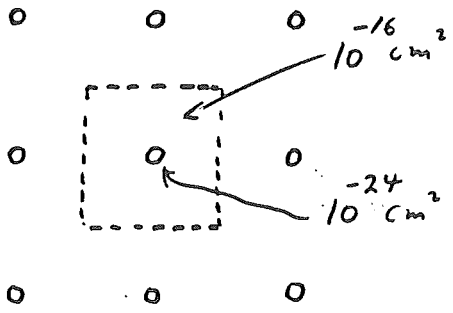

PER ATOMIC LAYER AN ACCELERATOR BEAM HAS A PROBABILITY P FOR A NUCLEAR COLLISION

$$P \sim 10^{-8}$$

FOR HIGH RESOLUTION EXPERIMENTS

TARGET HEATING LIMITS TARGET THICKNESS x_T TO A FEW HUNDRED ATOMIC LAYERS

$$x_T \leq 10^{19}\ \text{NUCLEI/CM}^2 \Rightarrow P \sim 10^{-5}$$

BEAM USAGE EFFICIENCY IS POOR (ONE PASS TARGET)

BRIGHTNESS OF A BEAM:

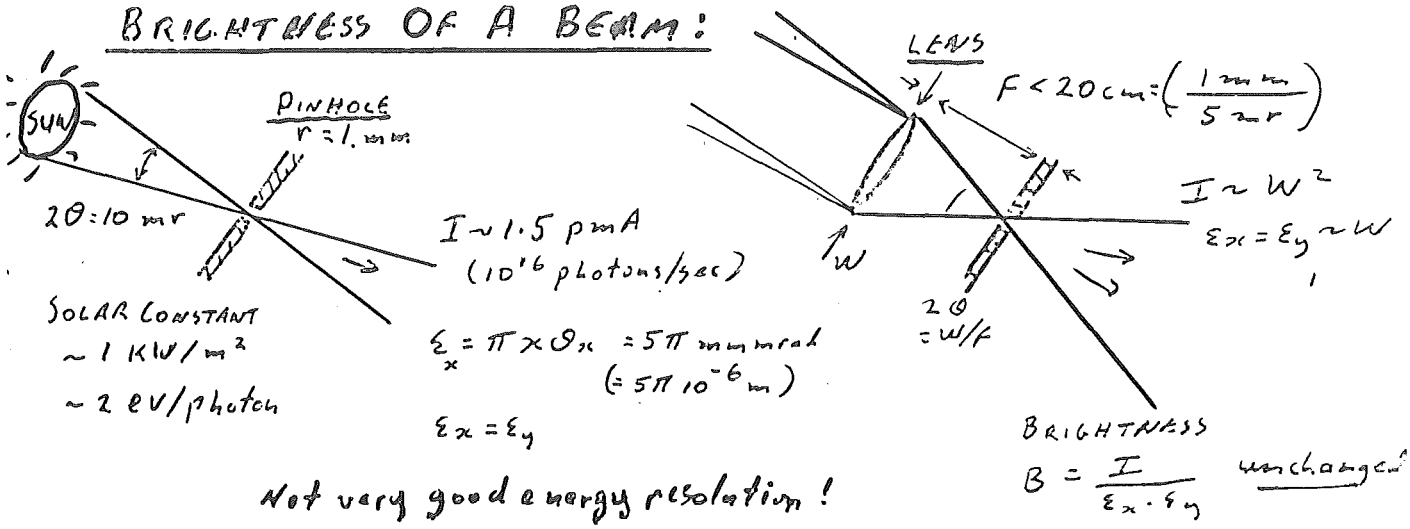

Not very good energy resolution !

FOR BLACKBODY RADIATION, BRIGHTNESS IS DETERMINED BY SOURCE TEMPERATURE (T^4 LAW)

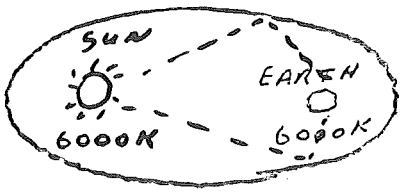

ELLIPTICAL REFLECTING CAVITY

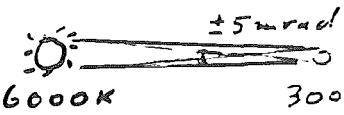

solid angle: $\pi\theta^2$

$$\frac{T_E^4}{T_S^4} = \left(\frac{300}{6000}\right)^4 = \frac{\pi(5\cdot10^{-3})^2}{4\pi}$$

EMITTANCE ε IS THE AREA IN TRANSVERSE PHASE SPACE OCCUPIED BY A PARTICLE BEAM

Defin: $\theta_x = \frac{p_x}{p}$

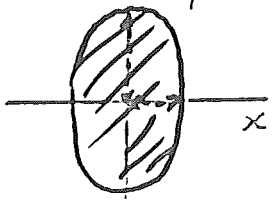

$\varepsilon = \pi \times \theta_x$

QUANTUM LIMITS:

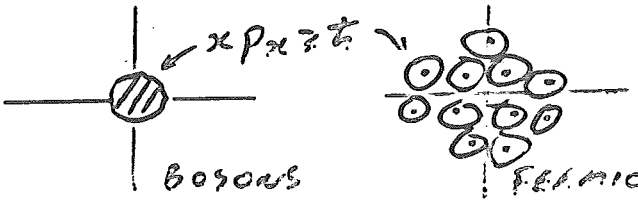

LASER $\varepsilon \sim \lambda \sim 10^{-6}$ m

NUCLEAR DENSITY !

SPACE CHARGE

BRIGHTNESS ENHANCEMENT BY STRIPPING
(FILL THE HOLES IN PHASE SPACE)

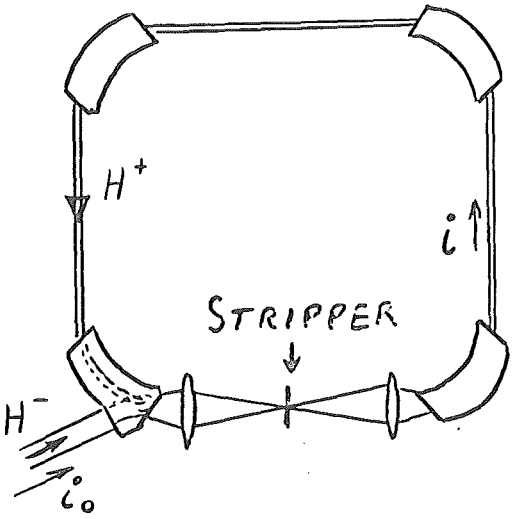

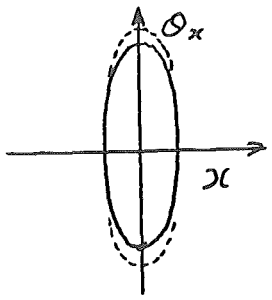

AT STRIPPER WAIST

EMITTANCE

$\varepsilon_x = \pi \times \theta_x$

SCALE LENGTH (COURANT BETA)

$\beta_x = x / \theta_x$

$\theta_x^2 = \varepsilon_x / \pi \beta_x$

$x^2 = \varepsilon_x \beta_x / \pi$

AFTER n TURNS:

$i = n\, i_0$ $\qquad \theta_x^2 = \theta_0^2 + \left(\frac{n+1}{2}\right)\theta_1^2$

θ_0 = input beam divergence

θ_1 = increase by stripper in one turn

DEFINE: BRIGHTNESS $B = i / \varepsilon_x \varepsilon_y$

MAXIMIZE: $\frac{\partial B}{\partial n} = 0$ $\qquad$ FIND: $n_{MAX} = 1 + 2\,\theta_0^2/\theta_1^2$

$\theta_{x\,MAX}^2 = 2\theta_0^2 + \theta_1^2$

$[\varepsilon_{MAX} \sim 2\varepsilon_0]$

$B_{MAX}/B_1 = 1/4\,(n_{MAX} + 2)$

EXAMPLE ($\beta_x = \beta_y = 1$ m)

BEAM ENERGY	10	200	MeV
FOIL THICKNESS [CARBON, 95% EFF.]	6	100	$\mu g/cm^2$
INPUT EMITTANCE	6.85π	1.45π	10^{-6} m
θ_0^2	6.85	1.45	10^{-6} sterad
θ_i^2	47.	5.5	10^{-10} "
n_{MAX}	2900	5300	turns
B_M/B_1	725	1325	→

CONCLUSION:

LARGE INCREASE IN BRIGHTNESS OVER WIDE ENERGY RANGE

(TRANSVERSE PHASE SPACE AREA)

BEAM EMITTANCE CONSIDERATIONS

BEAM LINE LENGTH, QUAD + DIPOLE SIZE, AS WELL AS HIGH RESOLUTION SPECTROMETER COST ARE SENSITIVE TO BEAM EMITTANCE

EXAMPLE : ANALYSIS MAGNET FOR 10 keV @ 1 GeV $P/\Delta p > 10^5$

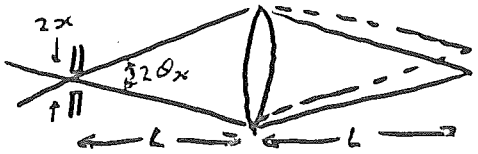

$\varepsilon = \pi x \theta_x$ $\quad 2w = 2L\theta_x$

$\Delta\theta/\theta_B = \Delta p/p$

JUST RESOLVED : $P/\Delta p = \dfrac{L\theta_B}{2x}$

$= \dfrac{[w\theta_B]}{2(\varepsilon/\pi)}$

$\propto \dfrac{\text{MAGNETIC FLUX}}{\text{EMITTANCE}}$

MAGNET VOLUME $\sim \rho^3$

FLUX $\sim \rho^2 \sim \text{cost}^{2/3}$

$\therefore$ ANALYZER COST $\propto \left[(P/\Delta p) \times (\text{EMITTANCE}) \right]^{3/2}$ or $\boxed{\dfrac{\rho}{\sigma_D} \left(\varepsilon P/\Delta p \right)^2}$

SIMILAR ARGUMENT FOR SPECTROMETER

FIX $\Delta\Omega$ + MAGNET MASS ; RESOLUTION IMPROVED AS BEAM SPOT GETS SMALLER (LENGTH LIMIT SET BY EMITTANCE !)

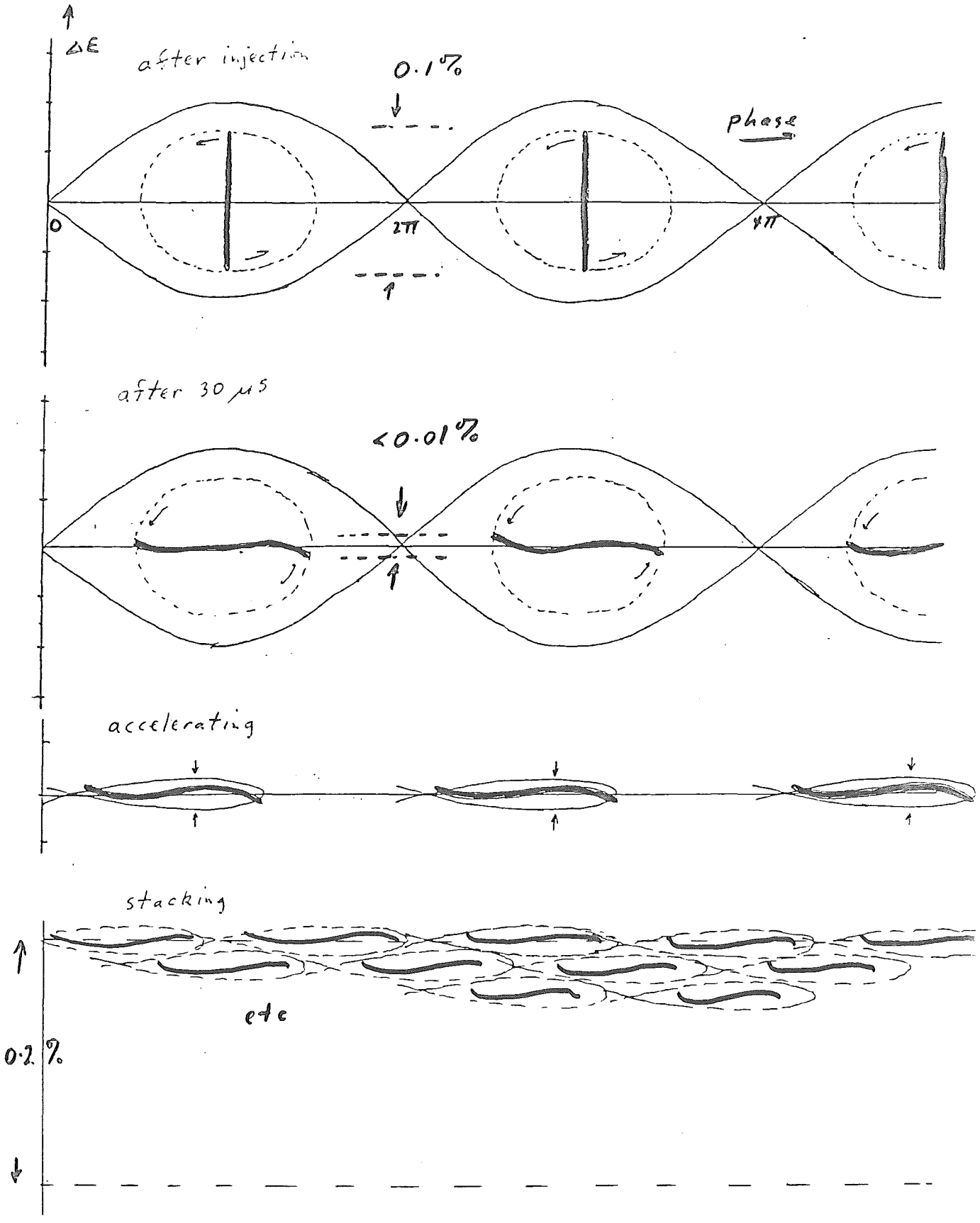
ΔE
after injection
0.1%
phase
0
2π
4π
after 30 μs
< 0.01%
accelerating
stacking
edge
0.2 %

BEAM COOLING

INCREASE BRIGHTNESS BY REDUCING EMITTANCE

COMMON FEATURES:

- $\vec{F} = -K\vec{v}$ DAMPING FORCE [WEAK COMPARED TO CONFINEMENT FORCES
- RANDOM (STOCHASTIC) DRIVING FORCE
- $10^{-2} < \tau < 10^{+2}$ SECONDS – SLOW APPROACH TO EQUILIBRIUM ⇒ CONFINEMENT REQUIRED
- ANISOTROPY (THERMAL)

DISTINGUISHING FEATURES:

- EQUILIBRIUM TEMPERATURE (SETS LOWER BOUND TO QUALITY IMPROVEMENT)
- RELAXATION TIME (LUMINOSITY LIMIT IN COOLED BEAM SCATTERING EXPERIMENTS)
- REGIME OF APPLICABILITY (BEAM SPECIES, ENERGY, INTENSITY)
- CONVENIENCE, COST, ...

SOME KNOWN BEAM COOLING METHODS:

I – SYNCHROTRON RADIATION $\gamma = E/mc^2 \gtrsim 10^3$ ⇒ ELECTRONS & POSITRONS

II – ACTIVE FEEDBACK (MAXWELL'S DEMON) DENSITY LIMIT

III – IMMERSION IN COLD CO-MOVING ELECTRON BATH $0.2 < v/c < 0.$

- TARGET IONIZATION HIGH TEMPERATURE
- DOPPLER-SHIFTED OPTICAL ATOMIC RESONANCE ABSORPTION SELECTI
- OTHERS

COOLING

SOME RECENT REFERENCES

GENERAL REVIEWS

F. T. COLE & F. E. MILLS - ANN. REV. NUCL. PART. SCI. 31 295 (1981)

A. N. SKRINSKII & V. V. PARKHOMCHUK - SOV. J. PART. NUCL 12 223 (1981)

W. D. PHILLIPS & H. METCALF - PHYS REV. LETT. 48 596 (1982)
LASER ABSORPTION

D. MÖHL ET AL - PHYSICS REPORTS 58 73 (1980)
STOCHASTIC COOLING

T. OGIRO & A. G. RUGGIERO JOURN. PHYS. SOC. (JAPAN) 49 1654 (80)
ELECTRON COOLING - THEORY

M. BELL ET AL - PHYSICS LETTERS 87B 275 (1979)
ELECTRON COOLING - EXPERIMENT

TARGET COOLING - reduce transverse vel., add back the longitudinal

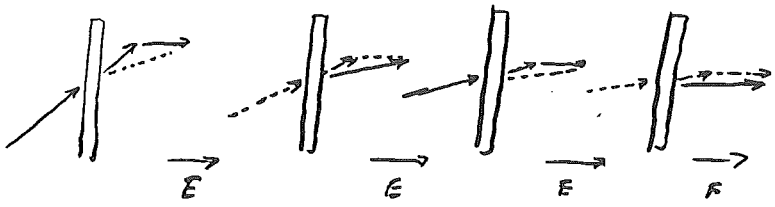

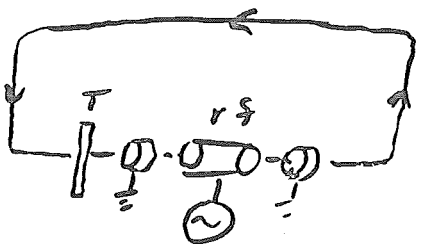

electrons cool
nuclei heat

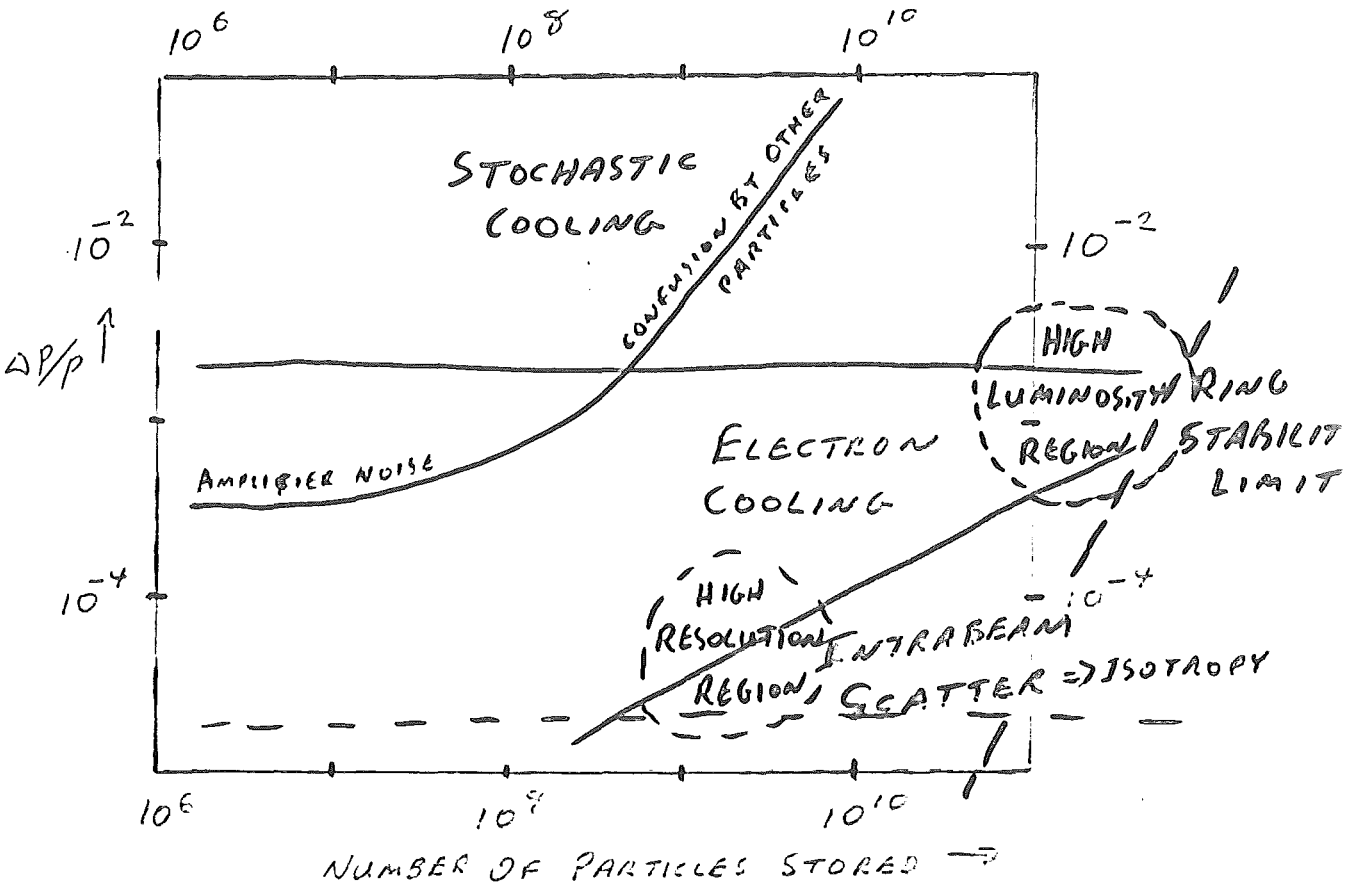

$\tau_{cool} \sim 1$ second (after Skrinskii & Parkhomchuk)

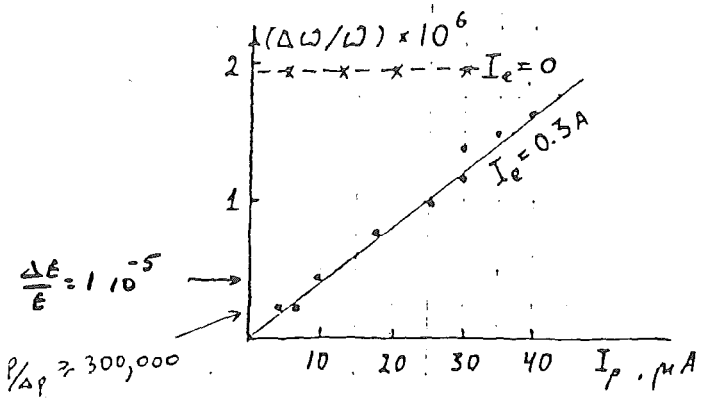

$\frac{\Delta p}{p} = 13.3 \frac{\Delta\omega}{\omega}$

NOVOSIBIRSK

ABOVE:
HIGHEST
RESOLUTION
$< 10^{-5}$

FIG. 5 - Measurements of proton revolution frequency spread by the debunching time method.

x x x x x x electron cooling is switched off
. . . . . electron cooling is switched on.

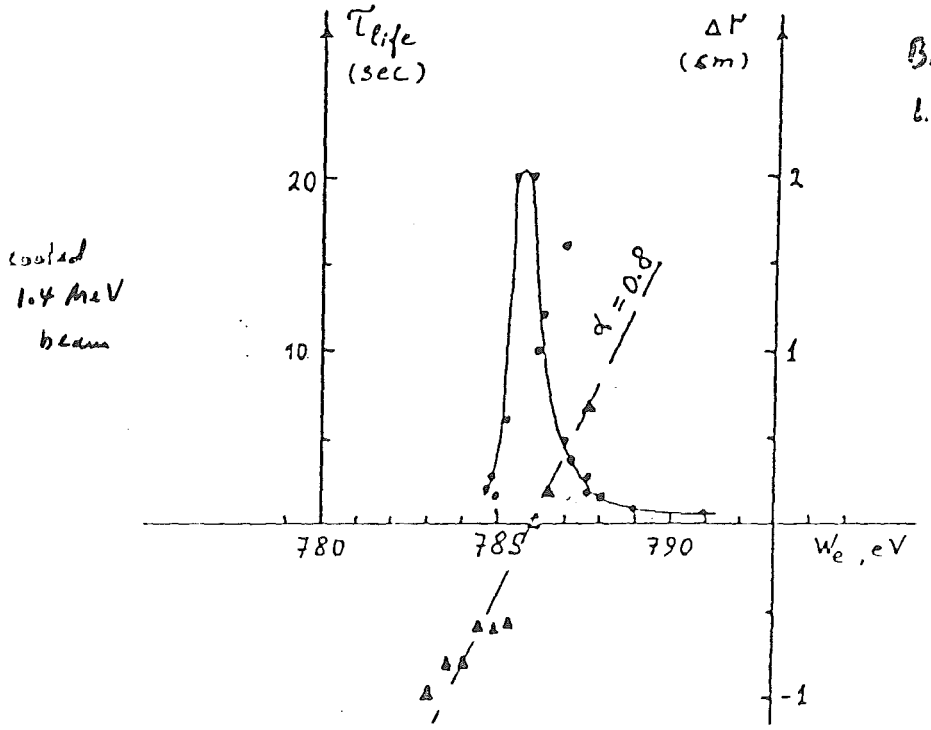

cooled
1.4 MeV
beam

BELOW:
LOWEST
ENERGY
1.4 MeV

FIG. 8 - The results of electron cooling experiments for low energy protons.

..... the dependence of proton life-time on electron energy

▲ ▲ ▲ the dependence of proton beam position from electron energy.

COOLER:

TARGET "HEATING" ⇌ ELECTRON "COOLING"

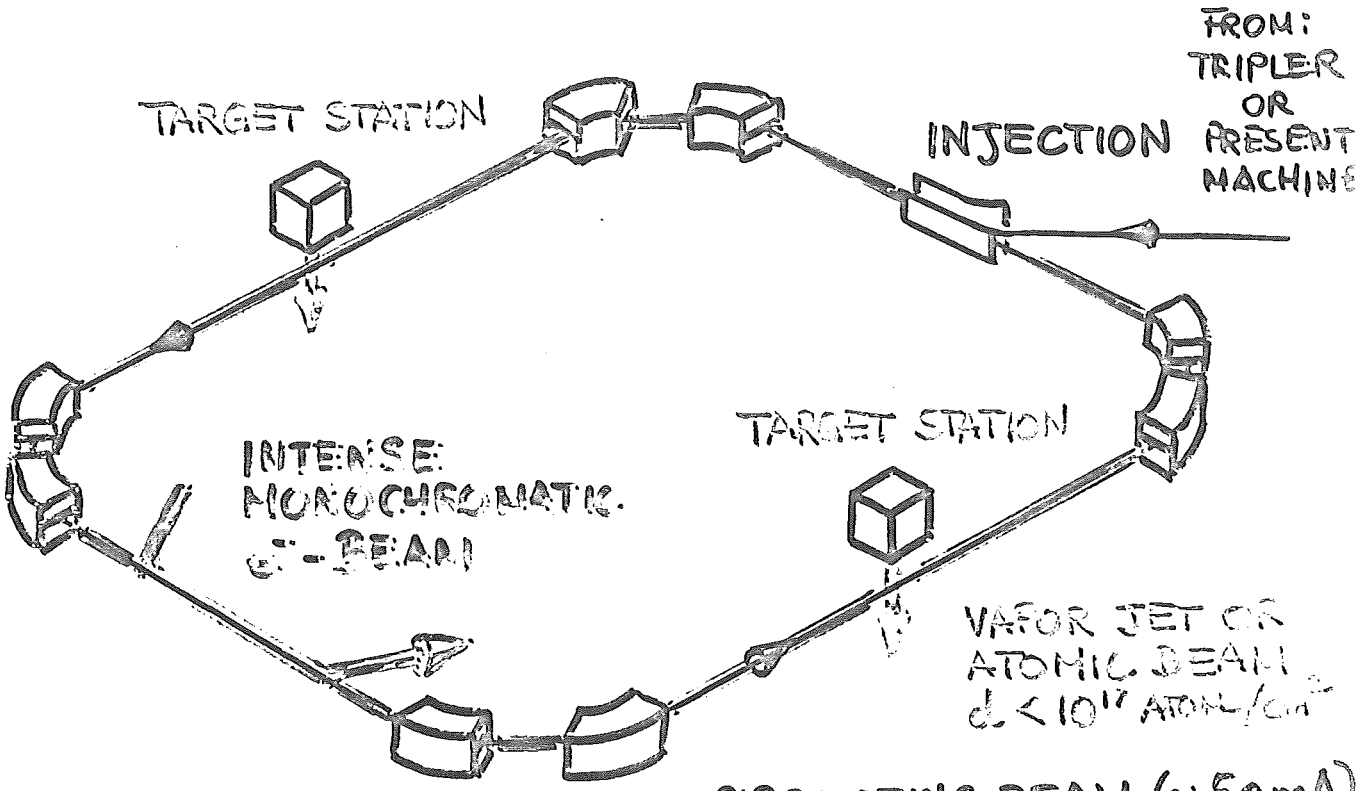

FEATURES: BEAM:

- MONOCHROMATICITY, LOW EMITTANCE
- DC-BEAM (OR ADJUSTABLE DUTY FACTOR)
- ADJUST ENERGY BY RAMPING e^- VELOCITY

EXPERIMENT:

- THIN TARGET
- POLARIZED ATOMIC BEAM TARGET
- RECOILS OBSERVABLE
- INFORMATION FROM STORED INTENSITY
- ULTRA-HIGH RESOLUTION

FACILITY:

- FILLING: USE ONLY MINOR FRACTION OF BEAM

Enhanced Experimental Capabilities with COOLER

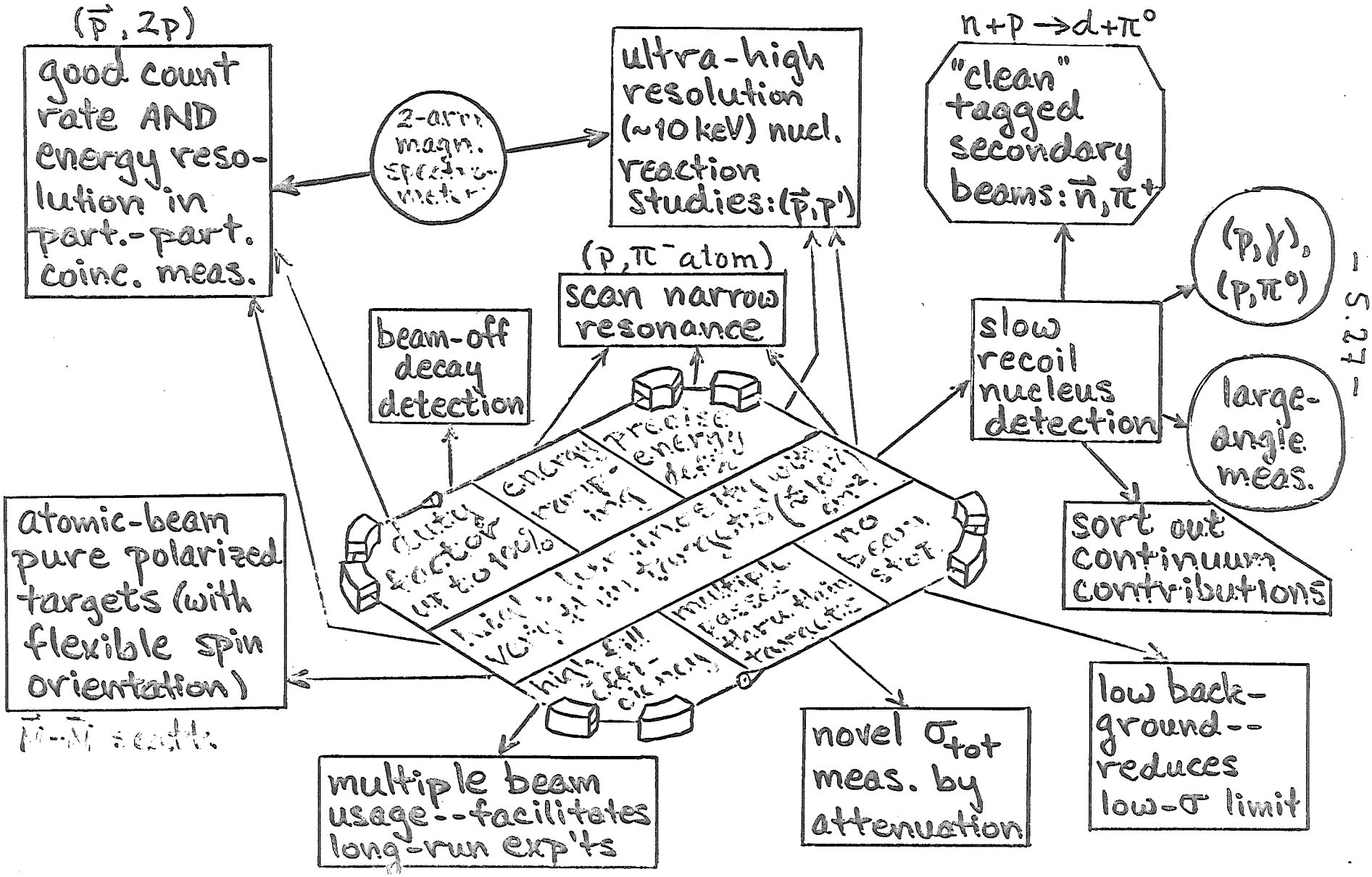

Third talk

Design and construction of the Indiana Cooler Ring

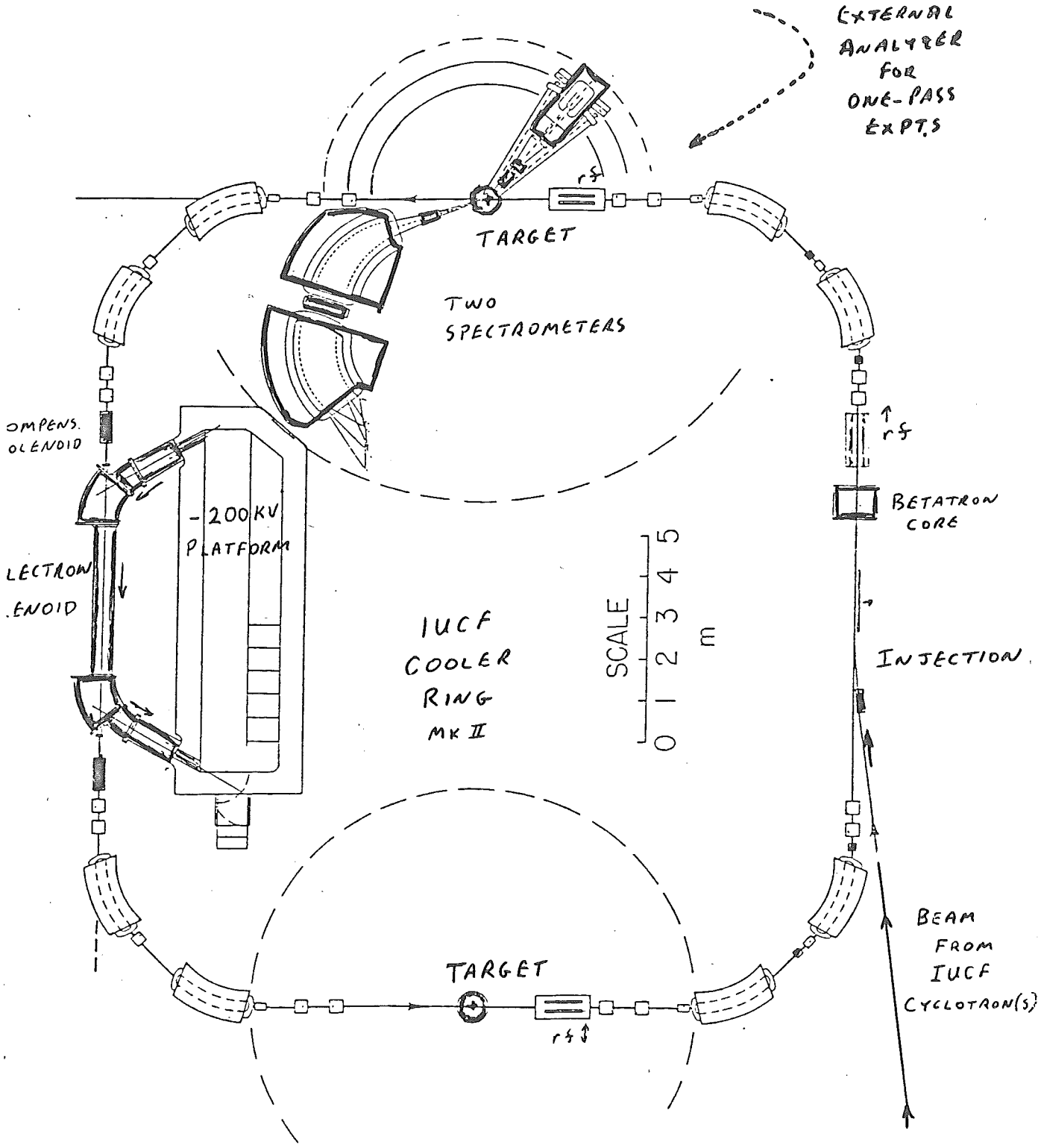
EXTERNAL
ANALYSER
FOR
ONE-PASS
EXPTS
rf
TARGET
TWO
SPECTROMETERS
OMPENS.
OLENOID
LECTRON
ENOID
-200 KV
PLATFORM
IUCF
COOLER
RING
MK II
SCALE
0 1 2 3 4 5
m
rf
BETATRON
CORE
INJECTION
BEAM
FROM
IUCF
CYCLOTRON(S)
TARGET
rf

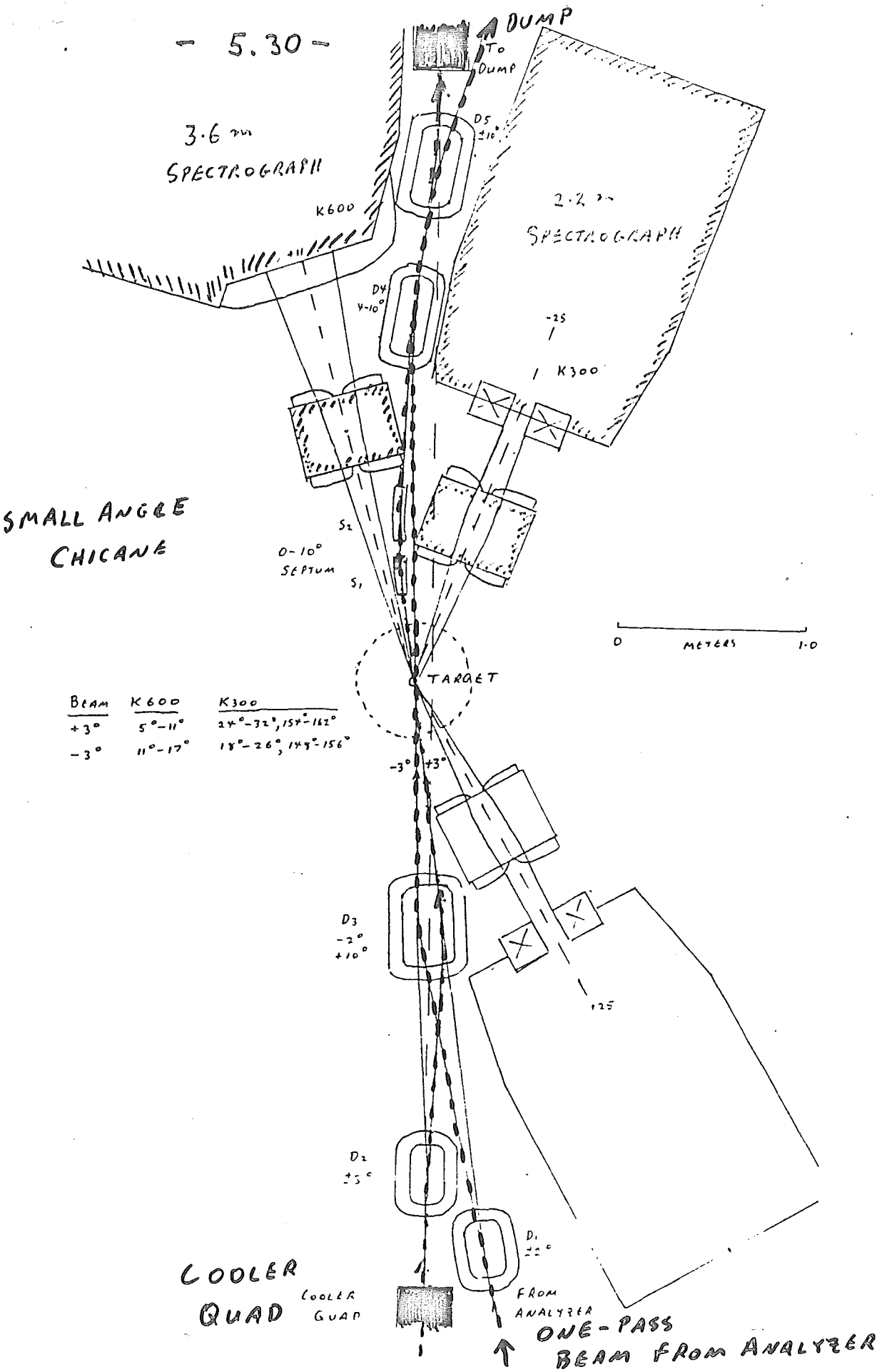
DUMP
To Dump
3.6 m SPECTROGRAPH
K600
D5 ±10°
2.2 m SPECTROGRAPH
D4 4-10°
-25
K300
SMALL ANGLE CHICANE
S2
0-10° SEPTUM
S1
0 METERS 1.0
TARGET
Beam K600 K300
+3° 5°-11° 24°-32°, 154°-162°
-3° 11°-17° 18°-26°, 148°-156°
-3° +3°
D3 -2° +10°
+25
D2 -3°
D1 -22°
COOLER QUAD
COOLER QUAD
FROM ANALYZER
ONE-PASS BEAM FROM ANALYZER

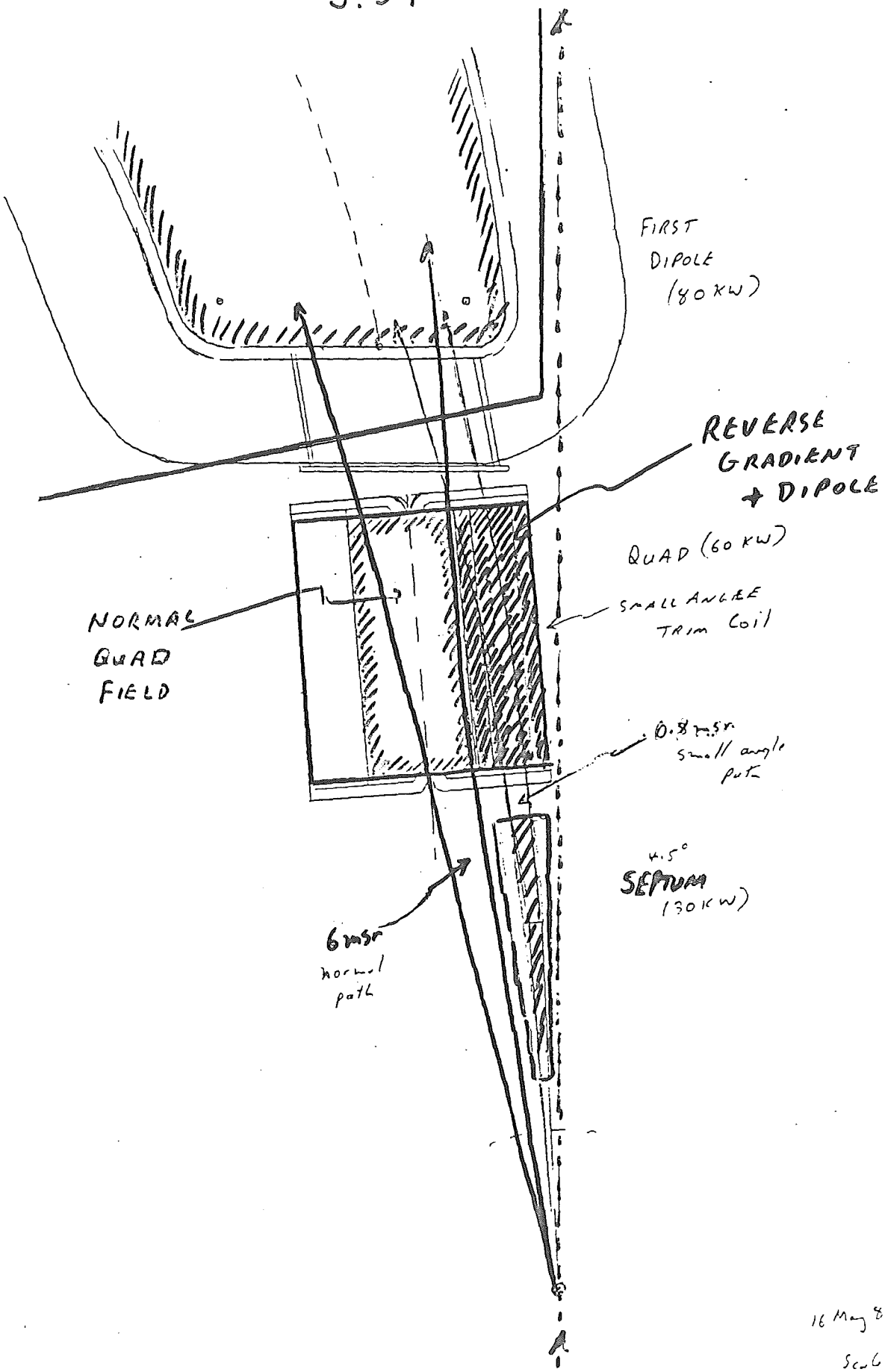

16 May 83

Scale

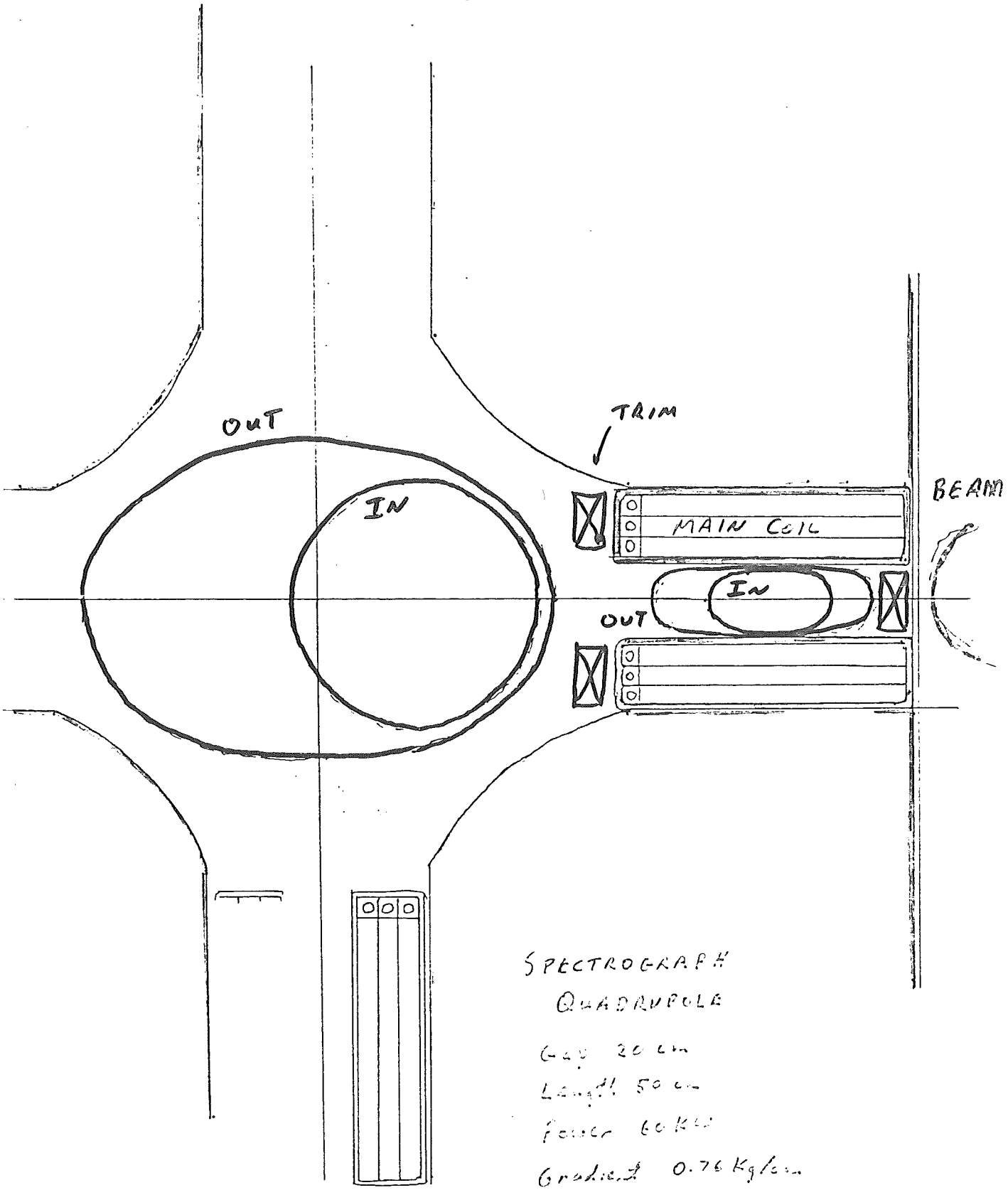

SPECTROGRAPH
QUADRUPOLE

Gap 20 cm
Length 50 cm
Power 60 KW
Gradient 0.76 Kg/cm

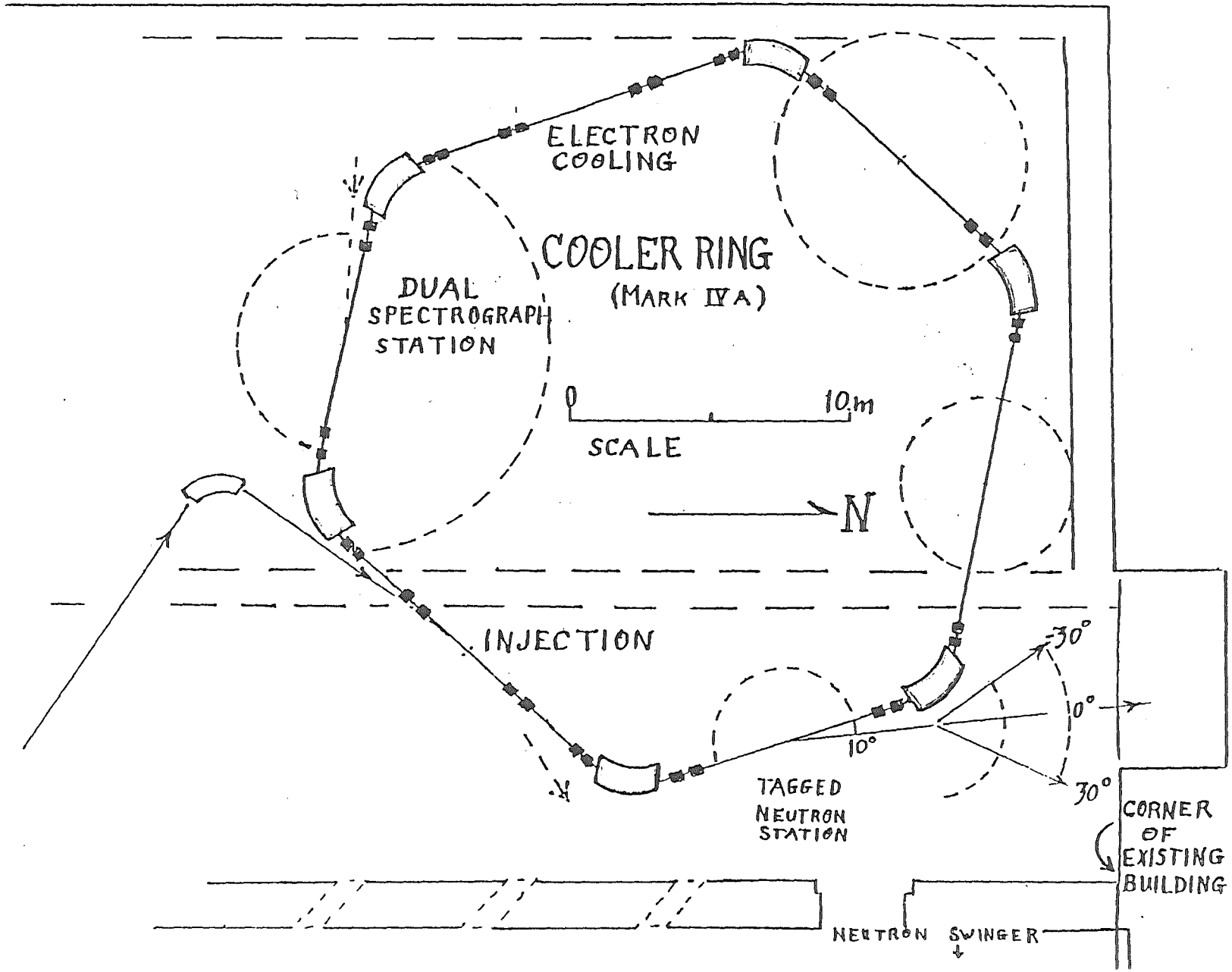
ELECTRON
COOLING
COOLER RING
(MARK IV A)
DUAL
SPECTROGRAPH
STATION
10 m
SCALE
N
INJECTION
30°
0°
10°
30°
TAGGED
NEUTRON
STATION
CORNER
OF
EXISTING
BUILDING
NEUTRON SWINGER

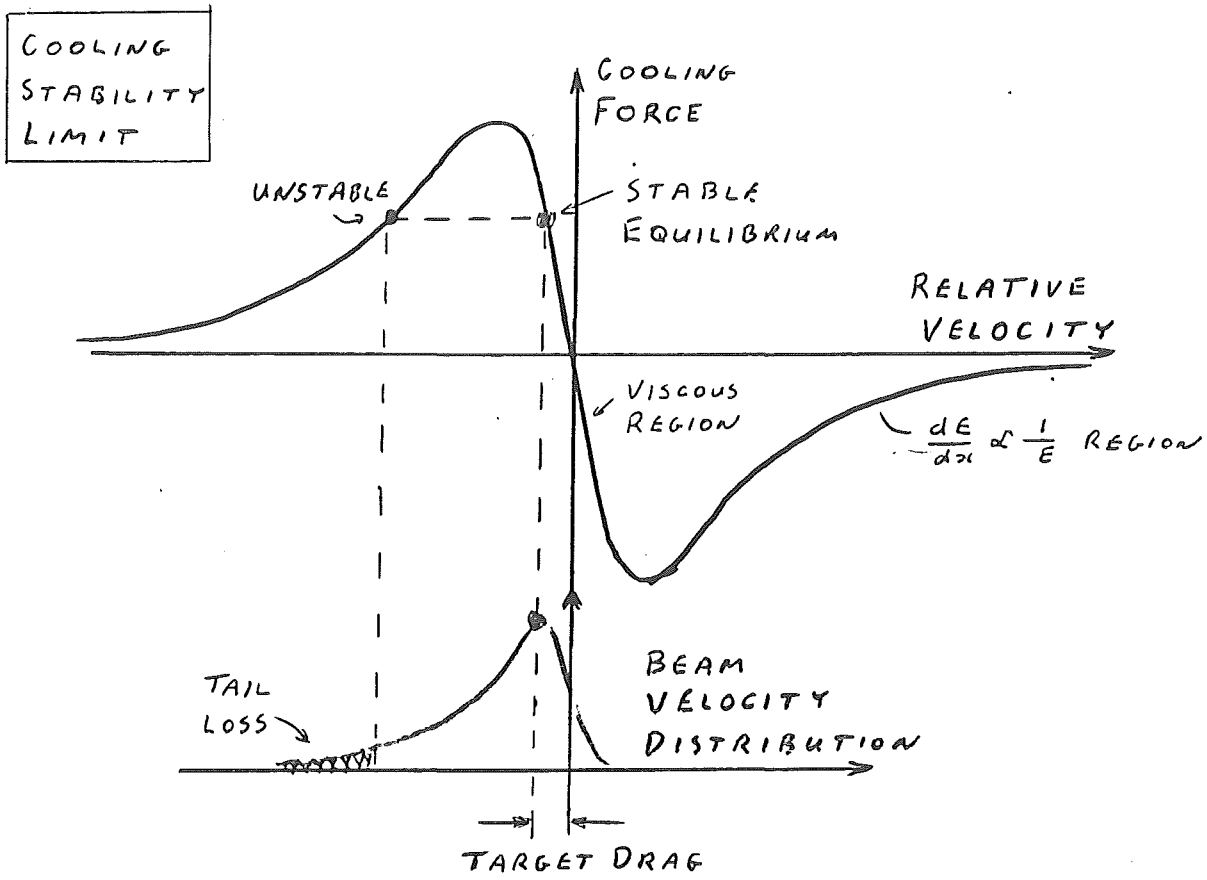
COOLING STABILITY LIMIT
COOLING FORCE
UNSTABLE
STABLE EQUILIBRIUM
RELATIVE VELOCITY
VISCOUS REGION
$\frac{dE}{dx} \propto \frac{1}{E}$ REGION
TAIL LOSS
BEAM VELOCITY DISTRIBUTION
TARGET DRAG

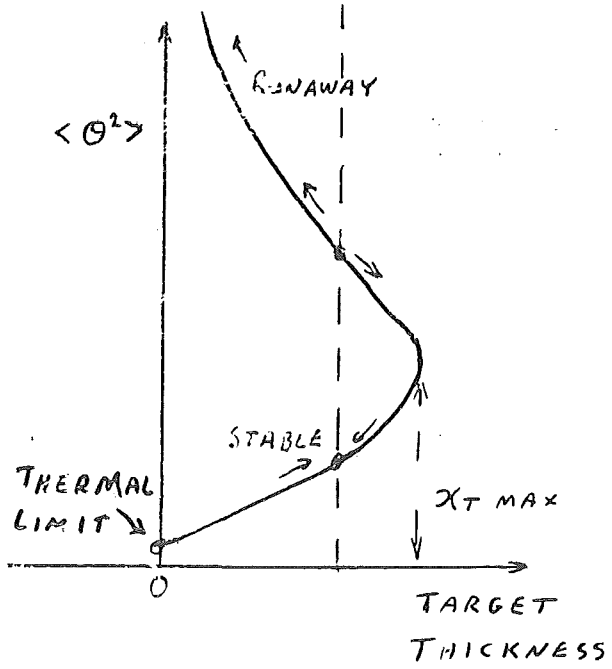
$\langle \theta^2 \rangle$
RUNAWAY
STABLE
THERMAL LIMIT
$x_{T\,MAX}$
0
TARGET THICKNESS

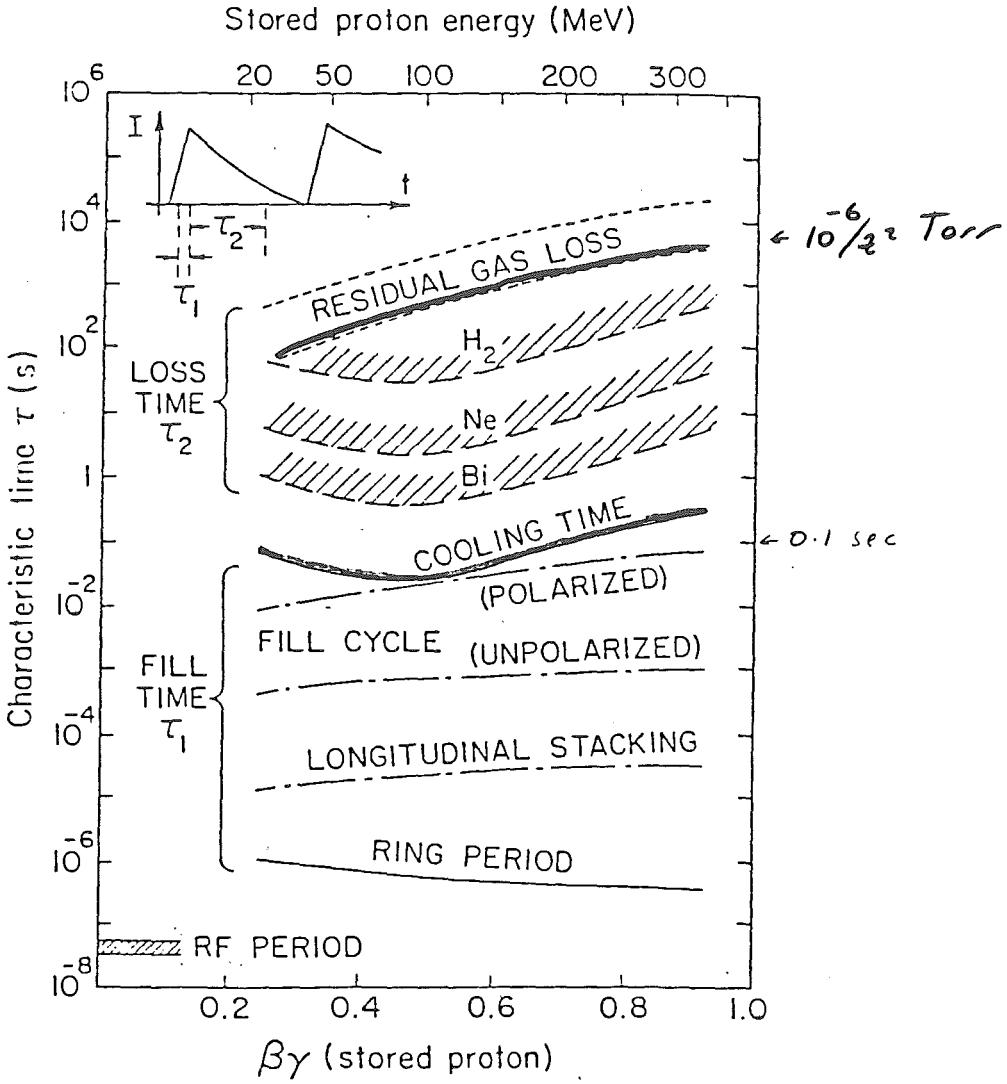

Fig.III-3: Characteristic times for filling and depleting proton current in the Cooler ring. For depletion by target scattering, the lower bound for each of the three materials corresponds to the thickest target that can be cooled. The two curves for beam lifetime in the absence of a target correspond to average ring pressures $p = 10^{-6}/Z^2$ Torr and $10^{-7}/Z^2$ Torr where Z is the atomic number of the residual gas.

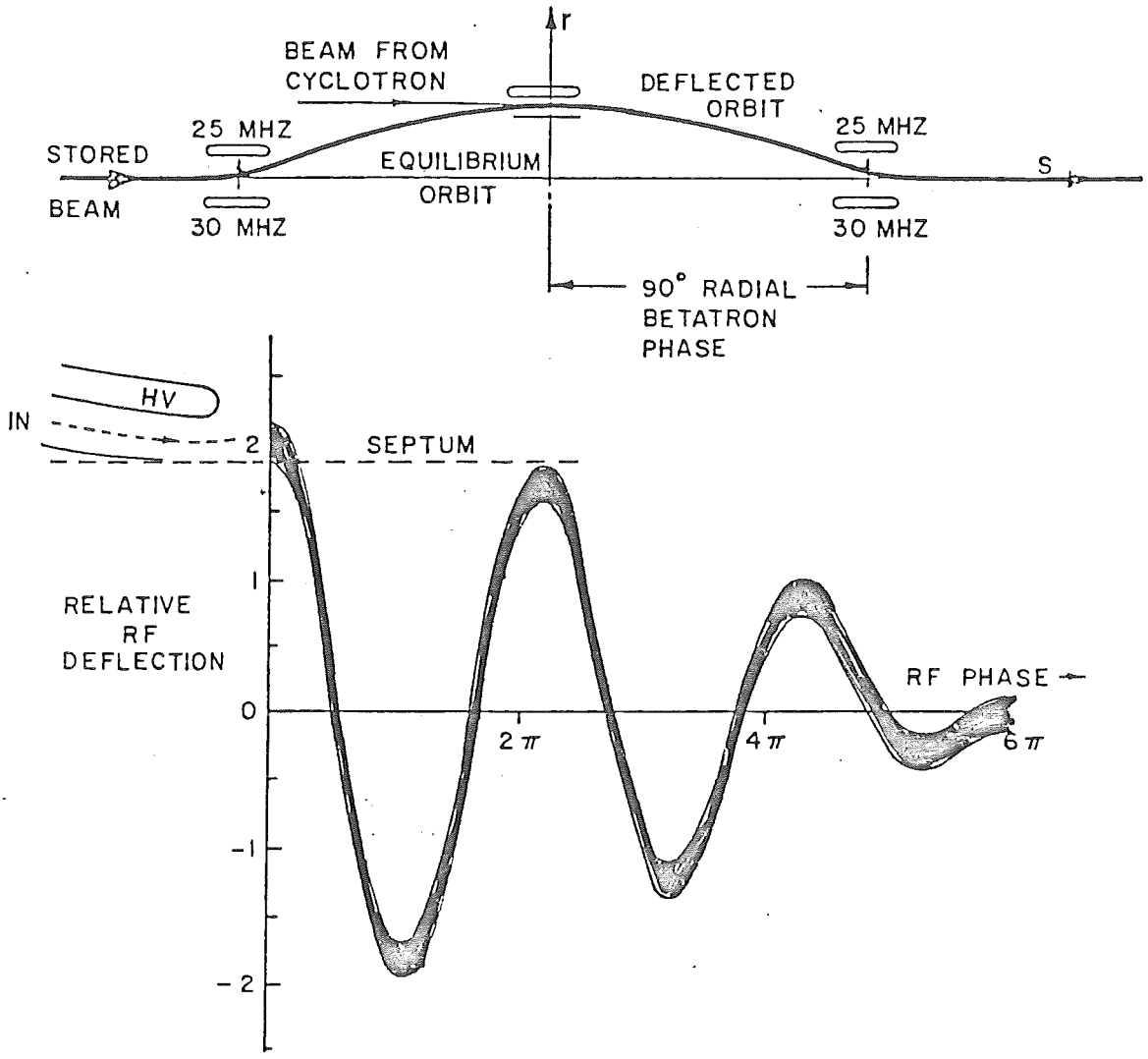

Fig.III-7: Longitudinal stacking scheme.

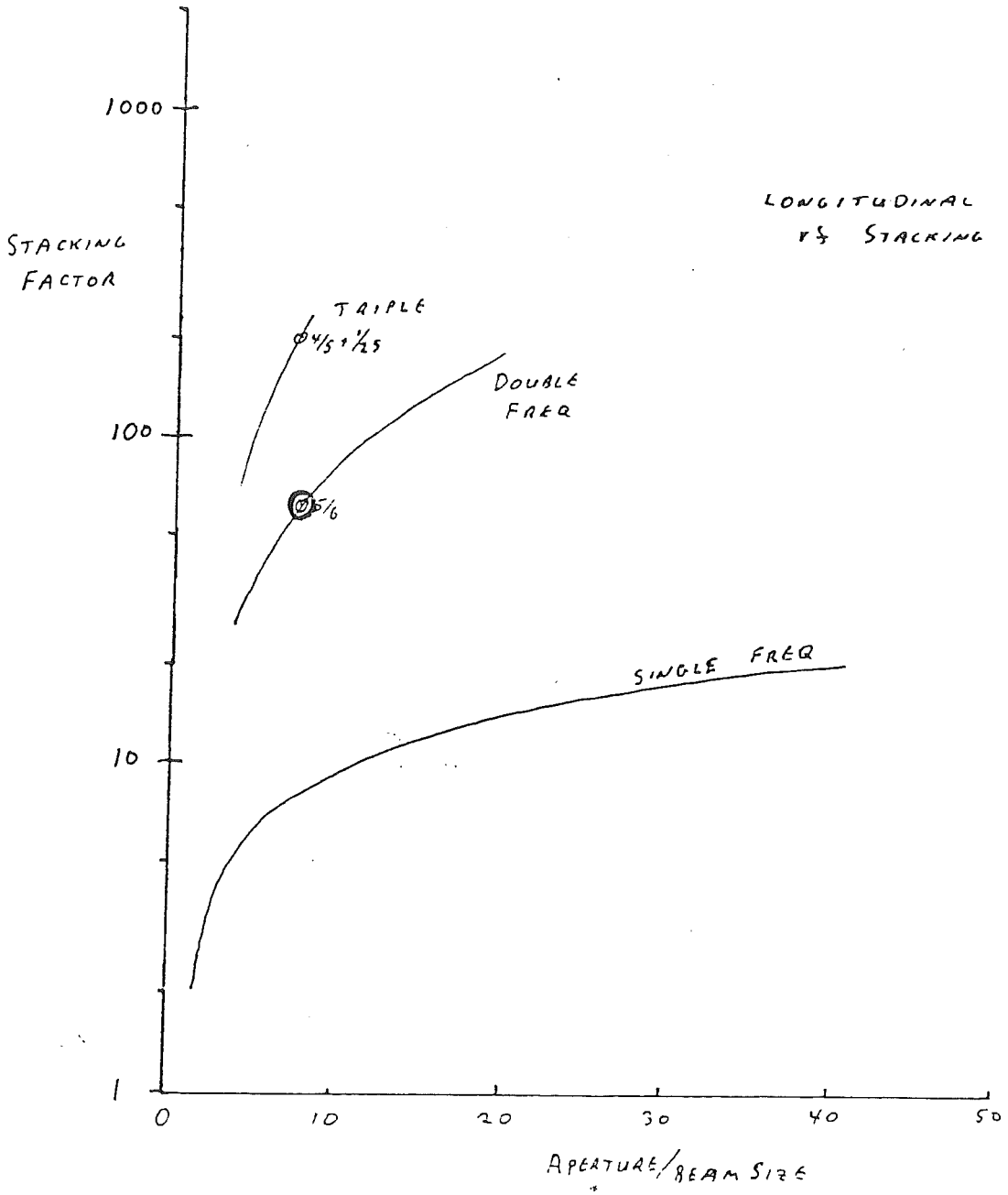
LONGITUDINAL
VS STACKING
STACKING
FACTOR
1000
100
10
1
TRIPLE
Φ4/5 + 1/25
DOUBLE
FREQ
Φ5/6
SINGLE FREQ
0
10
20
30
40
50
APERATURE/BEAM SIZE

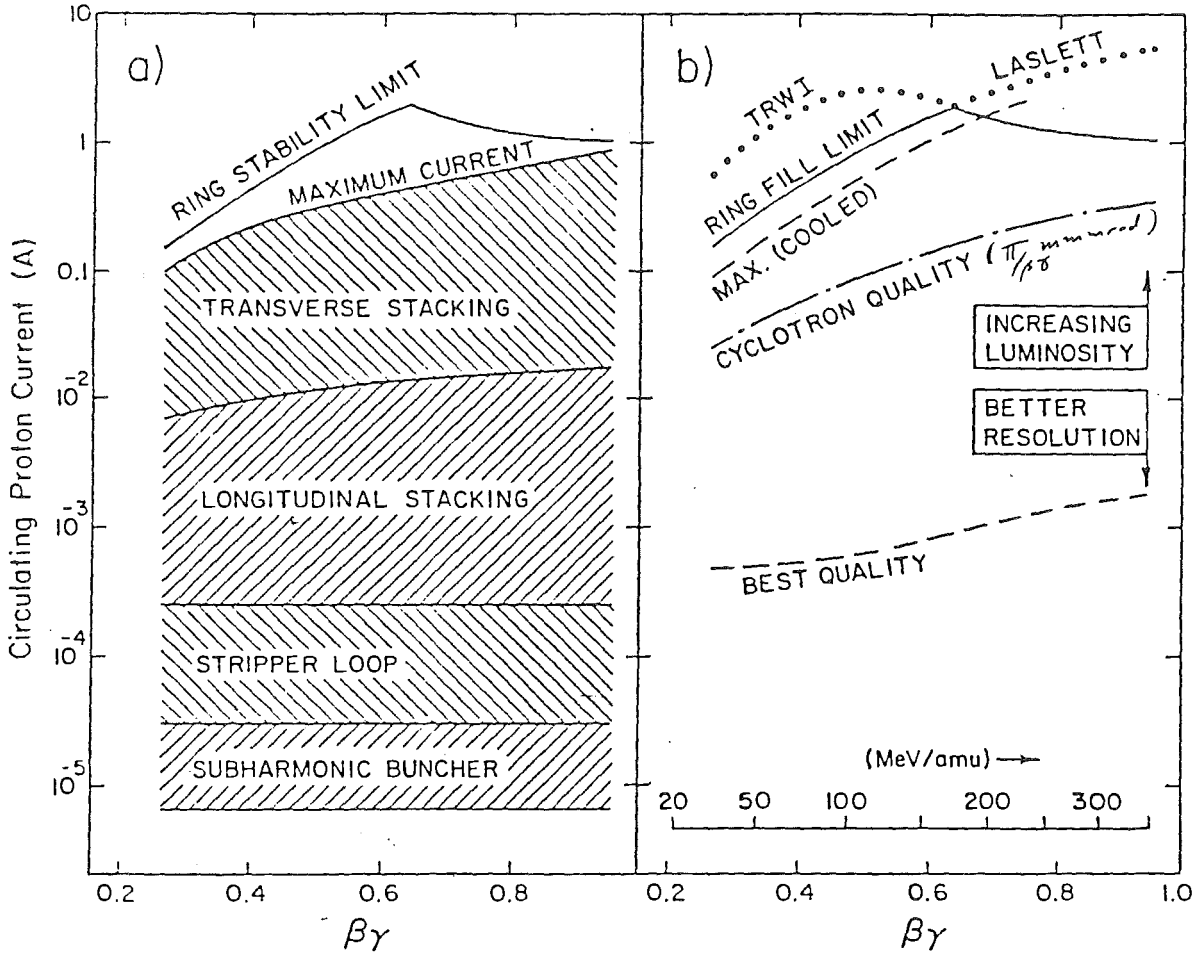

Fig.III-6: Energy dependence of ring proton current limits. On the left is shown the accumulation of current by cyclotron pulse preparation and ring stacking mechanisms. The maximum current approaches the ring stability limit. On the right is shown the effect of beam quality on the space charge limit. The emittance is varied by changing the target thickness.

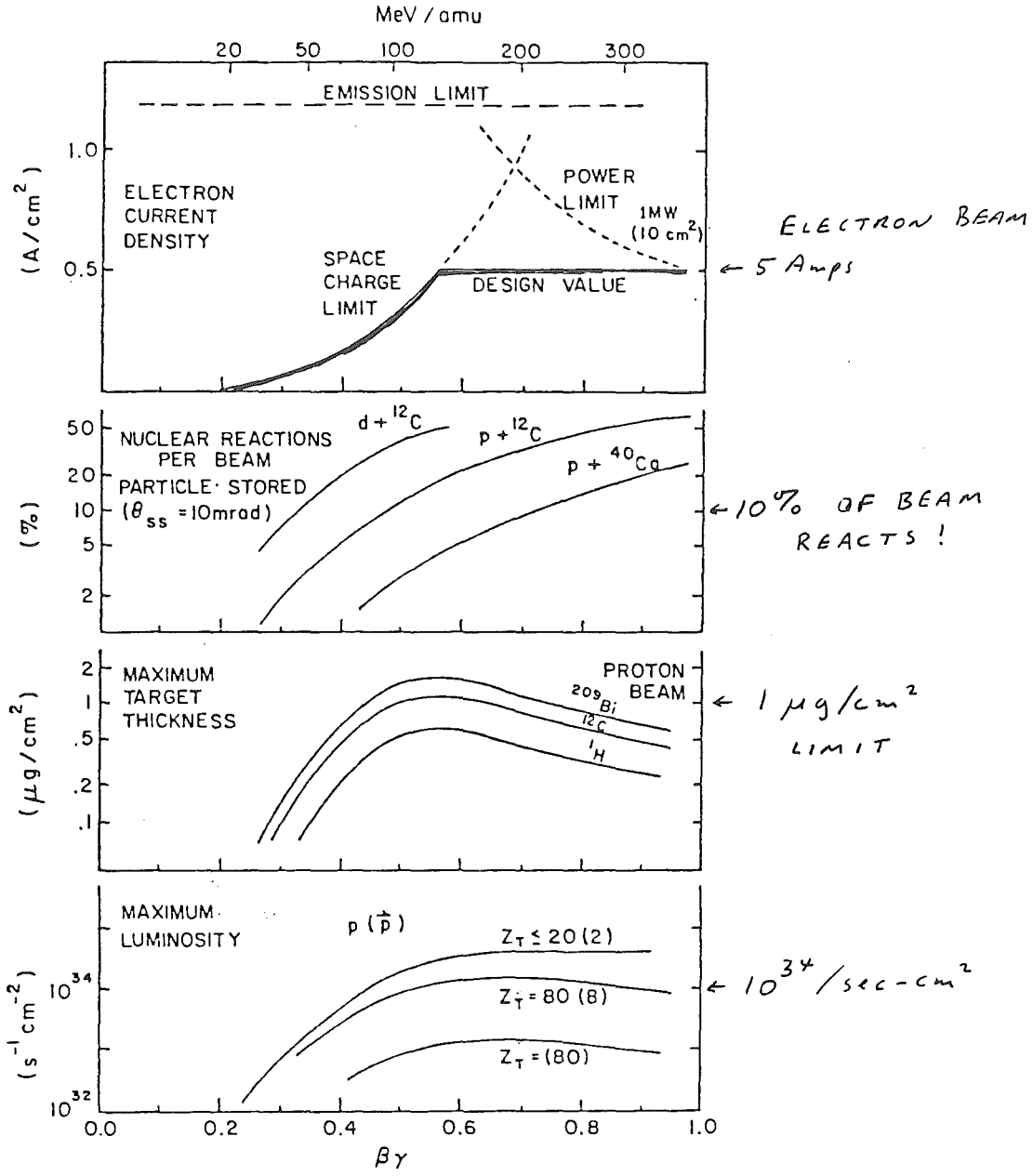

Fig. A-1: Energy dependence of various Cooler parameters.

COOLER RING RESONANCES

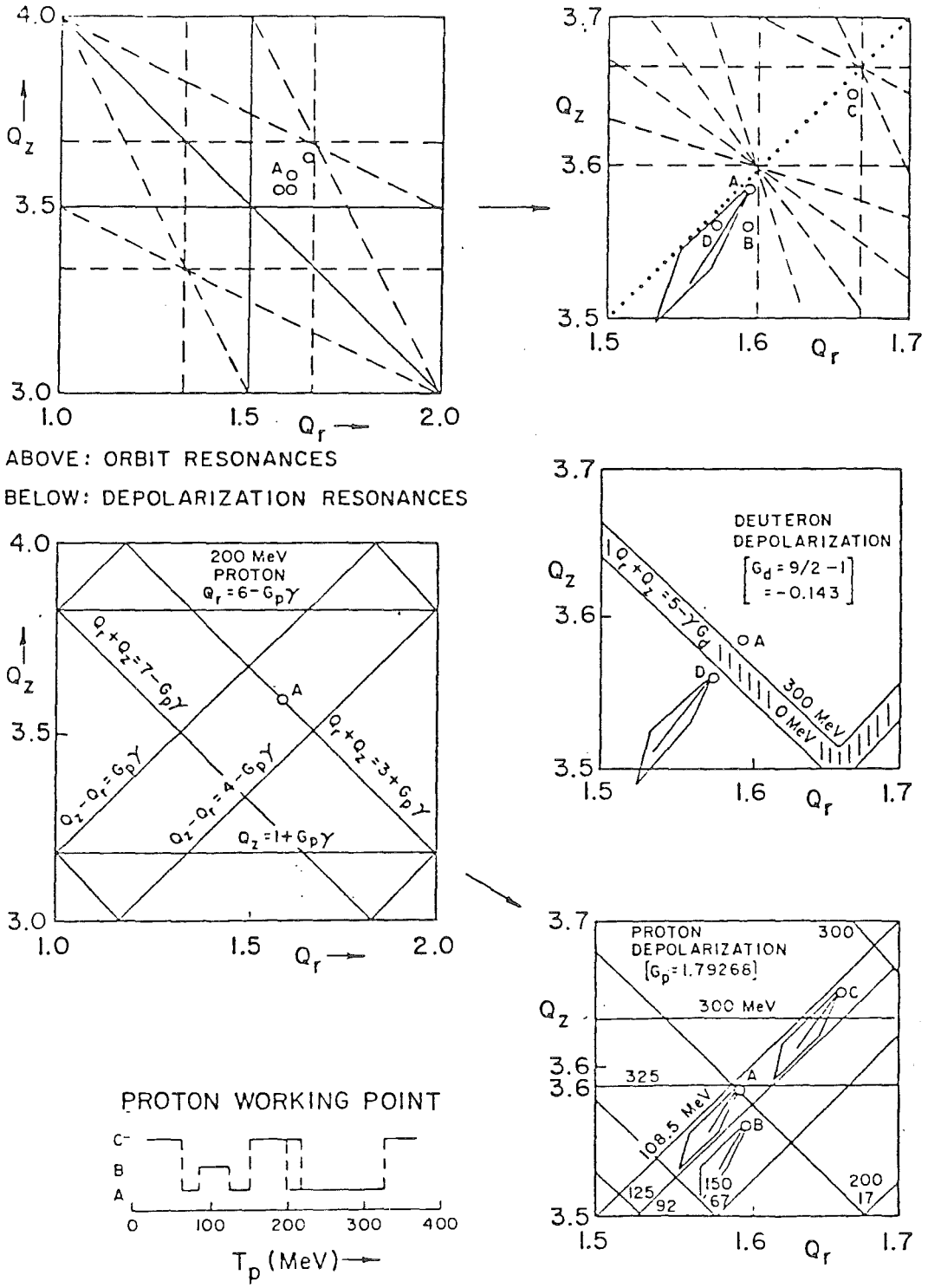

Fig.III-5: Cooler ring resonances.

Electron-cooling in combination with internal targets

H. Poth
Kernforschungsanlage Karlsruhe
and
LEAR-CERN

Electron cooling and internal targets

subjects

- Why electron cooling
- Why internal targets
- Combination electron cooling and internal target; performances

---

- Electron cooling experiments at ICE/CERN and results

- LEAR as a scheme for a highly versatile machine
- LEAR electron cooler
- Possible internal targets
- Other use of LEAR

- Operation of electron cooling for light (heavy) ion beams

Why electron cooling

- very short cooling times
- simultaneous cooling of emittances + momentum spread

Since cooling force increases for decreasing beam temperature (i.e. decreas emittances and momentum spread):

↯ cooling very effective for small beams
↯ rapid cooling of small perturbations ('superfast' cooling)
↯ very small equilibrium values achievable

- no change of operation conditions for change of particles to be cooled
- easy tuning of energy; cooling during acceleration/stacking possible
- acceleration/deceleration of stored beam with electron beam possible; rak ~100keV/se
- fine scan around desired energy
- precise calibration of stored beam energy through e-gun high voltage
- easily applicable at low energies: $\beta \approx \div 0.6$; gets technologically difficult for $\beta \to 0$
- delivers 'slowly extracted beam' through electron recombination with circulating pa

Applications

* phase space reduction of cooled beam ⇒ stacking + accumulation
* small apertures tolerable, when beam cooled (counter in vacuum tube)
* allows deceleration, cools down adiabatic blow up
* counteracting intrabeam, beam-beam interaction ↯ high luminosities
* increase of beam lifetime
* improvement of beam momentum spread ↯ high resolution spectroscopy
* improvement of beam emittances ↯ access to small forward angles
* allows efficient operation of internal target

Ref: G. Budker + A. Skrinsky, Sov. Phys. Uspeki 21 (1978), 277
Novosibirsk group, CERN yellow report 77-08, 1977
M. Bell Part. Acc 10, (1980), 201

Why internal targets

use of very thin ($10^{-9} \div 10^{-12}$ g/cm^2) targets with high efficiency

small target size ∿ well defined interaction vertex
∿ high bVillance

no windows ∿ no background
∿ spectroscopy of heavy particles

low target density; maximal one interaction per passage
∿ no multiple scattering correction: high ang. resol
∿ nearly no energy loss/straggling: high energy resolution

re-use of non-interacting particles ∿ high efficiency (economy)
∿ high count rates

use of polarized atomic beam as internal target:
∿ high polarization
∿ easy and rapid change of polarization direc
∿ pure target

Applications

SPS / CERN: molecular cluster target / polarized atomic beam target
$\bar{p}$/p beam no cooling required

ISR / CERN: molecular cluster target ($\bar{p}$ beam)
no cooling required

Novosibirsk: jet target, e^- storage, cooling by synchrotron radiation

LEAR: molecular cluster target foreseen
at low energies cooling required

Combination: electron cooling – internal target

the operation of an internal target at low energies requires a strong cooling system to compensate emittance blow-up due to repeated passage of beam through target and to compensate energy loss and straggling

- emittance blow-up rate by multiple scattering of protons on H_2 target:

$$\dot{E}_{ms} = \left(\frac{dE}{dt}\right)_{ms} = \frac{19}{\beta^3\gamma^2}\,\hat{\beta}_{H,V}\,\varrho d \quad [\pi\ \text{m rad s}^{-1}]$$

$\hat{\beta}_{H,V}$: beta function at target position

ϱd : target thickness [g/cm^2]

p	ϱd	$\dot{E}_{ms}$ ($\bar{\beta}$=10 m)	dE per sec	$\beta^3\gamma^2$
0.1 GeV/c	$6.5\cdot10^{-11}$ g/cm^2	9.8 π mm mrad s^{-1}	4.8 KeV	$1.2\cdot10^{-3}$
0.2	$5\cdot10^{-10}$	9.0	21	$9.5\cdot10^{-3}$
0.3	$1.2\cdot10^{-9}$	7.0	41	$3.1\cdot10^{-2}$
0.6	$3.8\cdot10^{-9}$	3.1	82	$2.2\cdot10^{-1}$
1.0	$5.0\cdot10^{-9}$	1.1	82	$8.3\cdot10^{-1}$

cooling reduces beam emittances according to $\left(\frac{dE}{dt}\right)_c = \dot{E}_c = -\frac{2}{\tau_c}E$

balancing blow-up and cooling: $\dot{E}_{ms} + \dot{E}_c = \frac{dE}{dt}$

$$E(t) = \left[1 - e^{-\frac{2t}{\tau_c}}\right]\frac{\tau_c\,\dot{E}_{ms}}{2} + E_0\,e^{-\frac{2t}{\tau_c}}$$

equilibrium emittance: $\boxed{E_{eq} = \frac{\tau_c}{2}\,\dot{E}_{ms}}$

Since $\tau_c \geq 1$ s the maximal admissible target thickness is for $E_{eq} = 1\pi$ mm mrad and low beta $\hat{\beta} = 1$ m:

$$\Rightarrow\ \boxed{\varrho d_{max}(H_2) = 0.1\cdot\beta^3\gamma^2\cdot10^{-6} \leq 10^{-9}\ \text{g/cm}^2}$$

M. Giesch, J. Gopann, K. Kilian, P. Lefèvre, D. Möhl, H. Poth, P. Riboni, CERN PS/DL Note 81-4/ KfK-Primärbericht 11.01.02P1

Ref.: J. Gopann, H. Poth, KfK-Report 3198, Karlsruhe, 1981.

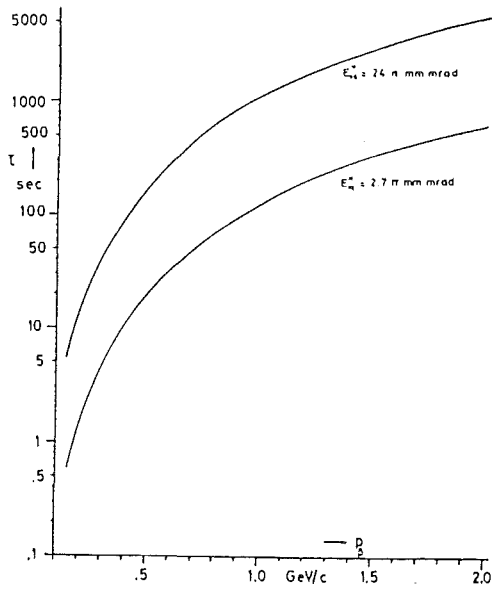

Required cooling times to obtain a horizontal equilibrium beam emittance of 24 π mm mrad and 2.7 π mm mrad respectively when operating with a $2 \cdot 10^{-10}$ g/cm^2 thick internal target (from Ref. 22). $\hat{\beta}_H = 10$ m

* Optimal target thickness + reaction rates *

beam decay time due to interactions in the target:

$$\tau_\ell = \frac{1}{\sigma_{tot} \cdot L/A \cdot \varrho d \cdot f}$$

f: beam revolution frequency

L: Avogadro's number

A: atomic number

$\sigma_{tot} = \sigma_{Strong} + \Delta\sigma_{Rutherford}$ $\quad \Delta\sigma_{Ruth.}(\theta_0)$: cross section for Rutherford scattering larger than angle θ_0

---

reaction rate R for a given reaction with cross section σ_1

$$R = N_0 \cdot L/A \cdot \sigma_1 \cdot \varrho d \cdot f$$

N_0: number of stored particles

$I = e \cdot f \cdot N_0$: circulating current

$$\Rightarrow \boxed{R = \frac{N_0}{\tau_\ell} \cdot \frac{\sigma_1}{\sigma_{tot}}}$$

in ideal case highest average count rates for $\frac{N_0}{\tau_\ell}$ = particle accumulation rate

i.e. for primary particle beams: N_0 = space charge limit,

$\tau_\ell \approx \tau_f$ = filling time to reach space charge limit

in most cases $\tau_{filling} \ll \tau_{cooling}$

$\rightsquigarrow$ for high resolution spectroscopy ϱd determined by E_{eq}:

$$\varrho d = \frac{0.1\,\beta^3\gamma^2 \cdot 10^{-6} \cdot E_{eq}}{\hat{\beta} \cdot \tau_c} \quad (\text{for } H_2)$$

$$\Rightarrow \tau_\ell = \frac{\hat{\beta} \cdot 10^7 \cdot \tau_c}{\sigma_{tot} \cdot L \cdot f \cdot \beta^3\gamma^2 \cdot E_{eq}} \quad \approx \quad 10^3 \div 10^4 \text{ sec}$$

$\Rightarrow$ count rate for 70 mA circulating beam

$$\boxed{R = \frac{\sigma_1}{\sigma_{tot}} \cdot [10^7 \div 10^9] \quad s^{-1}}$$

e.g. p-p at 500 MeV/c : $\sigma_{tot} \approx 100$ mb

$R = 0.1 \div 1\ s^{-1}$ for $\sigma_1 = 1$ nb

Achievable energy resolution

Attention: for intense beams blow-up of momentum spread by intrabeam scattering (particularly for small beams)

– counteraction through longitudinal electron cooling

$\Rightarrow$ equilibrium momentum spread depends on stored particle intensity

roughly :

N_0	$\Delta p/p$
10^7	$\sim 10^{-5}$
10^9	$\sim 10^{-4}$

<u>consequence:</u> define experimental needs

$\Downarrow$

E_{eq}, $\Delta p/p$

$\Downarrow$

chose : ϱd, N_0

Electron cooling experiments in ICE *

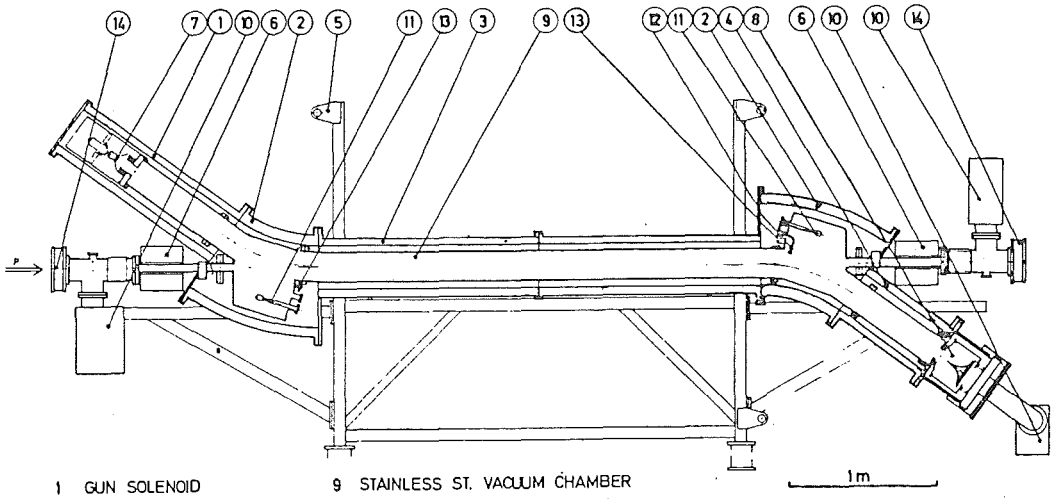

1 GUN SOLENOID
2 TOROID
3 CENTRAL SOLENOIDS
4 COLLECTOR SOLENOID
5 SUPPORTING FRAME
6 CORRECTION MAGNET
7 ELECTRON GUN CATHODE
8 COLLECTOR
9 STAINLESS ST. VACUUM CHAMBER
10 VACUUM PUMP (SPUTTER-ION)
11 VACUUM PUMP (Ti-SUBLIMATION)
12 SYNCHROTRON RADIATION ANTENNA
13 VIEWING PORT
14 SECTOR VALVE

The ICE electron cooling apparatus

1 ELECTRON COOLING DEVICE
2 HIGH VOLTAGE SUPPLY
3 FARADAY CAGE
4 TRANSFER LINE
5 INFLECTOR
6 FULL APERTURE KICKER
7 BEAM PROFILE MONITOR (HORIZ.)
8 BEAM PROFILE MONITOR (VERT.)
9 SCRAPER (HORIZ.)
10 SCRAPER (VERT.)
11 WIRE CHAMBERS
12 R.F. CAVITY
13 WIDE BAND KICKER (LONG.)
14 SCHOTTKY NOISE PICK-UP (LONG.)

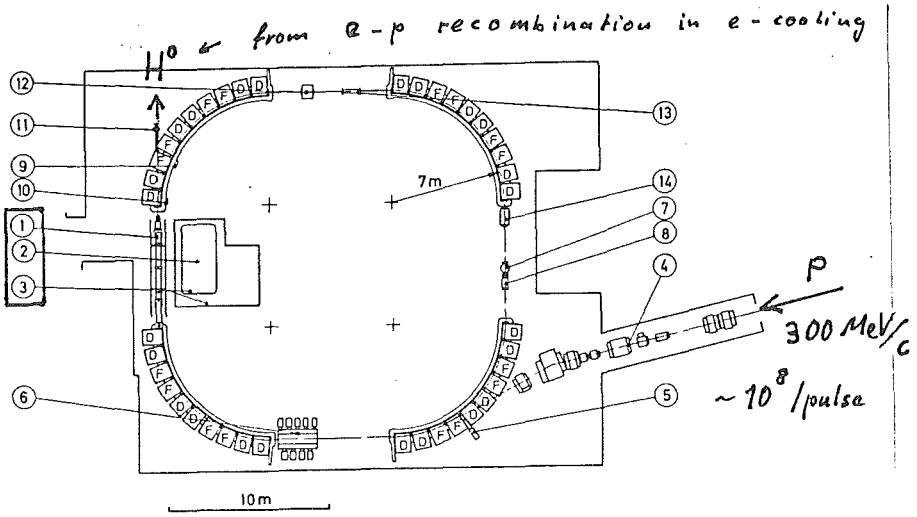

The ICE storage ring

* M. Bell et al. Phys. Lett. 87B, 275 (1979)
M. Bell et al. Nucl. Instr. Meth. 190, 237 (1981)

goals of the experiment

- production of cold electron beam:
  ∴ small longitudinal velocity spread ∧ 'flattened' distr.
  ∴ small transverse velocity spread, (flat cathod, high quality fie.
  ∴ efficient recuperation of power

- establish cooling

- determination of transverse damping rates for various conditions (e- current, amplitudes, ring working point)

- determination of longitudinal cooling rates for various conditions

- measurement of longitudinal frictional force

- determination of equilibrium values for various conditions (e.g. stored beam intensity)

- cooling studies of bunched beams

- stacking and accumulation

after matching velocities
immediate observation of cooling

increase of beam lifetime
by a factor of 10 - 40

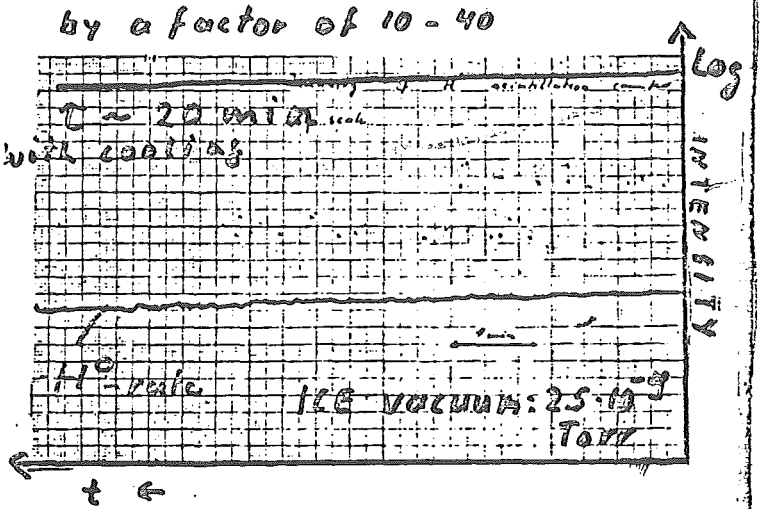

best results $\tau_{1/e}$ ~ 140 min

reduction of momentum spread

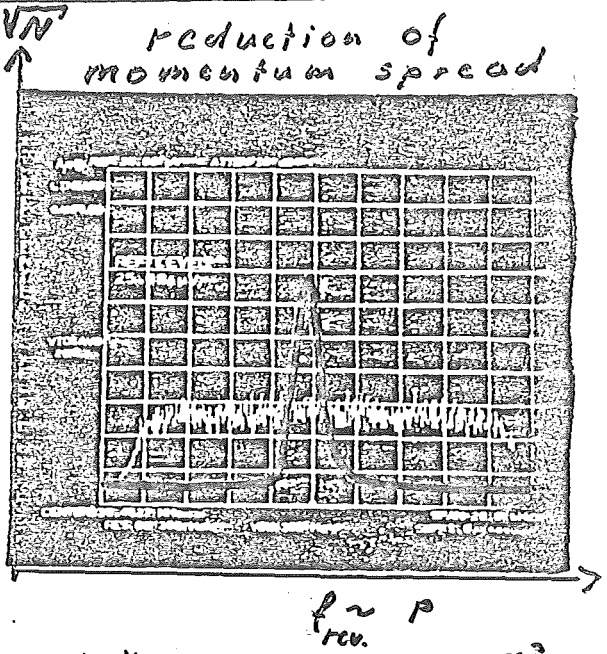

initially $\Delta p/p = 1.8 \cdot 10^{-3}$

after cooling $\Delta p/p = 2. \cdot 10^{-4}$

cooling of newly injected beam

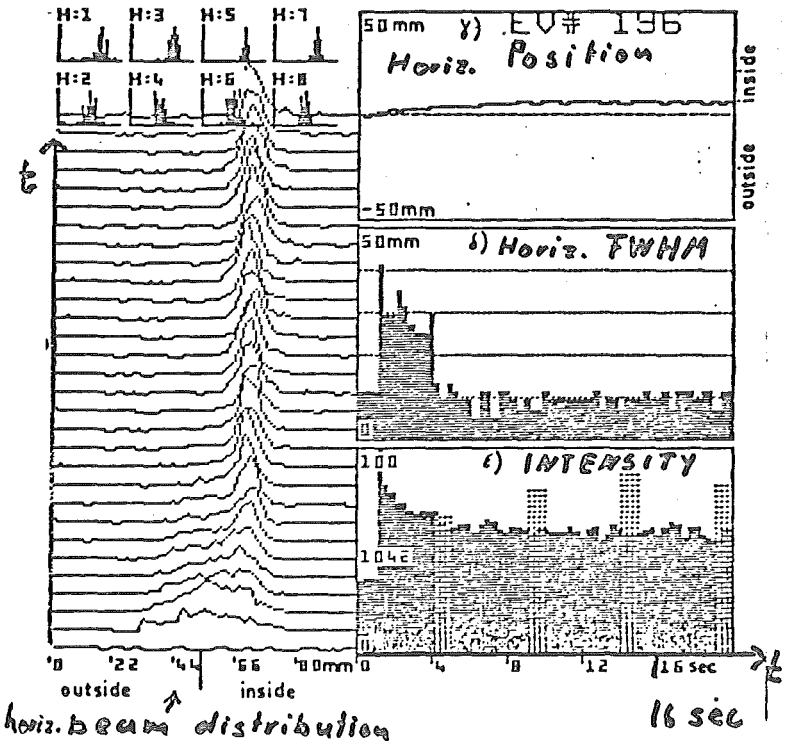

horiz. beam distribution every 400 ms

16 sec

neutral hydrogen (H^0 from e-p recombination)
beam profiles

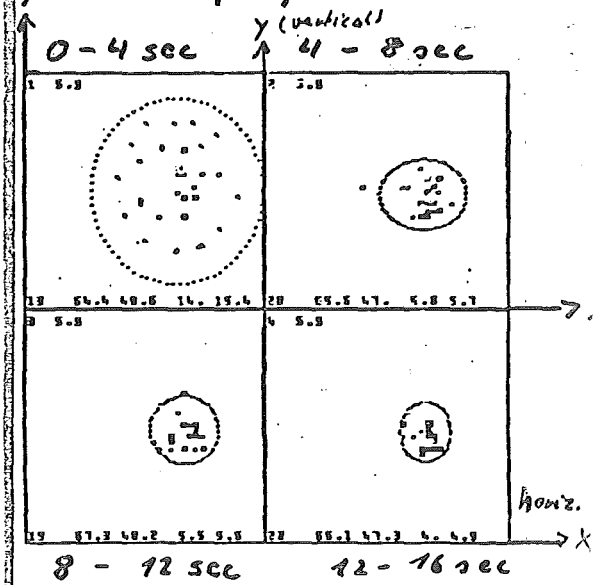

⇒ beam divergence < 0.5 mrad

detailed investigation of cooling process

- investigation of betatron oscil. cooling → transverse cooling times
- momentum cooling, acceleration, deceleration → measurement of frictional force $F_{\parallel} \sim \frac{1}{\Delta p}$
- measurements for different currents and working points of IUE (above, below transition), coupling and damped beams; different proton intensities; stacking and accumulation
- determination of e-beam characteristics → $\tau_{e\parallel}$ i $\tau_{e\perp}$

Excitation and damping of betatron oscillations

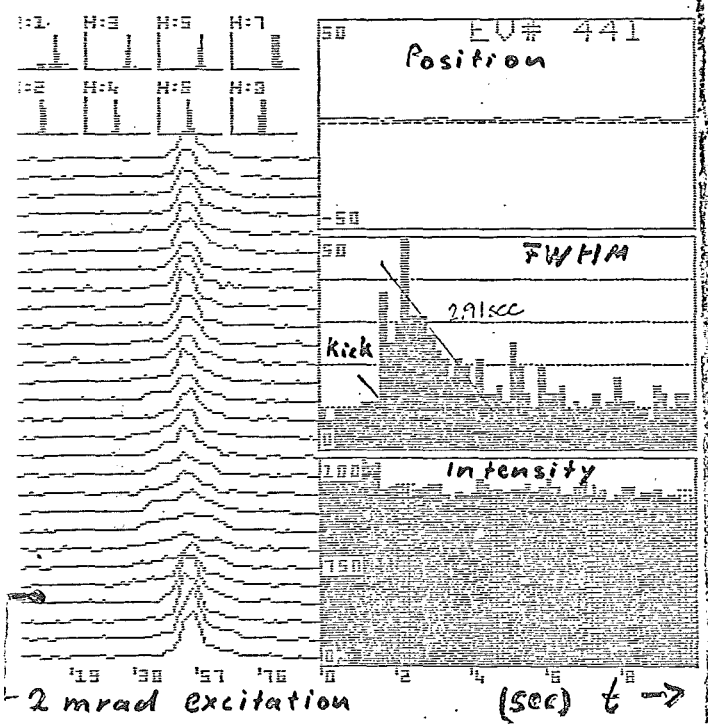

measurement of $F_{\parallel}$:
high voltage step: 120V, 5 sec

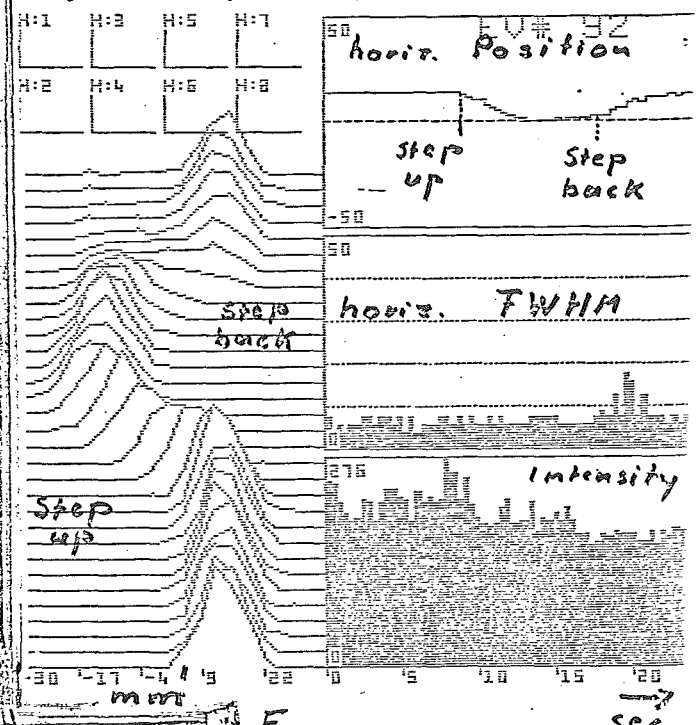

MEASUREMENTS OF TRANSVERSE COOLING TIMES

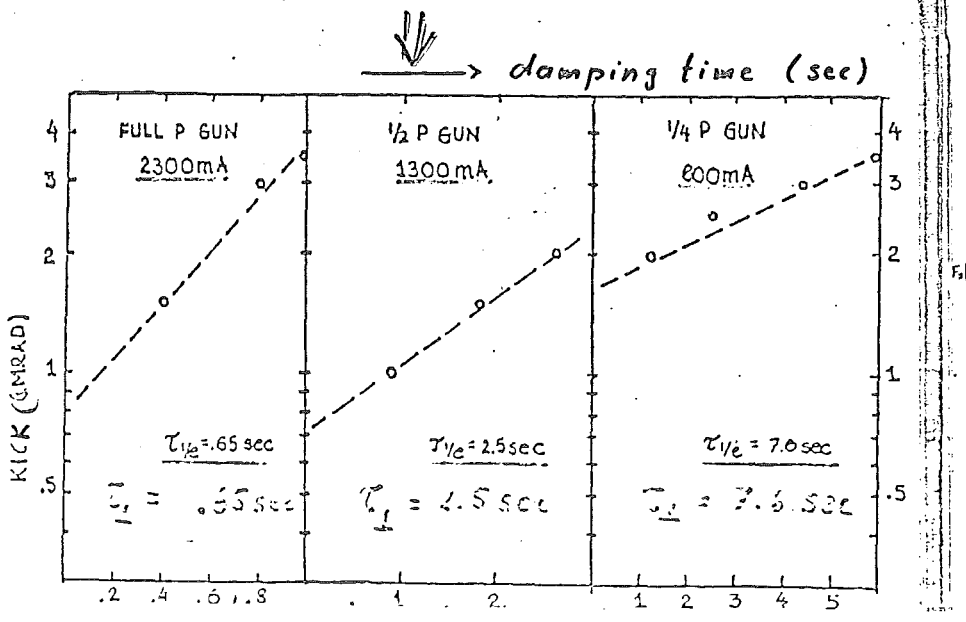

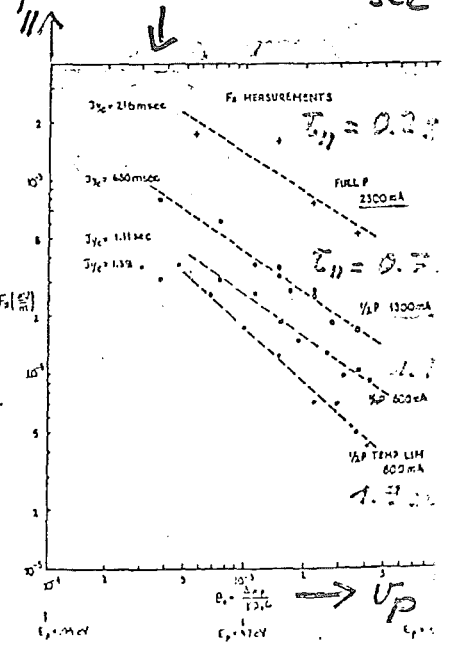

stacking and accumulation

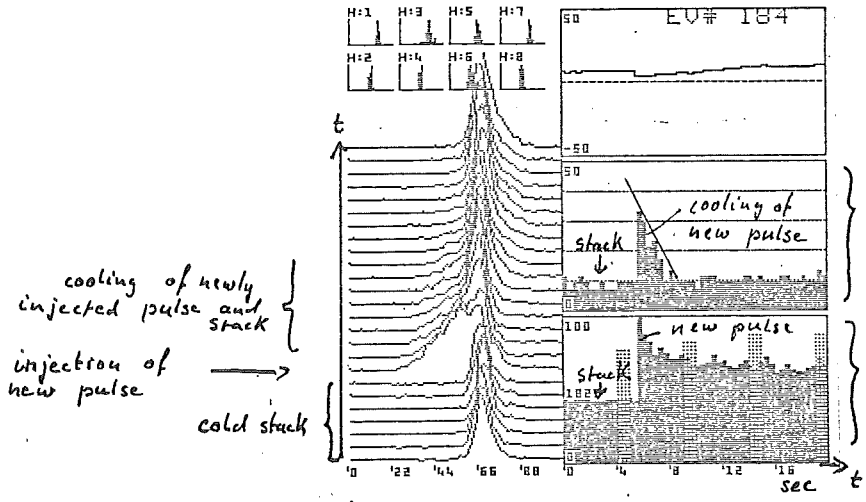

cooling of newly injected pulse and stack

injection of new pulse →

cold stack

horiz. beam profiles (scans every 400 ms)

FWHM of horizontal beam distribution as a function of time

stored beam intensity as a function of time

bunching factor 0.4

accumulation (continuous cooling of bunched beam)

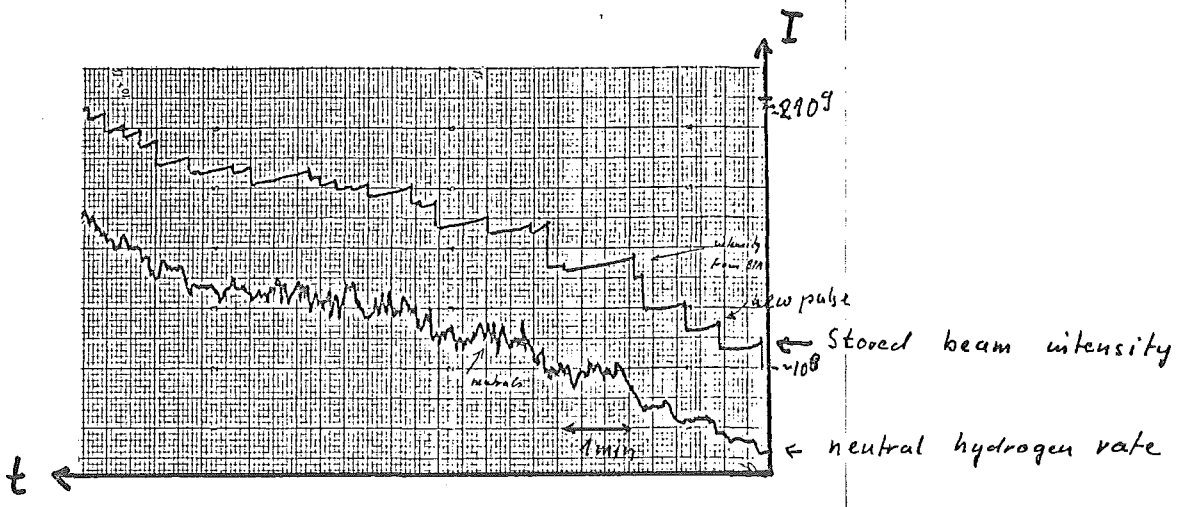

← Stored beam intensity

← neutral hydrogen rate

observation of self bunching (above transition)

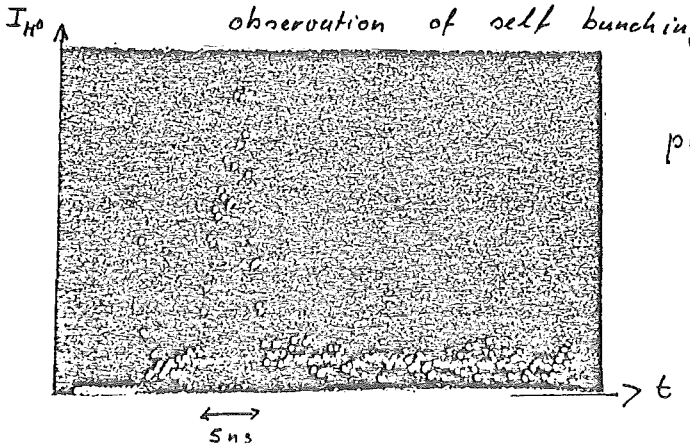

pulsed H^0 rate

Summary of ICE experiments

typical operation conditions

gun high voltage (electron energy)	:	26 KV (stability : $5 \cdot 10^{-5}$)
corresponding proton momentum	:	300 MeV/c (50 MeV)
electron beam current	:	2.3, 1.25, 0.6 A
stored proton beam intensity	:	$10^7 \div 10^9$
electron beam diameter	:	5 cm
collector high voltage	:	95 % of gun high voltage
collection efficiency	:	$\leq$ 98 %
solenoid field	:	~ 500 G
transverse electron temperature	:	0.2 eV $\quad \Theta_e \simeq 2 \cdot 10^{-3}$
average ICE vacuum	:	$2 \cdot 10^{-9}$ Torr N_2

momentum cooling times	:	0.2, 0.7, 1.1 s
transverse cooling times	:	0.7, 2.5, 7.6 s
equilibrium momentum spread	:	$4 \cdot 10^{-5} \div 6 \cdot 10^{-4}$
equilibrium beam size	:	$\leq$ 1 mm x 3 mm (hor x vert
equilibrium beam divergence	:	$\leq$ 0.3 mrad
equilibrium beam emittance	:	$\leq$ 1 (3) π mm mrad (vert.,
neutral hydrogen rate (for 10^9 p)	:	~ 400 s^{-1}
average beam lifetime	:	~ 30 min

$\therefore$ <u>note</u>: vacuum of $2 \cdot 10^{-9}$ Torr N_2 in ICE corresponds to

$$\varrho d = \varrho_0 \frac{p}{p_0} \cdot 2\pi R \cdot \underset{\uparrow}{49} \; (Z^2) = 9 \cdot 10^{-5} \cdot \frac{2 \cdot 10^{-9}}{760} \cdot 78 \cdot 10^3 \cdot 49 \; g/cm^2 \; H_2$$

an **internal target of ~ 10^{-9} g/cm² H_2**

Computer simulation of electron cooling

goals:
- reproduction of ICE experimental results
- detailed prediction for evolution of beam emittances and momentum spread for a given ring lattice and e-beam characteristic
- optimisation of cooling
- optimisation of cooling with internal target operation

method:
take representative ensemble of stored particles
calculate coordinates in cooler
calculate average cooling force for each particle
calculate emittance blow up and energy loss due to residual gas / internal target
calculate emittance blow up and momentum blow up due to intra beam scatt.
circulate particles with help of lattice functions and repeat calculations
find equilibrium values

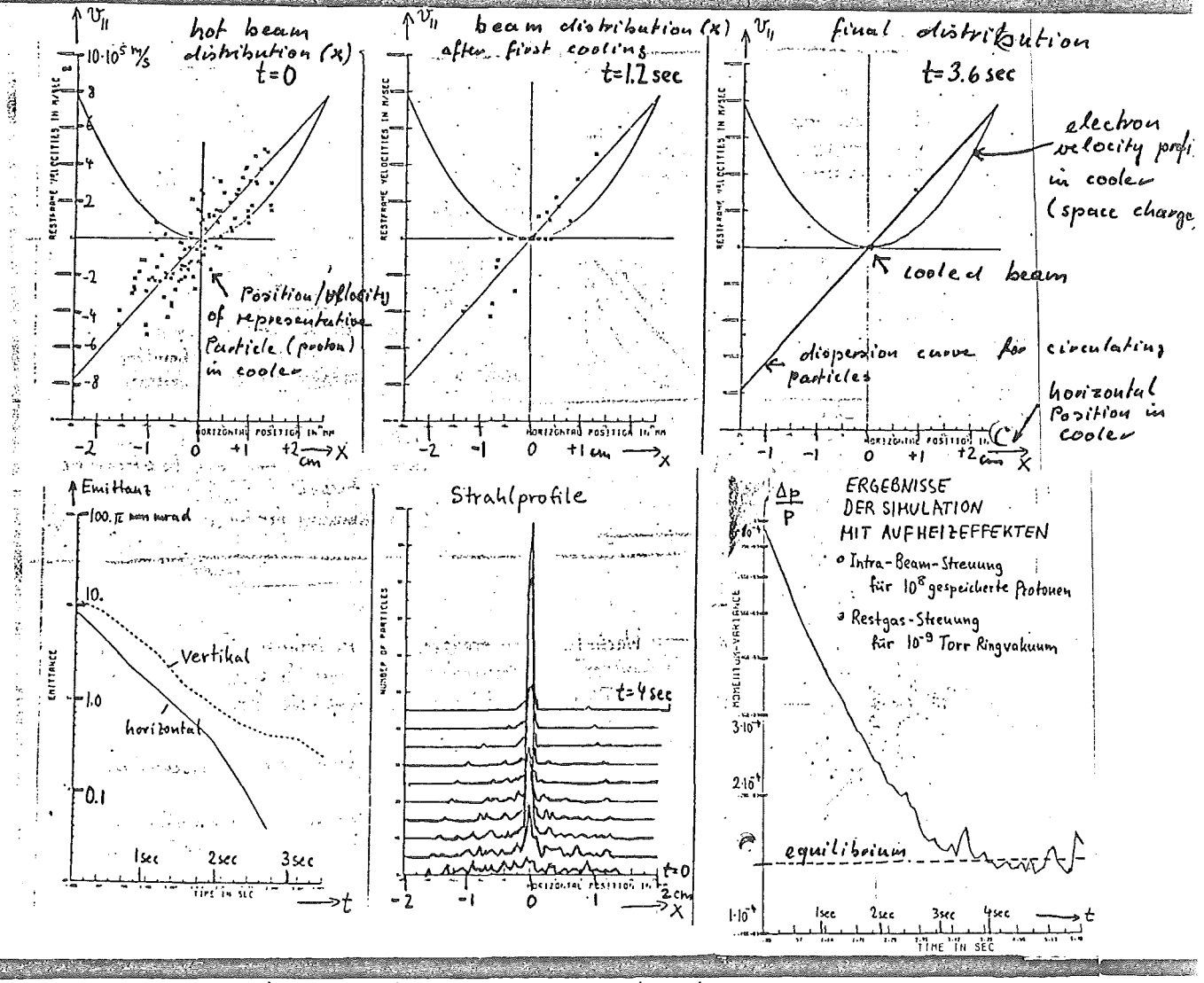

M. Bell, Cooling in ICE, CERN EP internal report 79-10, 1979

Ref.: A. Wolf, H. Poth, Germ. Phys. Soc. Meeting, March 1982

The Low Energy Antiproton Ring

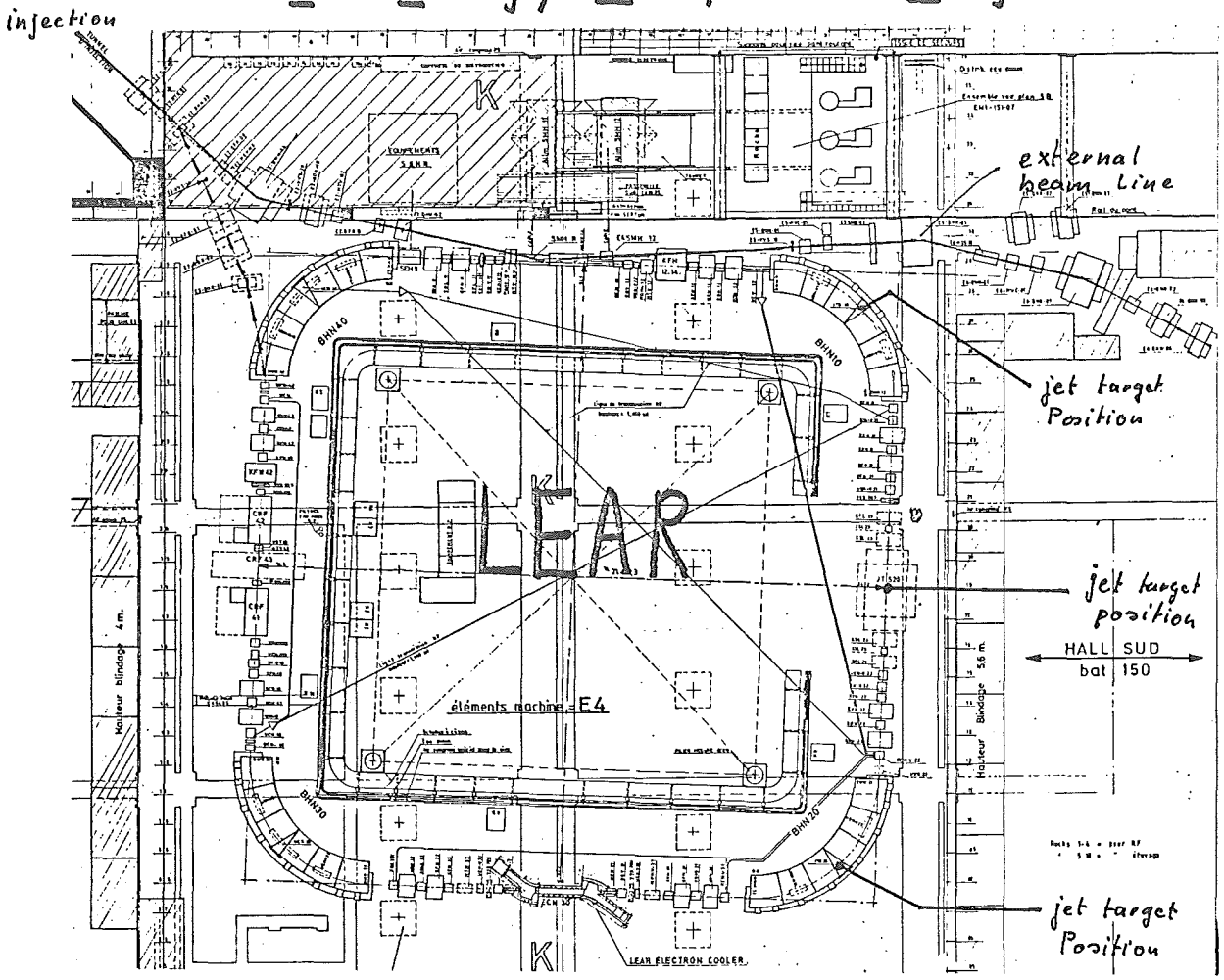

Synchrotron / Storage Ring

- range of operation : 0.1 GeV/c ÷ 2 GeV/c
- $\bar{p}$ injection momentum : 0.6 GeV/c
- p, H^- (from Linac I) injection momentum : 0.3 GeV/c
- operation modes : at all momenta
  - stretcher → Ultra slowly extracted beam, spill 10^3 s, 10^6 $\bar{p}$/s cl.
  - recirculator → Operation of internal target(s)
  - collider → simultaneous circulation of p and $\bar{p}$.

  between 0.3 - 0.5 GeV/c $\bar{p}$ H^- co-rotation → formation of neutral $\bar{p}p$ atoms in flight
- cooling systems : stochastic cooling at injection energy and above
  electron cooling at 0.1 - 0.37 (0.6) GeV/c

LEAR design report CERN/PS/DL 80-7
P. Lefèvre et al., Proc 11th Conf. on High Energy Accelerators, Geneva 1980

Ref.: Proc. Workshop on Physics with cooled low energetic Antiprotons, Karlsruhe, KfK report 283 1979
Proc. 5th European Symposium on $\bar{N}N$ interactions, Bressanone, 1980
Proc Workshop on Physics with low energy antiprotons at LEAR, Erice 1982

Electron cooling in LEAR

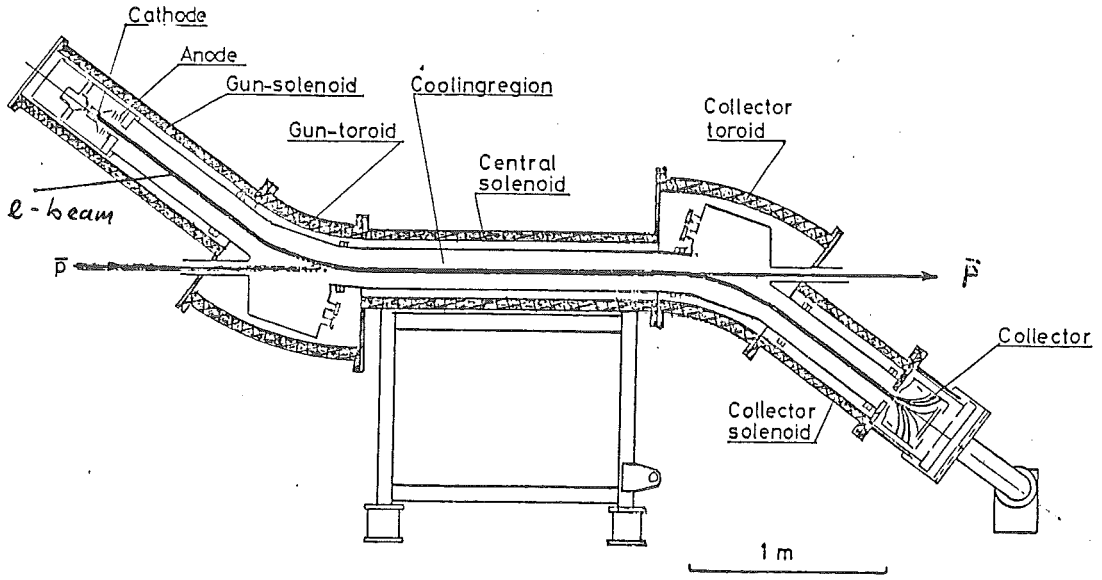

LEAR Electron cooler

- range of operation: 2.9 ÷ 40 KV (later 100 KV) $\beta = 0.1 - 0.37 (0.5$
  corresponding $\bar{p}$ momentum: 0.1 ÷ 0.37 GeV/c (0.63 GeV/c)
- electron current : 0.1 ÷ 5 A (20 A)
- electron beam size ϕ : 5 cm (1 cm)
- length of cooling region : 1.5 m = 2% of LEAR circumferen
- magnetic field : ÷ 1.5 kG
- recuparation efficiency : $1 - 10^{-3}$
- vacuum with cold cathode : $\sim 2 \cdot 10^{-12}$ Torr

applications: cooling in stretcher mode: small beam for extraction + further deceleration
cooling with internal target operation
cooling in co-rotating beam mode

particles to be cooled: $\bar{p}$, H^-, p

Ref.:
H. Haseroth, Ch. Hill, P. Møller-Petersen, H. Poth; CERN/PS/LR/Note 80-7, KfK – Primärbericht 11.01.02P07
L. Hütten, H. Poth, A. Wolf, H. Haseroth, Ch. Hill; Proc. Workshop on Physics with Low energy antiprotons at LEAR, Erice, 1982
CERN/PS/LI 82-9

A possible internal target for LEAR

molecular hydrogen cluster beam

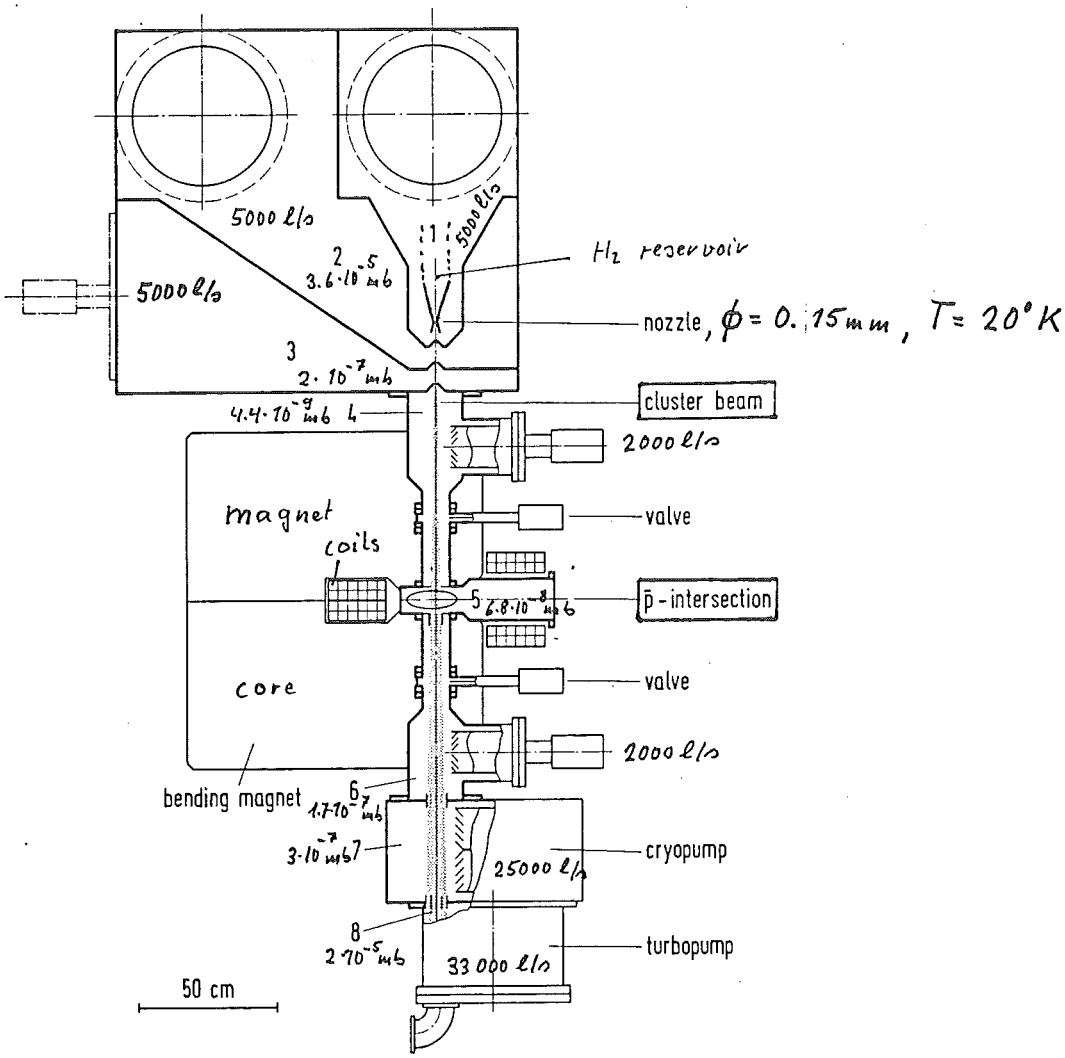

<u>advantages of cluster beams</u> (H_1, D, He ....):

- high densities ; high directivity of mass flow
- sharply bounded intensity (beam) profiles ⇝ least possible gas load on accelerator vacuum

<u>properties of above target</u> :

cluster beam intensity : 10^{22} H_2 / sterad·s ⇒ $2 \cdot 10^{10}$ g/cm² H_2

cluster beam size at $\bar{p}$ beam intersection : 40 × 40 mm² (could be ≤ 10 × 10 mm²)

pressure bump around target : 2 % of target thickness

Ref.: J. Gspann, H. Poth, KfK report 3198, 1981

Operation criteria for internal target in LEAR

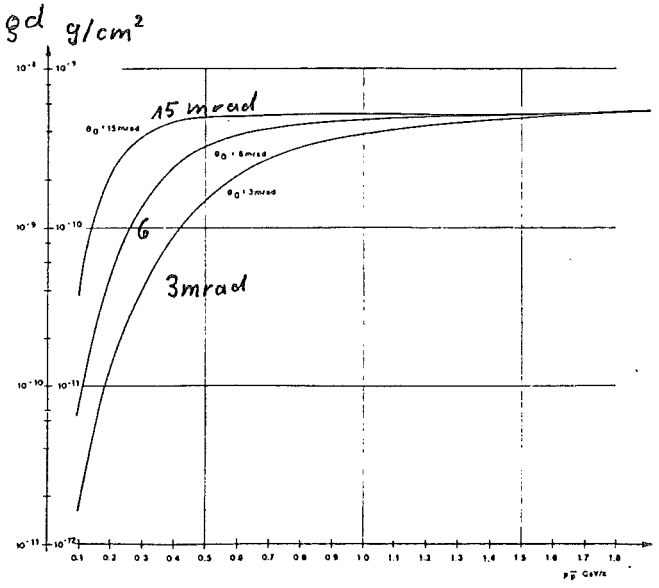

Optimal internal target density for an antiproton consumption rate of 10^6 $\bar{p}$/s and for three machine acceptance angles at the target position (Ref. 21). Left ordinate (thick target): number of stored $N_{\bar{p}} = 10^9$, beam decay time $\tau = 10^3$ s. Right ordinate (thin target): $N_{\bar{p}} = 10^{10}$, $\tau = 10^4$ s.

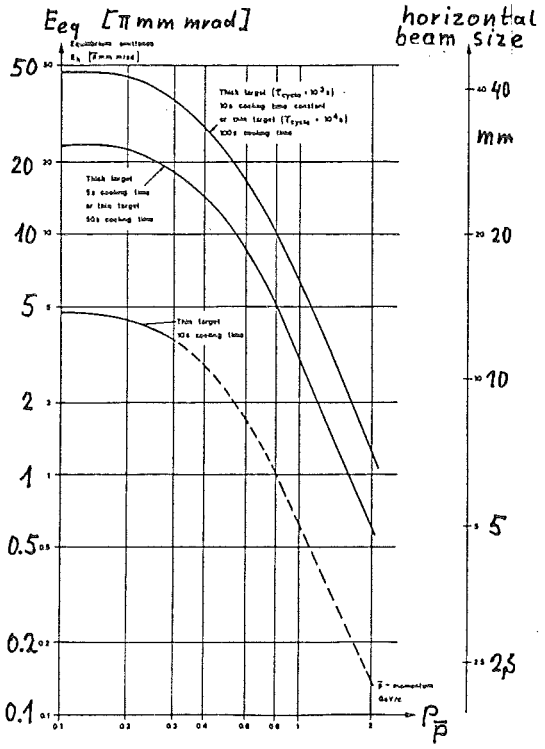

Equilibrium horizontal $\bar{p}$ beam emittance (left ordinate) and diameter (right ordinate) for "thick" and "thin" targets and various cooling times (from Ref. 21).

Ref.: M. Giesch et al. CERN PS/DL Note 81-4, KfK-Primärbericht 11.01.02.P10C;

molecular cluster beam target for ISR

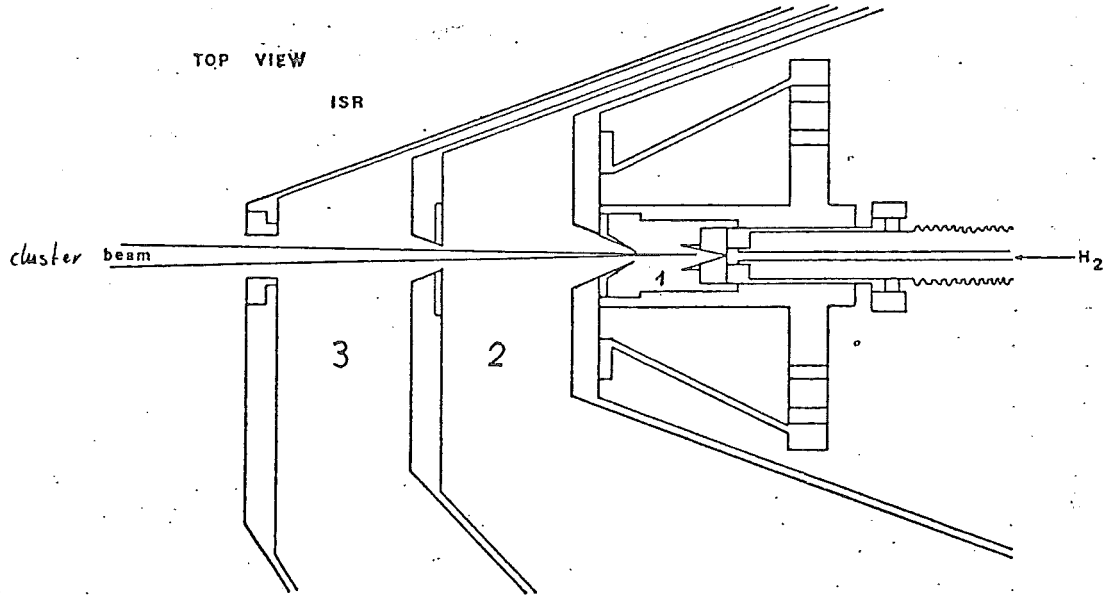

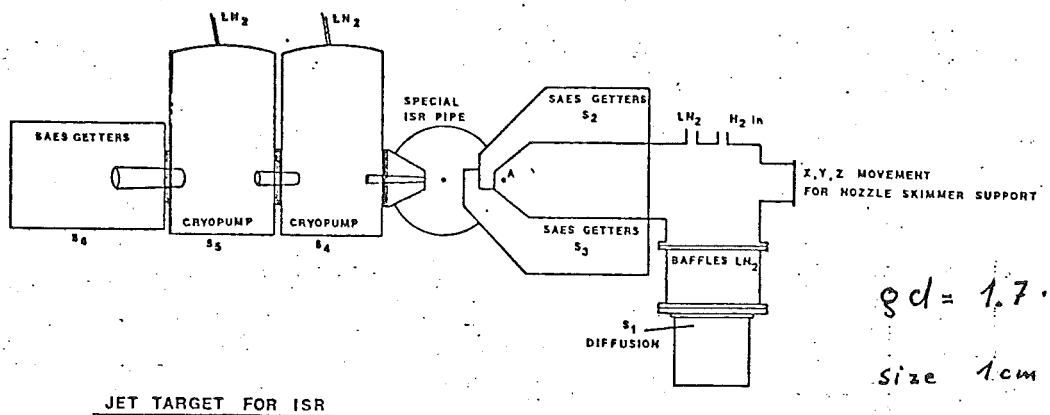

JET TARGET FOR ISR

$\varrho d = 1.7 \cdot 10^{-10}$ g/cm²

size 1 cm ϕ

50 cm

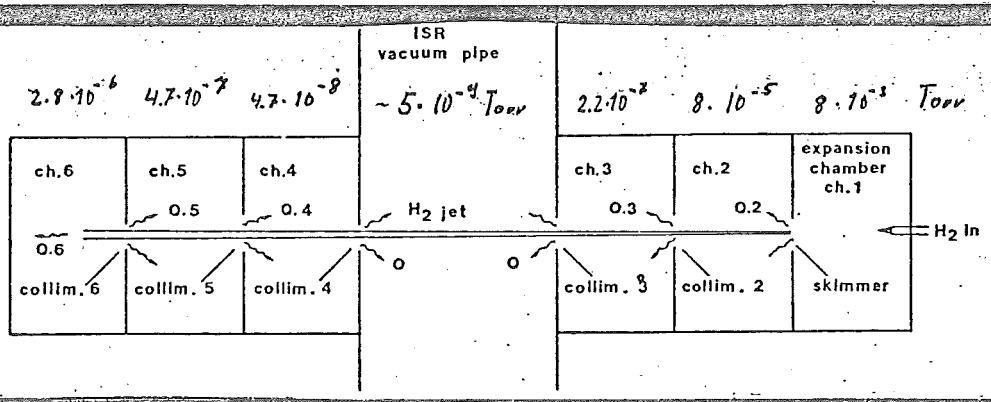

Ref.: C. Baglin et al.; CERN proposal CERN/ISRC/80-14, ISRC/P 106
experiment R704

Polarized hydrogen atomic beam target for SPS

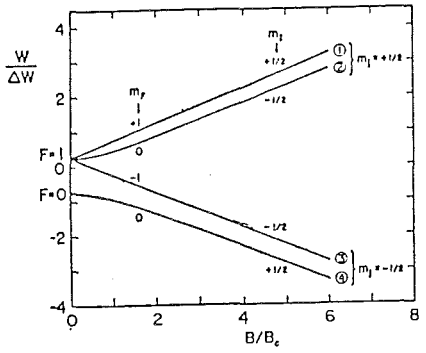

Energy level diagram of hydrogen atom ground state

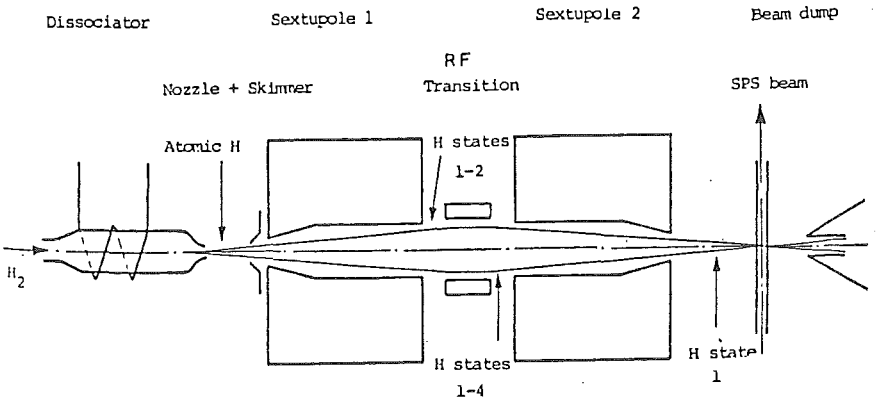

Schematic diagram of the polarized hydrogen jet target

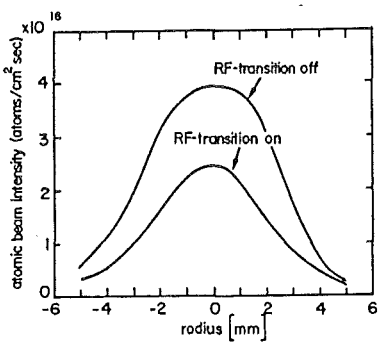

Atomic beam profile

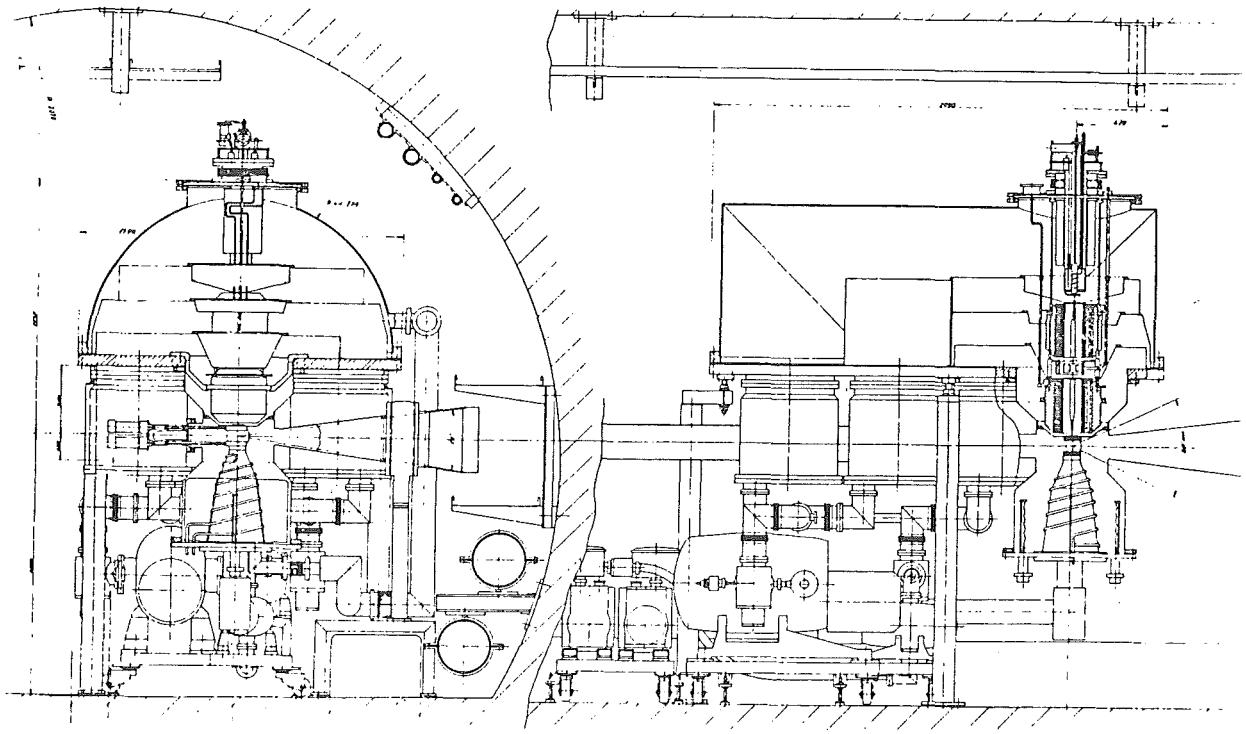

Target facility in the SPS tunnel

Ref.: L. Dick et al, Proc. High-Energy Physics with Polarized beams and Polarized target Lausanne, 1980, EXS 38

J. Antille et al, CERN SPS proposal SPSC/80-63, 1980

in far future: LEAR as a powerful intermediate energy machine ?!

- In final stage LEAR will be equipped with internal target(s) and power full cooling systems. (charge exchange injection)
- Independent operation (when not running with $\bar{p}$) from CERN accelerator complex by using Linac I as injector.

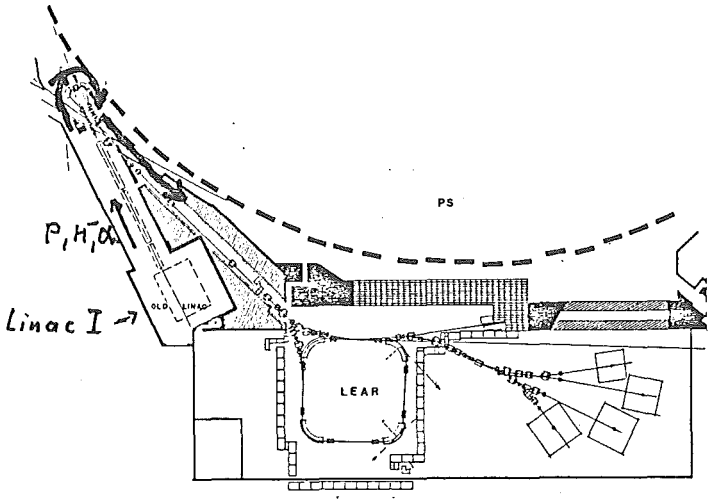

- Installation of ion source in Linac I anticipated
- Installation of polarized source also possible

$\sim$ high resolution, highly efficient nuclear physics machine

cooling of (heavy) ion beams

- cooling of (heavy) ion beams straight forward

cooling time: $\tau_c = \dfrac{K}{\underline{r_A} \cdot \underline{r_e} \cdot Z^2} \cdot T^{3/2}$ (r_A, r_e: $\uparrow$!)

recombination time: $\tau_R = \dfrac{K'}{\underline{r_e^2} \cdot Z^2} T^{1/2}$ (r_e^2: $\uparrow$!)

$\dfrac{\tau_c}{\tau_R} \approx A \cdot 10^{-5}$ $\sim$ recombination no problem

Is a recirculator for the BIG KARL spectrograph feasible?

C.A. Wiedner
Max Planck Institut Heidelberg

IS A RECIRCULATOR FOR THE BIG KARL SPECTROGRAPH FEASIBLE ?

Notes by: S.Martin,KfA Jülich
W.Schott,Physikdepartment TU München
C.-A.Wiedner,MPI Heidelberg

Storage Ring Design Considerations

1. Combined Cyclotron-Storage Ring-System

The BIG-KARL spectrograph is a powerful tool for doing physics with the light ion beams of the JULIC cyclotron.

In order to use the high resolution properties of the spectrograph the beam quality at the BIG-KARL target must be appropriate, i.e., matched to the dispersion of the spectrograph with an object width of the order of a millimeter. One step to meet these requirements is to let the beams pass through a monochromator before hitting the target. The characteristic figures for beams after the monochromator are

$$\tilde{\varepsilon}_x \approx \tilde{\varepsilon}_y \approx 1 \text{ mm mrad}$$

(phase area: π ε)

$$dp/p = 10^{-4}$$

$$I \approx 10 \text{ pn A.}$$

Thus, the intensity on target becomes low. In order to raise the particle current through the target, a storage ring is proposed by means of which many turns can be stored. If the spectrograph target is placed in the ring, the usable particle current might be enhanced by the number of turns. However, the target will change the energy of the stored beam. Therefore, accelera ting cavities are necessary for compensating the energy losses. Furthermore, the longitudinal and transverse phase space of the beam will be increased by energy- and angular straggling at the stripper. This will be discussed below.

How can the particles be brought into the ring? In order to answer this question, we must ask another one first: Do the particles obey Liouville's theorem during the injection process or not? The answer is simple: If the charge is changed at the stripper in the ring, there will be new particles for which Liouville's theorem holds only for the coordinates at the beginning of generation, which is at the center of the ring. In this case the density in phase space can be increased. If the particle charge is not changed, the inflecting beam line must be included into the beam optical system of the ring itself. Therefore, the phase space density of the stored beam cannot be increased by injecting more particles.

In table 1 the ions, which can be accelerated in JULIC, are listed. Included are ions for charge changing injection.

A combined function lattice consisting of twelve identical dipole magnets with edges was proposed for the storage ring (c.f. fig. 1). The number of pulses around the circumference of the ring must be an integer.

Thus the average radius R_s of the ring was chosen in such a way that the harmonic number h_s of the ring is given by $h_s = h_c \cdot \frac{R_s}{R_c} = 14$ where Rc is the mean extraction radius of JULIC being Rc = 1.54 m. In fig. 2 the envelopes of one turn of the beam $\tilde{x}_{max}$ and $\tilde{y}_{max}$ in radial and axial direction and the dispersion element R_{16} (Br 73) are drawn versus the path length. Fig. 3 shows the deviation elements R_{12} and R_{34} versus s, fig. 4 the resulting tune diagram. The lattice is rather weakly focussing.

At both ends of the half period (positions 0 and 4) there are achromatic points with waists in both directions. From the R_{12} (s)- and R_{34} (s) curves a tune of $\nu_x = 2$, $\nu_y = 1$ results which must be changed to a working point with a little smaller value of ν_x and ν_y (c.f. fig. 4) by a slight modification of the lattice in order to avoid resonances.

2. Storing Modes

Particles, which obey Liouville's theorem, can be stored in the two transverse and in the longitudinal phase areas of the storage ring. Usually, not all possibilities are achieved in one ring. The properties of the stored beams in the different modes are listed in table 2.

Transverse stacking.

The width of the stored beam at the target ($s = s_2$) is given by $(\tilde{x}_{max})_2 = \sqrt{\beta_2 \cdot \tilde{\varepsilon}_x}$, where $\beta_2 = \frac{(\tilde{x}_{max})_2}{\tilde{\varepsilon}_x}$ is the amplitude function of the lattice at s_2. For storing the beam in the (x,θ) area the reference orbit is shifted by $2 \cdot (x_{max})_1$ at s_1 using two kicker magnets at s_o and s_3 (in case of storing in the (y,ϕ)-area the second kicker must be placed at s_4 c.f. fig. 3). In the considered case (c.f. table 2) of $n = 100$ $(x_{max})_1 = 3.4$ cm results. The kicker field is given by

$$\frac{\theta_o \sqrt{2(T/A) \cdot E_u}}{(q/A) \cdot \ell \cdot c},$$

where ℓ means the length and $\theta_o = 2 \cdot (x_{max})_1 / (R_{12})_1$ the deflecting angle. Therefore, for protons of 45 MeV and ℓ = 1 m B_K = 198 Gauss is obtained, which is feasible. The beam passes then close to D1. During storing the bump must decrease by $2 \cdot (\tilde{x}_{max})_1$/turn in order to clear D1 for injecting the next turn. Thus, B_K must decrease as $-dB_K/d\tau_s$ = 0.04 Gauss/ns. For BIG-KARL, whose dispersion is in the radial plane, transverse stacking in the (y,ϕ)-plane might be considered. However, the beam extension in y-direction becomes quite large even at a moderate number of stored turns (c.f. table 2).

During the time of storage the RF-system must provide an accelerating voltage V which compensates for the energy loss in the target and delivers some bucket size big enough to take up the longitudinal phase area of the original beam and additional area caused by energy straggling of the circulating beam at the stripper. V depends on the target thickness and on the number of turns (c.f. below).

Longitudinal stacking.

Because of the rather small momentum spread dp/p it seems to be more useful to store "Liouville-particles" in the longitudinal phase area of the ring. In this case the RF-program is quite complicated. In order to inject the first turn, the reference orbit is bent by means of K1 and K3. The deviation at s_1 must be $2\cdot(\tilde{x}_{max})_1$ yielding a field of B_K = 21 Gauss. During stacking the target is out of the beam. The storing of 180 MeV α-particles is discussed as an example. During injection the first turn the reference orbit is shifted by $2\cdot(\tilde{x}_{max})_1$ by means of K1 and K3 (B_K = 21 Gauss). D1 is placed in such a way that the distorted orbit goes through the center of the channel. The r f- system values are ν = 27.8 MHZ, V = 2.44 Kv, ϕ_s = 0. After passing the first turn K1 and K3 are switched off (B_K = 0). The catching of the bunches into the bucket takes one synchrotron oscillation period τ_o. τ_o is given by (Bo 70)

$$\tau_o = \left\{ \frac{\cos\varphi_s}{4\pi^2} \frac{c^2}{2\pi R^2 E_o} \, heV \, \frac{1-\gamma^2/\gamma_{tr}^2}{\gamma^3} \right\}^{-1/2}, \text{ yielding}$$

τ_o = 325 µs (γ_{tr} see below).

The (dT,dϕ)-phase area dA of one turn is given by

$$dA = dT\cdot d\phi, \text{ where } dT = \frac{2\cdot dp}{p} T \text{ and } d\phi = \omega\cdot dt \text{ yieldin}$$

$$dA = 2\cdot 10^{-4}\cdot 180\cdot 10^{3}.2\pi\cdot 27.8\cdot 10^{+6}\cdot 0.7\cdot 10^{-9} = 4.4 \text{ keV}\cdot\text{rad}.$$

The injected particles are then accelerated to a larger mean radius

$R + \Delta R$. ΔR is related to the corresponding relative momentum increase $\Delta p/p$ by $\Delta p/p = \frac{\Delta R}{\langle R_{16} \rangle}$.

According to fig. 2 $\langle R_{16} \rangle$ = 2 cm/%, i.e., for ΔR = 2 cm $\Delta p/p = 10^{-2}$ results. The energy ΔT, which is to be added, is $\Delta T = 2 \cdot 10^{-2} \cdot T$ = 3600 keV. The relative shift in revolution frequency $\Delta \nu_s / \nu_s$ at the larger momentum Δp is given by (Bo 70)

$$\Delta \nu_s / \nu_s = (1/\gamma^2) \cdot \Delta p/p - \Delta R/R .$$

(below the transition energy T_{tr} = 835 MeV/N $\Delta \nu_s > 0$).
The total shift in rf-frequency is

$$\Delta \nu = h_s \cdot \Delta \nu_s = 175.6 \text{ kHz}.$$

The acceleration of the particles of the first turn to $T + \Delta T$ should take place with a moving bucket whose phase area must be exactly dA. In this way no empty phase area is diluted. Therefore the phase of the synchronous particle ϕ_s must be chosen in such a way that this condition is met.

The voltage/turn qV is given by (Bo 70)

$$qV = \frac{h (dA)^2 \cdot 2\pi\eta}{\alpha^2(\varphi_s) \cdot 16^2 \beta^2 (E_0 + T)} , \qquad (1)$$

where

$$\eta = \frac{1}{\gamma_{tr}^2} - \frac{1}{\gamma^2} , \quad \gamma_{tr} = \sqrt{\frac{R}{\langle R_{16} \rangle}} .$$

$\alpha(\varphi_s) = A(\phi_s)/A(0)$ describes the shrinkage of the moving bucket related to the stationary bucket.

Taking qV = 4.88 keV, dA = 4.4 keV rad $\varphi_s = 83^\circ$ results. Thus, the particles are accelerated close to the top of the voltage.

During acceleration ν must be increased to $\nu+\Delta\nu$ until $T + \Delta T$ is reached. Then the rf-voltage is switched off leaving the particles at $T + \Delta T$, where they distribute over 2π. The rf is restarted at ν = 27.8 MHz, V = 2.44 kV, ϕ_s = 0. Turn 2 is injected and accelerated by $\Delta T - \delta T$, where $\delta T = dA/2\pi$ is the energy width of one turn distributed over 2π. Turn 3 will be accelerated by $\Delta T - 2\delta T$ and so on until the whole ΔT-range is covered.

The filling time for n = 1000 turns will be

$$t_F = n\left(\tau_0 + \frac{\Delta T}{qV}\cdot\tau_s\right) =$$

$$= 1000\left(325\cdot10^{-6} + \frac{3600}{4.88}\cdot502.88\cdot10^{-9}\right) = 0.7\ s$$

After filling the target is placed into the beam and the measurement started. For a ^{12}C - target the equilibrium thickness d_{eq} is approximately (Hi 81)

$$d_{eq}\ (\mu g/cm^2) = 0.33\cdot T(MeV), \qquad (2)$$

yielding d_{eq} = 60 $\mu g/cm^2$.

With dT/dx = 0.143 keV/($\mu g/cm^2$)(No 70) an energy loss/turn due to the target of dT_T = 8.58 keV results. This energy loss is compensated for at an energy gain of qV = 100 keV/turn and ϕ_s = 4.92^o. Therefore, the rf voltage is switched on again at a medium frequency of the stack of ν = (27.8 + 0.176/2) MHz = 27.888 MHz and raised adiabatically (within one synchrotron oscillation period) to qV = 100 keV. The available bucket area A is, according to eq. 1, A = 10 400 keV·rad, i.e., in addition to the phase area of the stack of n·dA = 4400 keV·rad (n = 1000 turns) there is

ΔA = 6000 keV·rad left for (d T, dφ)-area increase due to energy straggling in the target. The full width at half maximum Γ of the energy straggling is given by (Hi 81)

$$\Gamma = 0,66 \cdot \sqrt{\frac{Z_p \cdot Z_T}{Z_p^{1/3} + Z_T^{1/3}}} \cdot \sqrt{d\,T_T} \qquad (3)$$

where Z_p and Z_T are the atomic numbers of the projectile and the target, respectively. Eq. 3 yields Γ = 3.82 keV for the considered case. Taking into account that the particles within the bucket cover about the phase π (half of the full phase) ΔA is given by

$$\Delta A \approx \Gamma \cdot \pi \cdot \sqrt{n_M} \qquad (4)$$

where n_M is the number of turns during measurements. Thus, after n_M = 250000, which corresponds to a measuring time $t_M = n_M \cdot \tau_s$ = 0.13 s, the bucket area is full and the measurement must be stopped. According to the section on target effects the emittances are doubled, i.e., $\varepsilon_x \approx \varepsilon_y \approx 2\tilde{\varepsilon}$ after n_M turns, due to angular straggling. More detailed calculations must take into account the cooling of the angular straggling due to the acceleration (c.f. section ...) The radial width $2(x_{max})_2$ of the beam at the target after the measuring time t_M can be calculated from the height dT_B of the bucket to be

$$2(x_{max})_2 = (R_{16})_2 \, dp/p = (R_{16})_2 \cdot \frac{1}{2} \frac{dT_B}{T}. \qquad (5)$$

The half bucket height is given by (Bo 70)

$$\frac{dT_B}{2} = \sqrt{\frac{V}{h}}\, Y(\varphi_s) \cdot \beta \cdot \sqrt{\frac{E_0 + T}{\pi \cdot \eta}}, \qquad (6)$$

where $Y(\phi_s = 4.92^\circ)$ = 1.31. With the above mentioned data $dT_B/2$ = 1468.3 keV results yielding with eq. (5) $2(x_{max})_2$ = 2.13 cm.

Non-Liouville-stacking

As an example of non-liouville-stacking we consider the case where two protons of 41 MeV are generated when H_2^+-ions of 82 MeV pass through the target. The Bρ-value of the H_2^+-ions is twice as large as that of the protons (c.f. table 1). Therefore, the radius of curvature within the dipole preceding the target at position 2 is twice as large providing an easy injection of the H_2^+-beam into the circulating p-beam (c.f. fig.5). The equilibrium target thickness deq = 27 $\mu g/cm^2$ results from eq.(2). The energy loss/turn in the target (c.f. section ...) is then dT_T = 0.351 keV. This energy loss is compensated for by a cavity voltage of V = 5 kV/turn at $\phi_s = 4.02^\circ$. The total bucket area, which is provided by these rf-data ($\alpha(\phi_s = 4.02^\circ) = 0.82$), is, according to eq. (1), A = 1164 keV·rad. At n_{max} = 21718 turns the brightness ratio R_B (c.f. section ...) has its maximum, i.e., each particle should make n_{max} turns in the ring. The total energy width δT is given by

$$\delta T = \sqrt{dT^2 + n\,\Gamma^2},$$

where dT is due to the beam energy spread ($dT/T = 2 \cdot 10^{-4}$) and Γ to the energy straggling being according to eq. (3) Γ = 0.571 keV. With the data given above δT = 84.55 keV results. The longitudinal phase area due to the energy width of the beam after n_{max} turns, is then $\delta A \approx \delta T \cdot 2\pi$ = 531 keV·rad which is well within the available bucket. Using eqs. (6) and (5), for the radial beam width at the target $2(x_{max})_2$ = 1.05 cm is obtained. In limiting $2 \cdot (x_{max})_2$

by means of slits to a value of 1.05 cm, the number of turns, which are stored, are set to n_{max}, thus, providing optimal beam conditions. At n_{max} turns the emittance has doubled yielding an object width which is by $\sqrt{2}$ larger than that of the incoming beam (c.f. table 2).

References

(Br73) K.L. Brown et al., Report CERN 73-16 (1973).

(Bo70) C. Bovet et al., Report CERN/MPS-SI/Int. DL/70/4 (1970).

(Hi81) G. Hinderer, F. Hinterberger, interner Bericht, TUM, München (1981)

(No70) L.C. Northcliffe, R.F. Schilling, Nucl.Data Tables A7 (1970) 233.

Table 1. Particles which are accelerated in JULIC to the energy T; $B\rho(Tm) = 3.3356\ pc(GeV)/q$. The cyclotron frequency ν_c and the RF-frequency ν are given. The numbers in brackets denote the values after stripping.

The time between particle bunches is $\tau = 35.92...\ 51.89$ ns; the pulse width ($d\phi = 7^\circ$) is $dt = 0.7\ ....\ 1.0$ ns; h_c being $h_c = \nu/\nu_c$ is the harmonic number.

T(MeV)	particle	γ	β	cp(MeV)	$B\rho$(Tm)	ν_c(MHz)	ν	h_c
22	p	1.023	.2128	204.4	.6817	6.606	19.82	3
45	p	1.048	.29906	294.0	.9809	9.2787	27.84	"
45	d	1.024	.21515	413.4	1.379	6.675	20.03	"
90	d	1.048	.29906	588.1	1.9617	9.2787	27.84	"
90	α	1.024	.21515	826.8	1.379	6.675	20.03	"
180	α	1.048	.29906	1176.2	1.9617	9.2787	27.84	"
67.5	τ	1.024	.21515	620.11	1.0342	6.675	20.03	"
135	τ	1.048	.29907	882.15	1.4712	9.2777	27.83	"
82.14 [41.07]	H_2^+ [2p]	1.0438		561.28 [280.63]		9.28	27.84	"
59.25	$^3He^+$ [τ]	1.0212		578.49	1.930 [0.965]	6.42	19.27	"
41.4	$^4He^+$ [α]	1.0111		557.23	1.859 [0.929]	4.64	27.84	6

Table 2. Beam properties after storing in different modes. Energy T in MeV; target thickness d in $\mu g/cm^2$; number of turns n; emittances ε_x, ε_y in mm·mrad (emittances of the incoming beam $\tilde{\varepsilon} = \tilde{\varepsilon}_x = \tilde{\varepsilon}_y$ = 1 mm·mrad, $dp/p = 10^{-4}$); momentum spread at the target $(\Delta p/p)_2$; total beam widths at target $2(x_{max})_2$ and $2(y_{max})_2$ in cm; object width in brackets; cavity voltage/turn V in kV; cavity frequency ν in MHz; the target is either in beam all the time (stationary), or it is out during filling time t_F and in during measuring time t_M (moving); filling time t_F in s; measuring time t_M in s.

Mode	T	d	n	ε_x	ε_y	$(\Delta p/p)_2$	$2(x_{max})_2$	$2(y_{max})_2$	V	ν	target	t_F	t_M
transverse (x,θ)			100	100	1	10^{-4}	2.0(1.0)	1.2			stationary		
" (y,φ)			100	1	100	"	0.2(0.1	11.9			"		
Longitudinal	180 α	60	1000	2	2	$2.2 \cdot 10^{-3}$	2.13(0.14)	1.4	50	27.8	moving	0.7	0.13
non-liouville	41 p	27	21700	2	2	$1.7 \cdot 10^{-3}$	1.05(0.14)	1.4	5	"	stationary		continously

Figure captions

Fig. 1 Combined function lattice of the storage ring. It consists of twelve identical homogeneous dipoles with an entrance edge angle 6.4^{o}. The average radius R_s is R_s = 7.19 m. The period of particle revolution is τ_s = 502.9...726.5 ns. The radius of curvature inside of the dipole is 1.52 m. Two cavities C_1 and C_2 at the positions 0 and 4 provide an accelerating voltage of 50 kV/turn at maximum within the frequency range ν = 19.27...28.02 MHz. There is one electrostatic deflector D1 at pos. 1 and two kicker magnets at 0 and 3. The position of the BIG-KARL-target is at 2.

Fig. 2 Beam envelopes $\tilde{x}_{max}$, $\tilde{y}_{max}$ of one turn of the beam and dispersion element R_{16} versus path length s over a half period (the other half of the ring being identical). For $\tilde{x}_{max}$ and $\tilde{y}_{max}$ the emittances $\tilde{\varepsilon}_x = \tilde{\varepsilon}_y$ = 1 mm mrad are assumed.

Fig. 3 R_{12} and R_{34} versus s.

Fig. 4 Tune diagram of the lattice.
Point 1 corresponds to a "single particle" calculation (the edge angle of the dipoles must be slightly changed and may be quads inserted to reach this point). The tune depends on the particle current I in the ring. Point 2 would be reached at I = 7.3 mA.

Fig. 5 Stored p-beam and incoming H_2^+-beam within the dipole preceding the target (position 2, fig. 1); beam data see table 1. The radius of curvature ρ of the p-beam is ρ_p = 1.516 m, $\rho_{H_2^+}$ = 3.032 m.

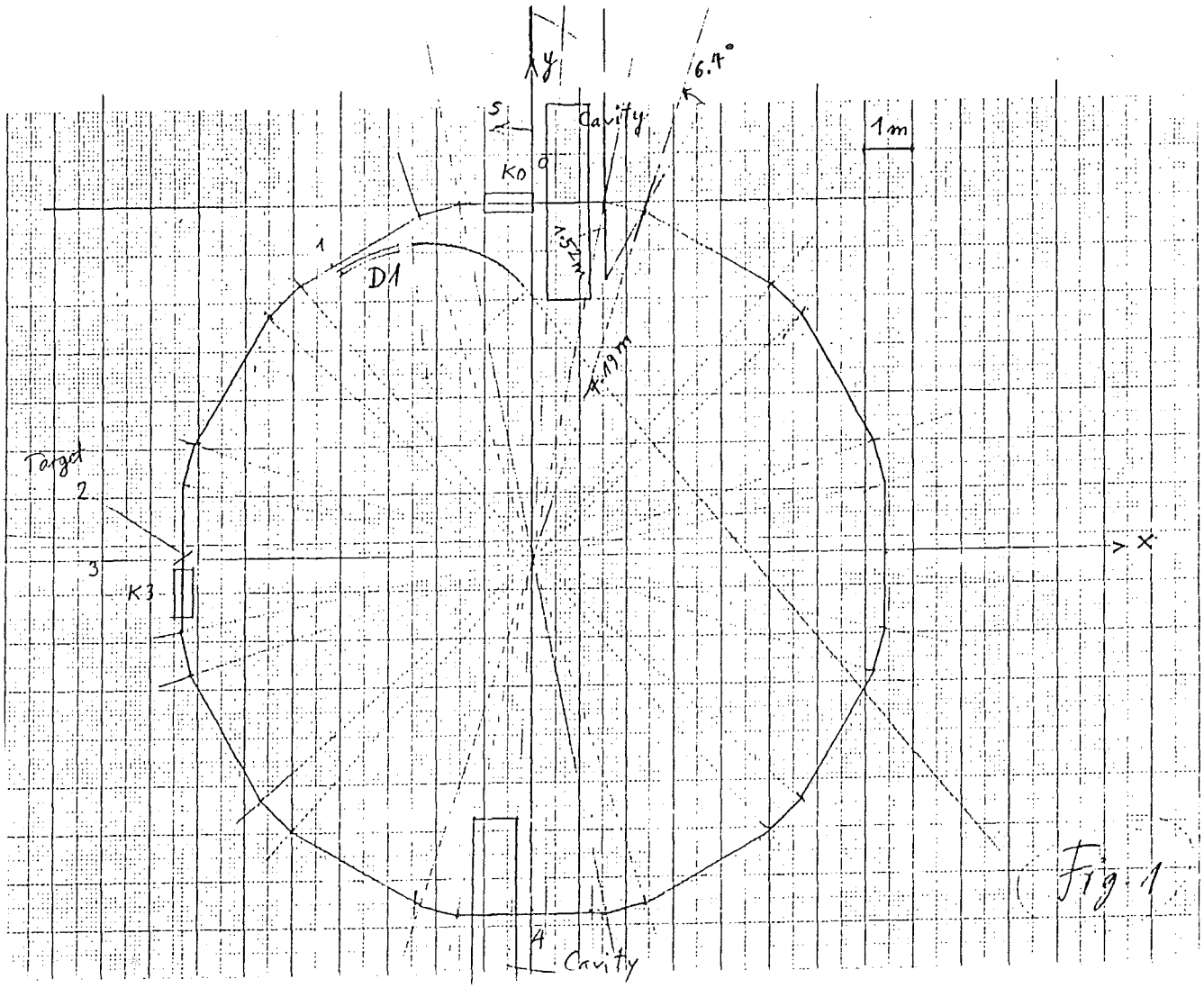

Fig. 1

Magnet Layout

B_{max} = 1.5 T, = 1.58 m , Ø = 30°

Uniform Field , 6.44° positive wedge angle at entrance side

N.I (A.turns) = 10^5

Poles: radial width -- ± 25 cm
gap 8 cm

Total weight (Iron) : 4.9 to (H-type)
5.4 to (C-type)

(Copper) : 0.2 to

Coils: watercooled copper conductor 8x8 mm^2, 3 mm Ø hole
2 coils 64 turns each, o.d. 8ox8o mm^2
.o58 x 2 Ohms

max.Current: 780 A
Voltage 90 V
Power 71 kW

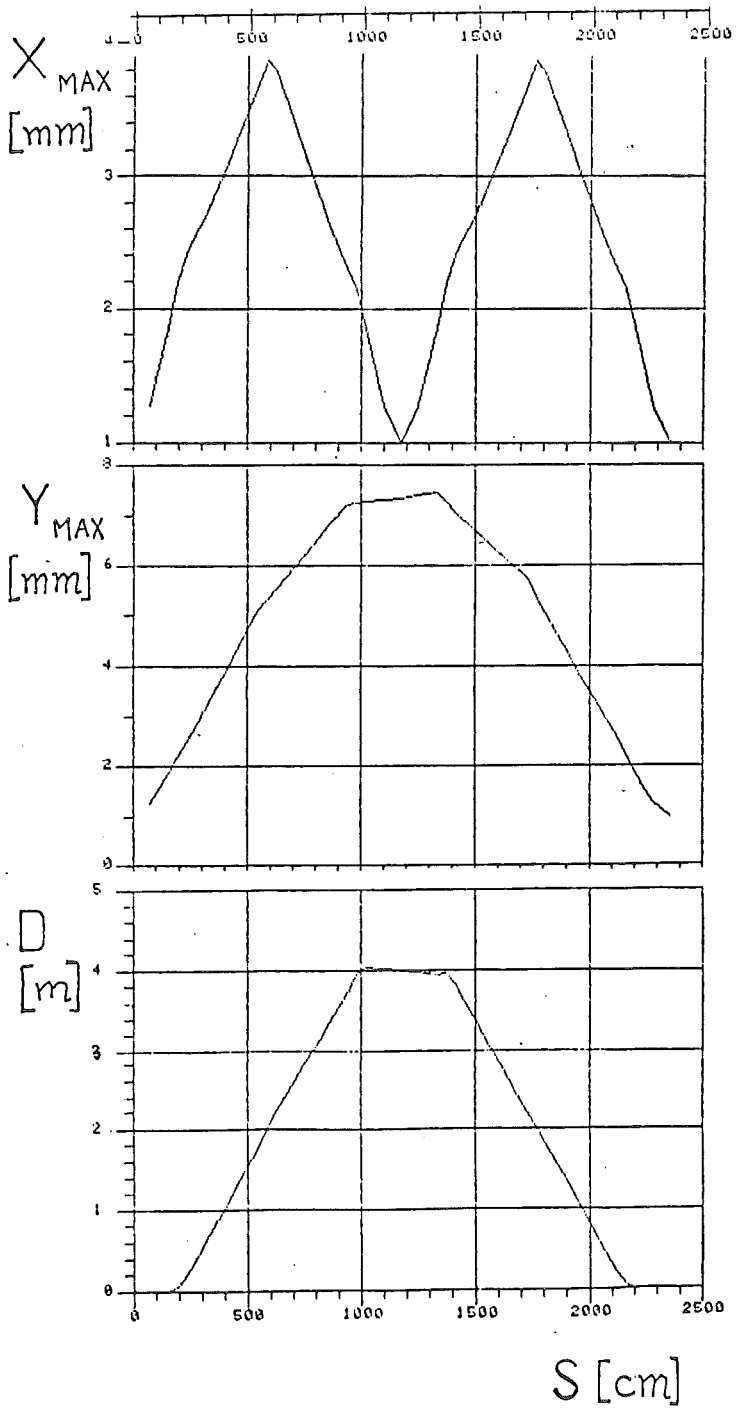

Fig. 2

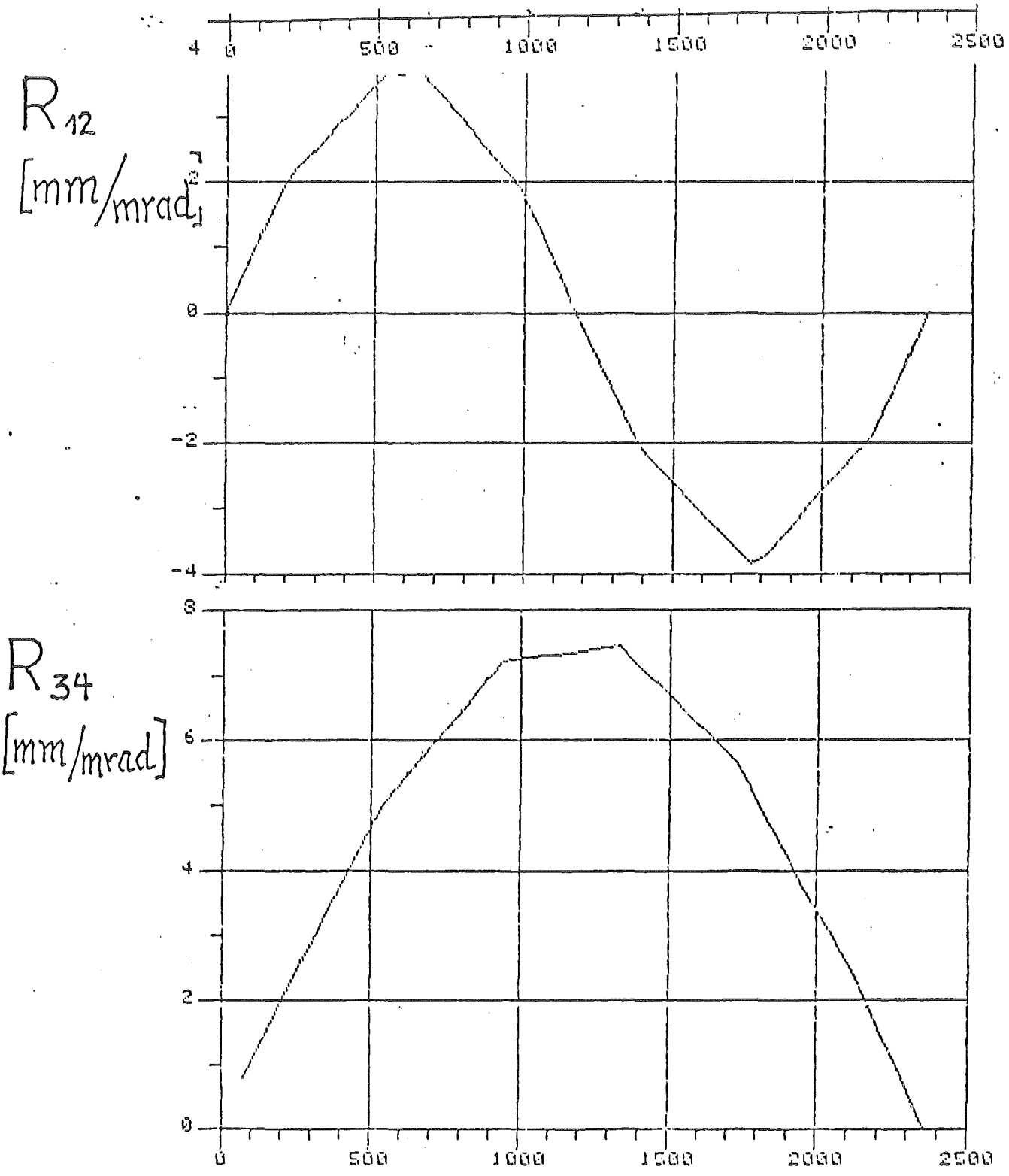
R12
[mm/mrad]
4
2
0
-2
-4
0
500
1000
1500
2000
2500
R34
[mm/mrad]
8
6
4
2
0
0
500
1000
1500
2000
2500
S [cm]

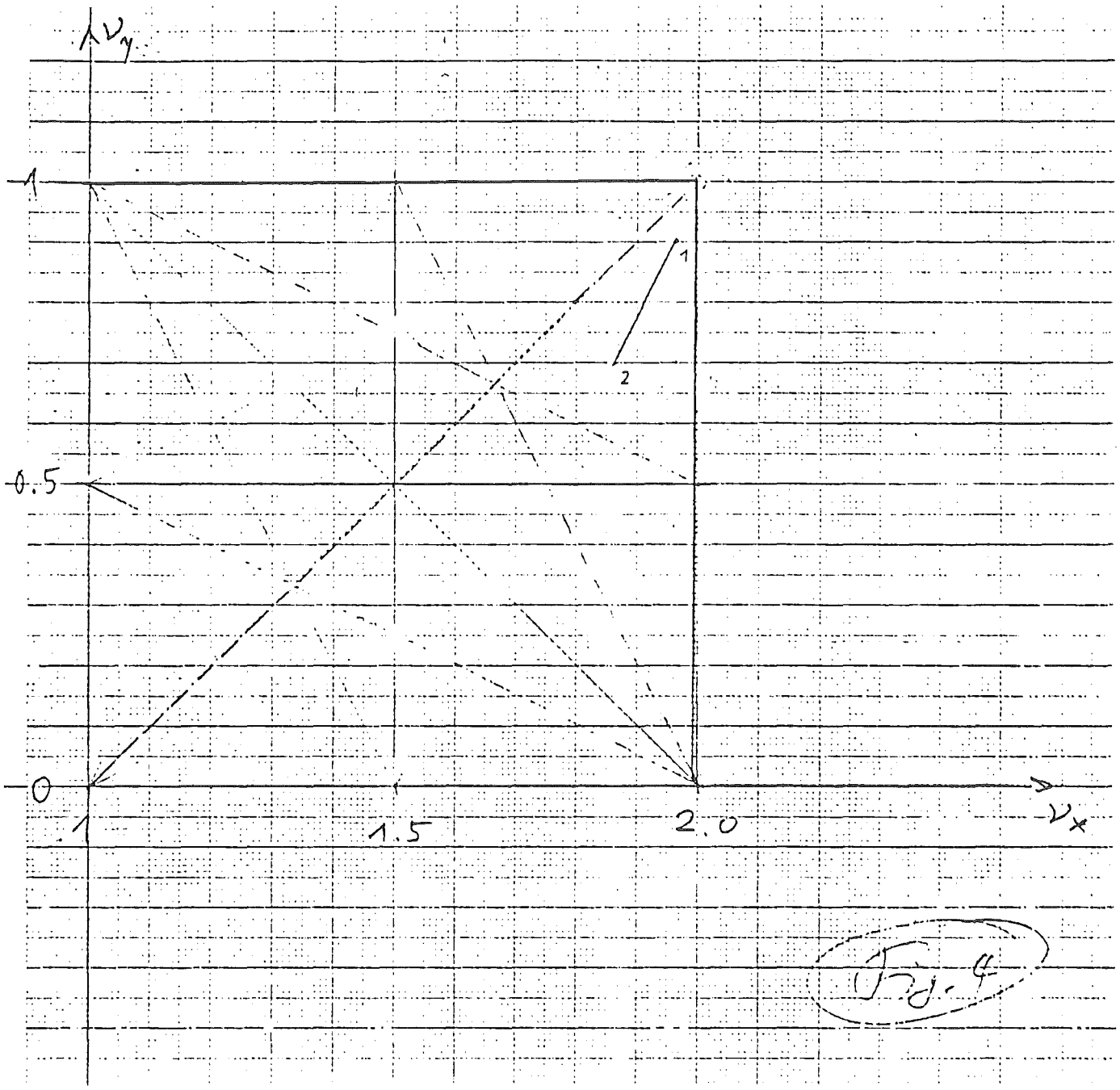

Fig. 4

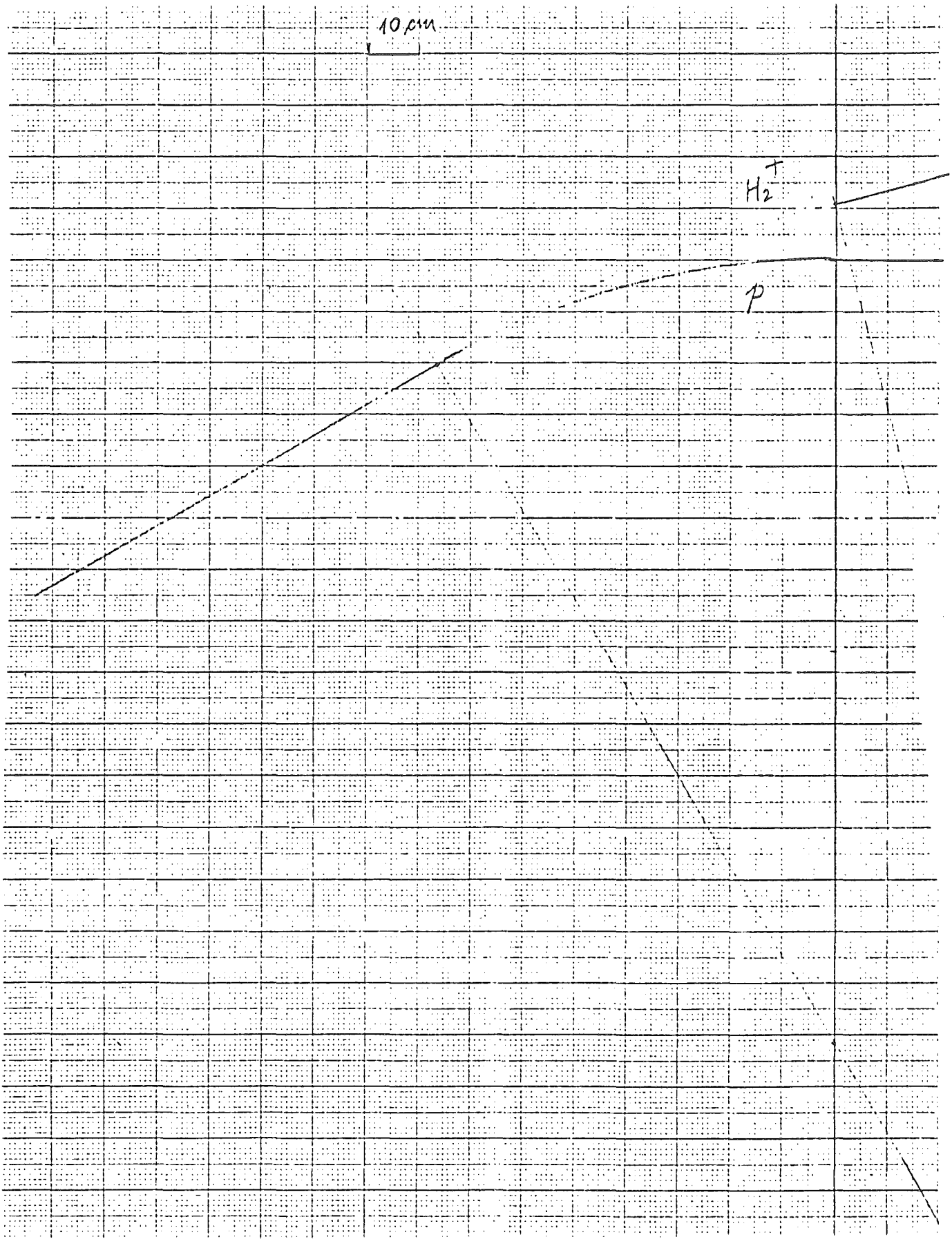

Fig. 5

Effects of Internal Targets

'Non-Liouvillian' Particles

Target Effects

To calculate the growth of the beam emittance in a storage ring with an internal target we employ the formalism of Cooper and Lawrence (Co 75). They predict large currents of stored protons for an H^- beam of 800 MeV injected onto and stripped by a 150 $\mu g/cm^2$ Carbon target.

The basic process for the beam blowup is Coulomb elastic scattering. Inelastic and nuclear scattering as well as residual gas scattering are assumed negligible. Also the circulating particles undergo no more than one Coulomb scattering per target traversal. The representation treats radial and axial effects alike.

With β, the betatron function in the ring and β_o its value at the target location, the injected beam of emittance ε_o is assumed to have a normalised distribution given by:

$$f_o(x,x') = \frac{1}{2\pi\sigma_o^2} \exp\left[-\frac{x^2 + x'^2}{2\sigma_o^2}\right] \qquad (1)$$

where $\varepsilon_o = \frac{2\pi}{\beta_o}\sigma_o^2$. After N turns the distribution is given by

$$f_N(x,x') = \frac{1}{2\pi(\sigma_o^2+\sigma_N^2)} \exp\left[-\frac{\hat{x}^2 + x'^2}{2(\sigma_o^2+\sigma_N^2)}\right] \qquad (2)$$

where σ_N the 'foil scattering width' is given by

$\sigma_N^2 = \frac{1}{2} N_s \cdot \beta_0^2 \cdot (\overline{\delta x'})^2$. The number of scatterings N_s is connected to the number of turns N, the number of atoms/cm^2, n · t and the Coulomb cross section σ_c for the mean square scattering angle $d\langle\Theta^2\rangle^{1/2} = \overline{\delta x'}$

$$N_s = N.\ n.t.\sigma_c$$

Thus the mean square betatron amplitude is given by

$$\langle \hat{x}^2 \rangle = 2(\sigma_0^2 + \sigma_N^2) \qquad (3)$$

The evaluation is complicated in a continuous injection: Particles injected in the first turn have traversed the target N times, those injected during the second turn N-1 times and so on. The resulting (betatron amplitude) distribution cannot be evaluated analytically. Following ref. (CO 75) it can be shown that numerically for not too large N it may be approximated by a Raleigh distribution:

$$p(\hat{x}) = \frac{\hat{x}}{\sigma_0^2 + \frac{1}{2}\sigma_N^2} \exp\left[-\frac{\hat{x}^2}{2(\sigma_0^2 + \frac{1}{2}\sigma_N^2)}\right] \qquad (4)$$

From phase space conservation - or, in other terms, the Courant-Snyder invariant, it follows that the phase space filled with particles with betatron amplitude less than

or equal to the RMS value $\langle \hat{x}^2 \rangle^{1/2}$ is

$$\varepsilon_N = 2\pi/\beta_o(\sigma_o^2 + \frac{1}{2}\sigma_N^2) \qquad (5)$$

$$\varepsilon_N = \varepsilon_o + \frac{1}{2}\pi\beta_o N\, nt\, \sigma_c \overline{d\Theta}^2 \qquad (6)$$

The additive term to ε_o represents the beam emittance growth being proportional to the betatron function at the target location β_o, the target thickness, the Coulomb cross section, σ_c, the square of the mean scattering angle and the number of the turns.

Evaluation of the Scattering Angle

The mean square scattering angle has been calculated following an analytical expression of Joy (JO 73)

$$d\Theta^2 = \langle\Theta^2\rangle = .25\left[\frac{Z_s(Z_s+1)}{A_s}\right]\frac{Z_i^2}{E_i^2} \qquad (7)$$

where A_s, Z_s denote the atomic mass and charge of the scatterer, Z_i, E_i (MeV) the atomic number and energy of the particle, L ($\mu g/cm^2$) characterises the target thickness.

This simple formula has been checked against the more refined evaluations of Marion and Zimmermann (MA 67). There, based on Moliere's theory of multiple scattering (Mo 47) and improve-

ments of Nigam, Sundaresan and Wu (NI 59), the $\Theta(1/e)$ angle is calculated. Since the evaluation is based on statistics, there are limitations concerning the number of collisions M. Therefore the formula is applicable only for $M \geq 15$.
The scattering angular distributions are normalised to unity at $\Theta = 0^{\circ}$, then they are approximated by a Gaussian. The $\Theta(1/e)$ angle defines the angle at which the distribution has reached its 1/e value, i.e., the fraction particles, which are scattered into the angular interval between 0° and $\Theta(1/e)$ - which is the half cone of the full distribution - would be for a Gaussian 0.695. For the exact distributions, however, - and for many cases (thin targets and/or high energies) here - this fraction is only .5. Another formula is given in ref.(PA 80) which may be a good approximation to very high energies. The number of particles scattered into an angular interval $d\phi$ is given by

$$g(\phi)\,d\phi = \frac{1}{\sqrt{\pi}\,\phi_0} \exp-\left(\frac{\phi^2}{\phi_0^2}\right) d\phi$$

and

$$\phi_0 = \frac{20\ \mathrm{MeV/c}}{p\beta} Z_i \sqrt{\frac{L}{L_R}} \left[1 + \frac{1}{9} \log_{10}\left(\frac{L}{L_R}\right)\right] \ (\mathrm{Rad})$$

where p, β and Z_i denote momentum in MeV/C, velocity, and atomic number of the beam particles and L/L_R the thickness of the scatterer in radiation lengths of the material. Al-

though the validity is good only to about 10^{-3} in L/L_R, also this formula has been used for a comparison of the rms values of the multiple scattering angles.
Tab. I contains this comparison, for 120 MeV α particles scattered from Al and various target thicknesses.

Tab. I

Comparison of calculated multiple scattering rms angles for 120 MeV α particles and Al.

$d(\mu g/cm^2)$	$2 \cdot \Theta(1/e)$*	$\langle\Theta\rangle$**	ϕ_{rms}*** mrad
100	.15	.22	.14
500	.43	.48	.37
1 000	.66	.68	.56

* Ref. (MA 67)
** Ref. (JO 73)
*** Ref. (PA 80)

It is readily seen that the approximations differ by about 20 %. In the following - mainly because of its simplicity - the approach of Joy is used for the evaluation of the multiple scattering angle.

In a paper of Cline (CL 69) experimental results are quoted for multiple scattering of ^{12}C and ^{32}S ions which are reproduced within the experimental error by the formula of Joy.

Evaluation of σ_c

For the calculation of the Coulomb scattering cross section σ_c the formalism reviewed by Kalbitzer (KA 80) has been applied. There the scattering function $f(t^{1/2})$ is derived in terms of the reduced energy and the cms scattering angle Θ:

$$f(t^{1/2}) = \sigma_c \cdot \frac{t^{3/2}}{\pi a^2} = \frac{1.309\, t^{1/6}}{[1+(2.618\, t^{2/3})^{2/3}]^{3/2}}$$

Here $t^{1/2} = \eta \sin(\Theta/2)$ where a is the screening radius,

$a = .8853 \cdot a_o \cdot Z^{-1/3}$

and

$$\eta = \frac{M_s \cdot E_i}{M_s + M_i} \Big/ \frac{Z_i \cdot Z_s \cdot e^2}{a}$$

$$Z = (Z_i^{2/3} + Z_s^{2/3})^{3/2}$$

a_o - Bohr Radius - .529 Å

As before the indices i and s stand for the particle and the scatterer respectively, with M,Z and E, the mass

atomic number and the cms energy. Kalbitzer discusses various limitations and different theories for the evaluation of $f(t^{1/2})$. Indeed, for $t^{1/2} \leq 5.10^{-2}$ the cross sections vary by a factor 2 and more, since the impact parameter has a length comparable to the size of the atom. For the cases considered here, however, - $t^{1/2} \geq .1$ - the formula quoted should be correct to within about 20 %, since it merges into the classical Coulomb cross sections.
For the calculations the difference between the lab and cms frame of reference has been neglected.

The emittance growth as a function of the number of turns N for different particles scattered by targets of various thicknesses is now readily calculated. From the physical concept , however, the brightness ratio characterises the net gain of the ring much better. Again following Cooper (Co 75) the brightness is defined to be proportional to the beam current divided by the product of the radial and axial emittances ε_a and ε_r

$$B = I/\varepsilon_r \cdot \varepsilon_a$$

After N turns, the current injected is N.I. At the same time the beam emittances $\varepsilon_{or}, \varepsilon_{oa}$ have grown to become $\varepsilon_{Nr}, \varepsilon_{Na}$, thus the ratio of the brightness is

$$R_B = B_n/B_o = (N \cdot I/\varepsilon_{Nr} \cdot \varepsilon_{Na})/(I/\varepsilon_{or} \cdot \varepsilon_{oa})$$

and with eq. 6 from p. 3 assuming β_o and ε_o to be the same in the radial and axial planes we derive

$$R_B \; N/(1 + \frac{1}{2\varepsilon_o} \pi\beta_o \cdot N \cdot nt \cdot \sigma_c \langle\theta^2\rangle)^2$$

This function has been evaluated for protons, deuterons, ^{3}He and α-particles for energies obtained at the Jülich Cyclotron and different target materials. The thickness of the target with 50-200 μg/cm^2 is typical for Big-Karl-experiments.

In fig. 1 the brilliance ratio R_B vs. N is shown for the extreme p-, d-, and ^{3}He energies, assuming an ^{27}Al target of 50 μg/cm^2. For α-energies of 40, 80, 120, 160, and 200 MeV and target nuclei differing in atomic mass by roughly a factor 2, i.e., C, Al, Ni, Sn, and Au, again for 50 μg/cm^2 R_B vs. N is plotted in figs. 2 - 6.
Increasing the target thickness reduces the brilliance ratio. In the lower part of the figures the difference ΔR_B defined as

$$\Delta R_B = R_B(50\ \mu g/cm^2) - R_B(n\ \mu g/cm^2) \;/\; R_B(50\ \mu g/cm^2)$$

for n = 100 and 200 μg/cm^2 has been plotted. The bell shaped curves have characteristic maxima in R_B the corresponding N is denoted by N_{max}. The following conclusions may be drawn:

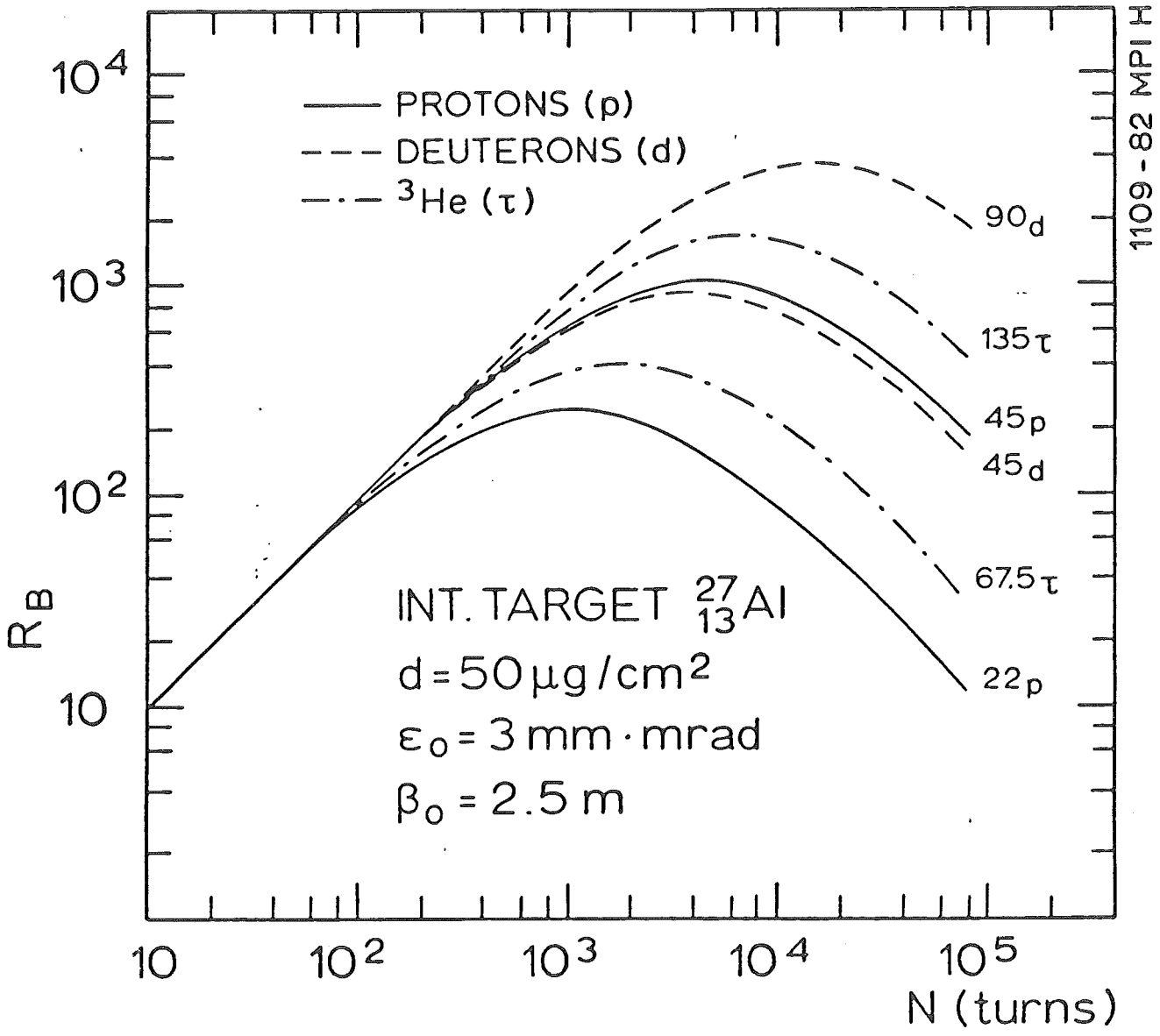
PROTONS (p)
DEUTERONS (d)
^{3}He (τ)
90d
135τ
45p
45d
67.5τ
22p
INT. TARGET $^{27}_{13}$Al
d = 50 µg/cm²
ε₀ = 3 mm · mrad
β₀ = 2.5 m
R_B
10
10^2
10^3
10^4
10^5
N (turns)
1109-82 MPI H

Fig. 1

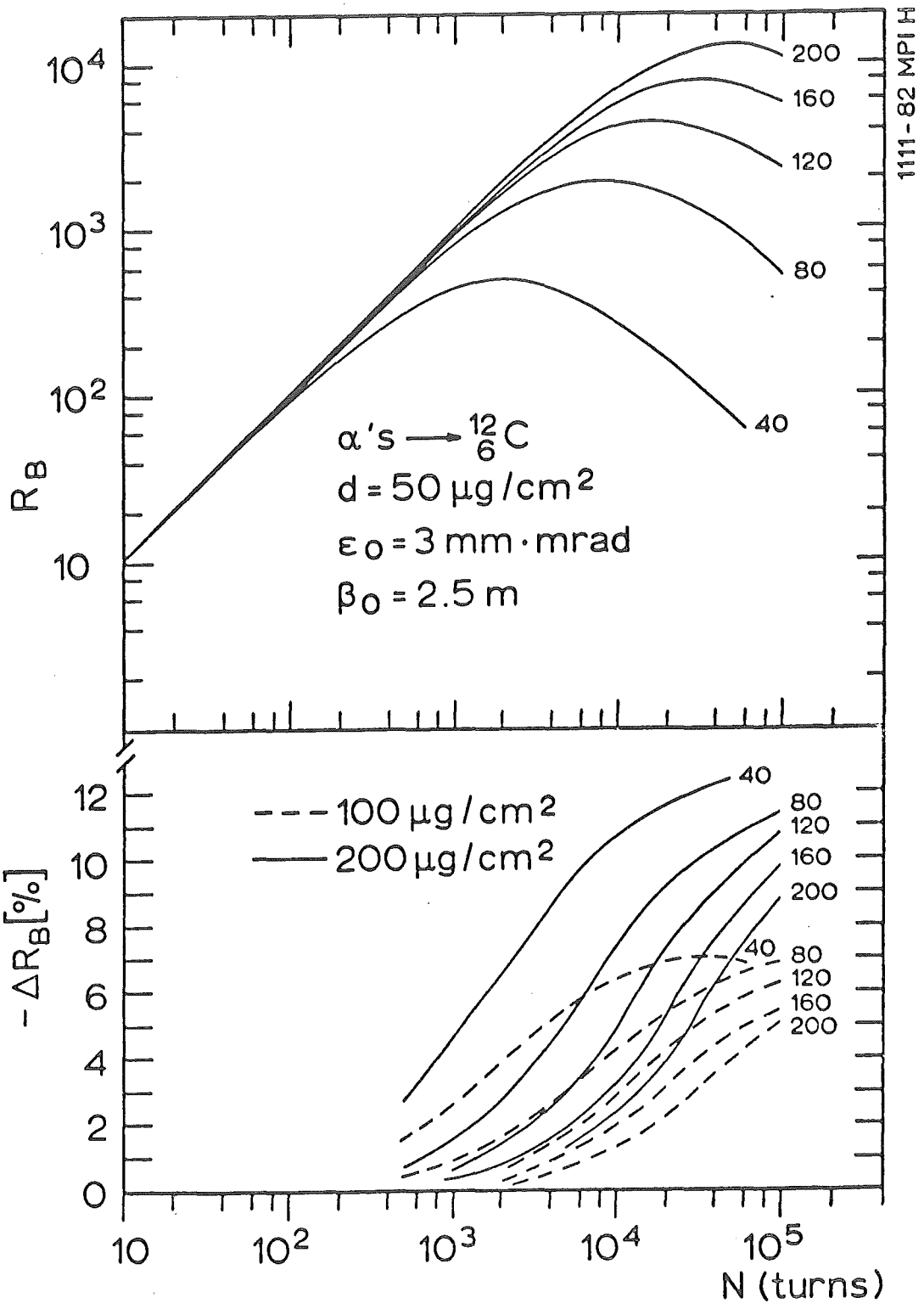
1111-82 MPI H
R_B
10^4
10^3
10^2
10
200
160
120
80
40
α's → $^{12}_{6}C$
d = 50 µg/cm²
ε_0 = 3 mm·mrad
β_0 = 2.5 m
$-\Delta R_B$[%]
12
10
8
6
4
2
0
100 µg/cm²
200 µg/cm²
40
80
120
160
200
10
10^2
10^3
10^4
10^5
N (turns)

Fig. 2

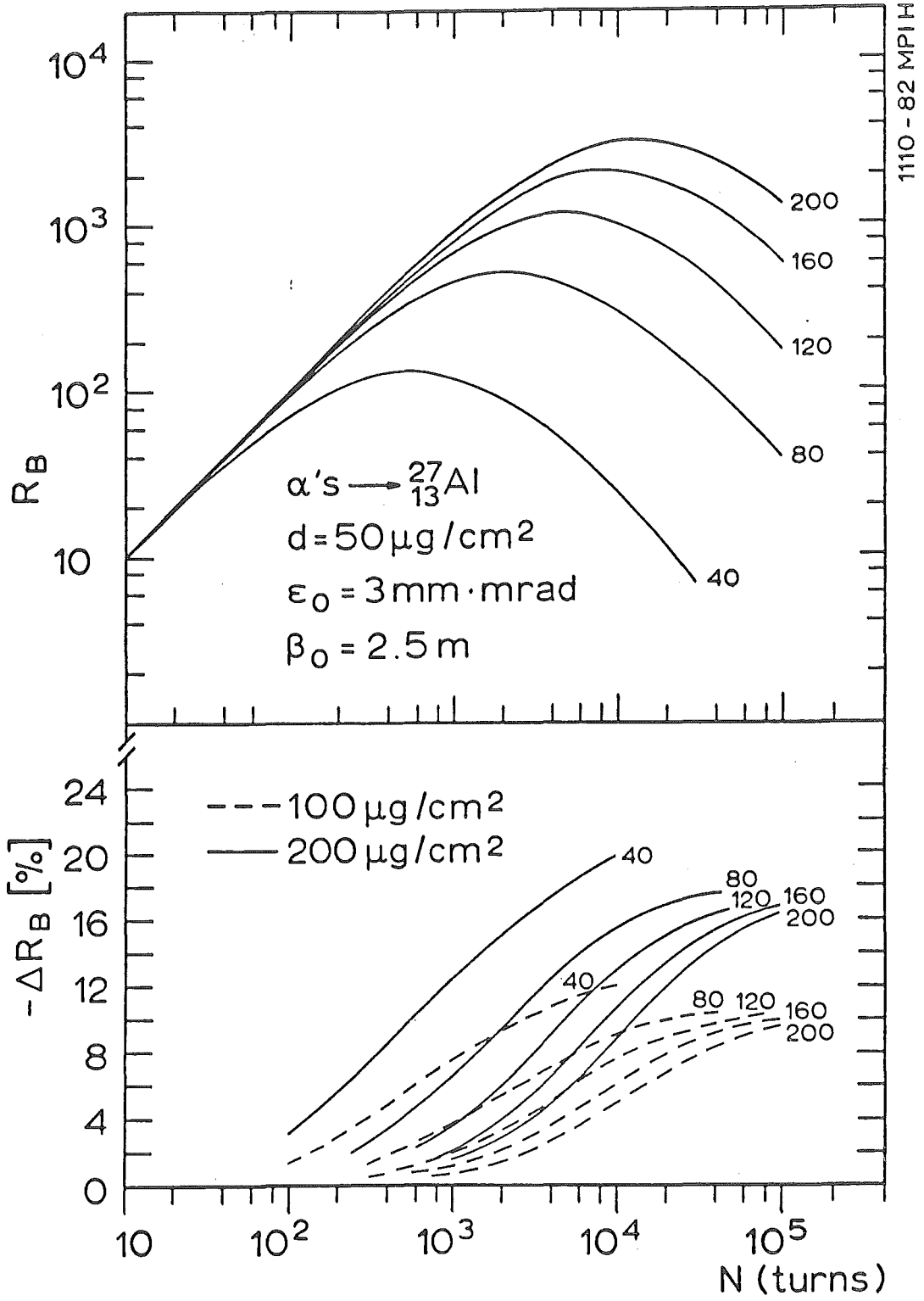
1110 - 82 MPI H
10^4
10^3
10^2
10
R_B
200
160
120
80
40
α's $\longrightarrow {}^{27}_{13}Al$
d = 50 µg/cm²
ε_0 = 3 mm · mrad
β_0 = 2.5 m
24
20
16
12
8
4
0
$-\Delta R_B$ [%]
--- 100 µg/cm²
—— 200 µg/cm²
40
80
120
160
200
40
80 120 160
200
10
10^2
10^3
10^4
10^5
N (turns)

Fig. 3

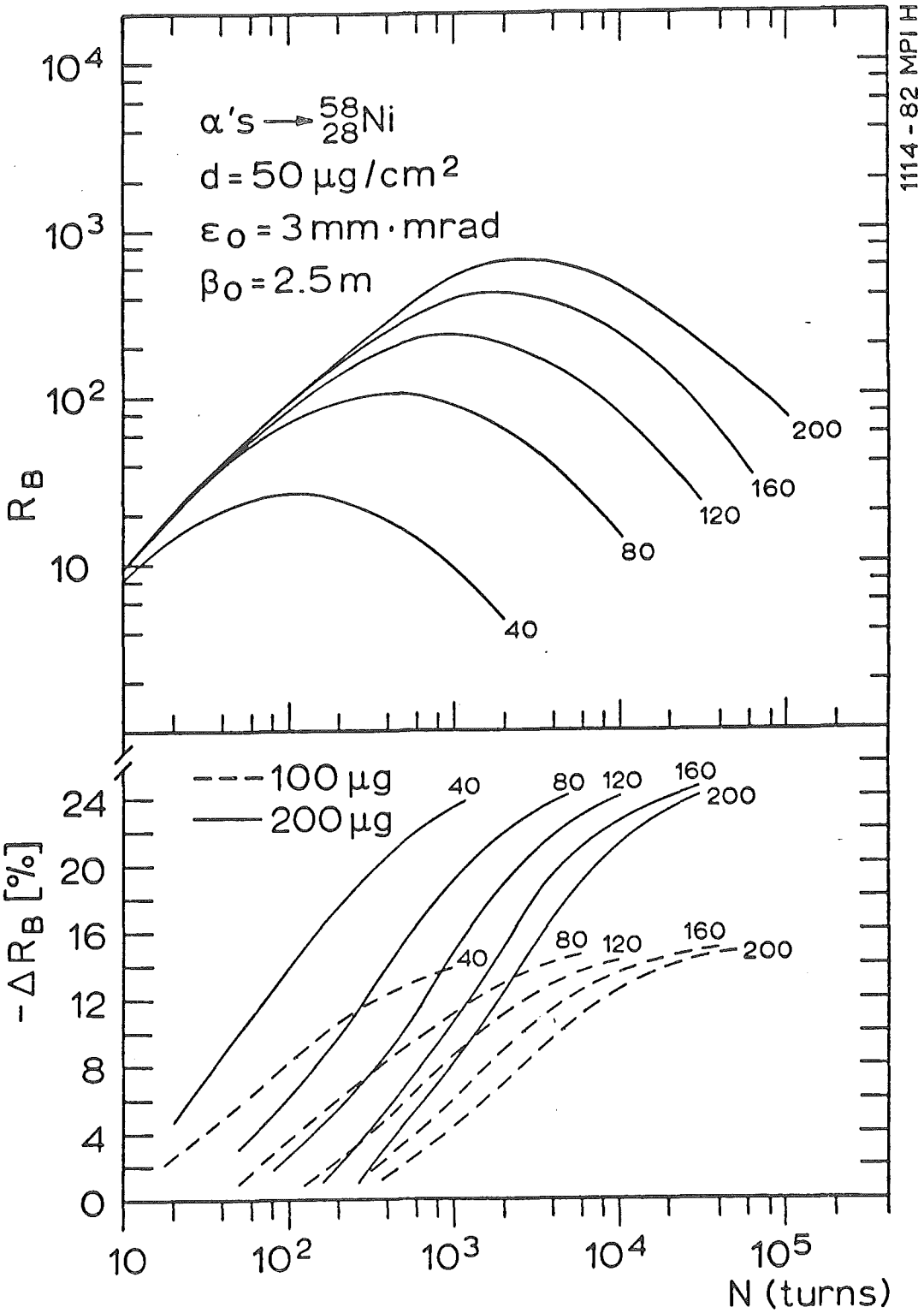
1114 - 82 MPI H
α's → $^{58}_{28}$Ni
d = 50 µg/cm²
ε₀ = 3 mm · mrad
β₀ = 2.5 m
R_B
200
160
120
80
40
---100 µg
——200 µg
-ΔR_B [%]
N (turns)

Fig. 4

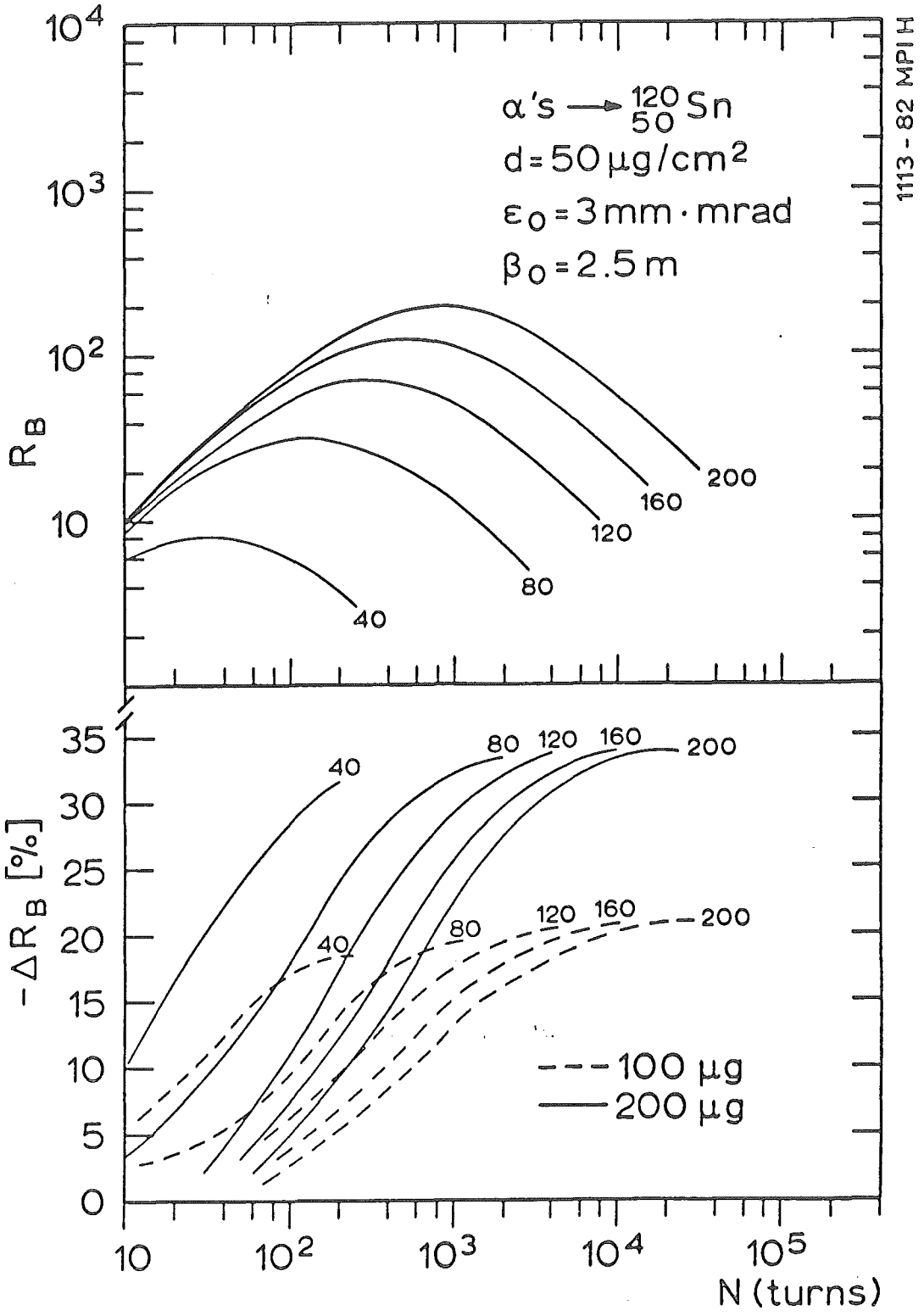
α's → $^{120}_{50}$Sn
d = 50 µg/cm²
ε₀ = 3 mm · mrad
β₀ = 2.5 m
1113 - 82 MPI H
R_B
40
80
120
160
200
-ΔR_B [%]
100 µg
200 µg
N (turns)

Fig. 5

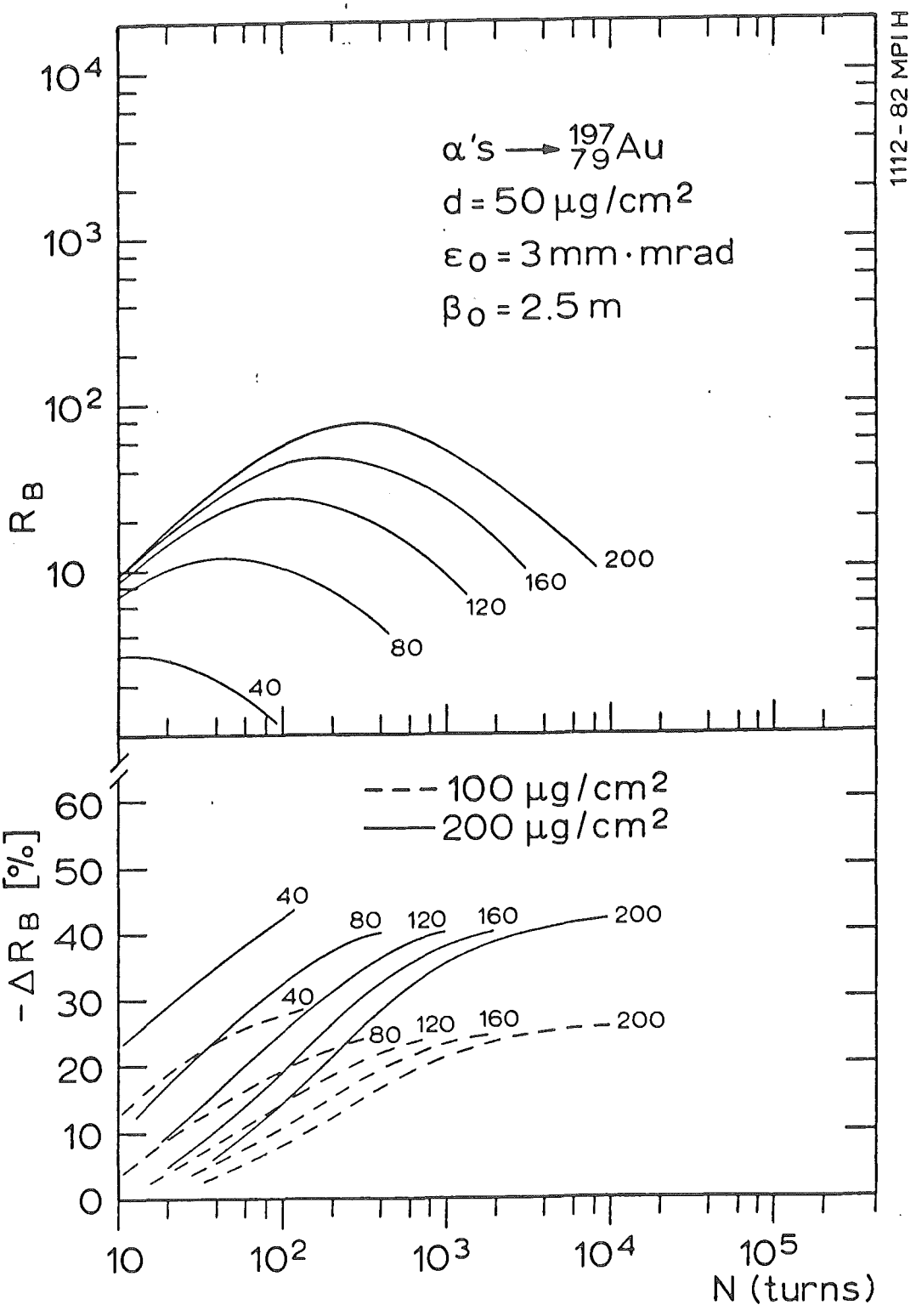
1112-82 MPI H
α's → $^{197}_{79}$Au
d = 50 µg/cm²
ε₀ = 3 mm·mrad
β₀ = 2.5 m
R_B
200
160
120
80
40
--- 100 µg/cm²
—— 200 µg/cm²
-ΔR_B [%]
N (turns)

Fig. 6

(i) For $R_B = 1$ the breakeven point is reached, i.e., assuming 100 % injection efficiency and no other losses than those due to Coulomb (single) scattering the beam intensity is the same as without the recirculator. For heavy ions - even with a thin target - $R_B(max)$ becomes small.*

(ii) The brilliance gain is positive for $N < N_{max}$. For $N > N_{max}$ the beam becomes diffuse, since the emittance grows, it misses the target and eventually hits the walls of the vacuum pipe.

What is quantitatively the corresponding emittance growth? For the emittance after N-turns, ε_N

$$\varepsilon_N = \varepsilon_o + c \cdot N \qquad \text{with } c = \frac{1}{2}\pi\beta_o \cdot nt \cdot \sigma_c \langle\Theta\rangle^2$$

$$R_B = N/\left(1 + \frac{c \cdot N}{\varepsilon_o}\right)^2$$

For the maximum $R_B(max)$ the corresponding N_{max} is given by

$$\frac{dR_B}{dN} = \frac{\left(1 - \frac{c}{\varepsilon_o} N\right)}{\left(\frac{c}{\varepsilon_o} N + 1\right)^3} = 0$$

---

* For a ^{12}C target of 10 $\mu g/cm^2$, $\varepsilon = \pi$ mm · mrad, $\beta_o = 2{,}5$ m, the following maximum R_B values are possible:

E(MeV/A)	ION	$R_B(max)$
10	^{7}Li	60
10	^{12}C	36
10	^{32}S	3.8
10	^{58}Ni	0.6

$$N_{max} = \frac{\varepsilon_o}{c}$$

Hence for $N = N_{max}$ the emittance ε_o has grown by a factor of 2. Since the operation should be in the regime where $dR_B/dN > 0$, this important result implies that for the stacking considerations the transverse "runaway" accounts for only twice the original emittance.

The maximum number of particles N with charge $\bar{z}$ and mass A in a storage ring is limited by the space charge limit. For a ring with circumference C, minor and major semiaxes a and b, respectively, where Q_o denotes the tune and ΔQ the tune shift N, is given by Craddock (CR 80)

$$N = \frac{A}{Q^2}\,\pi^2\beta^2\gamma^3\,\frac{b(a+b)}{C \cdot r_o} \cdot 2Q_o\Delta Q$$

$r_o = e/(4\pi\varepsilon_o mc^2)$ = classical proton radius

$= 1.535 \quad 10^{-16}$ cm

With a and b given as

$$a,b = \left(\beta_r,\ \beta_z \cdot \varepsilon_\theta,\ \varepsilon_{z/\pi}\right)^{1/2}$$

and assuming as before

$\varepsilon_o = \varepsilon_r = \varepsilon_z = 3\pi$ mm mrad and

$\beta_o = \beta_r = \beta_z = 2.5$ m hence

$a = b = 2.7$ mm and with $Q_o \cdot 2\Delta Q = .4$ (s. sect.)

$$\tilde{N} = 8.16 * 10^{11} A/Q^2 \beta^2 \gamma^3$$

In tab. 2 below for particles available from Jülich $\tilde{N}$ and the circulating current given by (BO 70)

$$I[A] = \frac{ec}{2\pi} \frac{\tilde{N}\beta}{R} \cdot Z = 7.644 * 10^{-12} \frac{\tilde{N}\beta}{R} \cdot Z$$

with the radius R of the ring $R = \frac{C}{2\pi} = 7.5$ m are listed.

E [MeV] , particle	22p	45p	45d	90d	90α	180α	675τ	135τ
βγ	.218	.313	.220	.313	.220	.313	.220	.313
$\tilde{N}(10^{11})$	.40	.84	.81	1.68	.41	.84	.30	.63
I mA	8.6	25.7	17.8	51.3	17.9	51.4	13.3	38.5
$\tilde{N}^*(10^{16}/\text{sec})$	5.36	16.0	11.1	32.0	5.60	16.0	4.2	12.0

The last row contains the number N^* of particles per sec. which pass the target: $\tilde{N}^* = 6.2418 * 10^{15} \cdot \frac{I}{Z}$ [mA] (Bo 70). The beam intensity and the luminosity are determined by N_{max}. The filling time τ necessarily is given by

$$\tau = N^{max} \tau_{sp} = N^{max} \frac{C}{\beta \cdot c}$$, with C = the ring circumference.

In fig. 7c for a 50 μg/cm^2 Al-target it is seen that for all light particles in the Jülich domain 1 ms < τ < 10 ms. For α-particles in fig. 7a the dependence of τ on the choice of the target material and thickness shows that

$$30\,\mu s < \tau < 50\,ms$$

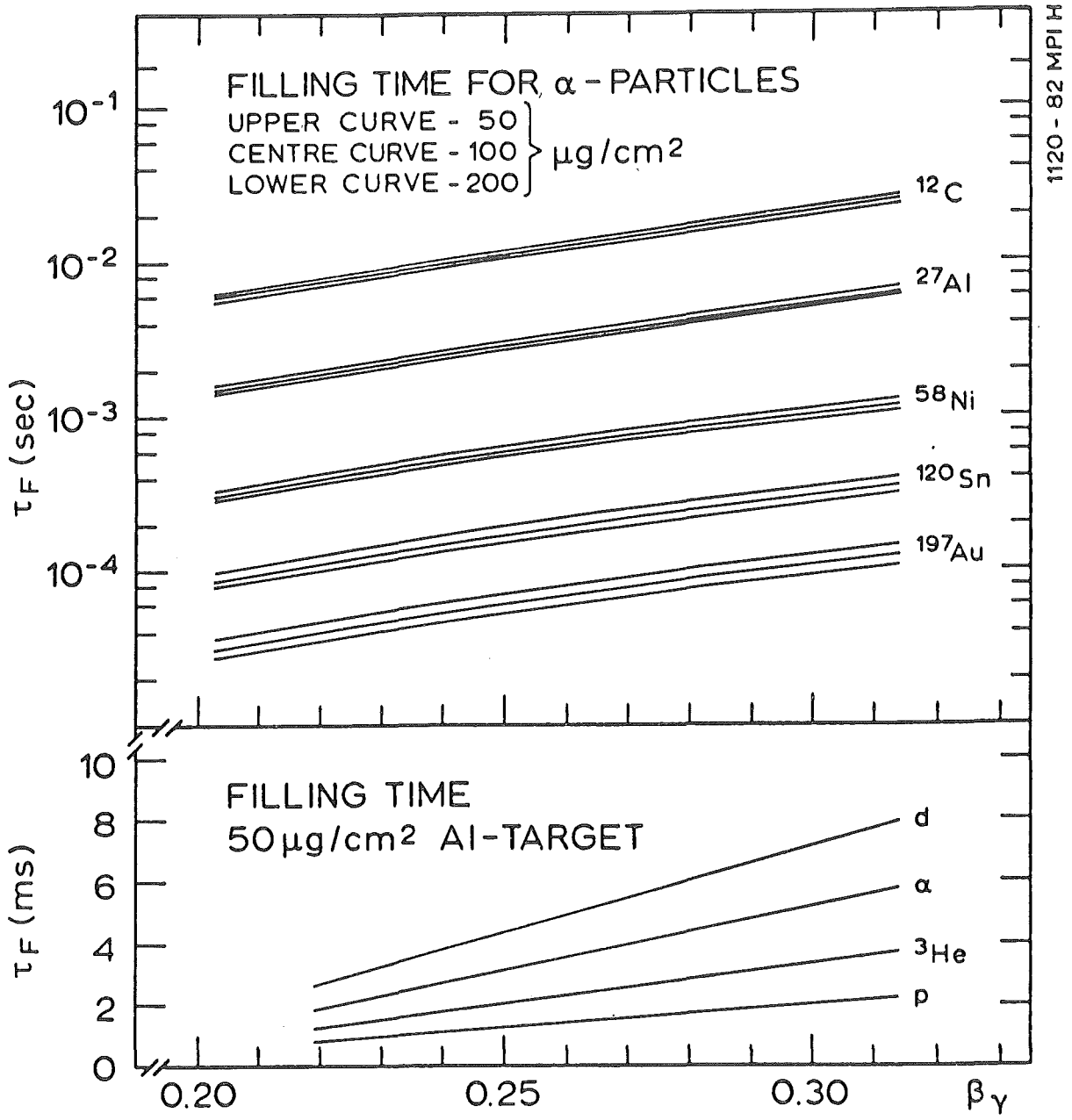
FILLING TIME FOR α - PARTICLES
UPPER CURVE - 50
CENTRE CURVE - 100
LOWER CURVE - 200
μg/cm²
12C
27Al
58Ni
120Sn
197Au
τF (sec)
10-1
10-2
10-3
10-4
FILLING TIME
50 μg/cm² Al-TARGET
d
α
3He
p
τF (ms)
10
8
6
4
2
0
0.20
0.25
0.30
βγ
1120 - 82 MPI H

Relation Between Longitudinal RF-"Cooling" and Transverse Heating

Let us define three regions in the storage ring: The subscript o shall represent physical quantities in front of the stripper, subscript 1 immediately after the target stripper and subscript 2 after RF cavity.

The beam ellipse is assumed to be upright at the stripper, i.e.,

$$\sigma_{0,1} = \begin{pmatrix} \sigma_{11} & 0 \\ 0 & \sigma_{22} \end{pmatrix} \qquad (1)$$

The stripper has the following effects on the beam:

a.) The energy is degraded by straggling and

b.) due to multiple scattering the beam is broadened.

The energy loss is accounted for by a momentum loss dp, whereas the multiple scattering is characterised by the angle $\alpha = \langle\theta^2\rangle^{1/2}$

Passing through the stripper the emittance changes from $A_o = \pi(\det\sigma)^{1/2}$ to

$$A_1 = \pi \cdot \left[\sigma_{11}\left(\sigma_{22} + \frac{\alpha^2}{2}\right)\right]^{1/2} \qquad (2)$$

. For $\alpha^2 \ll \sigma_{22}$

$$= \pi \cdot \left[\sigma_{11} \cdot \sigma_{22}\right]^{1/2} + \frac{1}{4}\frac{\alpha^2}{\sigma_{22}} \qquad (3)$$

$$= A_o + dA \qquad (4)$$

$$\text{with } dA = \frac{A_o\,\alpha^2}{4\sigma_{22}} \qquad (5)$$

The product of emittance and momentum stays constant when the beam traverses the RF cavity, i.e.,

$$B = A_1 p_1 = (A_o + dA)\ (p_o - dp)$$
$$= p_o(A_o + dA) - A_o dp \qquad (6)$$

The emittance after passage through the cavity is

$$A_2 = B/p_o = (A_o + dA) - A_o \frac{dp}{p_o} \qquad (7)$$
$$= A_o\left(1 + \frac{\alpha^2}{4\sigma_{22}} \rightarrow (dp/p_o)\right)$$

Apparently to avoid the beam blowing up in successive passages the relative increase in beam divergence relative to the unperturbed divergence should be smaller than energy degradation due to straggling and to be compensated by the RF cavity.

$$\alpha^2/4\sigma_{22} < dp/p_o \quad \text{and with} \quad dT/T = 2\, dp/p_o$$
$$\Theta_{max} = (\sigma_{22})^{1/2} > \alpha/(dT/T)^{1/2} = \Psi \qquad (8)$$

The energy losses $\overset{dT}{\gamma}$ were calculated following Fano (FA 63)

$$dT\,[MeV] = .307 \cdot d\,[g/cm^2] \cdot Z_T/A_T \left(z_i/\beta\right)^2$$
$$\times \left[\ln\left(\frac{2m_e c^2(\beta\gamma)^2}{I}\right) - \beta^2\right]$$

with d, the thickness of the target with charge and mass

number Z_T and A_T respectively and $Z_i, \beta \cdot \gamma$, the charge and momentum of the incident particle. The ionisation potential I is approximated by $I = 16 \cdot (Z_T)^{0.9}$ eV. The results were checked against the Northcliffe-Schilling tables(NO) to be consistent to within 10 % for the beam parameters and target thicknesses investigated. The mean energy loss has been calculated with the sophisticated computer code STRAGGL ( ) for some cases and compared to the energy loss from the evaluation above. Differences were at most for very small energy loss ~ 20 %.
In fig. 9 the quantity

$$\psi = \langle\theta^2\rangle^{1/2} \quad (\alpha T/T)^{1/2} \quad [\text{mrad}]$$

has been plotted for protons, deuterons, ^{3}He and α-particles, with $\langle\theta^2\rangle^{1/2}$ from eq. 7 p. 3 . This expression depends only very weakly on the target thickness at least in the range of 50-500 μg/cm^2. It is seen that for the present lattice the criterion eq. 8 is not fulfilled. In general without any cooling provisions the operation corresponds to a transverse "runaway".

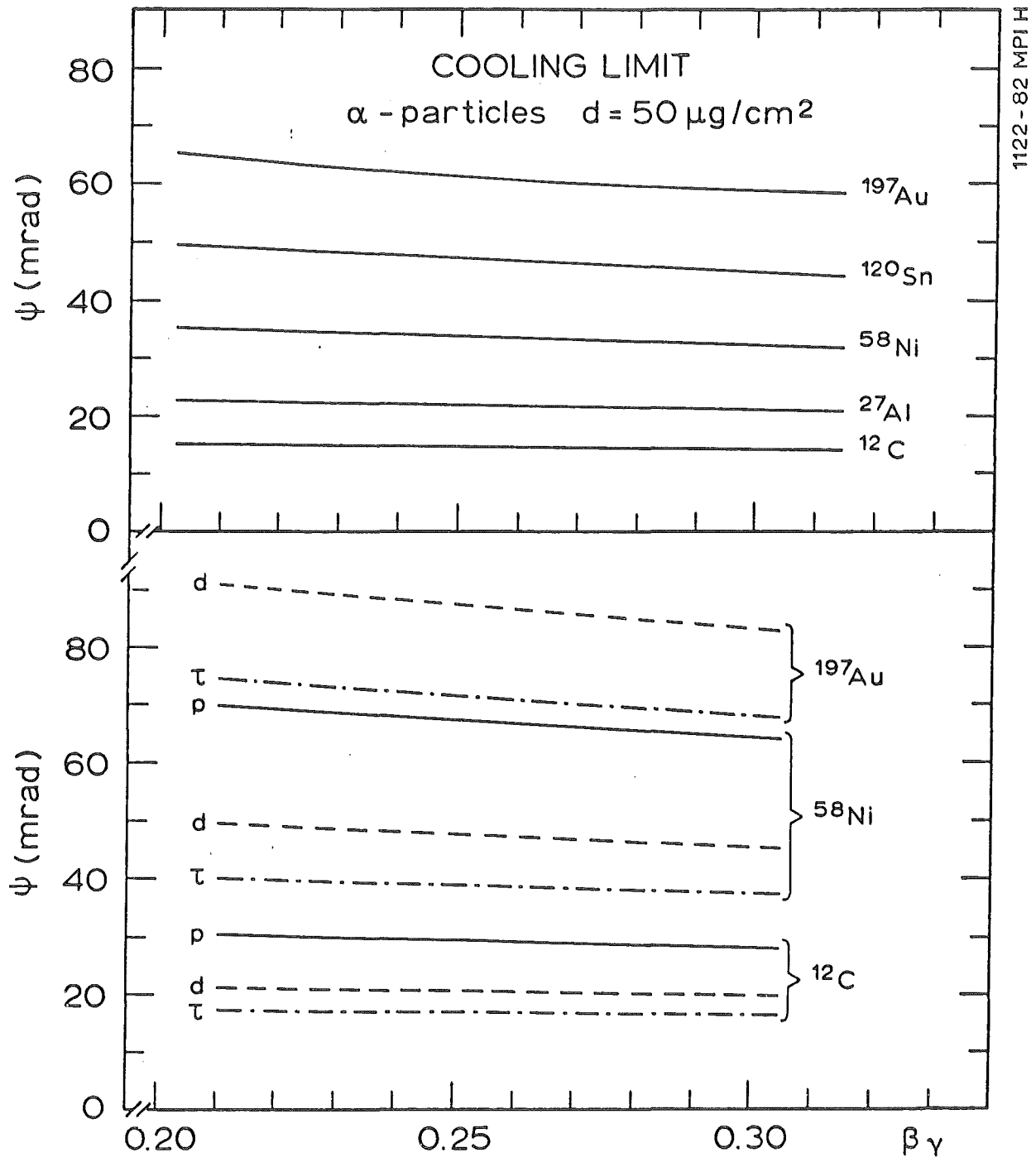
COOLING LIMIT
α - particles d = 50 µg/cm²
1122-82 MPI H
ψ (mrad)
80
60
40
20
0
197Au
120Sn
58Ni
27Al
12C
d
τ
p
197Au
58Ni
12C
0.20
0.25
0.30
βγ

References

Co75 - R.K.Cooper and G.P.Lawrence, IEEE Transactions on Nucl.Sc.Vol. NS-22, No.3(975) 1916

Jo73 - Joy, Nucl.Instr.and Methods 888 106 (1973) 237

Ma67 - J.B.Marion and B.A.Zimmermann, Nucl.Instr.and Methods 51(1967)93

Mo47 - G.Molière, Z.Naturf. 2a (1947) 133; 3a(1948) 78

Ni59 - B.P.Nigam, M.K.Sundaresan and T.-Y.Wu, Phys.Rev.115(1959)491

Pa8o - Particle Properties Data Booklet 1980, ed.CERN (1980) 81

Ka8o - S.Kalbitzer and H.Oetzman, Radiation Effects Vol.47(980)57

Fa63 - U.Fano, Ann. Rev. Nucl. Sci. 13 (1963) 1

No - Northcliffe

HU81 - B.Huck, Ph.d.thesis, Heidelberg 1981

CL79 - C.K.Cline et.al. Phys. Rev. 180 (1969) 450

Po 8(R.E.Pollock, Proposal for a Cooler-Tripler for the IUFC, Bloomington

JO73 - M.J de Jonge and F.W. Nesseschmid, Proc. 1973 Acc. Conf. S.Francisco, IEEE Trans. on Nucl Sci. 20 (1973) 796

The challenge of physics with a high-energy light-ion facility

F. Osterfeld
Institut für Kernphysik
Kernforschungsanlage Jülich

The challenge of physics with a high-energy light-ion facility

I. Nuclear reaction mechanisms and nuclear structure studies at E = 100-1000 MeV/am

II Mesonic degrees of freedom in nuclei

III. Test of fundamental symmetries

IV Study of the free nucleon-nucleon interaction over a large energy range

I Nuclear reaction mechanisms and nuclear structure studies at E = 100 - 1000 MeV/nucleon

A. Proton induced reactions

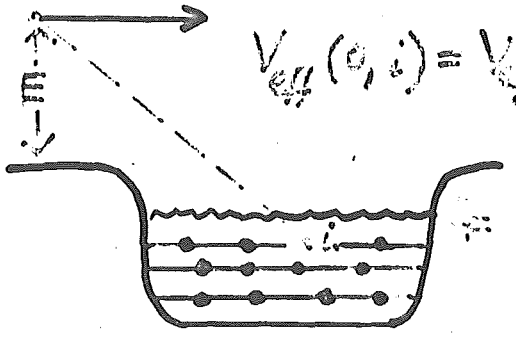

$$V_{eff}(\theta, i) = V_{eff}(\vec{r}_0, \vec{r}_t, \rho_T, E)$$

properties of V_{eff}:
1. energy dependent
2. density dependent
3. non local
4. complex (imaginary part)

Properties of V_{eff} at high incident energies

1. reaction mechanism is direct, i.e. multi step processes are suppressed

2. The Impuls approximation becomes valid (Kerman, McManus, Thaler)

$$V_{eff}(\theta, i) \longrightarrow t_{NN}(\theta, i)$$

free nucleon - nucleon t-matrix

density dependence ?

Love and Franey:

Free nucleon-nucleon scattering amplitude

↓ local representation of t (sum of 3 Yukawa's) (exchange is treated explicitly)

$$t(r;E) \equiv V_{eff}(r;E)$$

representation of $t(r;E)$ with spin-isospin components:

$$t(r;E) = \underbrace{\underbrace{t_c(r) + t_{\sigma\sigma}(r)\vec{\sigma}_1\cdot\vec{\sigma}_2}_{\text{spin-flip}} + \underbrace{t_{\tau\tau}(r)\vec{\tau}_1\cdot\vec{\tau}_2}_{\text{isospin-flip}} + \underbrace{t_{\sigma\tau}(r)\vec{\sigma}_1\cdot\vec{\sigma}_2\,\vec{\tau}_1\cdot\vec{\tau}_2}_{\text{spin-isospin-flip}}}_{\text{central}}$$

$$+ \underbrace{\underbrace{t_{LS}(r)\,\vec{L}_{12}\cdot(\vec{\sigma}_1+\vec{\sigma}_2) + \underbrace{t_{LS\tau}(r)\,\vec{L}_{12}\cdot(\vec{\sigma}_1+\vec{\sigma}_2)\,\vec{\tau}_1\cdot\vec{\tau}_2}_{\text{isospin flip}}}_{\text{spin-orbit}}}$$

$$+ \underbrace{\underbrace{t_T(r)\,S_{12}}_{\text{spin-flip}} + \underbrace{t_{T\tau}(r)\,S_{12}\,\vec{\tau}_1\cdot\vec{\tau}_2}_{\text{spin isospin flip}}}_{\text{tensor}}$$

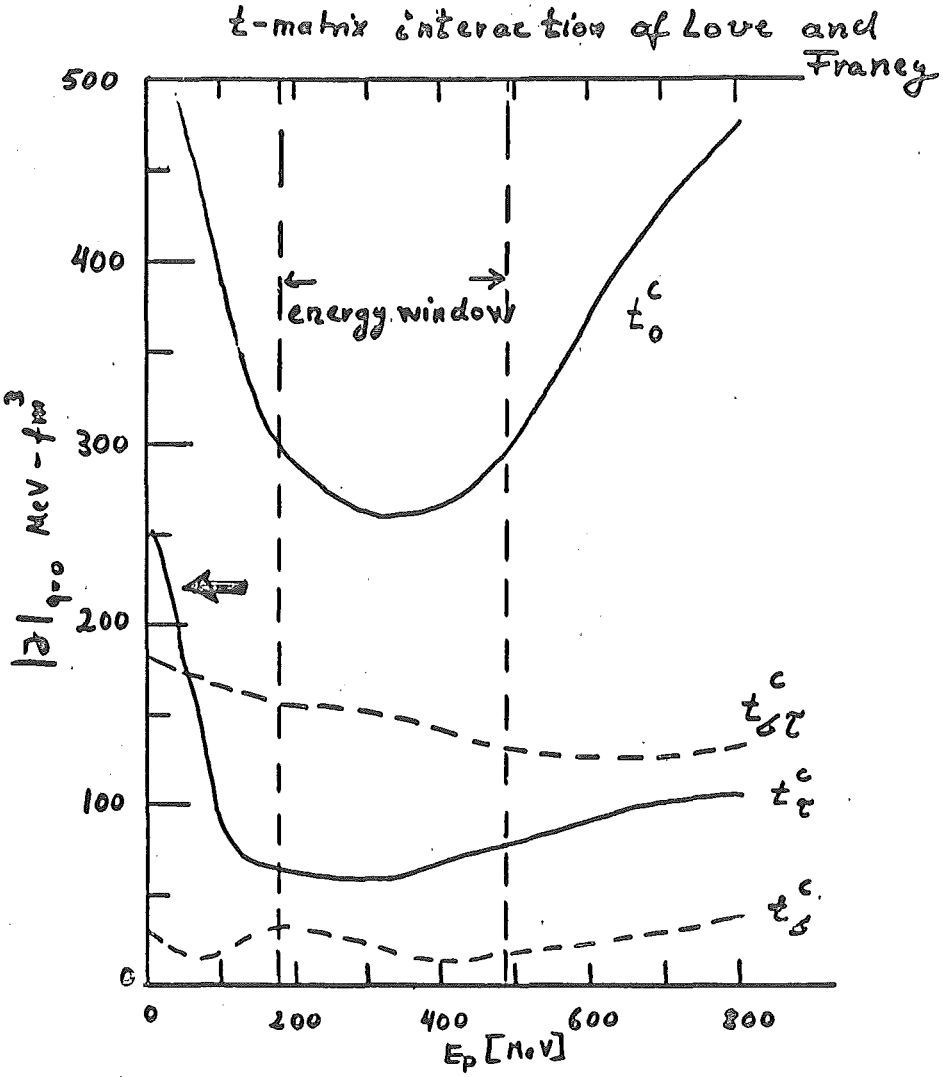

energy window: natural selectivity due to the choice of the incident energy

a. unnatural parity transitions are enhanced against the "background" of natural parity states

b. charge exchange: $\Delta S=1, \Delta T=1$-modes are much stronger excited than $\Delta S=0, \Delta T=0$-modes

Gamow-Teller Resonance (1^+)

C. Goodman et. al (1980)

IUCF

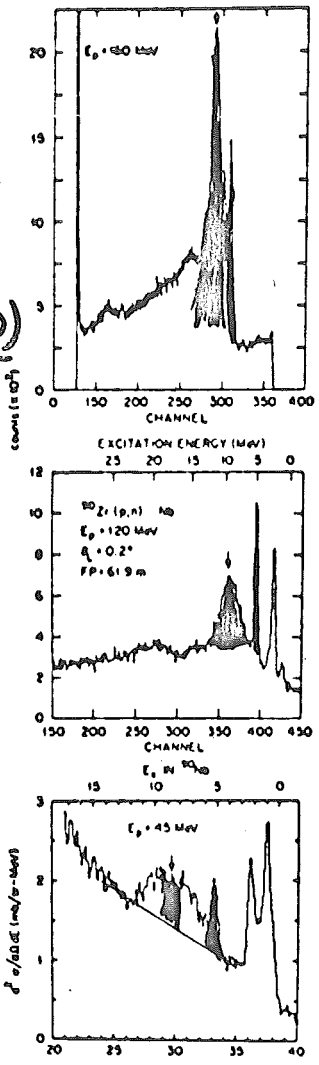

160 MeV

$^{90}Zr(p,n)$

120 MeV

45 MeV

Fig. 8 Forward angle excitation functions for $^{90}Zr(p,n)$ at E_p = 45, 120, and 160 MeV. The arrows mark the giant GT transition which grows markedly in strength with increasing energy.

Test of the impulse approximation

(or any other constructed effective NN-interaction)

1. nuclear scattering from light target nuclei

$$p + d \longrightarrow {}^3He + \gamma \qquad [V_{pd} = V_{pp} + V_{pn}]$$

2. generally: $p + A$

$$V_{NN}(E) \longrightarrow V_{NA}(E) \longrightarrow \sigma_{NA}(E)$$

(cross section)

3. Nucleus as filter

test of the different force components (central, spin orbit -, and tensor terms) of $t(r, E)$

Choose nuclear transitions where the structure of states is known either from (e,e') measurements or microscopic nuclear structure calculations

Test of

a.) Central- + $\vec{L}\cdot\vec{S}$-forces: Choose multiplett $0^+, 2^+, 4^+, \ldots 10^+, 1$
(simultaneous test of momentum (q) depend. of force)

b.) Tensor-forces: unnatural parity transitions stretched configurations $\left[\begin{matrix}\vec{j}_h \\ \vec{j}_p\end{matrix}\right] \vec{J}_f$

c.) $\tau\tau$-term: charge exchange: $\Delta T = 1, \Delta S = 0$ for example IAS

d.) $\sigma\sigma\tau\tau$-term: charge exchange: $\Delta T = 1, \Delta S = 1$ GT

e.) density dependence: medium corrections — 1^- $(\Delta T = 0)$ - transitions generally natural parity transitions $(\Delta S = 0, \Delta T = 0$

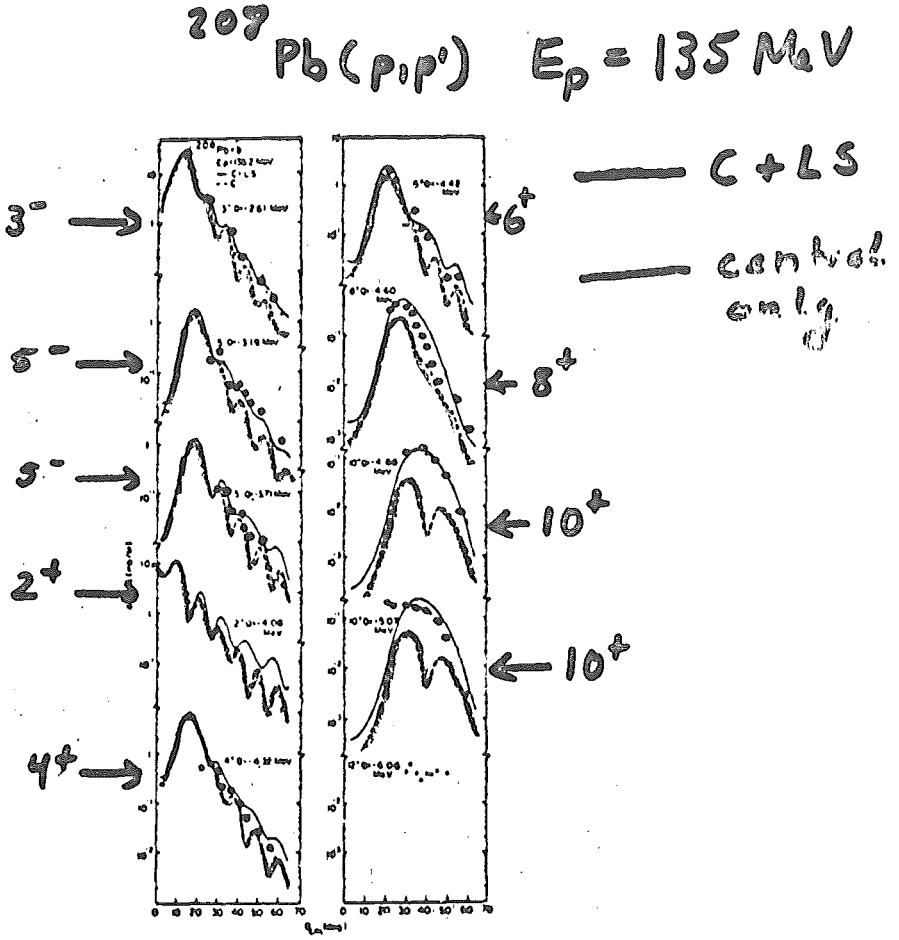

Fig. 11 The results of DWIA calculations for normal parity transitions in ^{208}Pb + p at E_p = 135 MeV. Results with (C + LS) and without (C) the spin-orbit interaction are shown separately. Note the decrease in the central contributions to the cross sections for transitions with J≥8.

Test of central and $\vec{L}\cdot\vec{S}$ - force

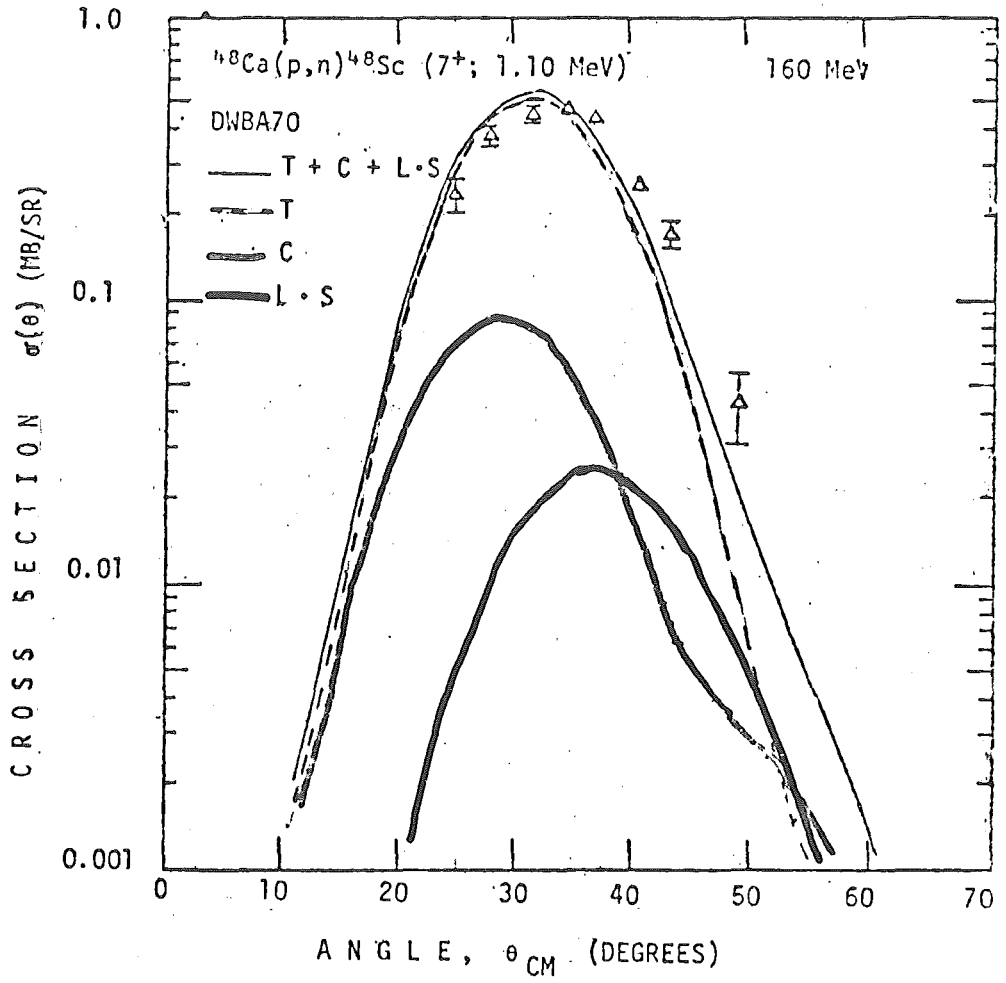

Fig. 3. Angular distribution of the $^{48}Ca(p,n)^{48}Sc$ (7^+; 1.10 MeV) reaction at 160 MeV. The dotted, dashed, dash-dotted and solid curves are DWBA70 calculations with the effective interaction of Love (1980) for the central only, tensor only, L·S only, and the coherent sum of all three terms, respectively.

Test of tensor force

J. Wambach : Doktorarbeit

^{208}Pb

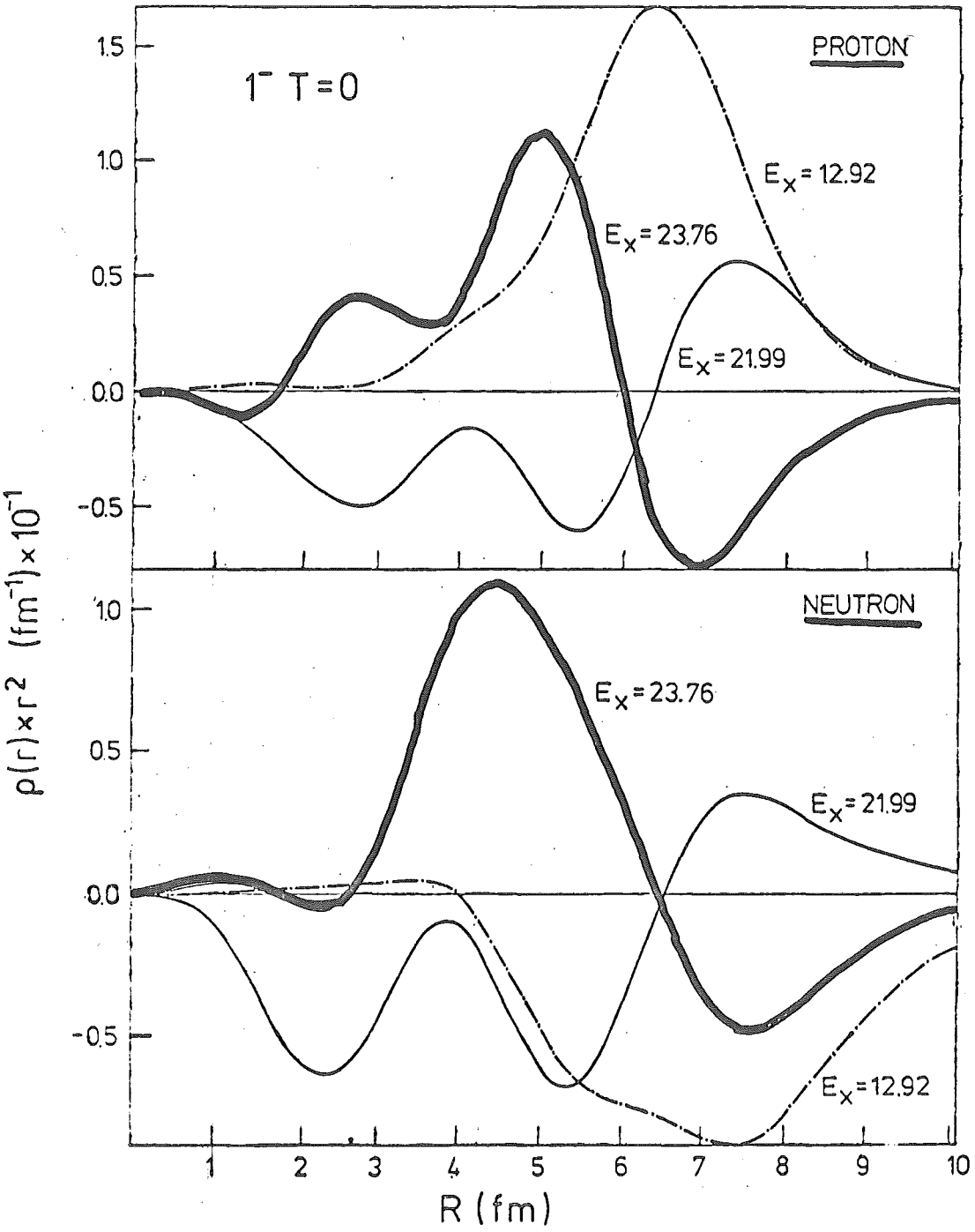

Test of the density dependence of the force [medium corrections]

B. Nuclear structure studies with Hadrons

1. elastic scattering
   a. form of nuclear potentials
   b. proton- and neutron mass distributions in nuclei

2. (p,p'),... (α,α') and (p,n) ; (^{3}He,t) ; (^{6}Li,^{6}He)..
   a. damping of nuclear states (coupling to 2p-2h)

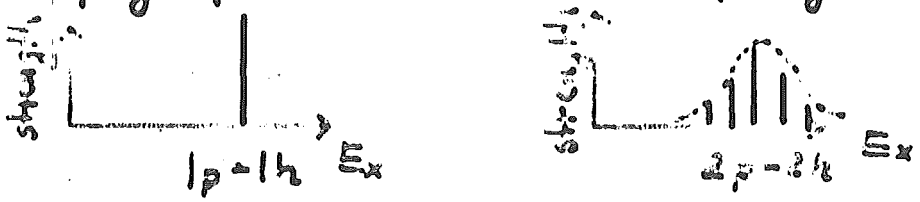

high spin states of simple configuration

   b. "new" giant resonances (identification and their decays (escape $\Gamma^\uparrow$ + spreading $\Gamma^\downarrow$)

   1. electric isovector resonances (0^+;T=1), (2^+;T=1

Δ(1232) - isobar degrees of freedom

   β. magnetic (M1,M2,...) resonances (Spin(σ)- and spin-isospin (στ)- contributions specific)

   c. Gamow-Teller transitions (and Fermi transitions)

[Quark-spin flip]

---

high spin/high energy: a good "signal" to background ratio

high beam intensity: b. Coincidence experiments

high resolution!

3. Single particle aspects of nuclei

a. knock out reactions: $(\vec{p}, 2p)$ and $(\vec{p}, pn)$
measurement of separation energies of deep hole states, momentum distributions, spectral functions

polarised projectile $(\vec{p})$ 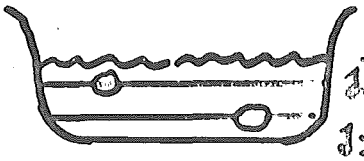

10 MeV ≤ E ≤ 50 MeV:

Distortion effets for projectile and knocked-out nucleon are smallest

b. pick-up - and stripping reactions
$(d, {}^3He)$,.... (d, t), ...

high energies:

α. favourable population of high spin single particle states (2 nucleon hole states)

β. width of $\begin{cases} \text{particle states} \\ \text{hole states} \end{cases}$ → width of ph-states

γ. variable energy ⟷ background

4. Test of many particle correlations in nuclei

cluster knock out reactions like (p, d), ...

advantage at E ≥ 100 MeV:

a.) "small" distortion effects

b.) multi step processes in the

S. Gales et al. (Orsay)

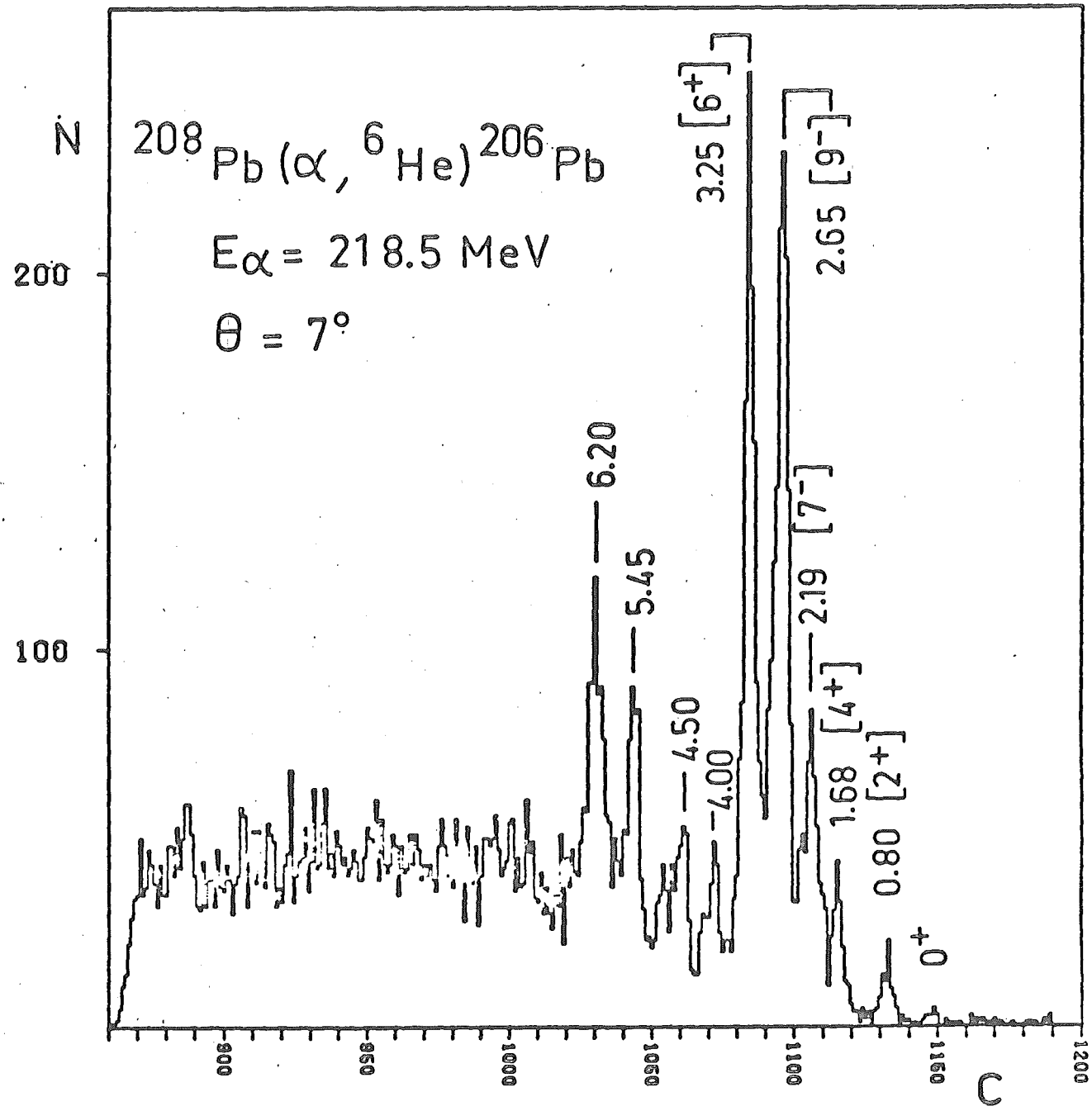

BENSON Créteil 890-10-90-192320133

projectile : ^{6}He

excites selectively high-spin states

Gales et al. (Orsay)

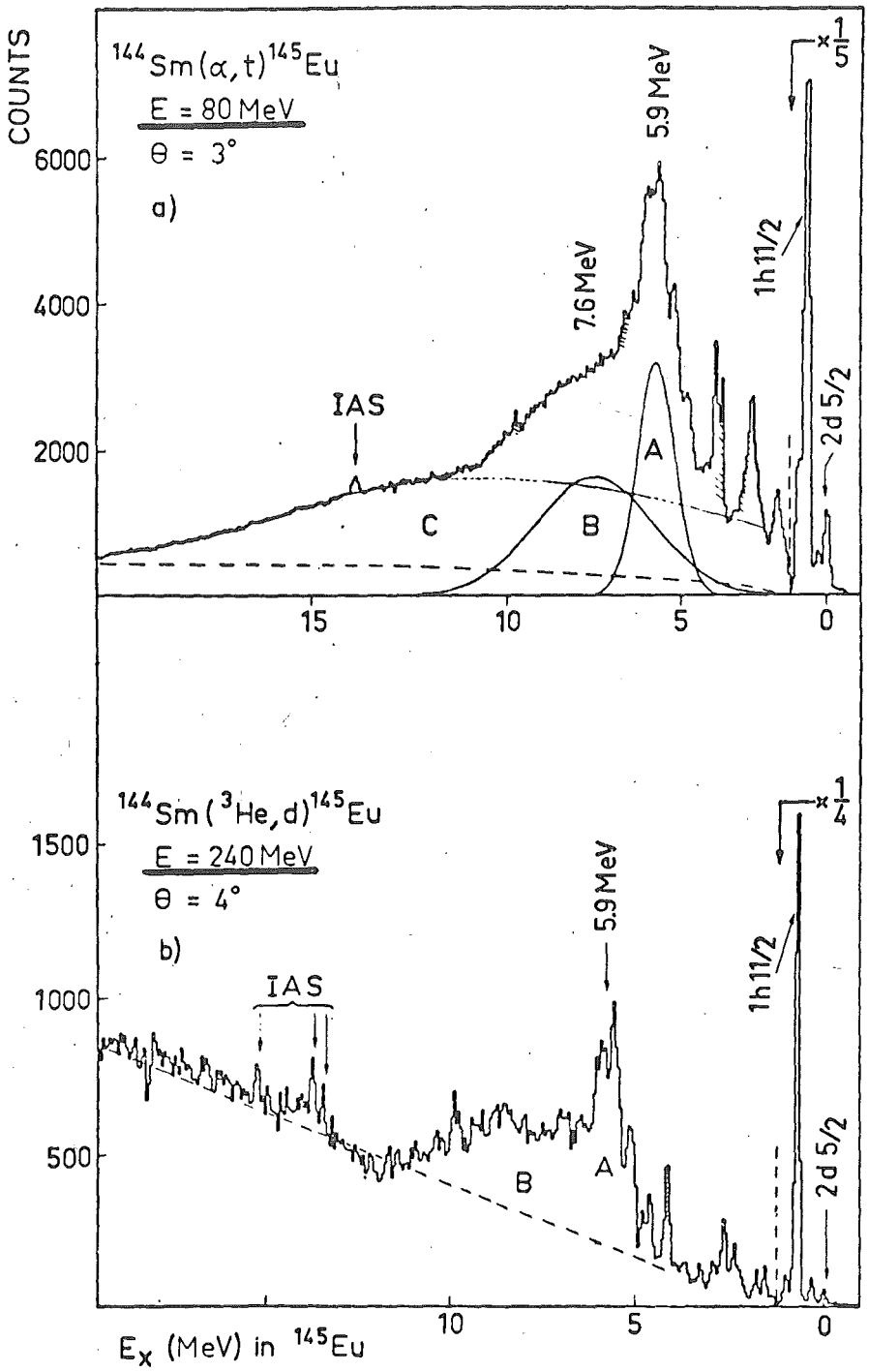

Variable energy → possibility to distinguish between "background" and peaks!

II Mesonic degrees of freedom in nuclei

1. The presence of virtual pions and isobars (Δ's) in nuclei affects the structure properties of nuclei like:
   a. magnetic moments ("quenching")
   b. unnatural parity transitions ($0^-, 1^+, 2^-, \ldots$-states)
   c. strength distribution of M1- and Gamow-Teller states
   d. short range two nucleon correlations
   e. three body forces

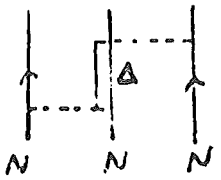

2. Pion production (Investigation of reaction mechanism)
   a. Pion production with discrete final states
      $A(p,\pi)A+1$
      high momentum transfer
   b. excitation of (collective?) Δ-hole states
   c. $A(d,\pi)A+2$ - reactions
      ↑
      correlated nucleon-nucleon pair
      Δ-component in wave function
   d. collective effects → pionic fusion
      $^3He + {}^3He \longrightarrow {}^6Li + \pi$

I. M1 - and GT - resonances

- collective nuclear excitations, which involve the spin (σ) - and spin-isospin ($\sigma\tau$) - degrees of freedom of the nucleons

a. M1-resonances (single particle model)

$|1^+, T_0, T_0\rangle =$ 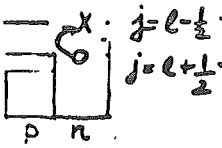

(for ex. ^{48}Ca)

transition oper.:
σ : isoscalar exc.
$\sigma\tau_z$: isovector exc.

b. GT-resonances (single particle model)

The GT-strength is split into various T-components:

$(T_- = \sum_k t_-(k))$

1. analogue to M1:

$|1^+, T_0, T_0-1\rangle = \frac{1}{\sqrt{2T_0}}$ 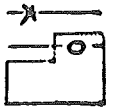 $+ \sqrt{\frac{2T_0-1}{2T_0}}$ 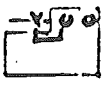

2. antianalogue to M1: $|1^+, T_0-1, T_0-1\rangle$

3. configuration state

$|1^+, T_0-1, T_0-1\rangle =$ 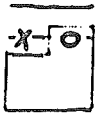

Important: We learn about spin (g_0) - and spin-isospin (g_0') correlations in nuclei

$F_{ph} = C_0 [g_0 \vec{\sigma}_1\vec{\sigma}_2 + g_0' \vec{\sigma}_1\vec{\sigma}_2 \vec{\tau}_1\vec{\tau}_2] \delta(\vec{r}_1 - \vec{r}_2)$

Quenching $\longleftrightarrow$ Δ_{33} - isobar effect

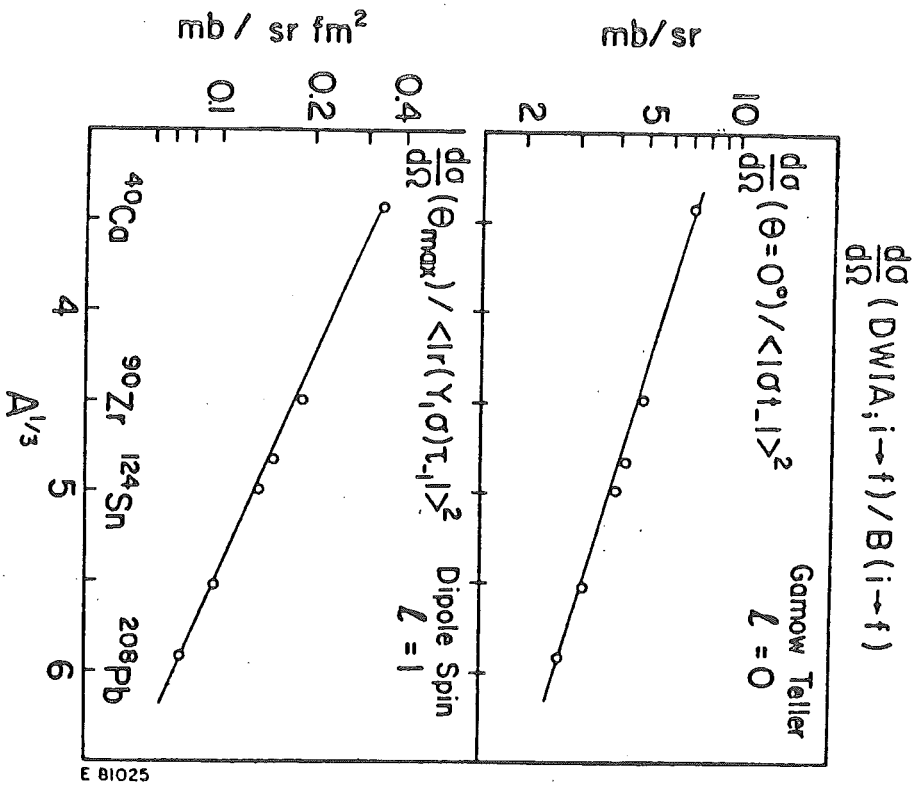

Gaarde, J. Rapaport, C. Goodman et al. Nucl. Phys.

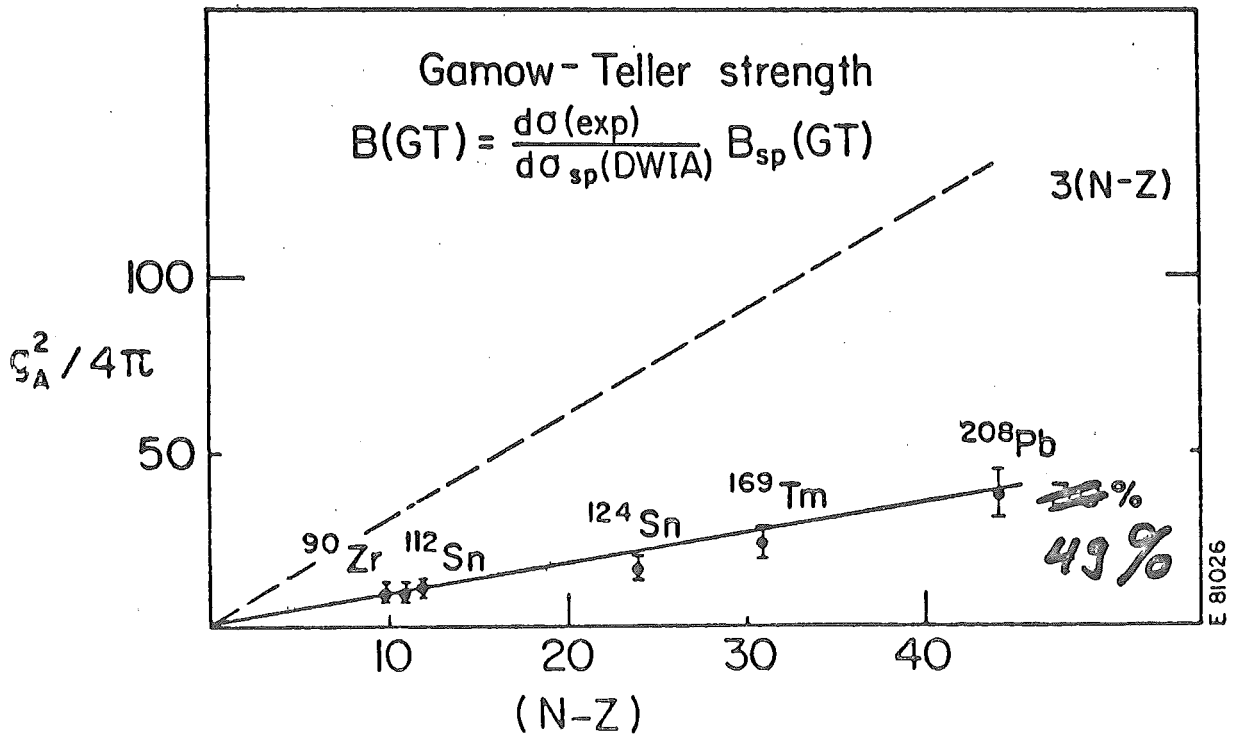

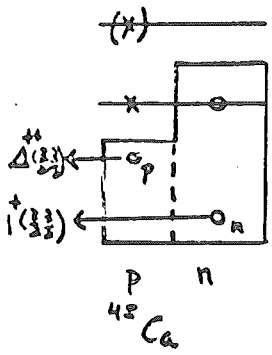

$$|1^+\rangle_{low} = a_1 \left[\pi f_{\frac{7}{2}} \nu f_{\frac{3}{2}}^{-1}\right]_{1^+} - a_2 \left[\pi f_{\frac{7}{2}} \nu f_{\frac{3}{2}}^{-1}\right]_{1^+}$$

$$|1^+\rangle_{high} = +a_2 \left[\pi f_{\frac{7}{2}} \nu f_{\frac{3}{2}}^{-1}\right]_{1^+} + a_1 \left[\pi f_{\frac{7}{2}} \nu f_{\frac{3}{2}}^{-1}\right]_{1^+}$$

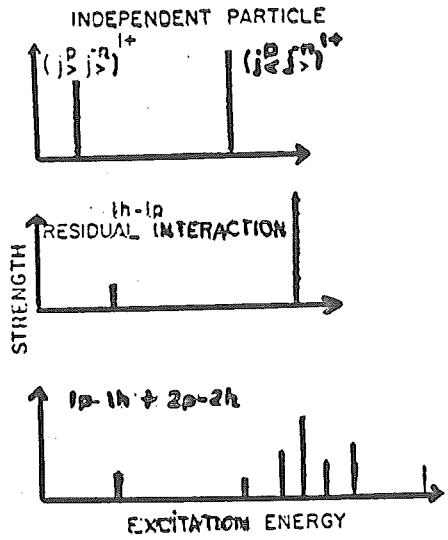

$$|1^+\rangle_{low} = a_1 |PN^{-1}\rangle - a_2 |\Delta N^{-1}\rangle$$

$$|1^+\rangle_{high} = a_2 |PN^{-1}\rangle + a_1 |\Delta N^{-1}\rangle$$

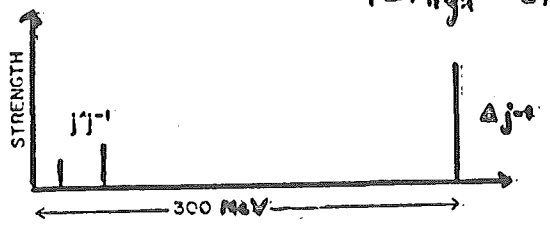

Osel and RHO

Towner and Khanna

Suzuki, Krewald, Speth

Sagawa v. Giai

Bertsch (Berkeley)

Bohr a. Mottelson Phys. Lett. 100 B

G. E. Brown and M. Rho Nucl. Phys.

$\Delta(1232)$-degrees of freedom in nuclei (test of Quark-models ...)

Properties of Δ's:

Spin: $= S = \frac{3}{2}$ Energy: 1232 MeV

Isospin: $= T = \frac{3}{2}$ 2 $\sqrt{3}$

Isospin multiplett:

	Δ_{++}	Δ_{+}	Δ_{0}	Δ_{-}	T_z
$p = \|uud\rangle \rightarrow \Delta^{++} = \|uuu\rangle$					
$n = \|udd\rangle \rightarrow \Delta^{+} = \|uud\rangle$	$+\frac{3}{2}$	$+\frac{1}{2}$	$-\frac{1}{2}$	$-\frac{3}{2}$	

I. Δ-hole admixtures to M1-transitions

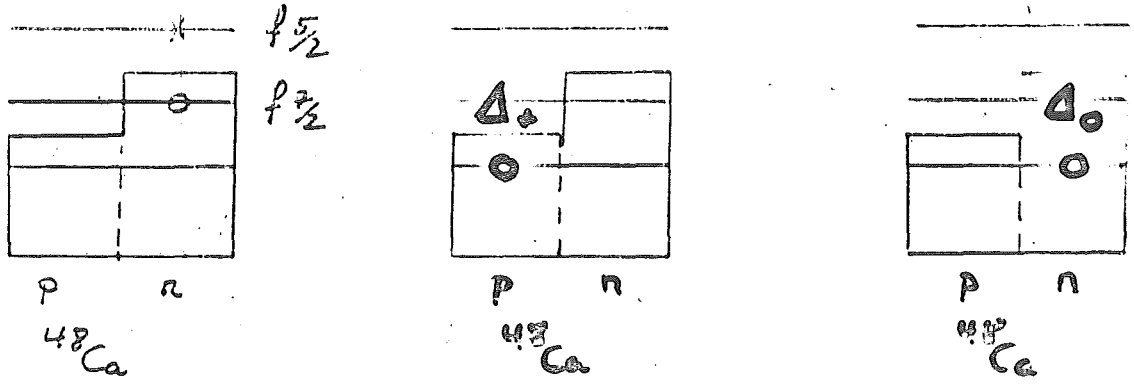

I. Δ-hole admixtures to GT-transitions (p,n) bzw. (n,p)

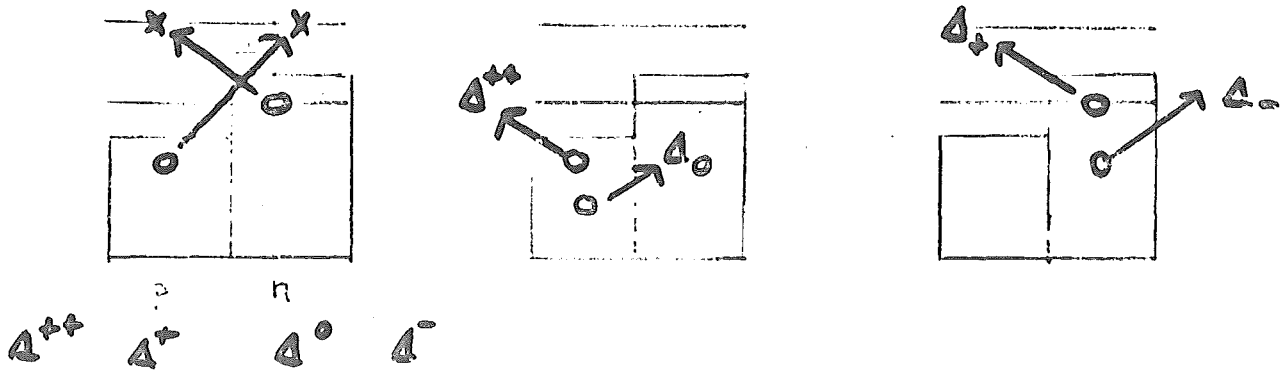

Reaction calculations for A(p,p') and A(p,n)

DWIA - calculations with G3Y - interaction of Love and Franey

replace: $\vec{\sigma} \rightarrow \vec{S}$; $\vec{\tau} \rightarrow \vec{T}$; $\frac{t^*}{t} = 2$

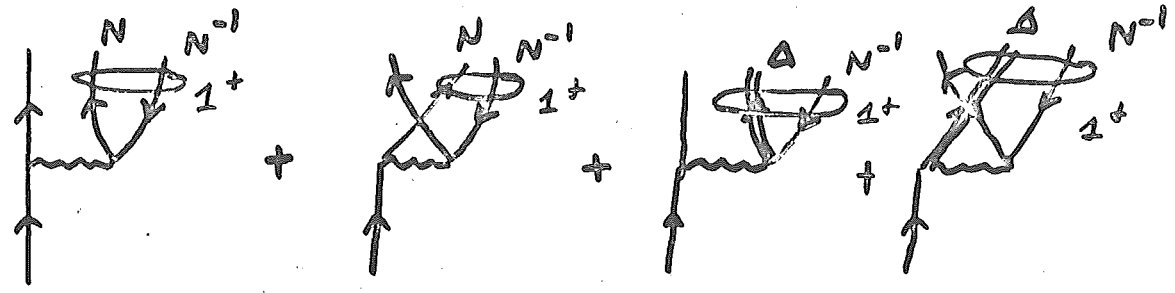

direct Knock out exch. direct Knock-out exch.

DWBA - code: FROST - MARS (F.O.)

RPA - wave function:

$$|\Psi(1^+)\rangle = \underbrace{\sum_{j_1 j_2}{}' \left(X^{NN^{-1}}_{j_1 j_2} - Y^{NN^{-1}}_{j_2 j_1} \right) a^+_{j_1} a_{j_2} |\tilde{0}\rangle}_{NN^{-1}\text{-part}}$$

$$+ \underbrace{\sum_{j_1' j_2'}{}' \left(X^{\Delta N^{-1}}_{j_1' j_2'} - Y^{\Delta N^{-1}}_{j_2' j_1'} \right) a^+_{j_1'} a_{j_2'} |\tilde{0}\rangle}_{\Delta N^{-1}\text{-part.}}$$

F. Osterfeld, S. Krewald, T. Suzuki, J. Speth
to Phys. Rev. Lett.

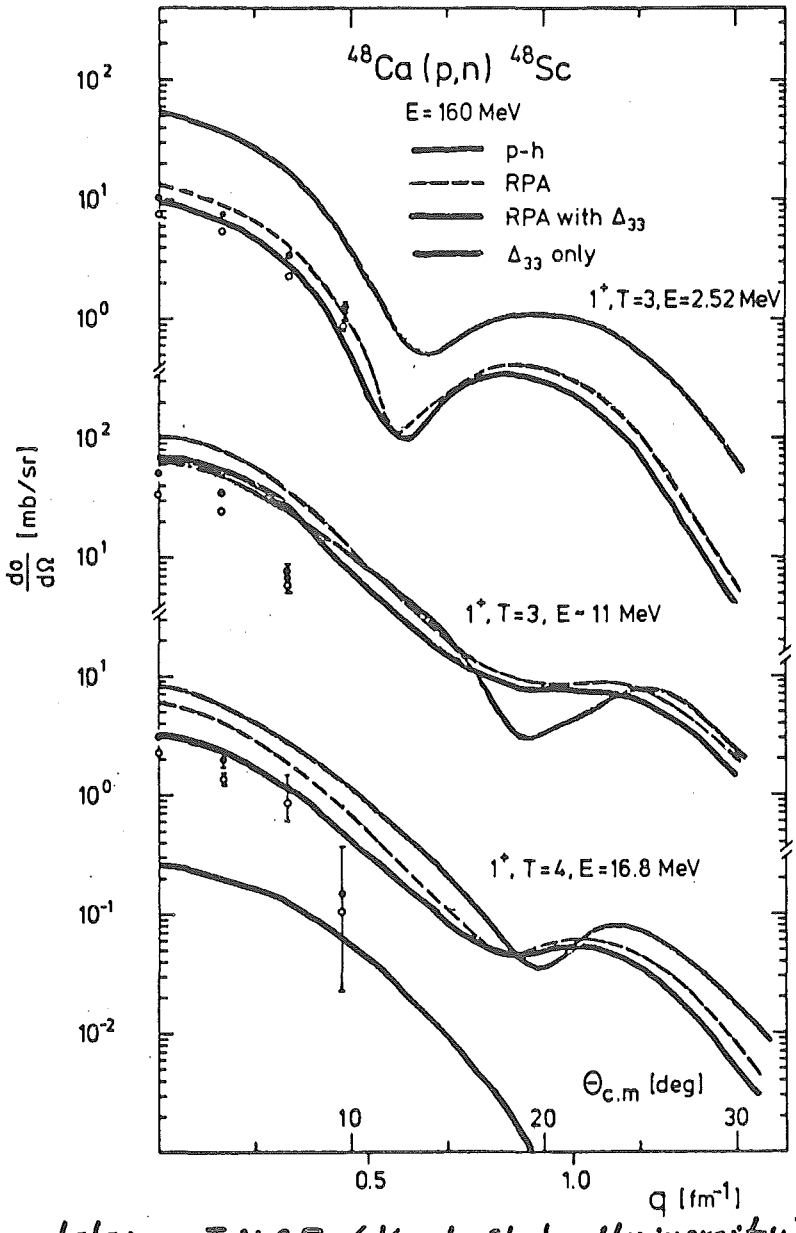

data: IUCF (Kent State University)

F. Osterfeld, S. Krewald, T. Suzuki, J. Speth
Phys. Rev. Lett.

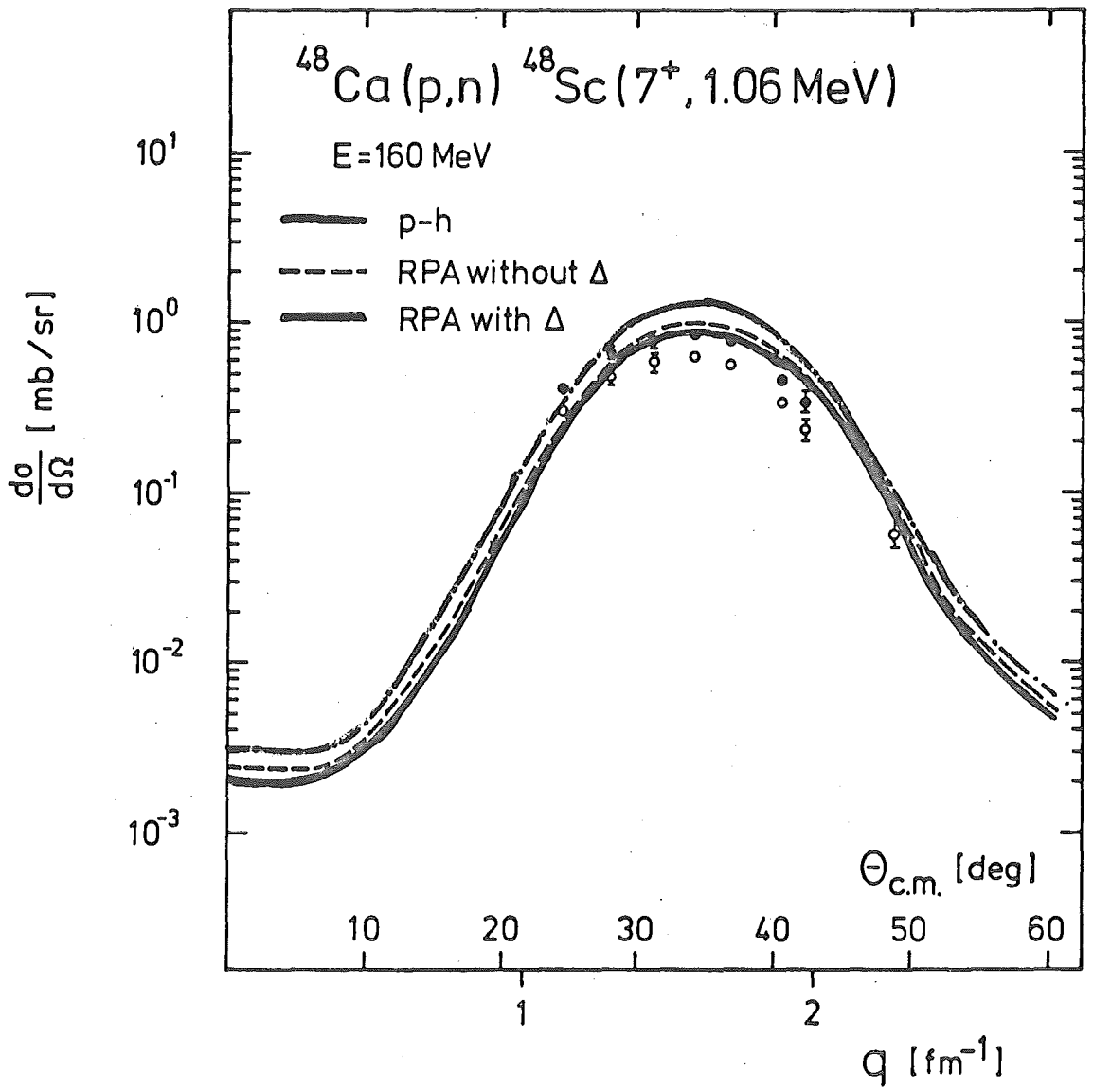

Background is not featureless

Background has "some structure"

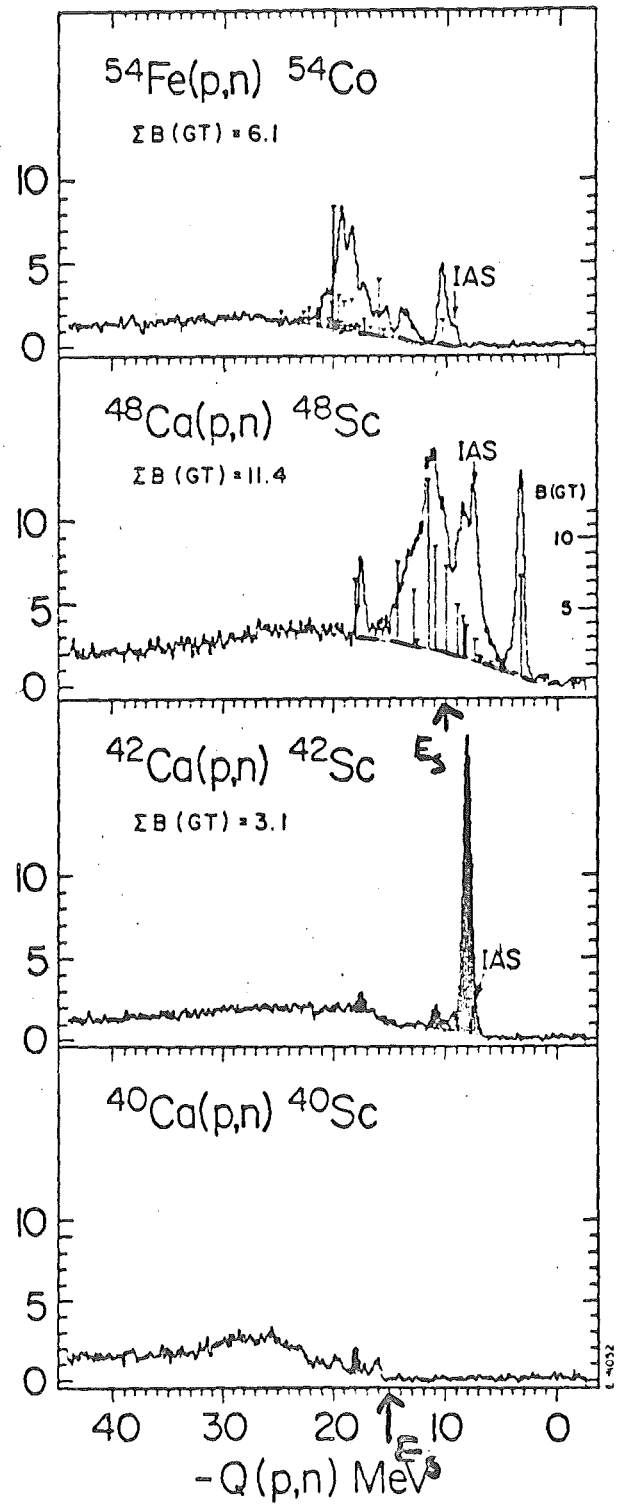

data: ← Ground state data: Anderson, Knudson, Tandy, Watson and Madey

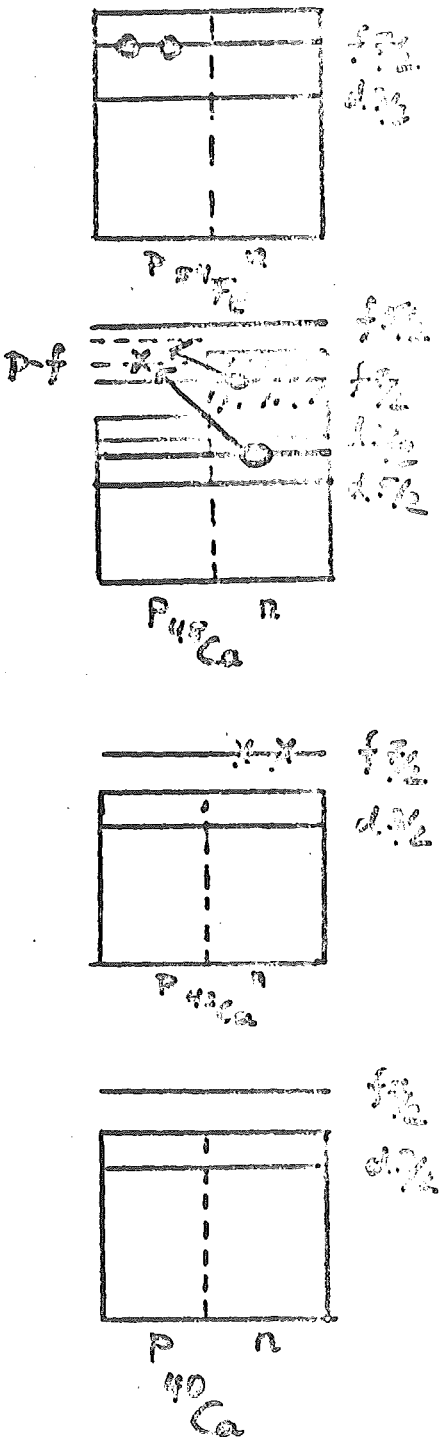

Data: C. Goodman, C.D. Goodman, J. Rapaport, J.S. Larsen, Foster, Goulding, Horen, Masterson, Sugarbaker (IUCF)

Microscopic model for background calculation
(particle-hole doorway model)

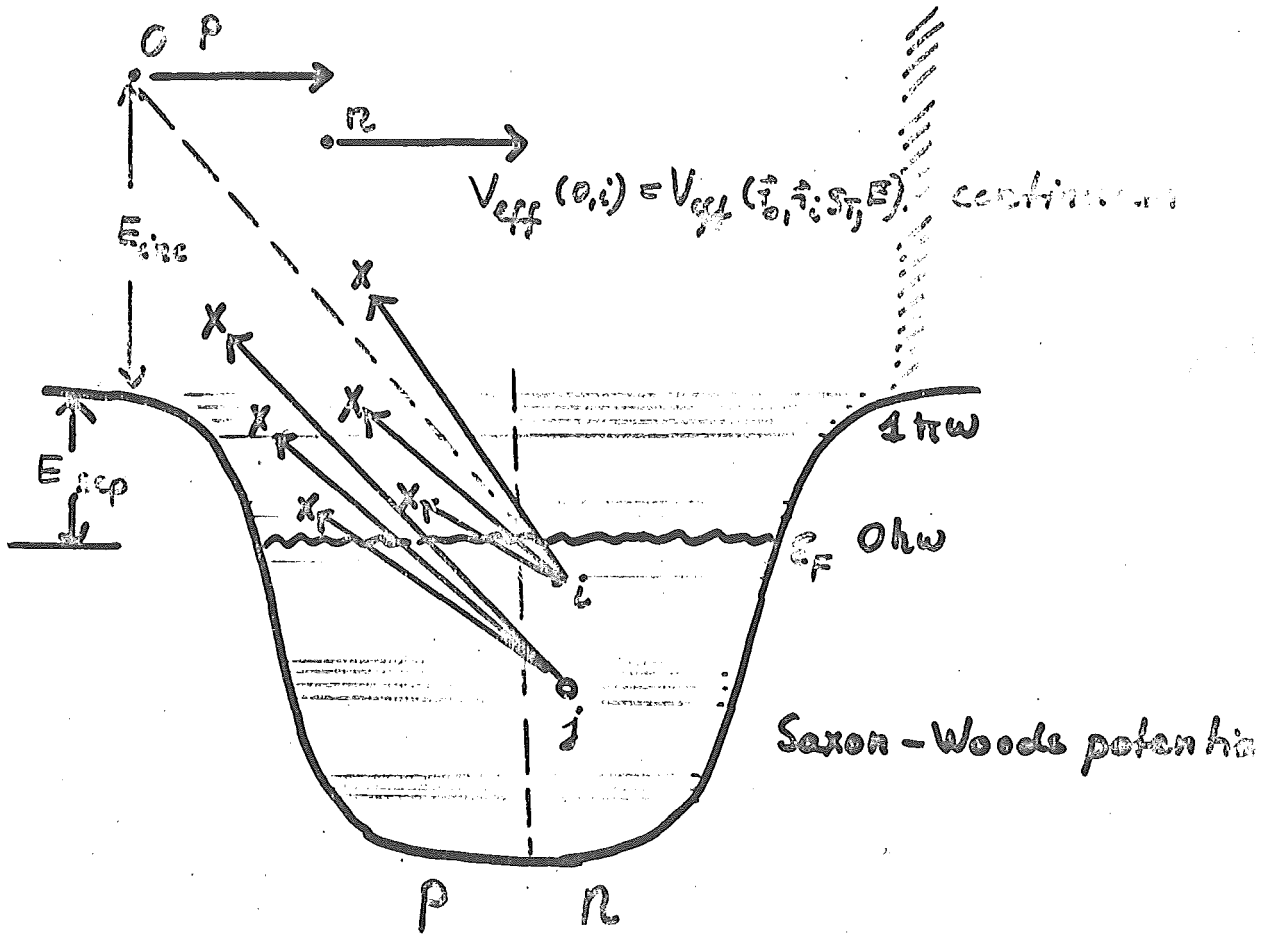

Properties of V_{eff} at $E \geq 100$ MeV

1. reactions are direct, i.e. multi step processes are suppressed

2. Impulse approximation is valid (Kerman, McManus, Thaler)

$$V_{eff}(0,i) \longrightarrow t_{NN}(0,i)$$

GJY: Love, Petrovich — real Energy.

free nucleon-nucleon t-matrix

3. only $\Delta S=1, \Delta T=1$-transitions contribute to the background

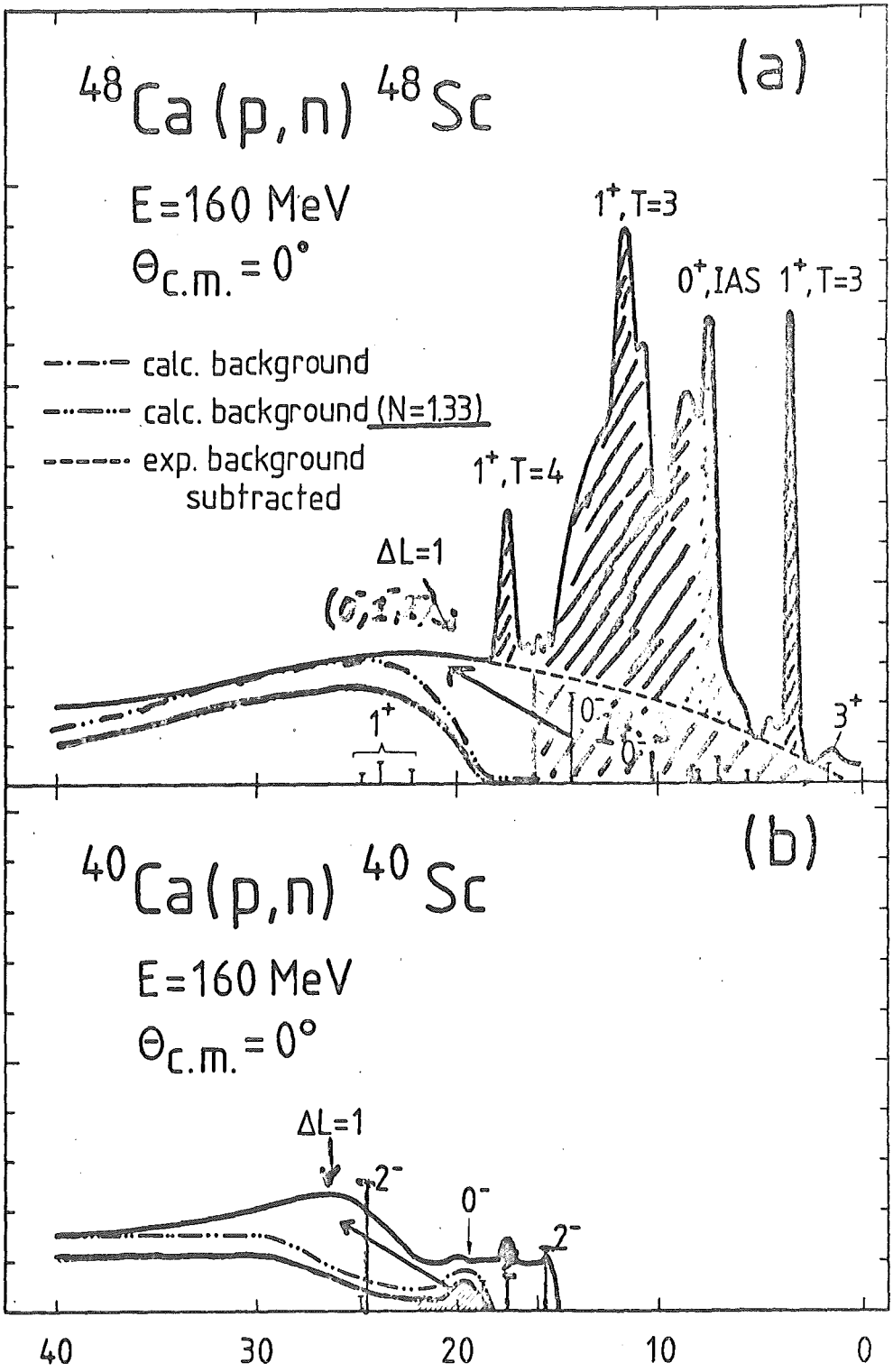

0⁻: 2.5 mb
2⁻: 1.4 mb
3⁺: 1.0 mb
sum: 4.9 mb

GT-strength in background:
~ 12 mb
2.5% eff.

$J^\pi = 0^-, 1^+, 1^-, 2^+, 2^-, 3^+, 3^-, 4^-$
$\Delta L = 0 - \Delta L = 3$

no calc. cross section to GTR and IAS shown

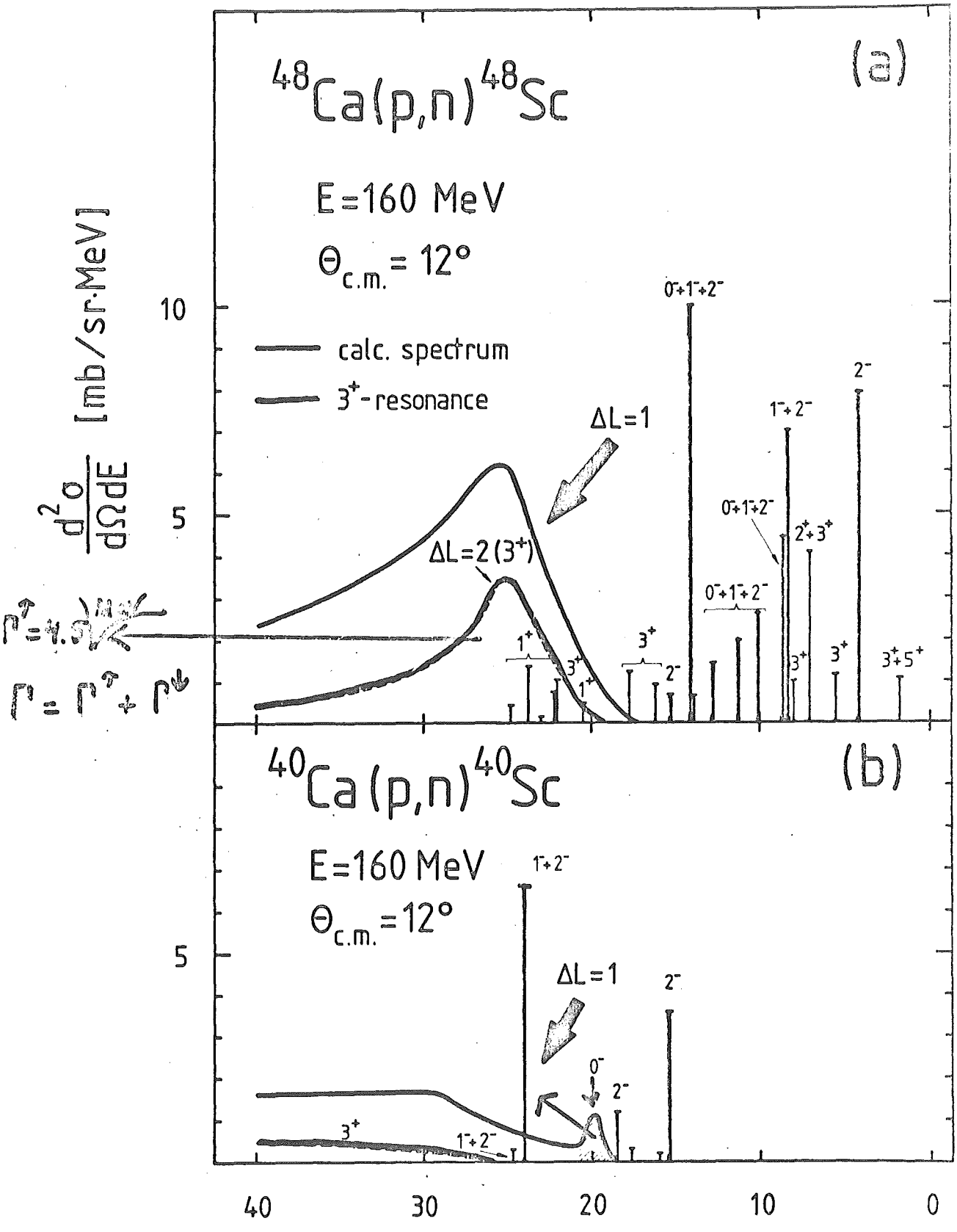

$\Gamma = \Gamma^{\uparrow} + \Gamma^{\downarrow}$

$J^{\pi} = 0^-, 1^+, 1^-, 2^+, 2^-, 3^+, 3^-, 4^-$

$\Delta L = 0 - 3$

no calc. cross section to GTR and IAS is shown

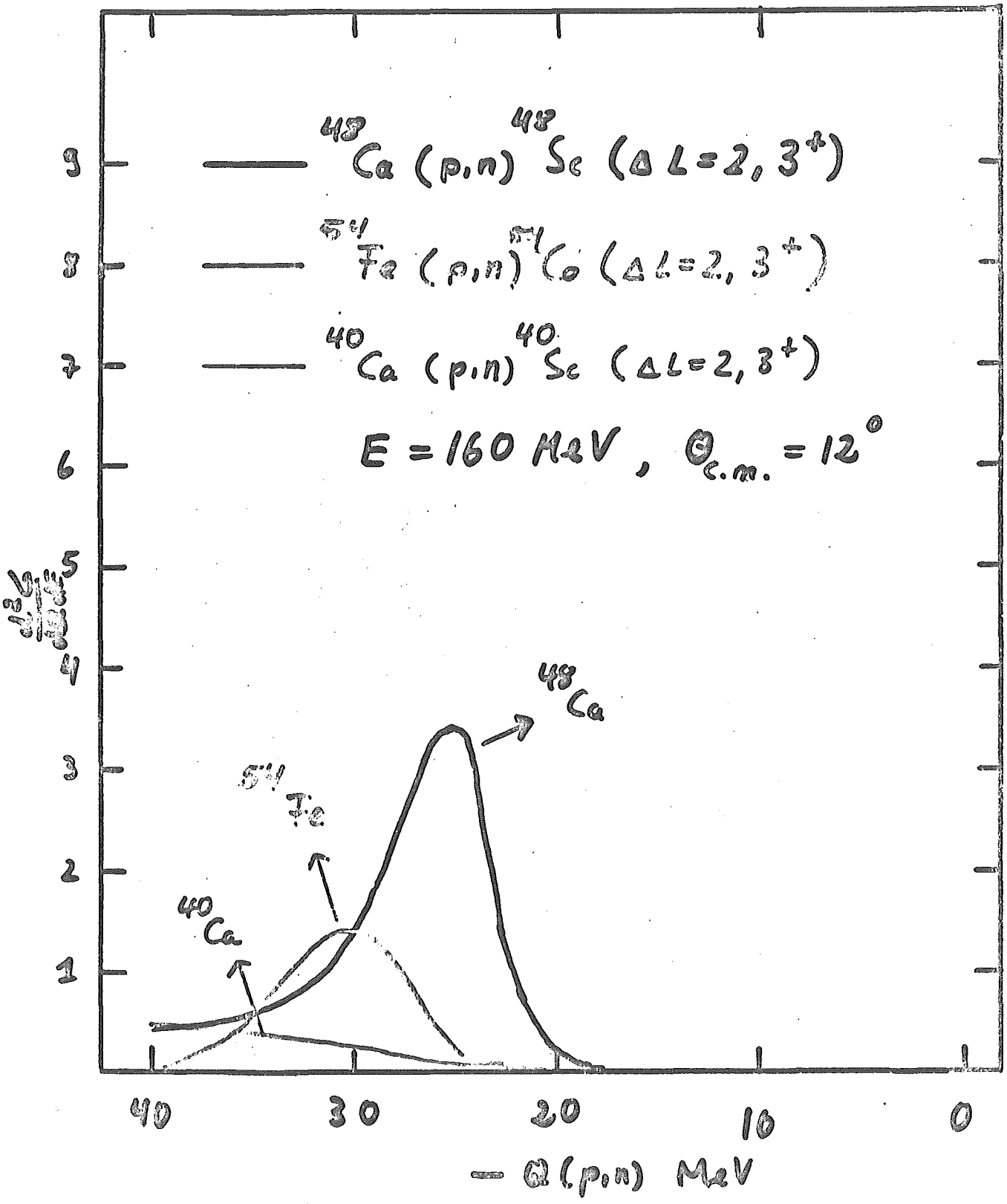
$^{48}Ca(p,n)^{48}Sc$ ($\Delta L=2, 3^+$)
$^{54}Fe(p,n)^{54}Co$ ($\Delta L=2, 3^+$)
$^{40}Ca(p,n)^{40}Sc$ ($\Delta L=2, 3^+$)
$E = 160$ MeV, $\theta_{c.m.} = 12^\circ$
^{48}Ca
^{54}Fe
^{40}Ca
9
8
7
6
5
4
3
2
1
40
30
20
10
0
$-Q(p,n)$ MeV

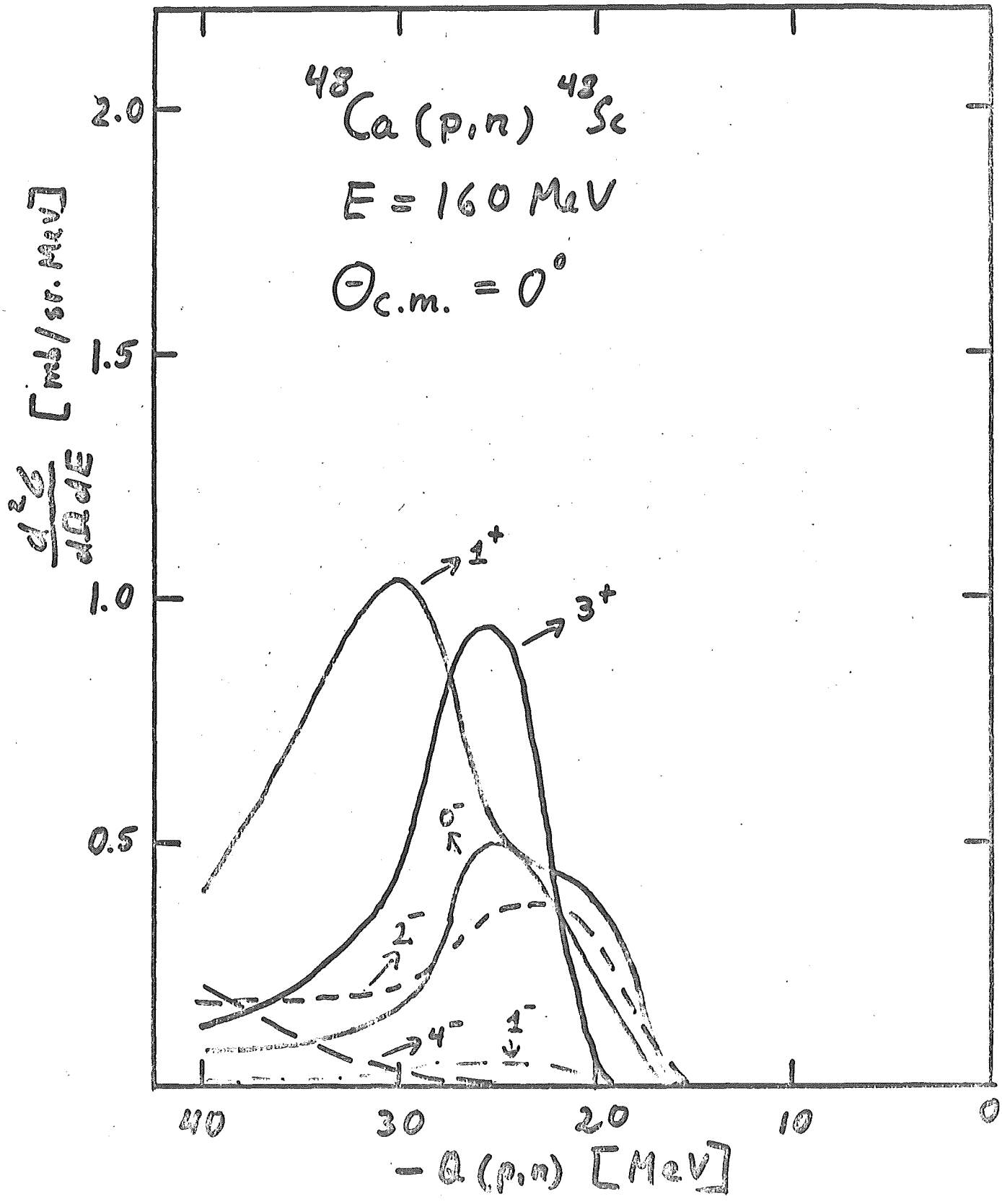
$^{48}Ca(p,n)^{48}Sc$
E = 160 MeV
$\Theta_{c.m.} = 0^\circ$
$\frac{d^2\sigma}{d\Omega dE}$ [mb/sr.MeV]
2.0
1.5
1.0
0.5
1+
3+
0-
2-
4-
1-
40
30
20
10
0
$-Q_{(p,n)}$ [MeV]

C. Gaarde, J. Rapaport, C. Goodman et al.
(Indiana University)

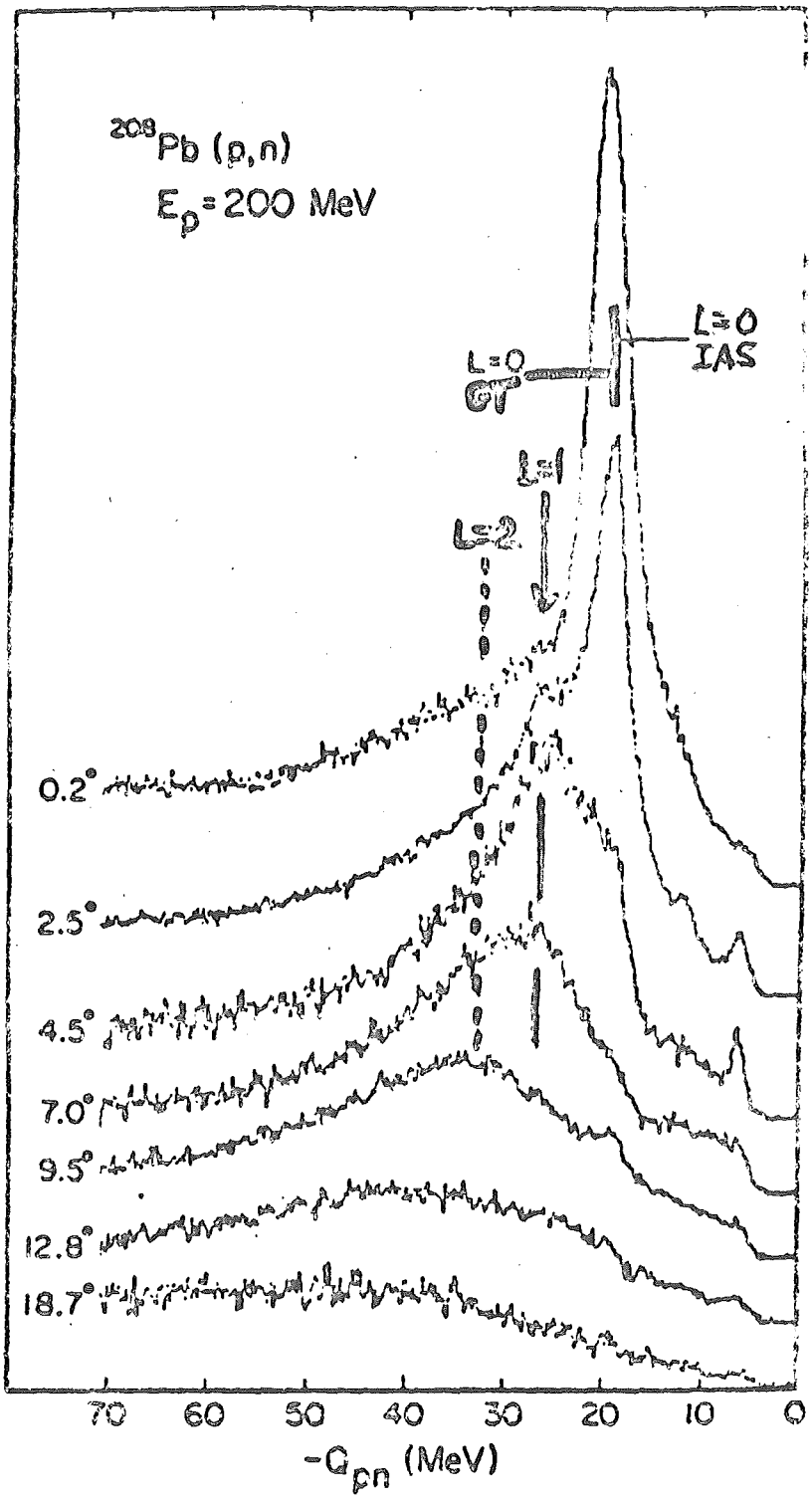

IUCF 546

Crawley, Bhattacharya, Galonsky, Djalali (MSU)
Marty, Nadal, Willis, Jourdain, Kitching (Orsay)

M1-strength in Zr-isotopes (Orsay)

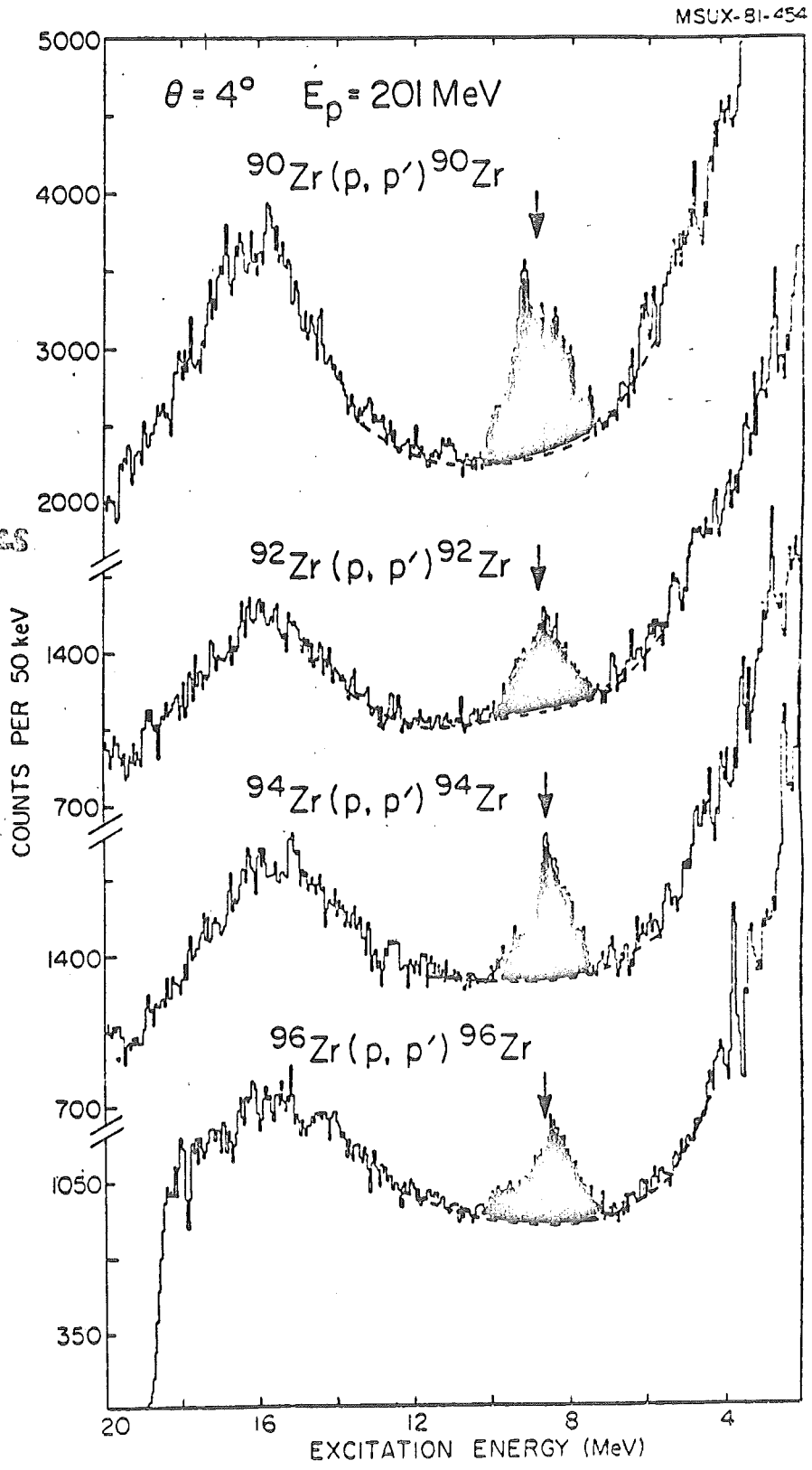

Jülich, BIG KARL - Spectrometer

Berg et al. Jülich
Gaul et al. Münster
Phys. Rev. C 25 (1982) 2100

$^{48}Ca(p,p')\ ^{48}Ca^{*}$, $E_p = 44.4$ MeV

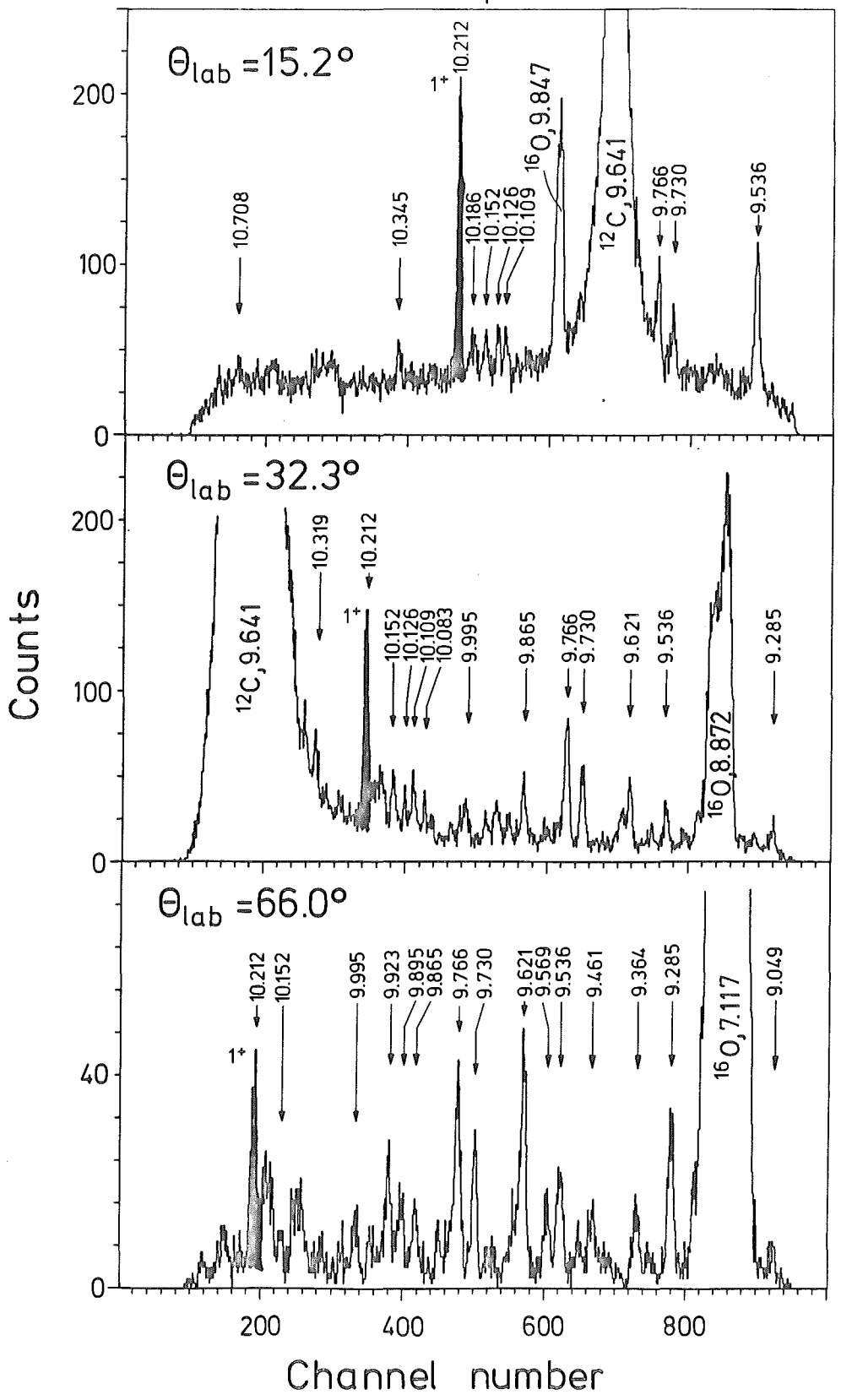

energy resolution
FWHM ≈ 120 keV

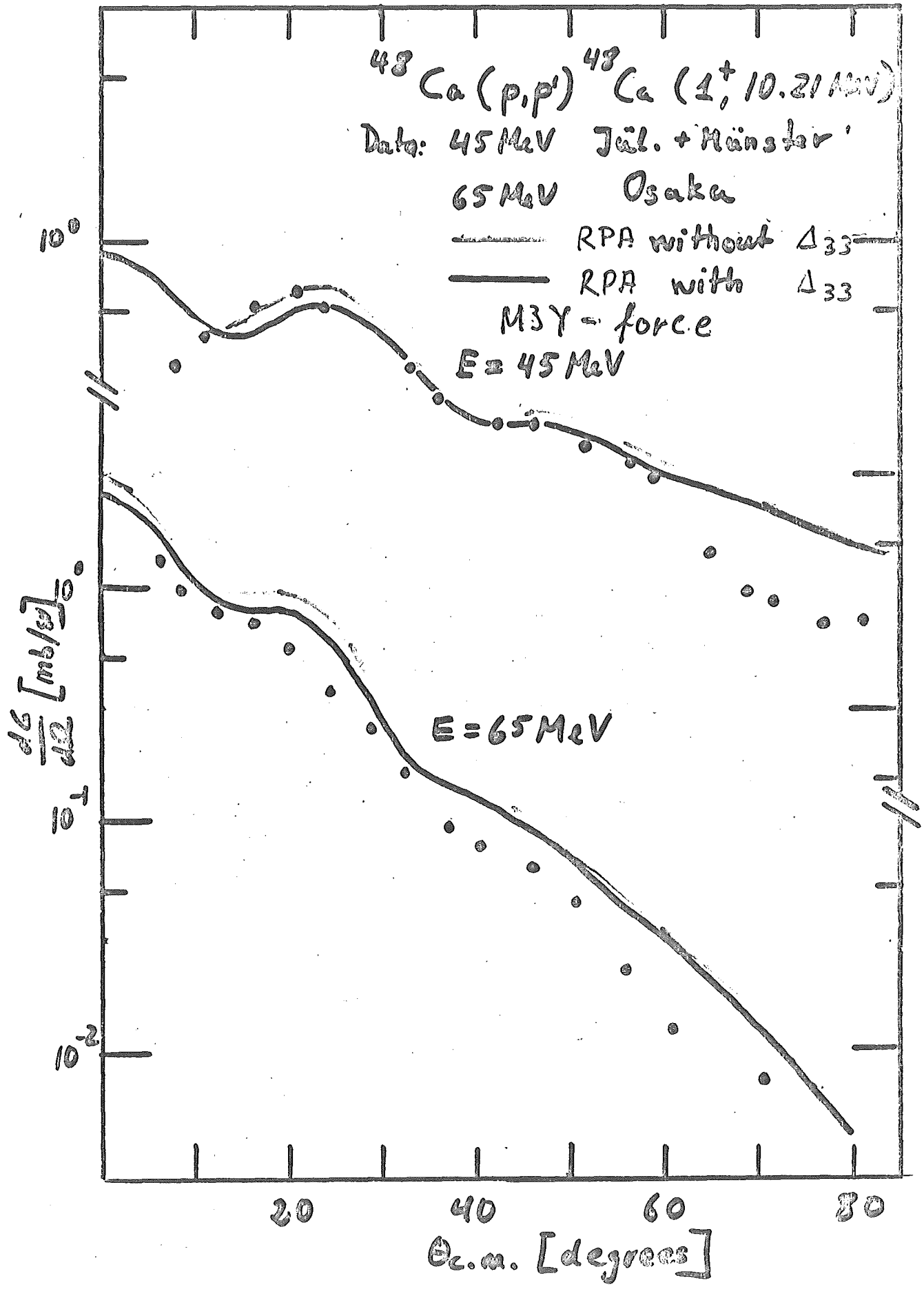
$^{48}Ca(p,p')^{48}Ca(1^+, 10.21\,MeV)$
Data: 45 MeV Jül. + Münster
65 MeV Osaka
RPA without Δ_{33}
RPA with Δ_{33}
M3Y - force
E = 45 MeV
E = 65 MeV
$\frac{d\sigma}{d\Omega}$ [mb/sr]
10^0
10^{-1}
10^{-2}
20
40
60
80
$\Theta_{c.m.}$ [degrees]

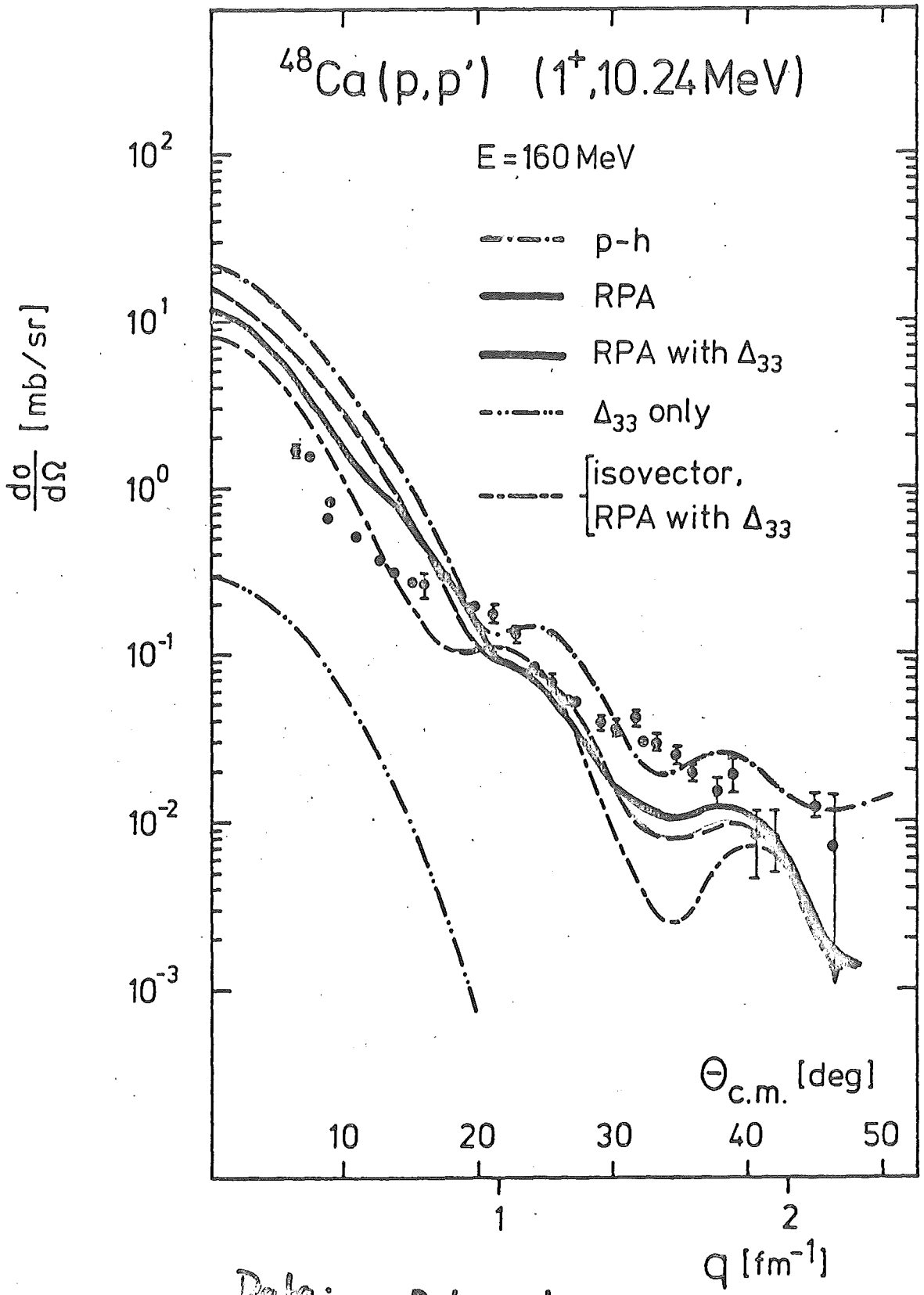

Data: Rehm, Kienle, Segel, Cowfort
IUCF

Saturn experiment (Saclay)

C. Gaarde, C. Goodman et al.

^{12}C (^3He, t)

E = 2 GeV

0°-spectrum

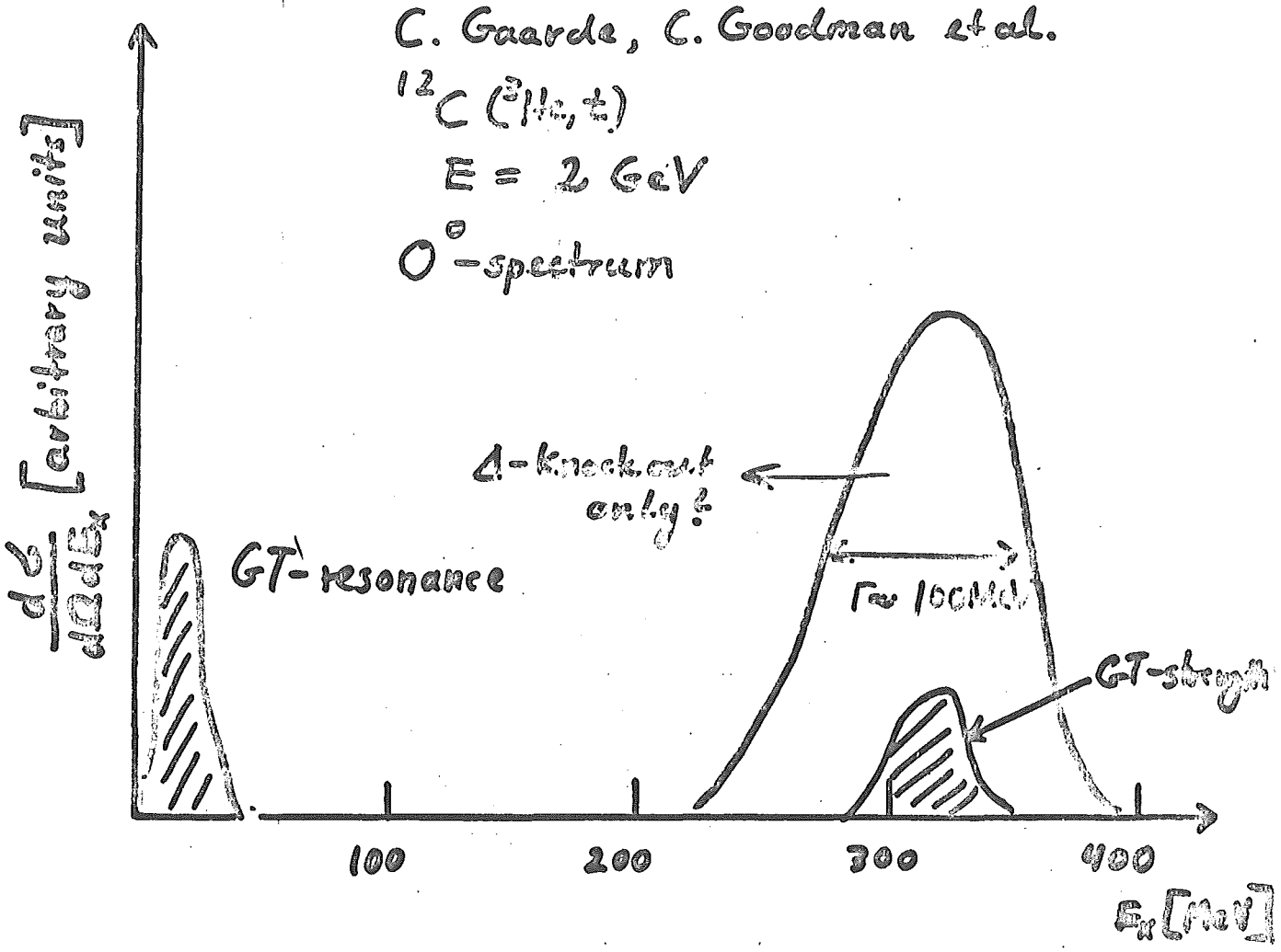

advantage of (^3He, t) over (p,n)

the charged particle in the exit channel allows for

a.) higher energy-resolution

b.) measurement of angular distributions

disadvantages of (^3He, t):

composite particle

M. G. Huber, K. Klingenbeck, W. Knüpfer
Modell der "Pionic Fusion" (Erlangen)

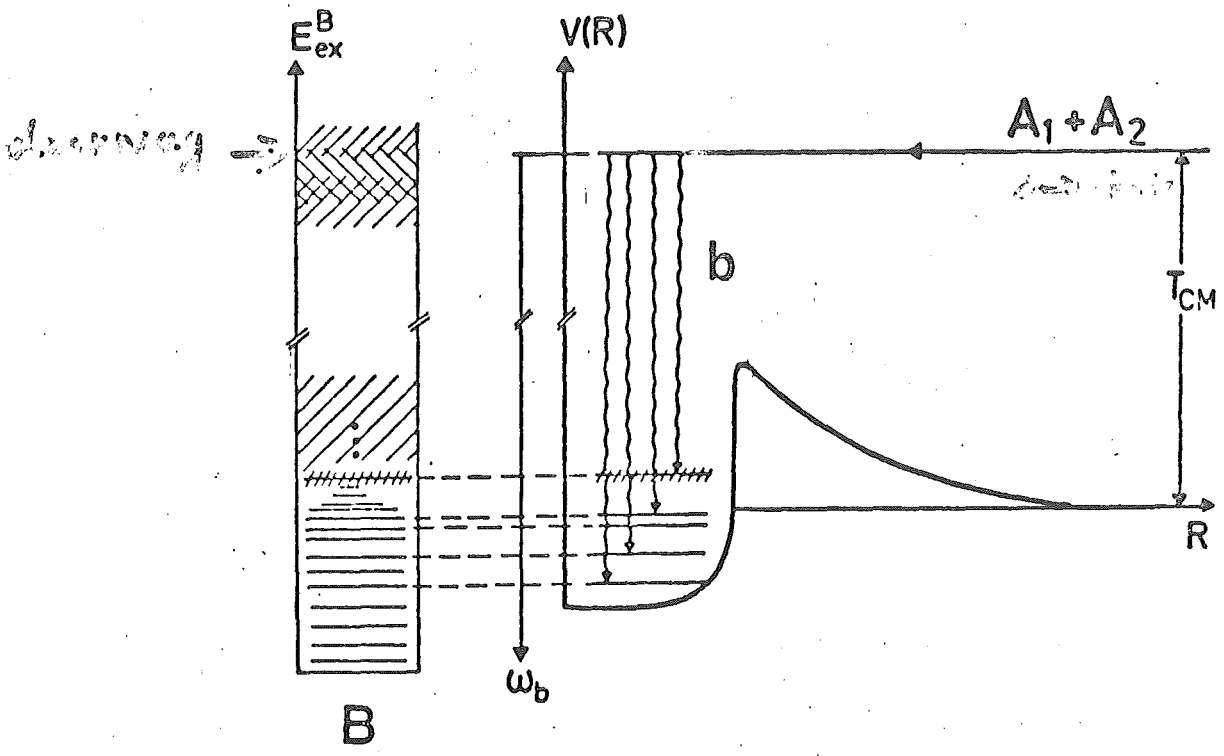

Fig. 3: Schematic representation of the coherent fusion reaction of eq. (6).

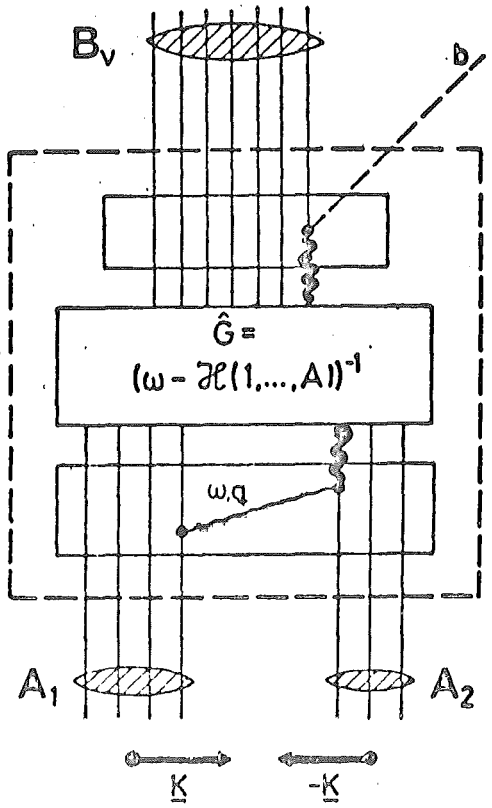

Fig. 4:
Resonant reaction mechanism for complete fusion (eq. (10)); the wavy line indicates a general single nucleon excitation, specified in chapters V and VI, respectively.

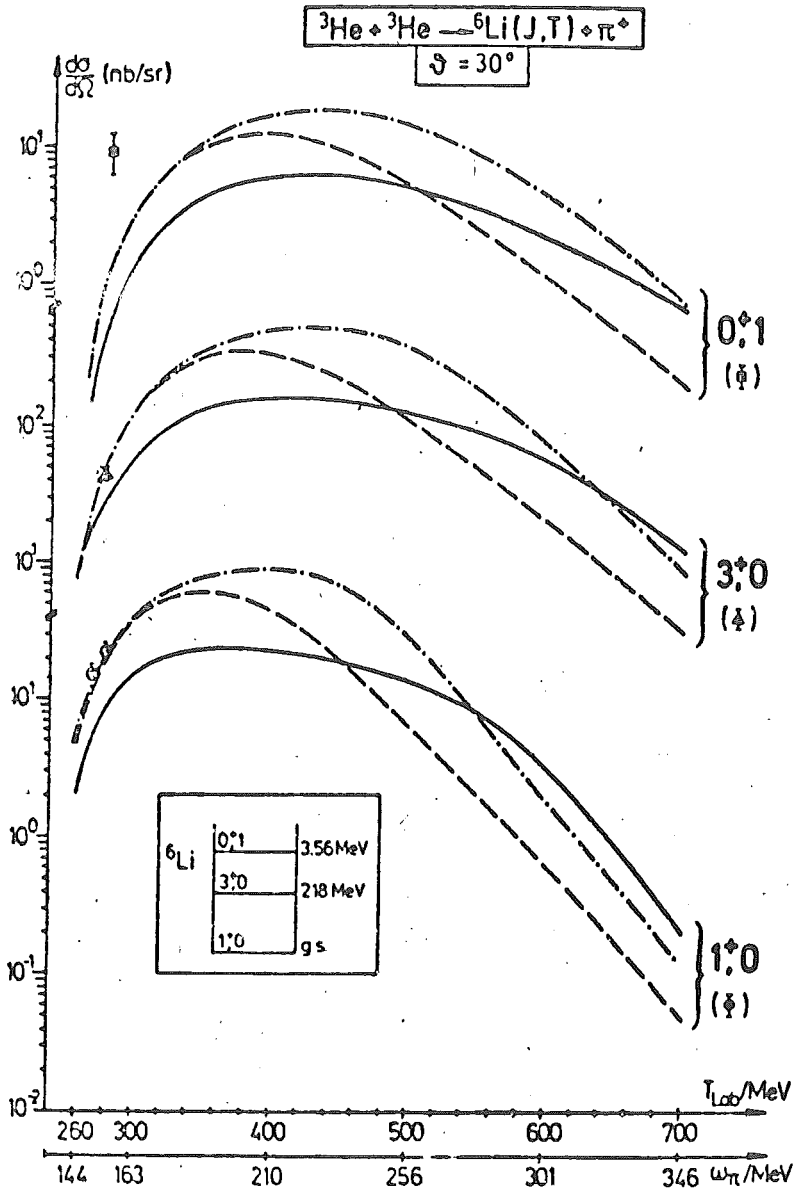

Fig. 7:
Excitation functions for a specific pionic fusion reaction: the three curves correspond to different assumptions on the closure energy, $\bar{\varepsilon}$, of eq. (18) (solid curve for a free Δ excitation; dashed and dashed-dotted curve for an energy shift of 50 MeV (see fig. 6) with a modified imaginary part, Γ_{free} and 2. Γ_{free}, respectively). The experimental points are from Le Bornec et al (ref. 2).

(iv) The reaction (20) can be used to produce new isotopes. This aspect might be particularly relevant for heavier systems where the bombarding energy must necessarily be quite large to overcome the Coulomb-barrier; here, the pion could be an efficient tool for a coherent "cooling" of the system.

It should be stressed that additional information may be obtained from the inverse reaction i.e. pion induced two body fission[6]:

$$\pi + B \longrightarrow A_1 + A_2 \ ;$$

This process will nicely complement the reaction of eq. (20). Furthermore, the investigation of radiative fusion, discussed in the following section, may similarly be used to reveal the existence of dinuclear structures in the nuclear excitation spectra.

III. Test of fundamental symmetries

A: Charge symmetrie breaking (CSB) nuclear forces

charge symmetry breaking $\not\Leftrightarrow$ $(n-n) = (p-p)$

theoretical: two classes of CSB-forces

1. $V^{(1)} = A[\tau_3(1) + \tau_3(2)]$

$[V^{(1)}(n,p) = 0]$

2. $V^{(2)} = I[\tau_3(1) - \tau_3(2)] + C[\vec{\tau}(1) \times \vec{\tau}(2)]_3$

general form:

$$[\tau_3(1) - \tau_3(2)]\,[\vec{\sigma}_1 - \vec{\sigma}_2] \cdot \vec{L}_{12}\; f(r^2, p^2, L^2)$$

experimental test:

Experiment I: elastic, polarised neutron-proton scattering

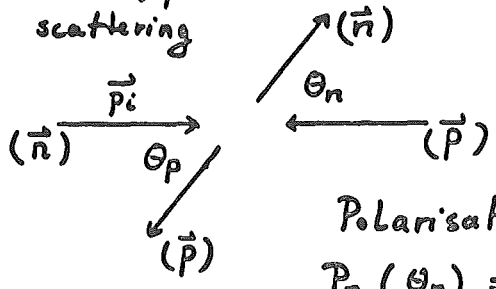

Polarisation:

$P_n(\theta_n) \overset{?}{=} P_p(\theta_p)$

Experiment II:

1. $n + p \rightarrow d + \pi^0$ (T=0, T=1) — symmetry around 90°
2. $d + d \rightarrow {}^4\mathrm{He} + \pi^0$ (T=0, T=0, T=0, T=1) — Barshay-Temmer!
3. $d + {}^4\mathrm{He} \rightarrow {}^3\mathrm{He} + {}^3\mathrm{H}$

Summary

high incident energies:

1. reaction mechanism is simple.
2. DWIA is valid
3. Distortion effects are relatively "small" in the energy window
4. the whole spectrum is essentially a result of one step process. "analyse in a microscopic way the whole spectrum including background.
5. selective excitation of certain classes of states (for ex: S=1, T=1)
6. study of mesonic degrees of freedom in nuclei
   Δ-isobars (Quark-model!)
   collective effects in π-production

New field of nuclear physics

7. Why not a

facility for (n,p)-reactions?

8. The physics, which we cannot foresee, which simply shows up, when we perform experiments in new energy regions and with better apparatus.

high energy (n,p) - reactions are highly interesting, especially for the study of Δ-isobar - effects in nuclei

purpose: production of high energetic neutrons
$E_n = 100 - 400$ MeV

procedure: E MeV protons + $^7Li \longrightarrow$ n + something

<u>Such a facility would be unique in the world!</u> (see Pollock talk)

<u>a high energetic, energy variable neutron beam.</u>

Acceleration and Storage of polarized particle beams

D. Husmann
Physikalisches Institut
Universität Bonn

Acceleration and Storage of Polarized Particle Beams

Circular Machines

Beams of Electrons a. Protons

not covered: Sources

main points:

Resonance Depolarization (e; p)

Sokolov-Ternov-Polarization (e)

Spin Diffusion (e)

Lit.

Proceedings of Conferences

High Energy Physics with Polarized Beams and Polarized Targets

Argonne, 1976: AIP Conf. Proc., No. 35

Lausanne, 1980: Experientia Supplementum Vol. 38 (Birkhäuser)

Equation of Spin Motion

Classical description of spin motion is sufficient.

Def.: $\frac{\hbar}{2}\vec{P} = \langle \psi | \vec{S} | \psi \rangle$.

Motion in an electromagnetic field (without Sokolov-Ternov polarization build-up):

$$\frac{d\vec{P}}{dt} = \vec{\Omega} \times \vec{P}.$$

Bargman-Michel-Telegdi-Equation

$\Omega(t)$: rotation vector

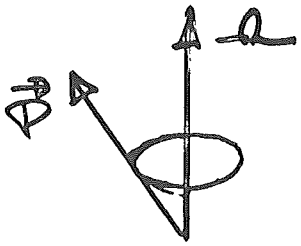

$$\Omega = \frac{e}{\gamma m_0}\left\{\vec{B}_\perp(1+\gamma a) + \vec{B}_\parallel(1+a) - \left(a - \frac{1}{\gamma+1}\right)\gamma\vec{\beta}\times\vec{E}\right\}$$

$$a = \frac{g-2}{2}, \quad a_e = 1.16 \times 10^{-3}$$
$$a_\mu = 1.29_3$$

$\vec{E} \equiv 0$:

$$\Omega = \frac{e}{\gamma m_0}\left\{\vec{B}_\perp(1+\gamma a) + \vec{B}_\parallel(1+a)\right\}$$

"Thomas-" "Larmor"-Precession

Spin motion in a plane perfect ring:

$$\vec{\Omega} = \frac{e}{\gamma m_0}(1+\gamma a)\vec{B}_\perp ,$$

$$\frac{d\vec{P}}{dt} = \frac{e}{\gamma m_0}(1+\gamma a)(\vec{B}_\perp \times \vec{P}) .$$

If $\vec{P} \parallel \vec{B}_\perp$: $\frac{d\vec{P}}{dt} = 0$.

'Closed Solution' $\hat{n}$

In the above given case: $\hat{n} = \hat{B}_\perp$.

Imperfect polarization:

$$(\vec{P}\cdot\hat{n})\hat{n} .$$

Components of $\vec{P} \perp \hat{n}$ precess around $\hat{n}$ and since different particles precess with different rates, rapidly smear out.

Resonance Depolarization

Angular frequency of precession of a spin with arbitrary direction around $\vec{\Omega}$:

$$\omega_{rL} = \frac{e}{\gamma m_0}(1+\gamma a)\cdot|\vec{B}_\perp|$$

With $\omega_c = \frac{e}{\gamma e m_0} \cdot |\vec{B}_\perp|$:

$$\omega_{TL} = (1 + \gamma a) \cdot \omega_c .$$

Spin rotation with respect to momentum rotation :

$$\omega_T = \omega_{TL} - \omega_c$$
$$= \gamma \cdot a \cdot \omega_c$$
$$= \nu \cdot \omega_c$$

ν : number of precessions per turn

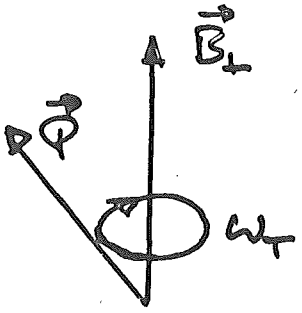

Influence of radial field components :

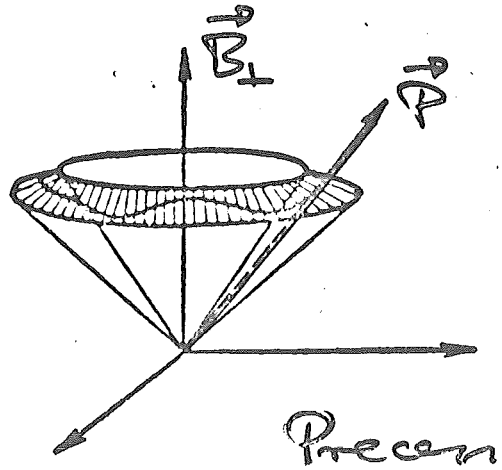

Precession cone for non resonant motion

Resonances:

Precession frequency = frequency of disturbing field influence

Disturbing field: f.i. radial field component

① Vertical betatron oscillation:

particles experience radial field components at frequency

$$\omega_\beta = (k \cdot p \pm Q_z)\,\omega_c$$

k: integer,
p: periodicity of ring,
Q_z: number of vertical betatron oscillation per turn

at resonance:

$$\omega_f = \omega_\beta$$

$$\Rightarrow \boxed{\gamma_a = k \cdot p \pm Q_z}$$

"Intrinsic Resonances"

② Ring with field errors:

$$p \cdot k = 1$$

$$\omega_f = n \cdot \omega_c$$

→ $\boxed{\gamma_Q = n}$.

"imperfection resonances"

Energies of resonances:

$T_e = n \cdot 440.65$ MeV

$T_n := 110$ MeV
634 "
1158 "
⋮ $\Delta T_n = 524$ MeV

In general resonances may occur at:

$$\boxed{\gamma_Q = n_0 \pm n_1 \cdot Q_z \pm n_2 \cdot Q_x \pm n_3 Q_s}$$

Experimental evidence:

(1) Argonne, ZGS
Saclay, SATURNE

(2) Orsay, ACO
SLAC, SPEAR
Bonn, 2.5 GeV Synchrotron

---

difference: accelerator - storage ring

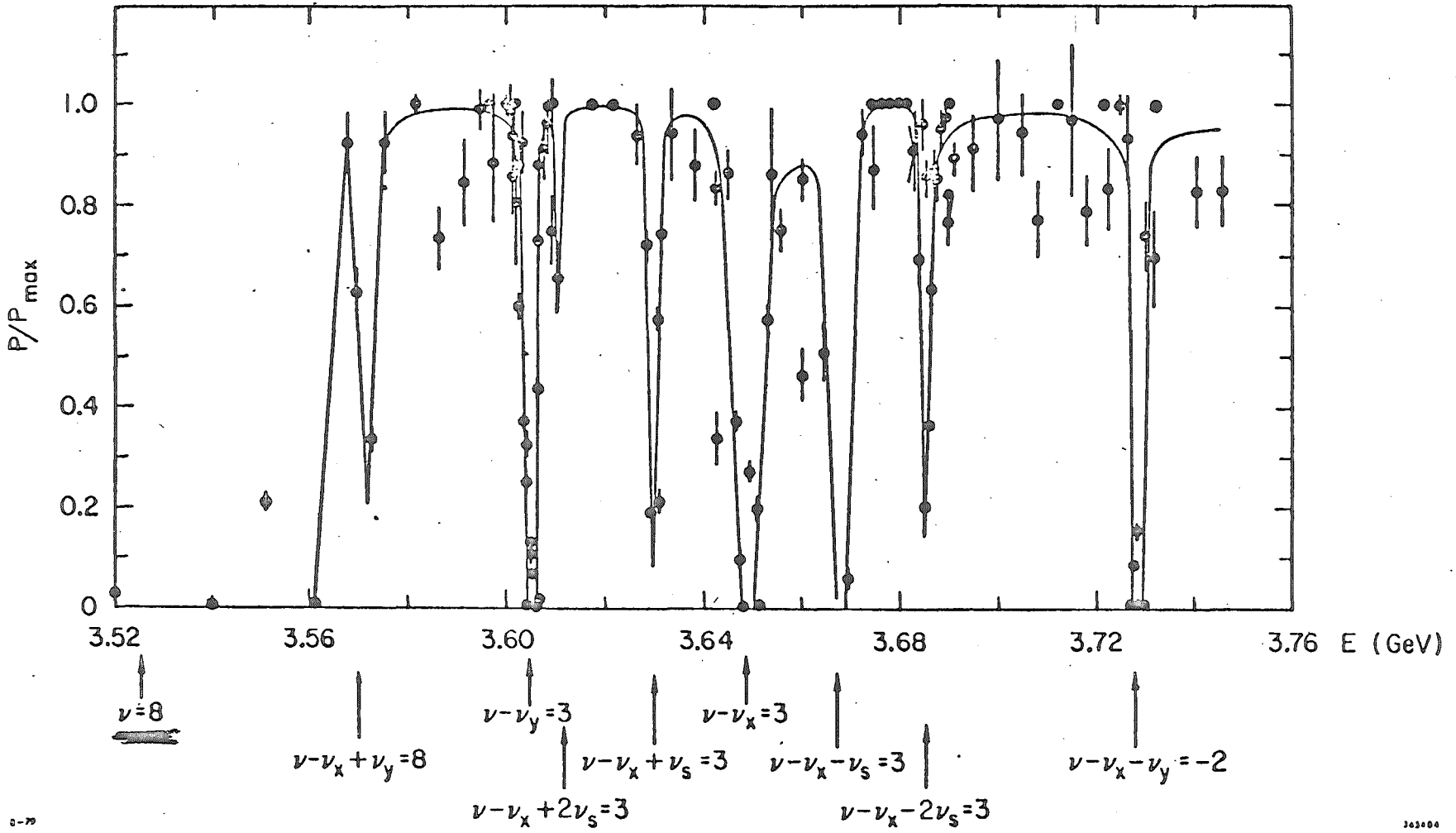

SPEAR, depolarizing resonances

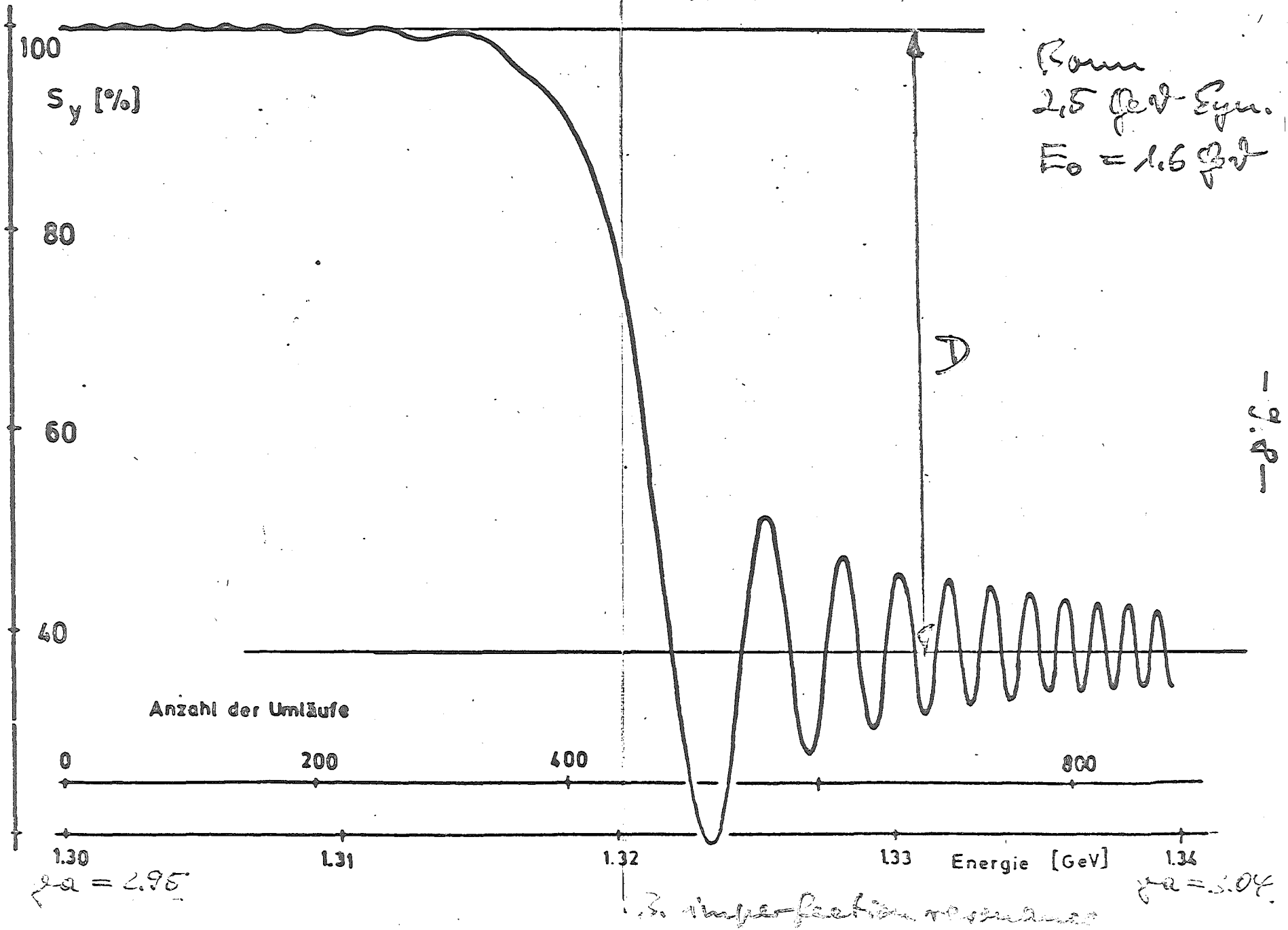
100
S_y [%]
80
60
40
Anzahl der Umläufe
0
200
400
800
1.30
1.31
1.32
1.33
Energie [GeV]
1.34
D
Ring
2,5 GeV-Syn.
E_0 = 1.5 GeV
Fig. 1

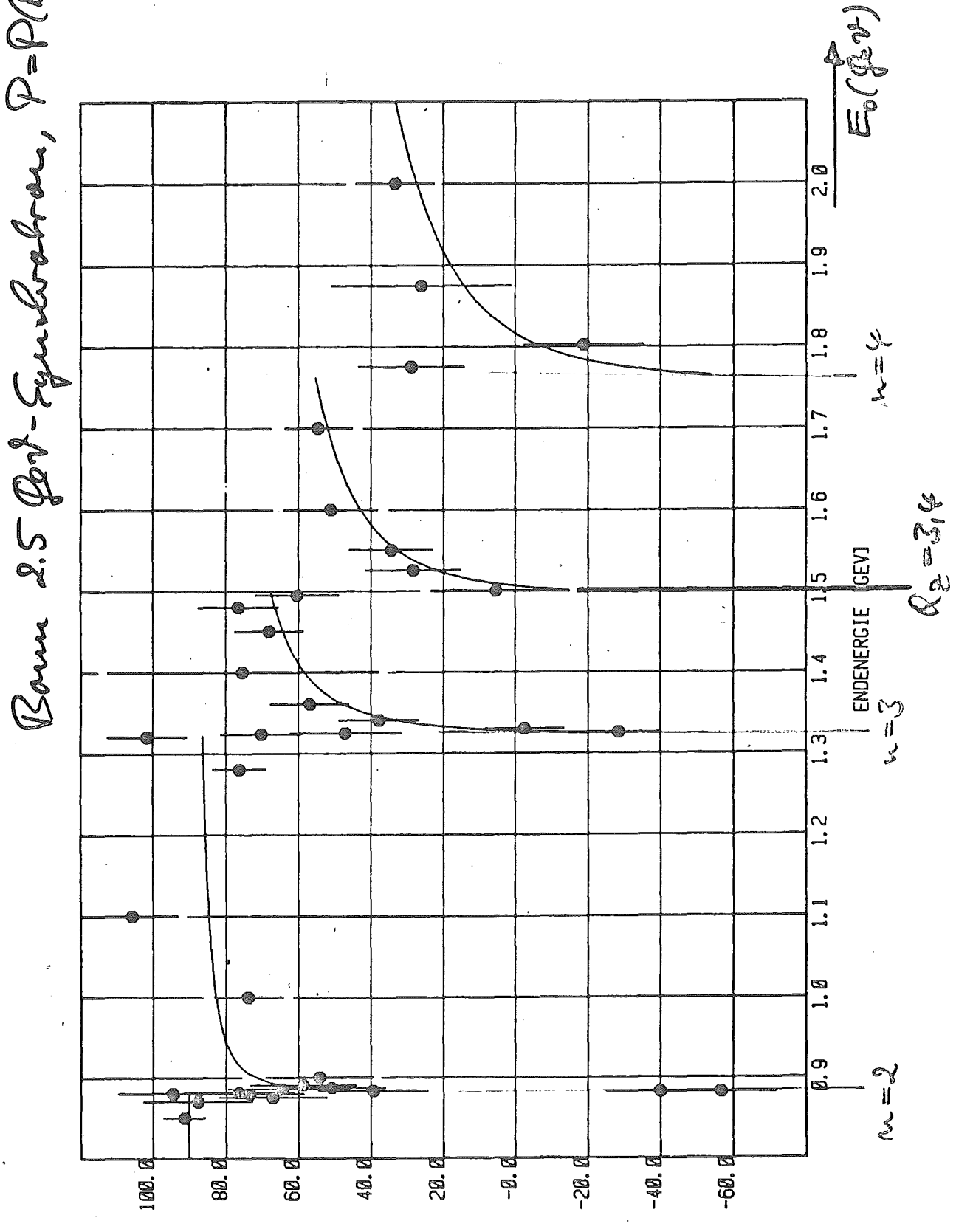
Bonn 2.5 GeV-Synchrotron, P=P(E0)
POLARISATION [%]
100.
80.
60.
40.
20.
-0.
-20.
-40.
-60.
0.9
1.0
1.1
1.2
1.3
1.4
1.5
1.6
1.7
1.8
1.9
2.0
ENDENERGIE [GEV]
E0(GeV)
n=2
n=3
n=4
Q2=3fm

Calculation of resonance strength mainly needs in case of

1.) intrinsic resonance:
vertical beam dimension,

2.) imperfection resonance:
responsible Fourier harmonic of closed orbit displacement.

Analytical calculation:
Froissart a. Stora (1959)

$$P_m = 2 \cdot \exp(-\eta^2) - 1$$

$$\eta = \frac{(1+m)\, b_m \cdot \pi}{2\sqrt{a \cdot \Delta\varphi}}$$

$$\Delta\varphi = 2\pi \cdot \frac{d\varphi}{d\theta} \,.$$

Computer calculation:
f. i. SLIM programme (Chao)

Correction Procedure

1.) Intrinsic resonance:
fast jump of working point,

2.) Imperfection resonance:
closed orbit correction.

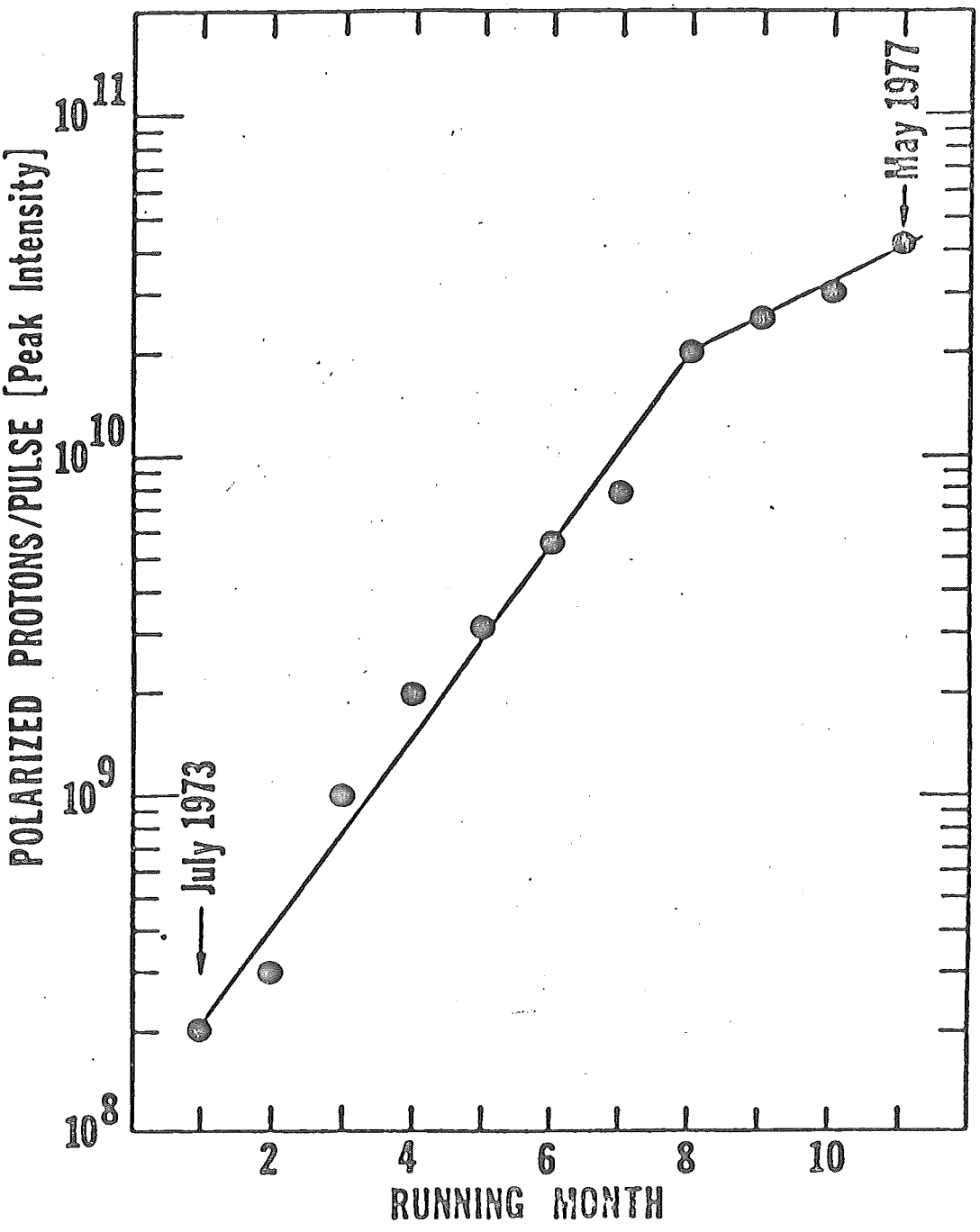

History of the Polarized Proton Intensity of the ZGS

Another possibility to avoid depolarizing resonances:

Insertion of a "Siberian Snake".

Spin rotation around particle velocity by 180° per orbital turn in the ring:

$$\underline{\nu = \frac{1}{2},}$$

$$\underline{\hat{n} \parallel \vec{\beta}.}$$

Realization:

wienoid at low energies,
transverse bends at high energies.

e: no Sokolov-Ternov polarization.

Sokolov - Ternov Polarization

Self - polarization of an electron beam circulating in a storage ring caused by synchrotron radiation. To a low extent synchrotron radiation emissions are connected to spin - flip transitions.

Spin-flip transition has an asymmetry with respect to spin direction being parallel or anti-parallel to the guide field:

$$\frac{W^{\uparrow\downarrow} - W^{\downarrow\uparrow}}{\Sigma} = 3 \cdot \frac{35}{32}\sqrt{3}\left(\frac{\nu}{\nu_c}\right)^4$$

$$\nu_c = \left(\frac{m_0 \cdot c \cdot r}{\hbar}\right)^{\frac{1}{2}}$$

r: bending radius

Polarization build-up:

$$P(t) = \frac{8}{5\sqrt{3}} \cdot \left(1 - e^{-\frac{t}{\tau}}\right)$$

$$\tau = \frac{8}{5\sqrt{3}} \frac{m_0^6}{\hbar^2 c^2 r_0} \frac{R r^2}{E^5}$$

$$= 92.66 \text{ sec} \frac{m^3}{\text{GeV}^5} \cdot \frac{r^2 \cdot R}{E^5}.$$

Maximum polarization is

$$P(t \to \infty) = \frac{8}{5\sqrt{3}} = 92.4\%$$

Examples:

SPEAR : $t_a \approx 10$ min,

PETRA : $t_a \approx 1$ h.

Polarization direction:

e^- : $\hat{S} \downarrow \hat{B}$

e^+ : $\hat{S} \uparrow \hat{B}$.

Siberian Snake (with $\hat{n} \parallel \vec{B} \perp \vec{B}_\perp$) does not allow Scalar-Tensor polarization!

Spin Diffusion

e- rings!

Suppose: Ring with closed orbit distortions (f.i. caused by radial field components)

General definition of

Closed Spin Solution

with help of the spin rotation matrix for one orbital turn:

$$T(s) = \exp\{-i\pi\nu\vec{\sigma}\cdot\hat{n}(s)\}$$

$\hat{n}(s)$ is the only real eigenvector of spin rotation for one orbital turn, if ν is non-integer.

Any other vector rotates around $\hat{n}(s)$ with angle $2\pi\nu$ per orbital turn.

The displaced closed spin solution shows a energy dependence.

Variation: $\mu \cdot \frac{\partial \hat{n}}{\partial \mu}$

~~Spin Chromaticity~~

~~Spin Dispersion~~

now: Spin. Orbit Coupling

It gives rise to an additional polarization, but also to a depolarization.

Sokier a. Ternov, 1966

Derbenev a. Kondratenko, 1973

$$P_\infty = \frac{8}{5\sqrt{3}} \cdot \frac{\langle |\dot\beta|^2 (\vec\beta \times \vec\beta)(\hat n - \gamma \frac{\partial \hat n}{\partial \gamma}) \rangle}{\langle |\dot\beta|^3 (1 - \frac{2}{9}(\hat n \cdot \vec\beta)^2 + \frac{11}{18}|\gamma \frac{\partial \hat n}{\partial \gamma}|^2) \rangle}$$

ultimate polarization!

σ – pol.

depol.

depolarization:

$$dP = -\frac{P}{2}\left(\frac{\Sigma}{E}\right)^2 |\gamma \frac{\partial \hat n}{\partial \gamma}|^2 .$$

depolarization time:

$$\tau_{depol} = \underset{\text{(Sok. Ternov)}}{\tau_{pol}} \cdot \frac{11}{18} \frac{\langle |\gamma \frac{\partial \hat n}{\partial \gamma}|^2 r^{-3} \rangle}{\langle r^{-3} \rangle}$$

To maximize electron beam polarization:

$$\hat n = \sqrt{\frac{7}{11}} \frac{\dot{\hat\beta} \times \hat\beta}{|\dot\beta|} \pm \sqrt{\frac{4}{11}}\,\hat\beta ,$$

$$\gamma \frac{\partial \hat n}{\partial \gamma} = \frac{2\sqrt{7}}{11}\left(-\sqrt{\frac{4}{11}} \frac{\dot{\hat\beta} \times \hat\beta}{|\dot\beta|} \pm \sqrt{\frac{7}{11}}\,\hat\beta\right)$$

$$\Rightarrow P_{max} = \frac{22}{5\sqrt{231}} = \underline{\underline{92{,}38\,\%}}$$

(A. Chao)

Antiproton accumulators at FERMILAB and recent results of electron-cooling

F. Mills
Fermi National Accelerator Laboratory
Batavia, Illinois

E- Cooling Program

A. Cooling at 200 Mev

Drag Forces
Cooling Rates
Proton Temperatures

B. Accumulation with e-beam

Correct Chromaticity — Use Full aperture
R.F. Stacking
Full aperture kickers
Vacuum improvements

$Q_x = 3.525$ $Q_y = 5.540$ File 23 1.05A

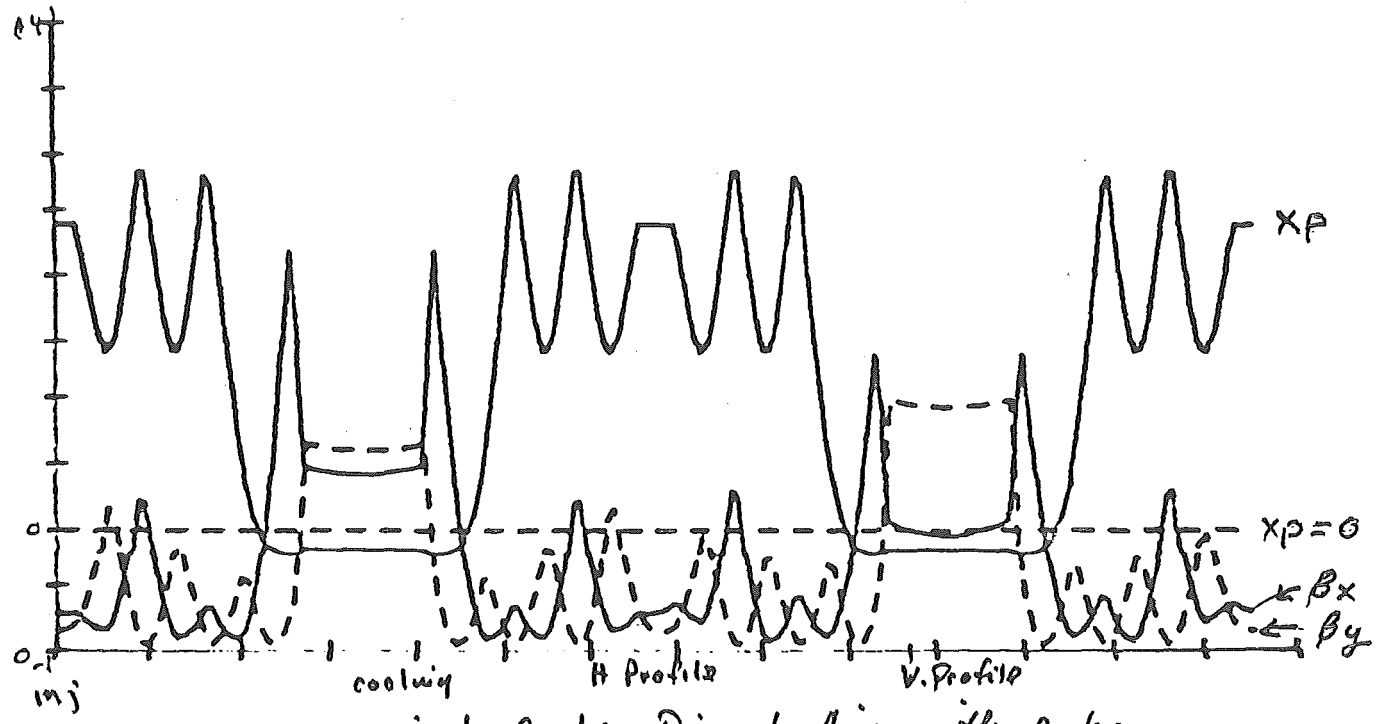

Typical Cooling Ring Lattice with e-beam

Schottky Bands at 450 MHz (1.25 MHz Separation)
Uncooled beam

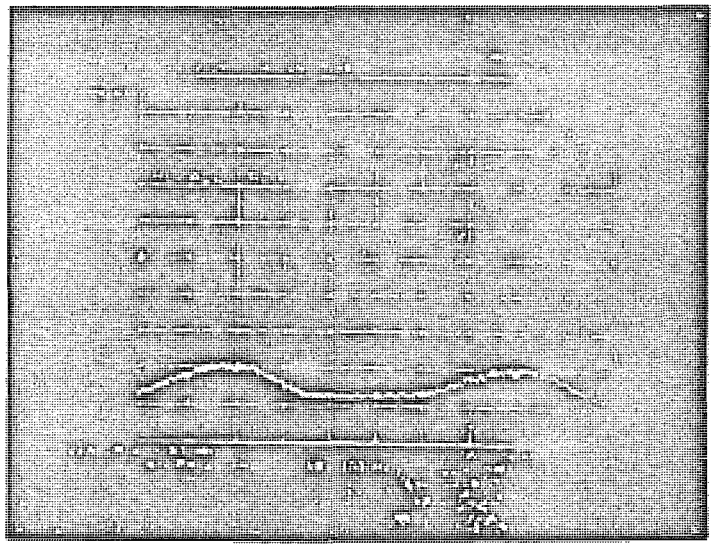

After several seconds

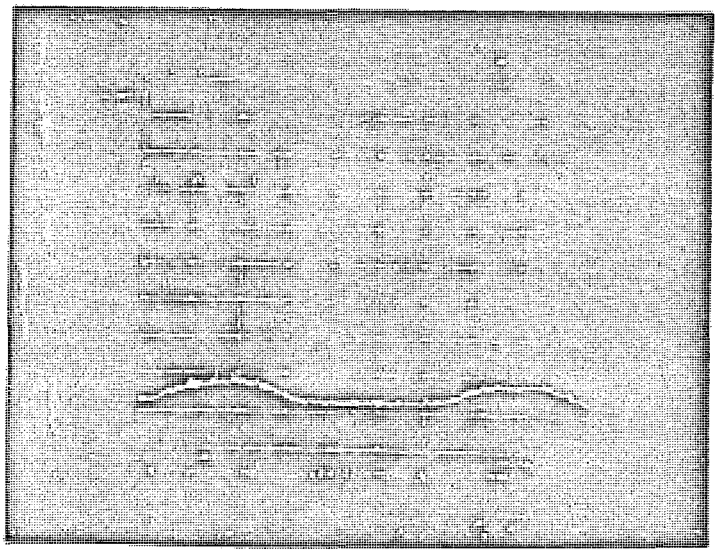

After several Minutes

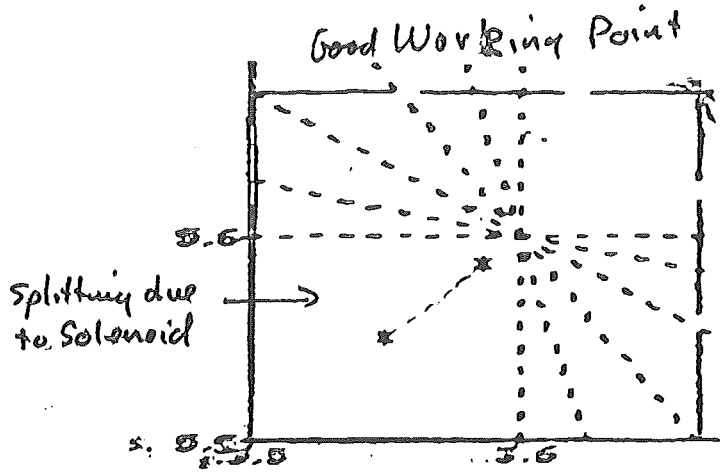

After several Seconds

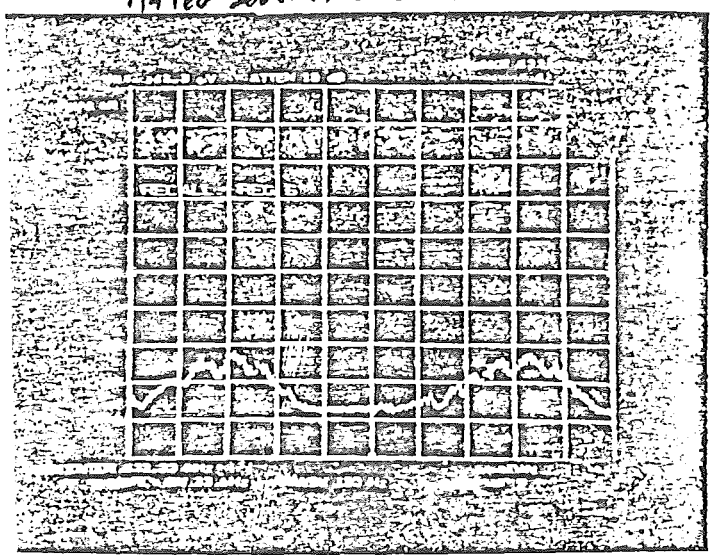

After several minutes

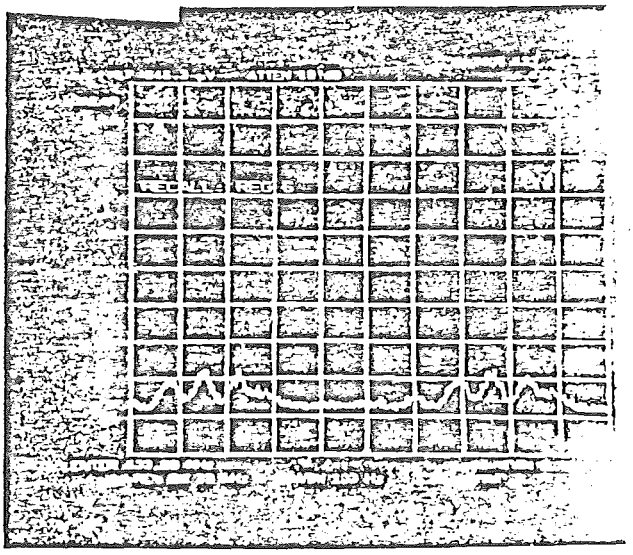

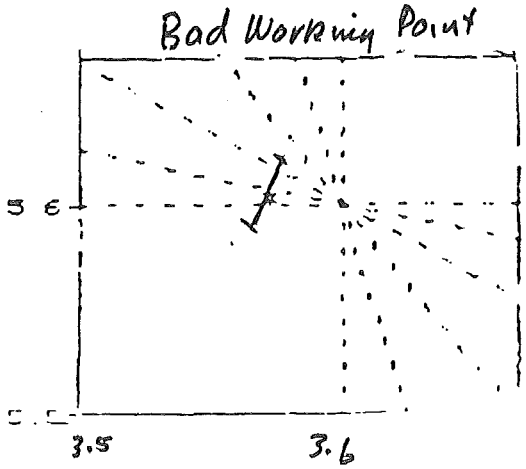

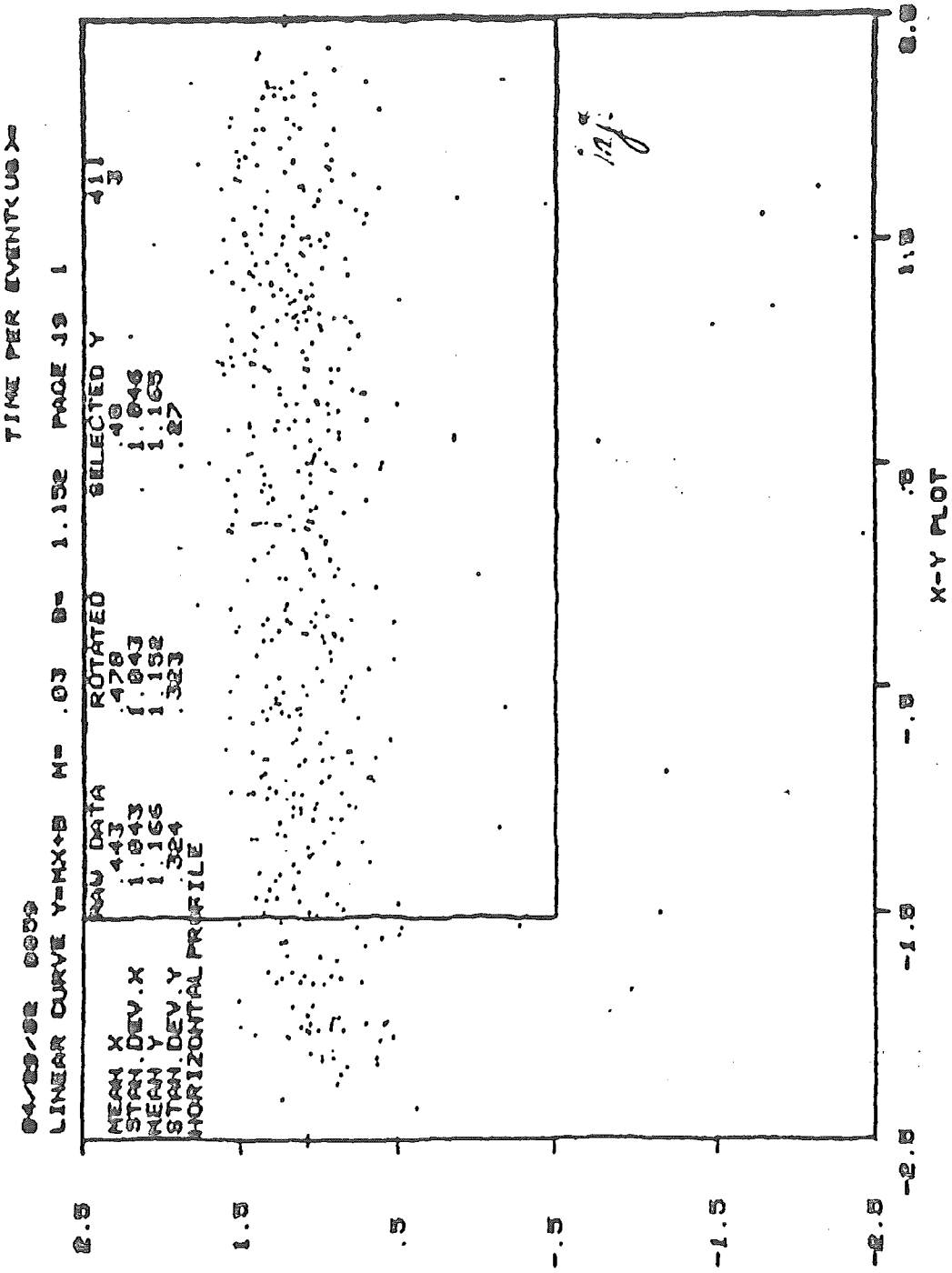
TIME PER EVENT(US)=
04/03/82 0059
LINEAR CURVE Y=MX+B M= .03 B= 1.152 PAGE 19 1
RAW DATA
ROTATED
SELECTED Y
411
50
MEAN X .443 .478 .478
STAN.DEV.X 1.043 1.043 1.046
MEAN Y 1.165 1.152 1.165
STAN.DEV.Y .324 .323 .327
HORIZONTAL PROFILE
2.5
1.5
.5
-.5
-1.5
-2.5
2.0
1.0
.0
-1.0
-2.0
X-Y PLOT

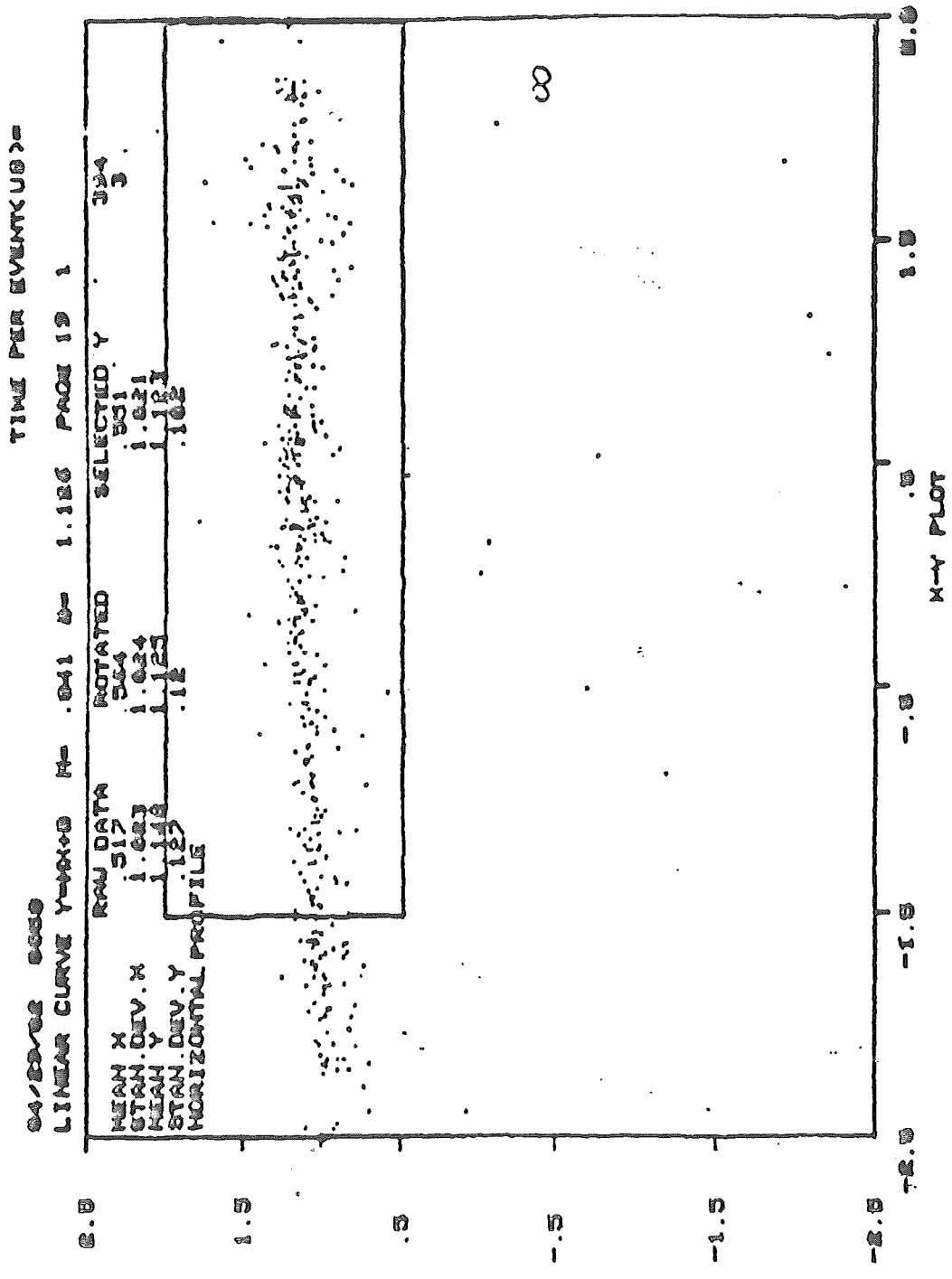
TIME PER EVENT(US)=
LINEAR CURVE Y=MX+B M= .041 B= 1.136 FROM 19 1
RAW DATA
317
MEAN X 1.623
STAN.DEV.X 1.144
MEAN Y .127
STAN.DEV.Y .12
HORIZONTAL PROFILE
ROTATED
344
1.624
1.123
.1
SELECTED Y
331
1.621
1.183
.102
334
3
8
2.0
1.5
1.0
.5
0.
-.5
-1.0
-1.5
-2.0
-2.0
-1.5
-1.0
-.5
0.
.5
1.0
1.5
2.0
PLOT Y1X

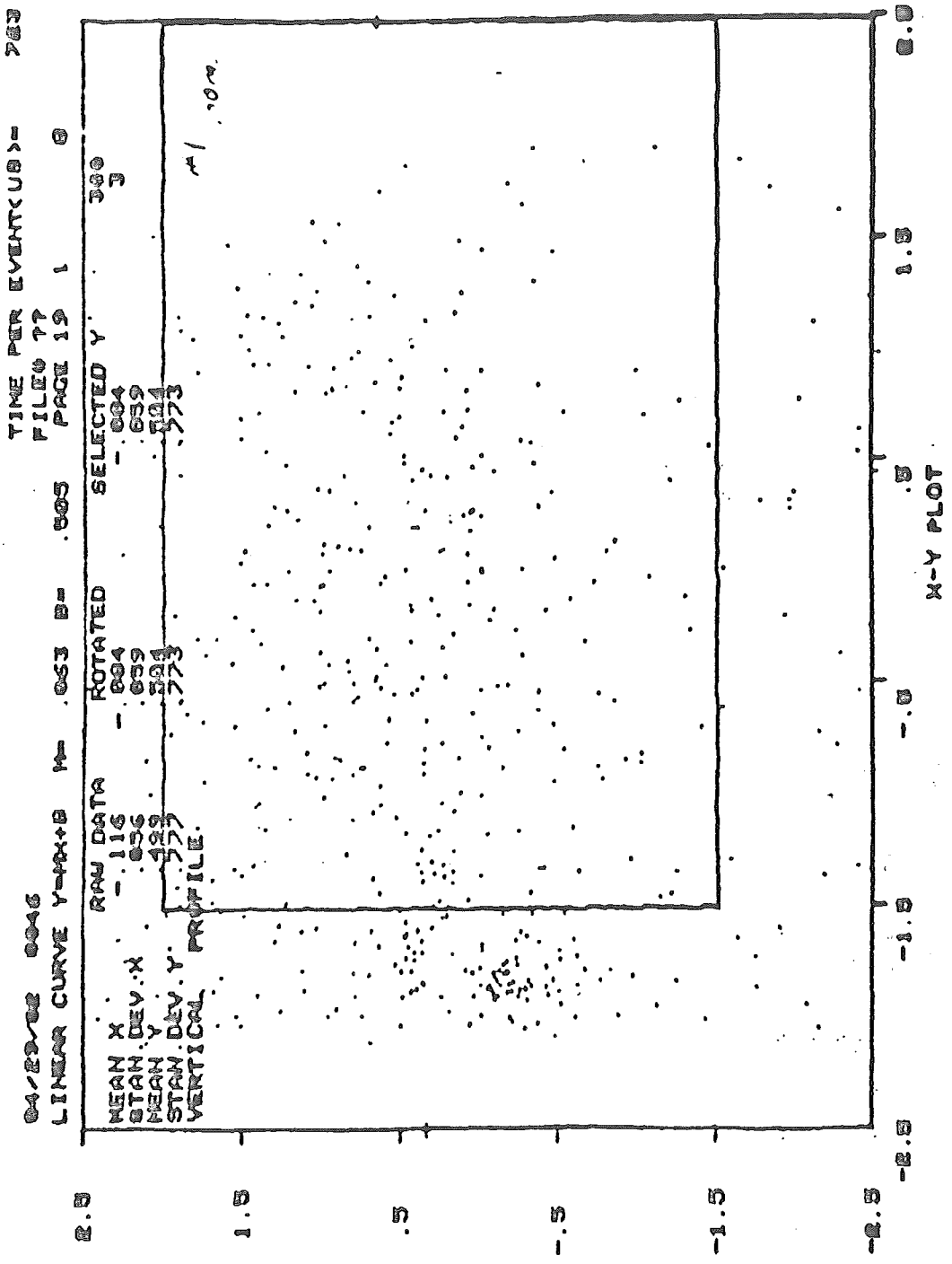
TIME PER EVENT(USA)
FILE 77
PAGE 19 1
LINEAR CURVE Y=MX+B M= .053 B= .005
RAW DATA
MEAN X -.116
STAN.DEV.X .856
MEAN Y .122
STAN.DEV.Y .773
VERTICAL PROFILE
ROTATED
-.804
.659
.591
.773
SELECTED Y
-.804
.659
.591
.773
X-Y PLOT
2.5
1.5
.5
-.5
-1.5
-2.5
-2.5
-1.5
-.5
.5
1.5
2.5

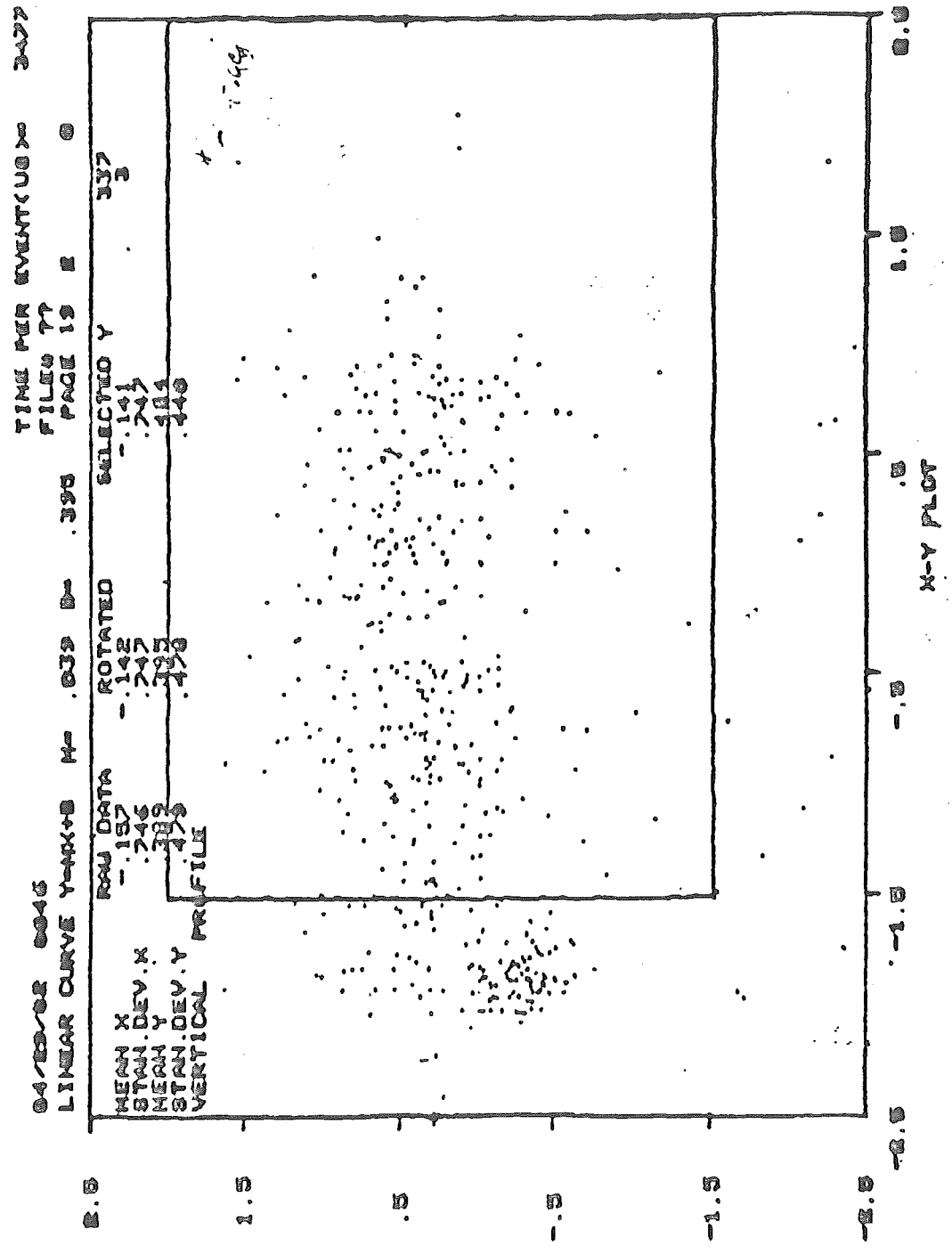
TIME PER EVENT<USEC> DATA
FILE= TT
PAGE 19
04/20/82 0046
LINEAR CURVE Y=AX+B M= .839 B= .395
ROW DATA
MEAN X -.157
STAN.DEV.X .246
MEAN Y .389
STAN.DEV.Y .477
VERTICAL PROFILE
ROTATED
-.142
.245
.433
SELECTED Y
-.141
.241
.444
337
X-Y PLOT
2.0
1.5
1.0
.5
0.0
-.5
-1.0
-1.5
-2.0

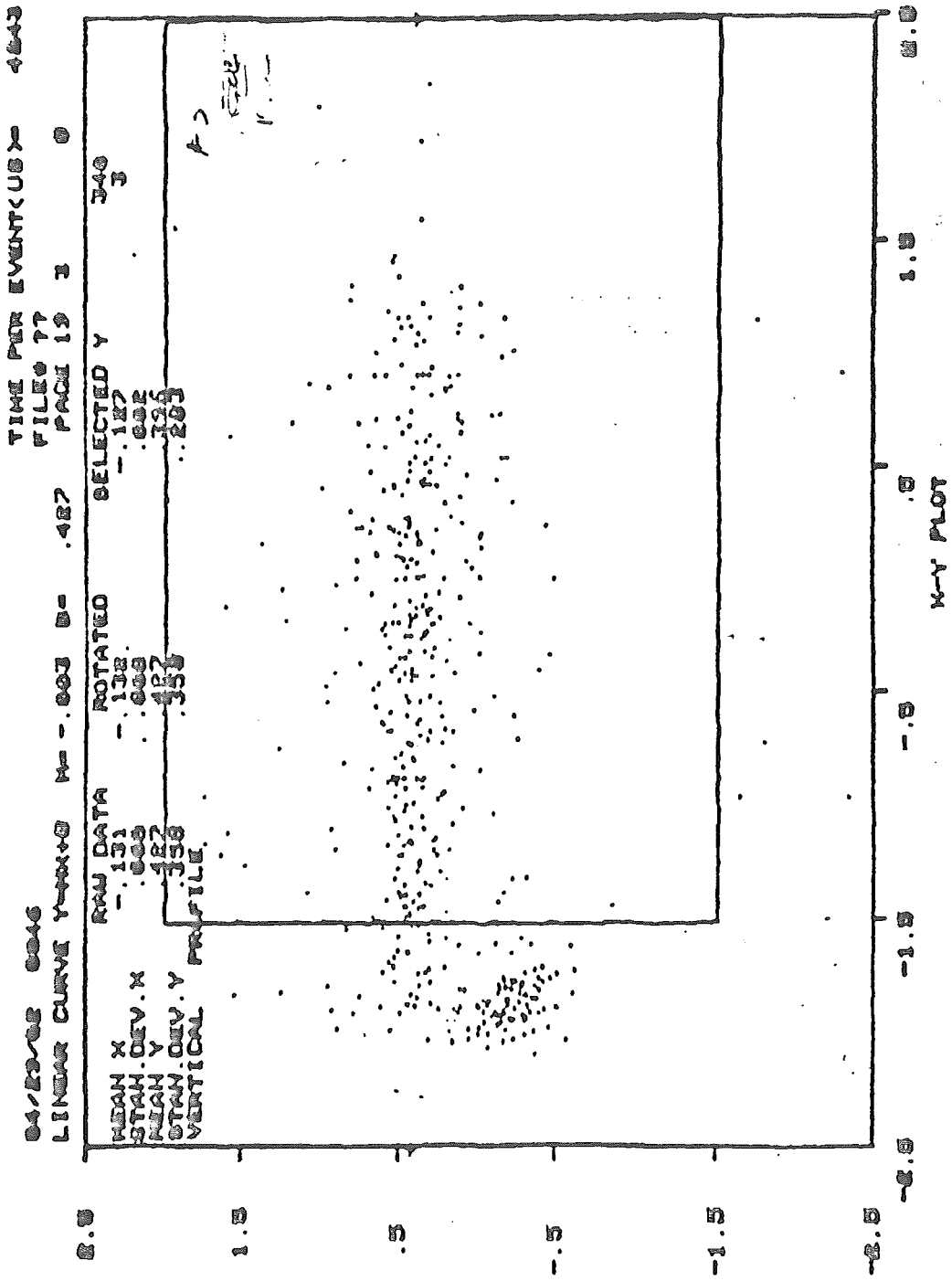
TIME PER EVENT<USE> 4643
FILE# 77
PAGE 19 3 0
LINEAR CURVE Y=MX+B M= -.003 B= .487
RAW DATA
MEAN X -.131
STAN.DEV.X .003
MEAN Y 182
STAN.DEV.Y 358
VERTICAL PROFILE
ROTATED
-.138
.003
182
358
SELECTED Y
-.182
.002
126
283
340
5
K-Y PLOT
0.0
-.5
-1.0
-1.5
-2.0

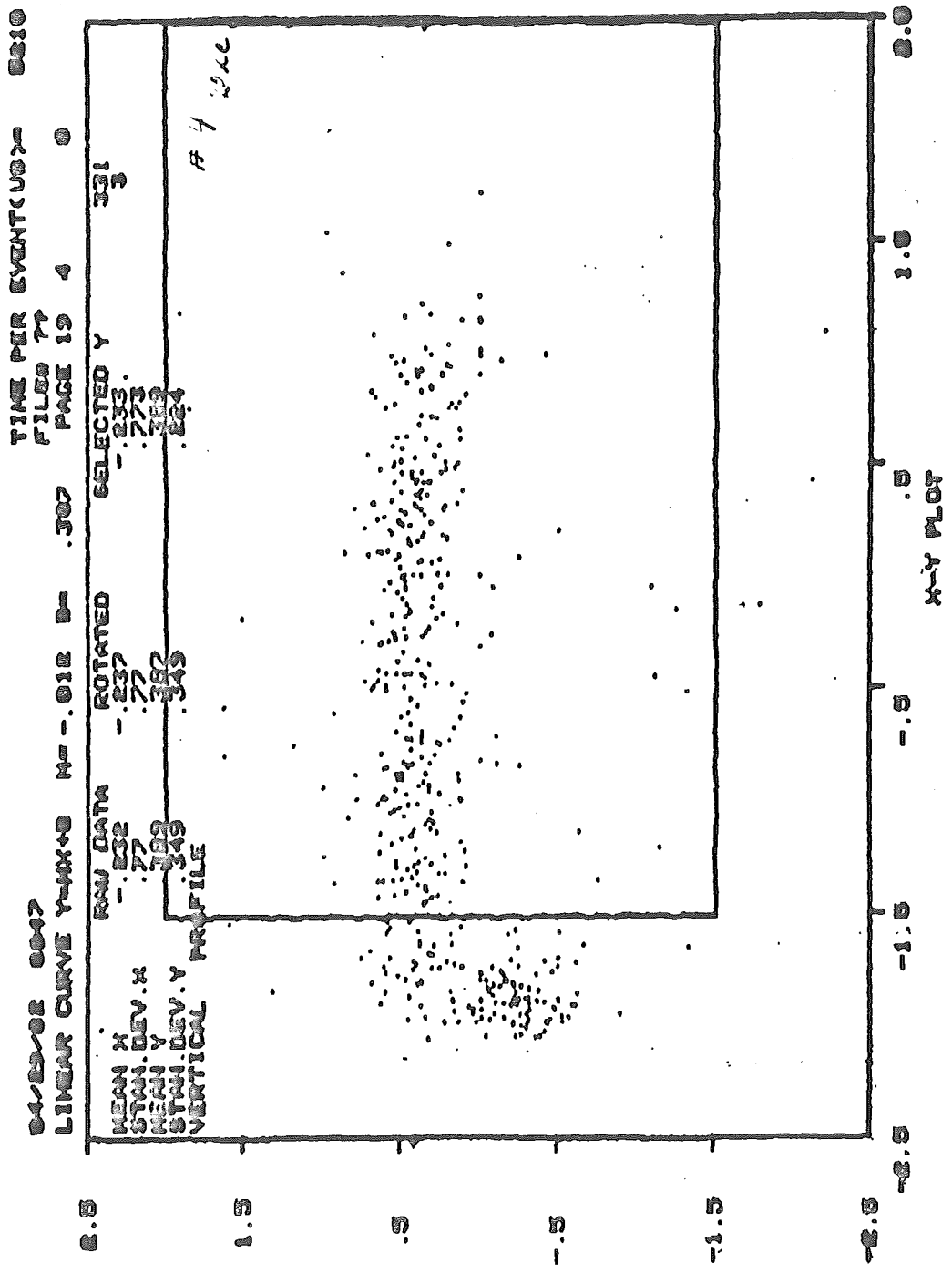
TIME PER EVENT(USX= 0.10
FILE# 77
PAGE 19 4 0
LINEAR CURVE Y=MX+B M= -.018 B= .307
RAW DATA
MEAN X -.232
STAN.DEV.X .27
MEAN Y .782
STAN.DEV.Y .349
VERTICAL PROFILE
ROTATED
-.237
.27
.782
.349
SELECTED Y
-.233
.273
.783
.324
331
3
4 wire
X-Y PLOT
2.5
1.5
.5
-.5
-1.5
-2.5
-2.0
-1.0
-.5
.5
1.0
2.0

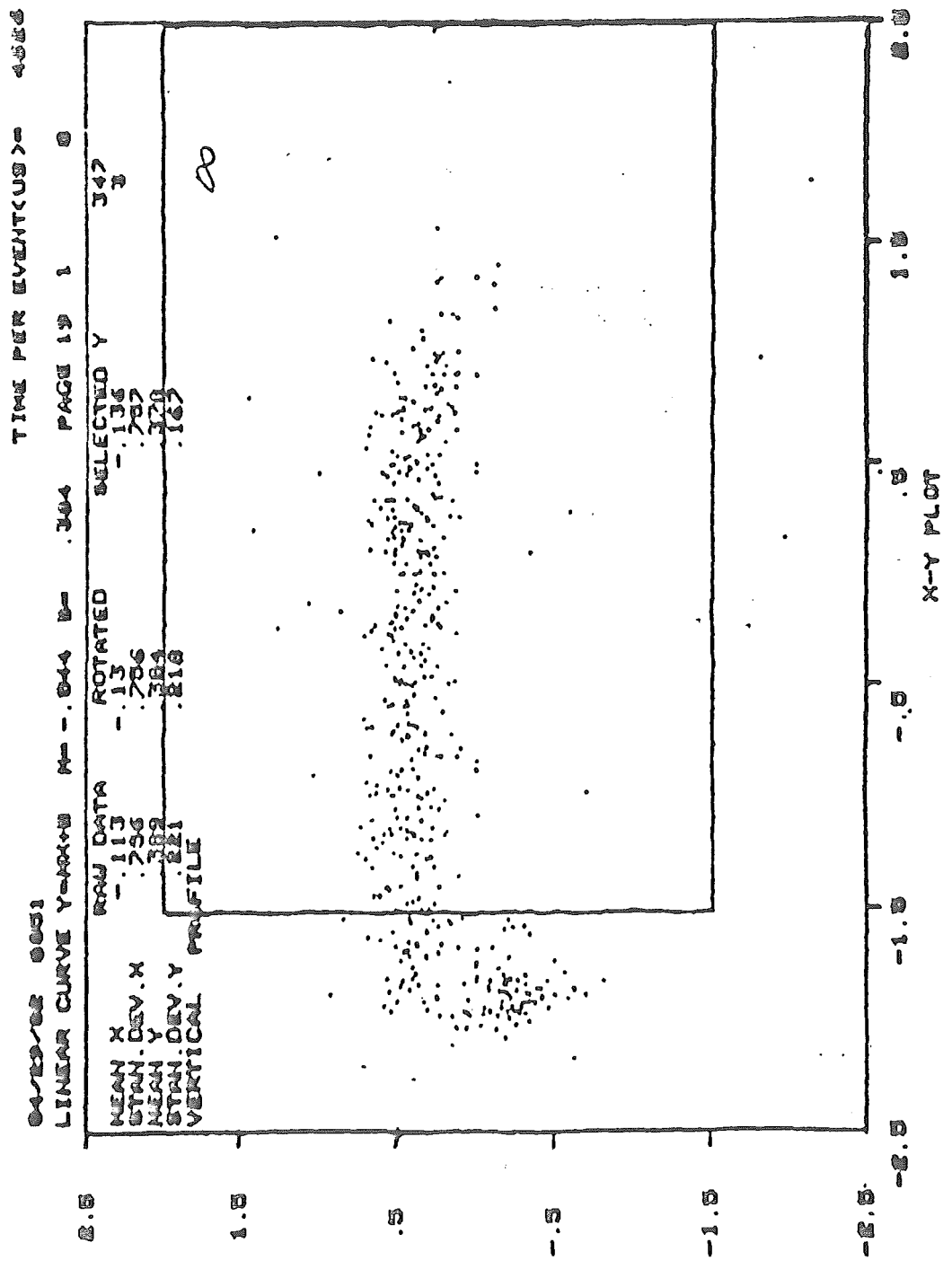
LINEAR CURVE Y=AX+B M= -.044 B= .304 PAGE 19 1 0
TIME PER EVENT(US)= 4.6
RAW DATA ROTATED SELECTED Y
NEAN X -.113 -.135
STN.DEV.X .236 .787
NEAN Y .382 .384 .370
STN.DEV.Y .221 .218 .163
VERTICAL PROFILE
X-Y PLOT
2.5
1.5
.5
-.5
-1.5
-2.5
-2.5
-1.5
-.5
.5
1.5
2.5

Accumulation

How to merge a stacked beam of $\sim 10^{-5} = \frac{\sigma p}{p}$ with a hot beam of $2 \times 10^{-3} = \frac{\sigma p}{p}$?

Answer: Put the hot beam inside the cold beam!

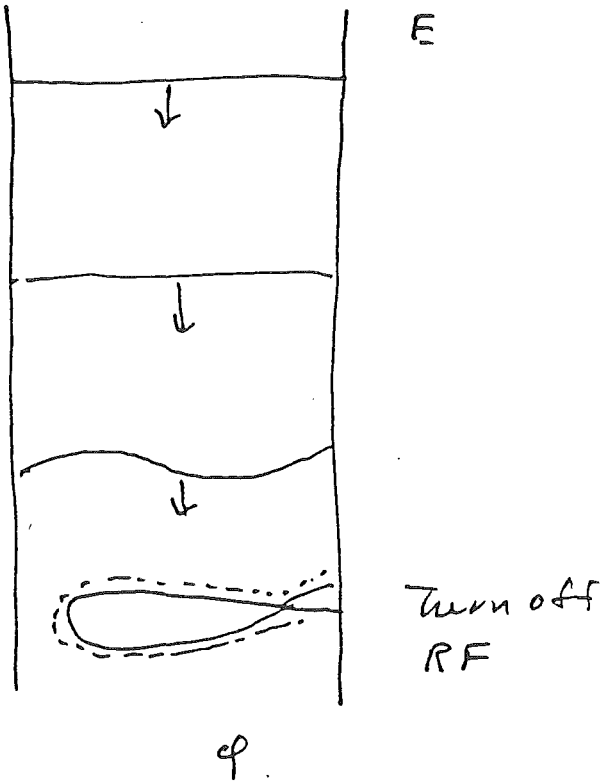

Schottky Signals after stack.

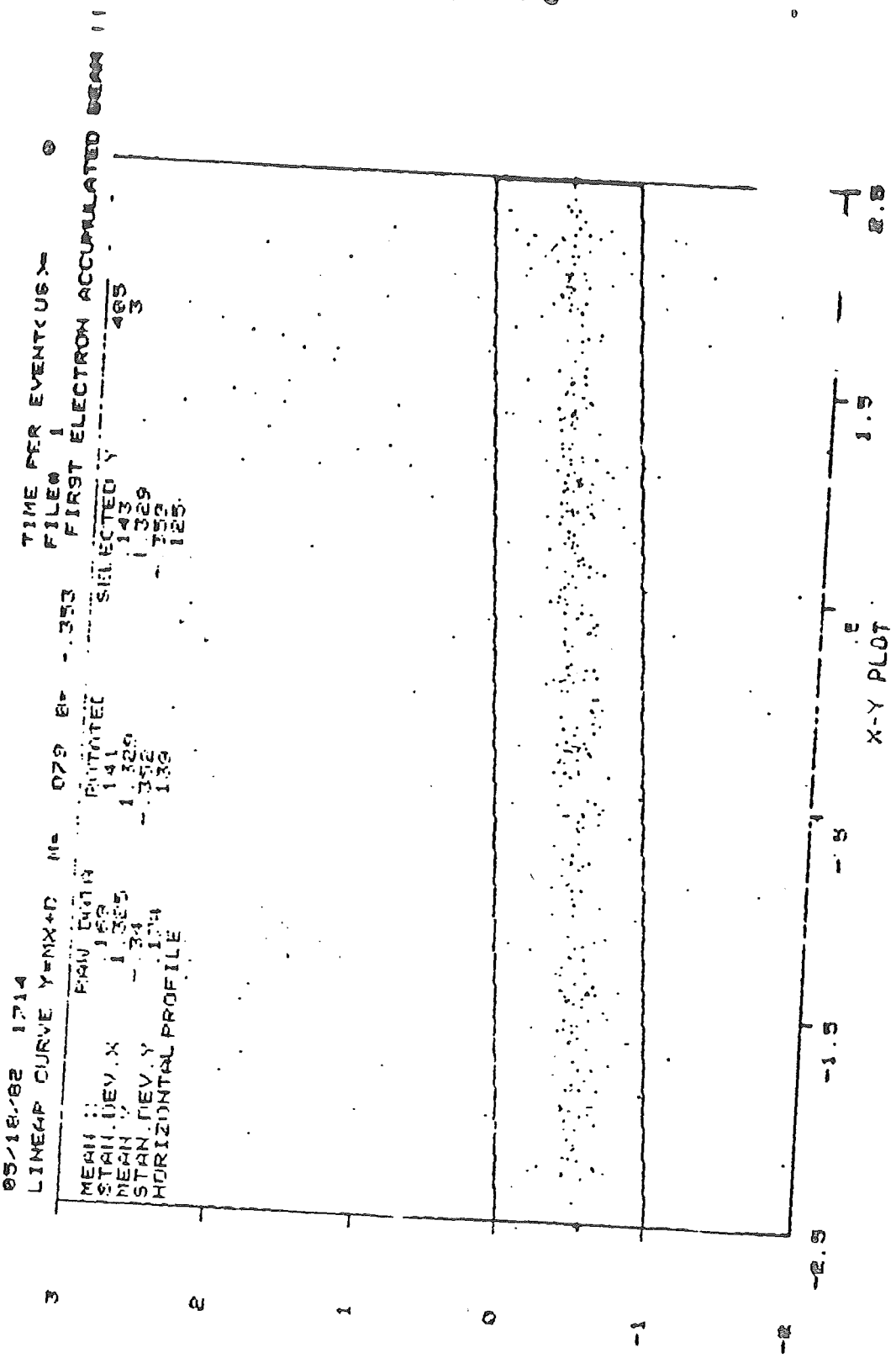
05/18/82 1714
LINEAR CURVE Y=MX+B M= 079 B= -.353
TIME PER EVENT<US>= 0
FILE# 1
FIRST ELECTRON ACCUMULATED BEAM
RAW DATA
PLOTTED
SELECTED Y
MEAN :: 1.329
STAN.DEV.X 1.325 1.329
MEAN :: -.34 -.352 -.352
STAN.DEV.Y 1.14 1.39 1.25
HORIZONTAL PROFILE
465
3
143
X-Y PLOT
3
2
1
0
-1
-2
-2.5
-1.5
-.5
.5
1.5
2.5

IM INNOV21

Sweeping

V = proton velocity

V_0 = electron velocity

$$\frac{d\vec{V}}{dt} = -K\frac{\vec{V}-\vec{V}_0}{|\vec{V}-\vec{V}_0|^3} = K\nabla_v\frac{1}{|V-V_0|}$$

Let $\vec{u} = \vec{V} - \vec{V}_0$ $\quad \dot{\vec{u}} = \dot{\vec{V}} - \dot{\vec{V}}_0 = -K\frac{\vec{u}}{u^3} - \dot{\vec{V}}_0$

$$= \nabla_u\left[\frac{K}{u} - \vec{u}\cdot\dot{\vec{V}}_0\right] \qquad \text{Choose } V_0 = -a\,\hat{n}_{\parallel}$$

$$= \nabla_u\left[\frac{K}{u} + a\,u_{\parallel}\right.$$

Electrostatic Analogy $\qquad q = K \quad \dot{\vec{u}} = E$

a = external field.

Question: at what V_+, when particle start at large $-V_{\parallel}$ do particle get cooled?

Electrostatic Analogy: What is the radius of the bundle of electric flux lines which end on q ! $\quad u=\infty$

electrostatics E_{ext} → ; q

$$\pi R^2 E_{ext} = 4\pi q \qquad R^2 = 4q/E$$

electron cooling a $\xrightarrow{T u_\perp}$ °K

$$\pi u_\perp^2 a = 4\pi K$$

$$u_\perp^2 = \frac{4K}{a}$$

SIS 12 - A Heavy Ion Accelerator for the range up to 1 GeV/u. Look to Cooling of H.I. Beams.

Bernhard Franzke, GSI - Darmstadt

1. SIS 12 - Characteristics

In the heavy ion programme of GSI-Darmstadt, described in the SIS-proposal for a two-stage synchrotron facility for 15 GeV/u[1], the synchrotron SIS 12 plays a double role as booster for the large SIS 100 and as exploring machine for experiments in the energy range from 20 MeV/u up to 1 GeV/u.

The latest design of SIS 12 lead to a ring of nearly 200 m circumference containing 12 identical separate function focusing periods, each with 30 degree bending magnets (see Fig. 1). The maximum magnetic rigidity of ions is B×R = 12 Tm at a bending field B = 1.2 T corresponding to maximum energies of 0.5 MeV/u for uranium, 1.2 GeV/u for Z = A/2 (neon), and 2.7 GeV for protons. There is still the possibility to raise the field to 1.8 T corresponding to 1 GeV/u for uranium, 2 GeV/u for neon, and 4.5 GeV for protons.

The transversal acceptances of SIS 12 - horizontal 200 π mm mrad, vertical 50 π mm mrad - will be filled by radial multiturn injection of the UNILAC - beam the emittance of which is around 5 π mm mrad. Optimal use of the apertures of bending and focusing magnets is achieved at injection by quadrupole triplett focusing. During acceleration the shrinking of the beam emittance is allowing for a transition to doublet focusing whereby the gradient of the third lense of the triplett is left at injection level.

The working pressure in the SIS 12 vacuum chamber has to be below 1×10^{-10} mbar. Under this condition beam losses due to stripping of accelerated ions at the residual gas molecules are probably below 1 %.

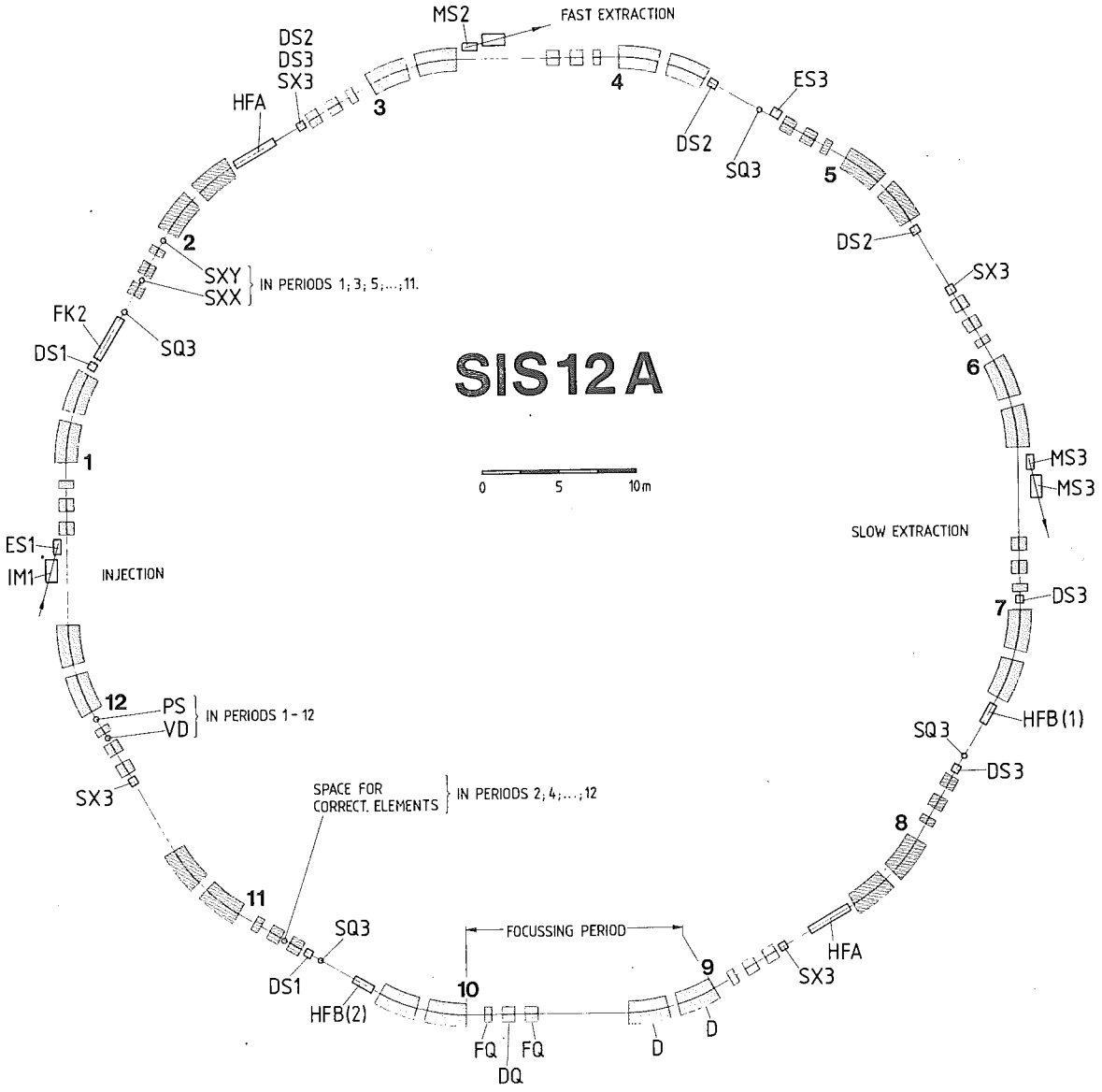

SYMBOLS:

D	DIPOLE MAGNET	SXX, SXY	CHROMAT. SEXTUPOLES
FQ	FOC. QUADR. MAGNET	IM.	INFLECTOR MAGNET
DQ	DEFOC. QUADR. MAGNET	MS.	SEPTUM MAGNET
VD	CORR. DIPOLE (VERTICAL)	ES.	ELECTROSTATIC SEPTUM
HFA	ACCEL. CAVITY (0.9-6 MHz)	SX.	FAST SEXTUPOLE MAGNET
HFB	ACCEL. CAVITY (9-54 MHz)	SQ.	FAST QUADRUPOLE MAGNET
PS	BEAM DIAGNOSTIC	..1	INJECTION ELEMENT
FK.	FERRITE KICKER	..2	FAST EXTRACTION ELEMENT
		..3	SLOW EXTRACTION ELEMENT

Fig. 1: The SIS 12 lattice

2. The SIS 12 beam

a) Energy range

The energy of the SIS 12 beam will be continuously variable between 20 MeV/u and 1 GeV/u. The reproduction of energy values should be possible with an relative error of $\Delta E/E \leq \pm 1 \times 10^{-4}$. The dependence of maximum energies on the atomic number of ion and on injection conditions is shown in Fig. 2.

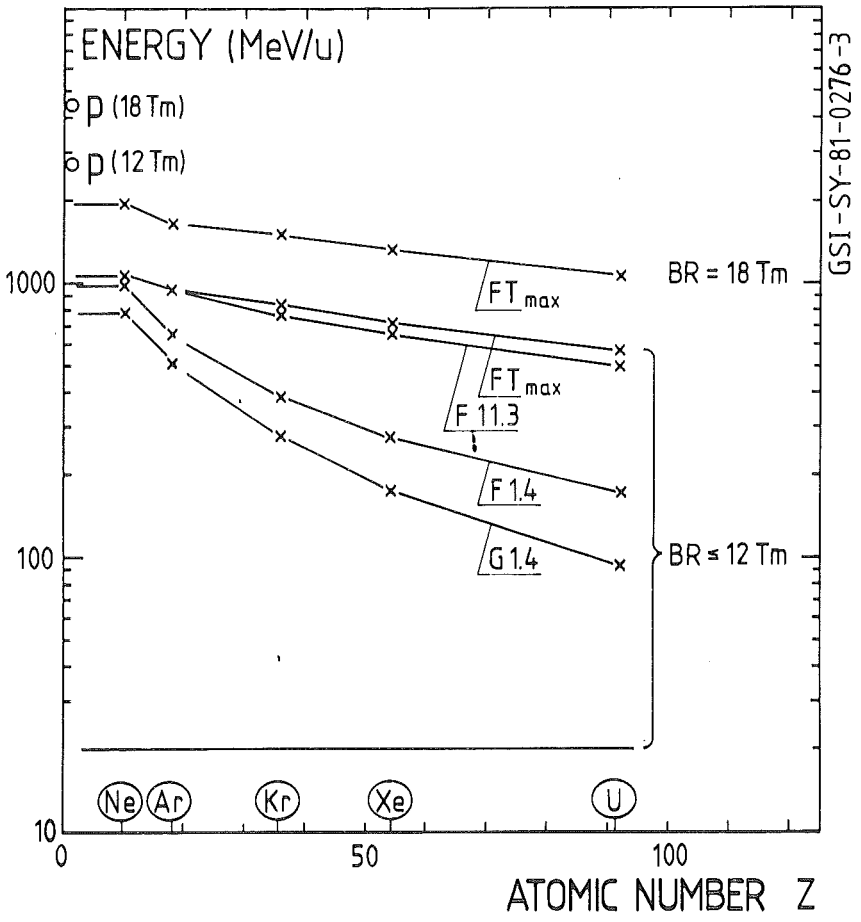

Fig. 2: Energy range for ions accelerated in SIS 12. The curves for maximum energies are determined by the charge states attained by foil (F) and gas (G) strippers in and behind the UNILAC at 1.4 MeV/u, 11.3 MeV/u and the maximum UNILAC energy T_{max} (17.3 - 20.6 MeV/u).

b) Beam currents

The average beam current from SIS 12 is determined by the cycling rate f_c and the number of ions per pulse N_{max} which principally is limited by space charge effects at injection (incoherent detuning of betatron oscillations). In Fig. 3 the product $N_{max} \times f_c$ is plotted vs. extraction energy, assuming 20 % duty factor for slow extraction.

At present the UNILAC is not able to fill SIS 12 up to the space charge limit. Therefore it will be upgraded by a high current pre-injector (probably rfq-structure) within the coming years.

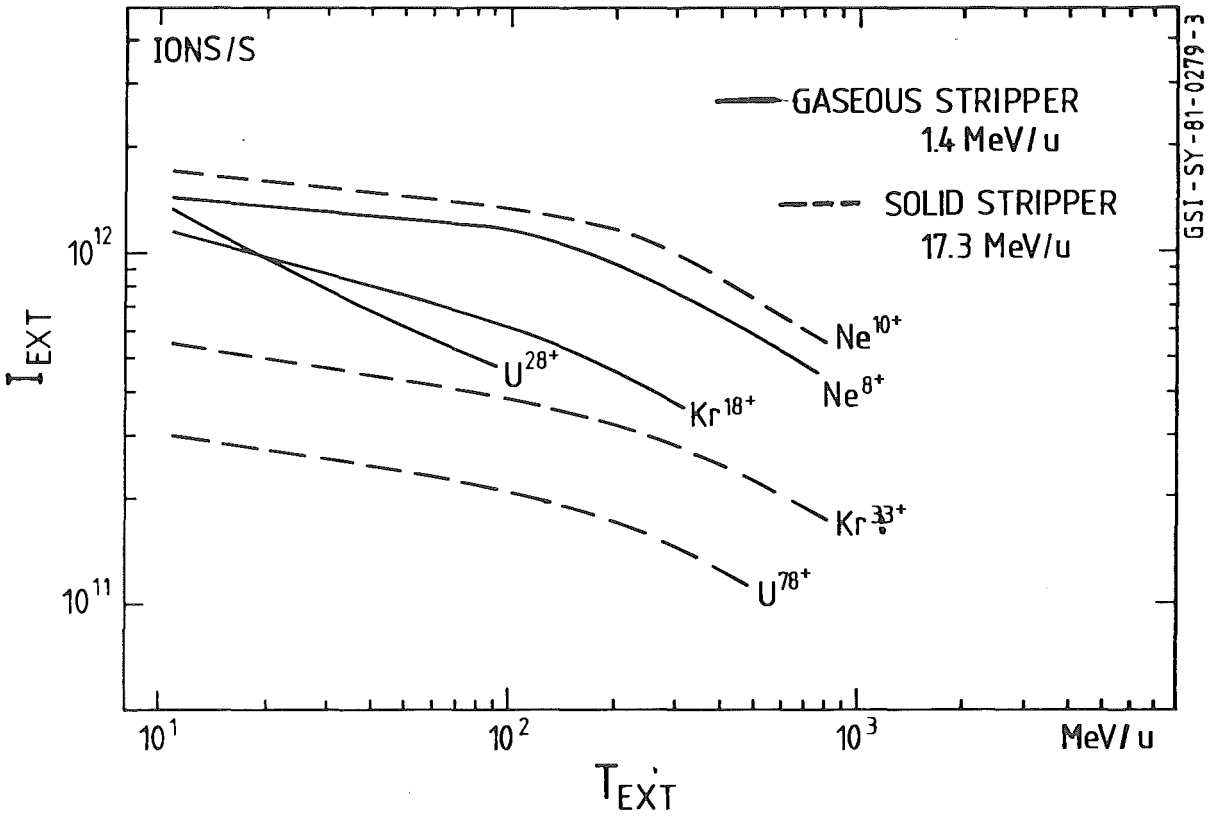

Fig. 3: Maximum average particle currents from SIS 12 vs. specific ion energy. A duty factor of 20 % for slow extraction is assumed.

c) Emittances

The emittances which can be achieved with the full beam intensities (see Fig.3) depend on the extraction energy as shown in Fig. 4. These values may be reduced by reducing the beam current. The dependence between current and vertical emittance is linear, whereas the horizontal emittance is influenced roughly by the square root of beam current.

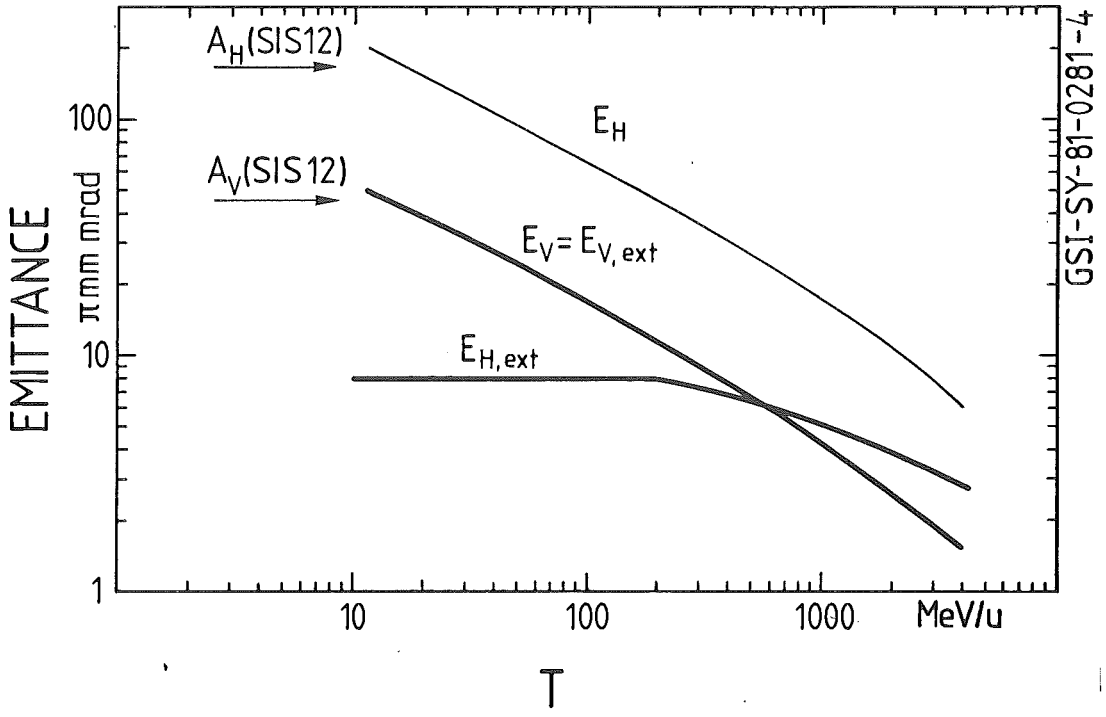

Fig. 4: Horizontal and vertical emittances of the SIS 12 beam injected at 11.3 MeV/u. The constant value of $E_{H,Ext}$ below 200 MeV/u may only be exploited to the point where - at the beginning of extraction - the beam fills less than half of the aperture.

d) Momentum spread and time structure

During the adiabatic r.f. capture at injection energy, the momentum spread of the beam increases to around $\Delta p/p = \pm 3.5 \times 10^{-3}$, nearly independently of the momentum width of the injected beam. The decrease of $\Delta p/p$ with energy is proportional to $(\beta\gamma)^{-1}$. $\Delta p/p = 10^{-3}$ is a value typical for SIS 12. At the maximum bunch frequency of 6 MHz the bunch length is roughly 50 ns, i.e. without practical worth.

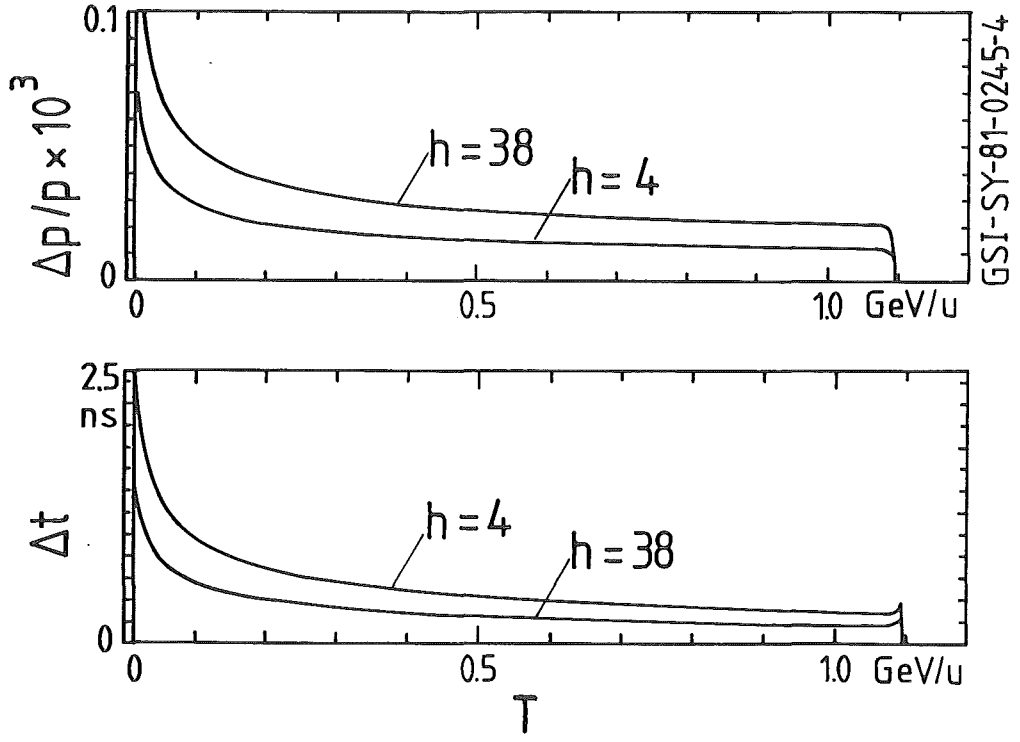

Fig. 5: Momentum spread and pulse width for neon ions vs. extraction energy in the case of 'bunch into bucket' injection.

Essential improvements can be achieved if the UNILAC micropulse structure can be conserved during injection into SIS 12. This 'bunch into bucket' capture is planned to be realized by using a second accelerating system, working in the interval from 9 to 55 MHz. Under idealized conditions one should reach the values for $\Delta p/p$ and Δt plotted in Fig. 5 vs. extraction energy with optimal values $\Delta p/p = \pm 2 \times 10^{-5}$ and $\Delta t = \pm 0.2$ ns. These will probably be increased by technical imperfections (non-ideal synchronisation between UNILAC and SIS 12 or limited phase stability of the SIS 12 r.f.). Furthermore, one has to expect essentially lower average beam currents because of strongly increased transversal and longitudinal space charge effects.

3. Option for beam cooling at GSI

At GSI, the discussion of beam cooling has been mainly stimulated by rather extreme beam parameters thrown on the market by the SUSE proposal[2]. Nevertheless, there are - so far - no mentionable research and development activities concentrated on heavy ion cooling. Electron beam cooling seems to be more promising than stochastic cooling techniques because of shorter cooling times, independence of beam current and higher cooling efficiency at low ion energy. However, there are many effects which may lead to difficulties in praxis and therefore, should be theoretically or experimentally investigated as soon as possible:

1. Cross sections for capture of cooling electrons by ions? Dependence on Z.

2. Equilibrium phase space volume of highly charged ion beam? (Space charge limits, Instabilities?)

3. Vacuum requirements, cooling of partially stripped ions?

4. Internal and/or external targets? Comparison of cooling rate with heating of ions by internal target? Space requirements for internal experiments?

5. Energy and mass range? Energy variation?

6. If necessary: Extraction concept for extremely cold beams?

Table I:

Tentative Parameters for a Cooling Section in SIS 12

Eff. length, L_{eff}	:	3 m
Ion energy	:	30 - 200 MeV/u
Electron energy	:	16.5 - 110 keV
Beam Diameter	:	5 cm
$\eta = I_{eff/U}$	:	1.5 %
Electron current	:	10 A
Current density	:	0.5 A/cm²

Cooling time (transversal compoents):[3]

$$\tau_c = \frac{k}{\eta L_c} \left(\frac{A}{q^2}\right) \cdot \beta^4 \gamma^5 \frac{(\theta_e^2 + \theta_i^2)^{3/2}}{r_e r_N (j/e)}$$

k	= 0.6 (Maxw. Dist.)	$\beta^4\gamma^5$	= 0.0044 (30 MeV/u)
η	= 0.015		0.27 (200 MeV/u)
L_c	= 10	$r_e r_N = 1823\, r_e^2$	$= 8\times10^{-26}$ cm²
A/q^2	= 0.2 (Ne^{10+})	j/e	$= 3.13\times10^{18}$ cm^{-2} s^{-1}
θ_e	~ 0.001	θ_i	= 0.005

τ_c = 2 ms at 30 MeV/u

110 ms at 200 MeV/u

Table I presents a rough estimation of cooling time constants for 30 MeV/u and 200 MeV/u Ne(10^+)-ions circulating in SIS 12. A cooling section of about 3 m length installed into one of the 12 straight sections is assumed. The result seems to indicate that electron cooling may be a suitable tool for improvements in beam quality of a fast cycling synchrotron. The installation of a cooling test section, by means of which most of the questions listed above may be answered, should be taken into consideration.

References:

[1] SIS - Eine Beschleuniger-Anlage für schwere Ionen hoher Energie; GSI-Darmstadt, November 1981

[2] SUSE-Daten, Universitaet Muenchen, November 1980

[3] A.M. Sessler, Proc. Workshop on High-Luminosity High-Energy pp-Collisions, Berkeley (LBL-7574,1978) p.53

PANEL DISCUSSION

Chairman: K.H. Maier (HMI Berlin)

Discussion

R. Santo

Requirements of typical experiments (1. spectroscopy of spin-isospin resonances, 2. particle-particle correlation experiments) on momentum resolution, current, the measurement of angular distributions and the required time structure.

	spectroscopy of spin-isospin resonances	particle-particle correlation
$\Delta p/p$	optimal	average
current	decent	high
angular distribution	yes (forward angles)	yes
time structure	-	important

R. Santo

Questions from the experimentalists' point of view about the performance of a new accelerator facility using the electron cooling scheme

1. What are the limits on the target thickness for use in cooled beams?
   a. Dependence of the maximum target thickness from beam energy
   b. Losses of beam and beam quality
   c. How can the cooling time be improved?
2. Problems related to the extraction of cooled beams
3. Time structure of extracted cooled beams
4. Cooling of heavy ion beams
5. Energy variation using the electron beam?

R. Santo

Special questions related to experiments using a cooled beam.

a) What types of experiments require external targets?

b) To what extent can Big Karl be used with internal targets?

c) Vacuum requirements

d) Preparation of internal targets (size, thickness, isotopes...)

e) Scattering chamber experiments with the recirculator?

R. Santo presents a table which shows the properties of the beam and the target.

	E_p (MeV)	Beam optimal $\Delta p/p$	Beam current (μA)	Beam reasonable $\Delta p/p$	Beam current (μA)	Target d($\mu g/cm^2$) extern	intern	limited by spectrum	limited by machine	costs DM
JULIC[1]	45	(2)1×10^{-4}	0.05	1.5×10^{-3}	10					
		(3)6×10^{-4}	1.0			x		50		-
Recirculator[4]	45	2×10^{-4}	2.5[1]	(3)2×10^{-4}		x	x	50		3×10^6
R. Pollock (Tripler)	200	5×10^{-5}	5 mA				x		.05	
S. Martin (COSY)	500	2×10^{-5}	30 mA				x		.5	20×10^6
COSY	45[5]									

1) The geometrical emittance of the Jülich cyclotron is $\varepsilon = 6\pi$

2) Dispersive mode of the JULIC beam line

3) Achromatic mode of JULIC beam line

4) The circulating current is strongly dependent in the target and the lattice (see contribution 7)

5) Electron cooling is faster at low energies, but the injection from the cyclotron in the synchrotron may be a problem (F. Mills)

R. Pollock

A good understandable figure of merrit is the plot of the luminosity vs. resolution

C. Wiedner

The recirculator discussed in sect. 7 does not match the maximum resolving power of the Big Karl spectrometer. This recirculator allows only $p/\Delta p$ = 4000, the Big Karl is made for 20 000.

K.H. Maier

The figure of merrit should show
1. the increase in current
2. the increase in peak to background

There may be a problem with a variable resolution spectrometer like Big Karl and a fixed dispersion recirculator.

The dispersion is transformed to the aperture of the ring, giving the size of the magnets.

K.L. Brown

Also higher order aberrations third and higher order will limit the resolution of recirculator systems. This must be calculated.

R. Pollock

A way to a variable resolution system would be to keep the dispersion of the ring constant and adjust the ß-function.

C. Wiedner

In Big Karl high resolution requires high dispersion $D \gtrsim 20$ cm/%

O. Schult

Is it possible to inject during cooling?

F. Mills

Generally yes.

We do it in batch mode, i.e. the experimentor switches off the detector during filling.

K.L. Brown

Cooling is a wonderful way to wipe out the aberrations of a system.

S. Martin

Advantage of synchrotrons: it is easy and relative cheap to increase the energy up to $\sim$ 1 GeV.

F. Mills

Charge exchange injection will easy work.

Injection of Liouville particles is difficult.

P. v. Brentano

Is it possible to achieve an energy resolution of 500 eV at 20 MeV (independent of target effects)?

R.E. Pollock

$E/\Delta E$ = 40 000 should be available for the IUCF cooler.

S.A. Martin

The recirculator does not improve the beam quality and the spectrometer limit is around $E/\Delta E$ = 20 000 (1 keV at 20 MeV).

H. v. Geramb

Why is the energy of COSY limited to 500 MeV? There are more resonances expected in the region above 1 GeV. A nice feature would be a maximum energy of 1 GeV in the first step and 3 GeV in the second step.

F. Mills

One may vary the dispersion of a ring between 0 and twice of the value of the natural ring dispersion.

S. Martin

According to the dispersion matching, not only the dispersion but also the resolution needs to be matched.

J. Reich

Is the cooled beam so good, that matching is not needed?

R. Pollock

With e-cooling you can achieve emittance improvement in the order of $m_e/m_p \sim 1/1800$ and a factor of $\sqrt{1800} \sim 40$ in beam spot size.

v. Brentano

If the internal target thickness changes in the ring is the system detuned?

R. Pollock

You have to drive the r. f. in a closed loop to correct for target thickness changes during experiment, a matched system is more stable against such changes.

O. Schult

Is it possible to build a compact mini-COSY at 45 MeV?

F. Mills

The cooling is faster at low energy, may be the injection from the cyclotron is a problem.

S. Martin

For the Jülich COSY system the 500 MeV maximum energy is not limited. the 2 GeV as maximum energy is possible.

C. Poth

One should try to reach the energy of the baryon resonances but at higher energies ($\gtrsim$ 500 MeV) the electron cooling gets difficult. Also polarized beams and targets would be nice.

H. v. Geramb

Does the cooler allow polarized beams?

R.E. Pollock

Yes, but it must be polarized transverse.

SUMMARY

R.E. Pollock
Indiana University Cyclotron Facility
Bloomington, Indiana

1. Purpose of the Workshop

- Regional plan for nuclear physics after 1985
- Try to find an agreement on energy, particle and beam quality
- Keep talking together! In order to find the right compromises

2. Resources

- People:
  The number of participants at this workshop demonstrates the strong interest in the future plans. KFA Jülich should be a solid basis in terms of man power as well as technological know how.

- Possible spallation source:
  All future plans are influenced by the engagement of the NRW universities for the spallation neutron source (SNQ)

- BIG KARL:
  The high resolution spectrometer BIG KARL is an existing important element for a future system.
  BIG KARL works for particles up to 3.5 Tm (ca. 500 MeV protons)
  First ideas for future plans are developed by the BIG KARL group.

3. Cooling Technology

- The electron cooling has been well studied for energies between 20 and 200 MeV protons. There is no doubt that it works also for higher energies.
- Electron-cooling is a good research and development program for future application e.g. heavier ions.

4. A cooled synchrotron?

- It is certainly possible to do cooling and accelerate in the same Ring. For a 6 Tm ring (1100 MeV protons) the high quality cooled external beam would have an average current also about < 30 nA $>$ with a duty factor of 20 %.

- The lattice for such a system needs more careful studies.
- One should study a system of 2 rings, one for cooling and acceleration the other for the experiment.
- even with cooling the resolving power is limited.

5. An uncooled recirculator

- This is a quick way to get a selective improvement (stripping injection using atomic H_2^{1+} and $^3He^{1+}$)
- to build a recirculator will accumulate design experience for a later system
- the better brightness allows a higher data rate at a given resolution
- the acceleration of the circulating beam may open up new experimental possibilities
- cooling in the recirculator may be done as a further extension

6. This workshop has opened more questions than it has answered questions, e.g.
   - the use of fibre targets in cooled beams?
   - slit-free clean up with electron beam edges?
   - heavy ion cooling?
   - 500 eV experimental resolution with high luminosity?
   - extraction of cooled beams?
   - stacking problems
   - small angle measurements
   - variable dispersion lattice

7. Remarks on workshop environment

   - an excellent meeting

Bad Honnef Workshop Summary

Purpose
- regional plan for 1985-1998..
- must agree on energy and particle and ΔE
- compromises! keep talking together!

Resources
- people
- Big Kahl
- possible spallation source
- ideas!

Cooling Technology
- proven: 20 < Tp < 200 MeV → (×100)
- good R+D to build on

6T-m A) Cooled Synchrotron: < 30 mA > thru put 20% DF
same ring can cool and accelerate lattice?
Better with separated rings? resolving limit

2T-m An Unsolicited Recirculator? assist + encourage!
H₂⁺ quick way to get selective improvement + design experience
better brightness allows higher data rate
at given resolution accel? coul?
in principle

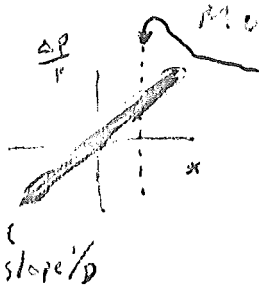

More Questions
fibre targets?
slit-free cleanup with e. beam edges?
heavy ion cooling?
500 eV with high luminosity?
extraction of cooled beam?
stacking
small angles

variable dispersion lattice?

Remarks on Workshop Environment
an excellent meeting